On the control through leadership of multi-agent systems

Dissertation zur Erlangung

des naturwissenschaftlichen Doktorgrades
der Julius-Maximilians-Universität Würzburg

vorgelegt von

Suttida Wongkaew

aus
Phayao, Thailand

Würzburg 2015

Eingereicht am: August 2015.
Tag der mündlichen Prüfung : 5. Oktober 2015.
Hauptreferent : Prof. Dr. Alfio Borzì, Julius-Maximilians-Universität Würzburg.
Korreferent : Prof. Dr. Marco Caponigro, Conservatoire National des Arts et Métiers.

Erkärung/ Declaration

Hiermit erkläre ich, dass ich die eingereichte Doktorarbeit eigenständig, d.h. insbesondere selbständig und ohne Hilfe einer kommerziellen Promotionsberatung angefertigt und keine anderen als die von mir angegebenen Quellen und Hilfsmittel benutzt habe.

I hereby declare that I executed the thesis independently, i.e. in particular self-prepared and without the assistance of a commercial doctorate consultancy and that no sources and tools other than those mentioned have been used.

Würzburg, 2015

Unterschrift / Signature

Acknowledgements

Life is like a book and the chapter as a Ph.D. student began when Prof. Dr. Alfio Borzì gave me the opportunity to study and work under his supervision. Honestly, if he would not give this opportunity, I would give up to continue my study in Germany and could not continue my journey to this point. My motivation on this dissertation came from the first paper that he gave me *"Cucker-Smale Flocking under Hierarchical Leadership"* inspired me and enabled me to find out what I actually want to study and which directions I should go though. I would like to express my special appreciation and thank to him for his generous guidance not only about mathematics but also my personal problems; moreover, for all the sound and fruitful discussions. This dissertation and corresponding papers would not be possibly completed without his help.

I also would like to sincerely thank Prof. Dr. Marco Caponigro for his valuable guidance, friendship and specially agreeing to be the co-referee of my thesis. Moreover, I thank him for kind hospitality during my stay in Paris. Cooperating work with him was significantly influence the accomplishment. I appreciate all his contribution of time and idea to my work. It stimulated my attention and also enriched my master experience. Further I would also like to thank Prof. Dr. Krzysztof Kułakowski. Although we have never met, collaborating work with him via emails, I found him such a nice professor. He always replied me with valuable detailed answers; thank to him.

I gratefully acknowledge the Commission on Higher Education and the Royal Thai government for the Higher Education Strategic Scholarship for Frontier research Network to provide the financial support. Without this scholarship, it would not be possible for me to pursue my Ph.D. here in Germany.

Acknowledgments are also extended to Mrs. Petra Markert-Autsch for kindly helps in preparation important documents and for organizing WiReMIX group's activities; many thanks to her. To all my friends, my time in Germany was made enjoyable because of them and graduallly they become a part of my life. I would like to thank all of them for always staying by my side and encouraging me. Special thank to Gabriele Ciaramella who is an excellent office mate. He is a very good friend. I thank him very much for providing me a good suggestion in which broaden my skills and knowldege. In addition, he taught me to cook several italian recipes and made lots of good times with me. A huge thanks for my friends in WiReMIX group. I really enjoyed the time that we spent together. It is kind of feeling at home. Also friends from Thailand that we usually organized good social activities, I thank them for bringing me to the joyful world which helped me a lot to release my stress.
Lastly, I wish to express my gratitude to my family for all their love, patience and encouragement.

Suttida Wongkaew

Kurzzusammenfassung

Die Untersuchung von interagierende Multiagent-Modellen ist ein neues mathematisches Forschungsfeld, das sich mit dem Gruppenverhalten von Tieren beziehungsweise Sozialverhalten von Menschen. Eine interessante Eigenschaft der Multiagentensysteme ist kollektives Verhalten. Eine der herausfordernden Themen, die sich mit diesen dynamischen Modellen befassen, ist in der mathematischen Sicht eine Entwicklung der Regelungsmechanismen, die die Zeitevolution dieser Systemen beeinflussen können.

In der Doktorarbeit fokussieren wir uns hauptsächlich auf die Studie von Problemen der Steuerbarkeit, Stabilität und optimalen Regelung für Multiagentensysteme anhand drei Modellen wie folgt: Das erste ist die Hegselmann- Krause opinion formation Modell. Die HK-Dynamik beschreibt die Änderung der Meinungen von einzelnen Personen aufgrund der Interaktionen mit den Anderen. Die Studie dieses Model fokussiert auf bestimmte Regelungen, um die Meinungen der Agenten zu betreiben, damit eine gewünschte Zustimmung erreicht wird. Das zweite Model ist das Heider social balance (HB) Modell. Die HB-Dynamik beschreibt die Evolution von Beziehungen in einem sozialen Netzwerk. Ein Ziel der Untersuchung dieses Systems ist die Konstruktion der Regelungsfunktion um die Beziehungen zu steuern, damit eine Freundschaft erreicht wird. Das dritte Modell ist ein Schar-Modell, das in biologischen Systemen beobachteten kollektive Bewegung beschreibt. Das Schar-Model unter Berücksichtigung beinhaltet Selbstantrieb, Friktion, Attraktion Repulsion und Anpassungsfähigkeiten. Wir untersuchen einen Regler für die Steuerung des Schar-Systems, um eine gewünschte Trajektorie zu verfolgen. Üblich wie alle dieser Systeme soll laut unsere Strategie ein Hauptagent, der sich mit alle anderen Mitgliedern des Systems interagieren, hinzugefügt werden und das Regelungsmechanismus inkludiert werden.

Unserer Regelung anhand dem Vorgehen mit Führungsverhalten ist unter Verwendung von klassischen theoretischen Regelungsmethode und ein Schema der modellprädiktiven Regelung entwickelt. Zur Ausführung der genannten Methode wird für jedes Modell die Stabilität der korrespondierenden Linearsystem in der Nähe von Konsensus untersucht. Ferner wird die lokale Regelbarkeit geprüft. Nur in dem Hegselmann-Krause opinion formation Modell. Der Regler wird so bestimmt, dass die Meinungen der Agenten gesteuert werden können. Dadurch konvergiert es global zu eine gewünschten Zustimmung. Die MPC-Vorgehensweise ist eine optimale Regelung Strategie, die auf numerische Optimierung basiert. Zu Verwendung des MPC-Shema werden die optimalen Regelungsproblemen für jedes Modell formuliert, wo sich die objektive Funktionen in Abhängigkeit von den gewünschten objective des Problems unterscheidet. Die erforderliche Optimalitätsbedingungen erster Ordnung für jedes Problem sind präsentiert. Außerdem für die numerische Prozess, eine Sequenz von offenen diskreten Optimalitätssystemen ist nach dem expliziten Runge-Kutta Schema

gelöst. In dem Optimierungsverfahren ist ein nicht linear konjugierter Gradientlöser umgesetzt. Schließlich sind numerische Experimenten in der Lage, die Eigenschaften der Multiagent-Modellen zu untersuchen und die Fähigkeiten der gezielten Regelstrategie zu beweisen. Die Strategie nutzt zu betreiben Multiagentensysteme, um einen gewünschten Konsensus zu erreichen und eine gegebene Trajektorie zu verfolgen.

Abstract

The investigation of interacting multi-agent models is a new field of mathematical research with application to the study of behavior in groups of animals or community of people. One interesting feature of multi-agent systems is collective behavior. From the mathematical point of view, one of the challenging issues considering with these dynamical models is development of control mechanisms that are able to influence the time evolution of these systems.

In this thesis, we focus on the study of controllability, stabilization and optimal control problems for multi-agent systems considering three models as follows: The first one is the Hegselmann Krause opinion formation (HK) model. The HK dynamics describes how individuals' opinions are changed by the interaction with others taking place in a bounded domain of confidence. The study of this model focuses on determining feedback controls in order to drive the agents' opinions to reach a desired agreement. The second model is the Heider social balance (HB) model. The HB dynamics explains the evolution of relationships in a social network. One purpose of studying this system is the construction of control function in oder to steer the relationship to reach a friendship state. The third model that we discuss is a flocking model describing collective motion observed in biological systems. The flocking model under consideration includes self-propelling, friction, attraction, repulsion, and alignment features. We investigate a control for steering the flocking system to track a desired trajectory. Common to all these systems is our strategy to add a leader agent that interacts with all other members of the system and includes the control mechanism.

Our control through leadership approach is developed using classical theoretical control methods and a model predictive control (MPC) scheme. To apply the former method, for each model the stability of the corresponding linearized system near consensus is investigated. Further, local controllability is examined. However, only in the Hegselmann-Krause opinion formation model, the feedback control is determined in order to steer agents' opinions to globally converge to a desired agreement. The MPC approach is an optimal control strategy based on numerical optimization. To apply the MPC scheme, optimal control problems for each model are formulated where the objective functions are different depending on the desired objective of the problem. The first-oder necessary optimality conditions for each problem are presented. Moreover for the numerical treatment, a sequence of open-loop discrete optimality systems is solved by accurate Runge-Kutta schemes, and in the optimization procedure, a nonlinear conjugate gradient solver is implemented. Finally, numerical experiments are performed to investigate the properties of the multi-agent models and demonstrate the ability of the proposed control strategies to drive multi-agent systems to attain a desired consensus and to track a given trajectory.

Contents

Chapter 1

Introduction

In recent years mathematical models of multiple interacting agents have been increasingly investigated. These models are inspired by systems observed in biology and life science, as for instance, collective motion of birds, school of fishes, and motion of group of animals, as well as of cells that are attracted by a chemical substance. Also human social behavior is intensively studied by means of multi-agent systems.

From the mathematical point of view, the dynamics of multi-agent systems poses a wealth of questions concerning stability, synchronization, and phase transition of the formed structures [37]. On the other hand, research on these systems essentially relies on computer simulation that requires the development of accurate discretization schemes and their analysis. In addition, in application there is the important issue of controlling these systems to attain given objectives, for example, a group of birds moving toward food sources, people making decision to vote a political party, etc. In many situations, only few individuals are aware of a given task and thus convergence to consensus of the whole group is relevant. For this propose, observation in nature and computer simulation suggest that a hierarchical group dynamics is fundamental for coherent control of multi-agent systems [66]. In particular, this hierarchical leadership concept is discussed in [3, 13, 16, 33, 39, 75, 82, 83], where an external leader is considered that interacts with all member agents giving rise to aggregation states and convergence towards consensus.

This thesis contributes to the mathematical investigation of multiple agent systems focusing on the modeling of a new control mechanism based on hierarchical leadership in the sense that the control function does not apply directly to all agents but indirectly through the interaction with a controlling leader. In particular, we aim at studying the stabilization, controllability, and optimal control problems with multi-agent dynamical systems based on leadership.

The main focus of this work is to investigate control strategies for three representative multi-agent models outlined as follows:
The first model that we consider is the opinion formation model known as the

Hegselmann-Krause (HK) model where the evolution of the opinion depends on interactions among the agents taking place in a bounded domain of confidence; see [51]. We consider the HK model with leadership where the control function is implemented on the leader dynamics. We develop a feedback control to globally achieve the consensus and then discuss local controllability. Moreover, we investigate an optimal control problem governed by the HK model with given objectives.

The second multi-agent model that we consider is the Heider social balance (HB) model describing the dynamics of social balance. The key concept of the social balance according to the Heider theory is defined based on the relation of triads of people represented as graphs, where each node represents an individual and edge connecting two people represents their social relation. To each edge, a value corresponds to friendship or hostility: positive values represent a friendly relationship, while, a negative value corresponds to a conflicting relation. Our purpose is to investigate an optimal control strategy for the continuous time Heider balance model proposed in [55]. For the control strategy, an additional 'reference' agent enters in the network with a connection to all people of the network. This agent acts on the network by modifying the values of the edges that connect to it with the purpose to attain a desired objective. However, in this case, the control functions represent the values of the edges connecting to the reference agent, while in the HK model the control is implemented in the leader agent.

The third multi-agent model that we investigate is a refined flocking model that includes self-propelling, friction, short-range repulsion, long-range attraction, and alignment features. This model draws primary references on [8, 9, 27, 56, 58, 78], that have been continuously refined by numerous researchers by introducing additional interaction forces to explain different observed behaviors in real multi-agent systems; see [1, 24, 25, 64]. On the other hand, the presence of a leader in flocking has been considered in, e.g., [3, 33, 75]. Based on a refined flocking model, we develop an optimal control scheme where the control mechanism is implemented on the leader of the flock and the control action applies to all agents through the mutual interaction mechanism. The purpose of constructing the control strategy is to steer the evolution of flocking to converge to group pattern or track a desired trajectory.

Summarizing, the main purpose of this thesis is to model and validate a new implementable and effective control strategy that accommodates model nonlinearities and different optimization objectives for multi-agent systems that include most of the recently proposed interaction mechanisms.

This thesis consists of three main parts. In the first part, we discuss the control strategies in order to steer the system to attain consensus for multi-agent systems focusing on HK, HB, and flocking models that can be put in the following general

control affine form,

$$\dot{\mathbf{x}} = \mathbf{f}(\mathbf{x}) + \sum_{i=1}^{nc} g_i(\mathbf{x}) u_i, \tag{1.1}$$

where $\mathbf{x}$ is state of the system. The control variable u_i represents an external input that is able to influence the evolution of the state variable. The vector field $\mathbf{f}(\mathbf{x})$ describes the free dynamics. The vector fields $g_1(\mathbf{x}), \ldots, g_{nc}(\mathbf{x})$ are the control vector fields. However, in our study the vector field $g_i(\mathbf{x})$ are constant. Therefore, the system (1.1) can be simplified by introducing a control matrix, say $\mathbf{B}$. The system (1.1) can be written as follows

$$\dot{\mathbf{x}} = \mathbf{f}(\mathbf{x}) + \mathbf{B}\mathbf{u}. \tag{1.2}$$

Additional issues like stability, controllability are also considered in this part.

In the second part, we consider the formulation of optimal control problems for the multi-agent systems. A control can be required to achieve a target configuration and to follow a desired trajectory. This optimal control problem can be formulated as follows

$$\begin{aligned} \min_{\mathbf{x},\mathbf{u}} \quad J(\mathbf{x},\mathbf{u}) &:= \frac{1}{2}\|\mathbf{x}(T) - \mathbf{x}_{des}(T)\|^2 + \int_0^T l(\mathbf{x})dt + \frac{\nu}{2}\|\mathbf{u}(t)\|^2_{L^2}, \quad (1.3)\\ \text{subject to} \quad \dot{\mathbf{x}} &= \mathbf{f}(\mathbf{x}) + \mathbf{B}\mathbf{u}(t), \quad t \in [0,T],\\ \mathbf{x} \in H^1((0,T);\mathbb{R}^{nx}), &\qquad \mathbf{u} \in \mathbb{U} = L^2((0,T);\mathbb{R}^{nc}). \end{aligned}$$

We consider a tracking functional of the agents' trajectories that includes the cost of the control function. The first tracking term in (1.3) measures the tracking error to the given configuration with respect to a desired target position. The second term of the objective functional, $l(\mathbf{x})$ represents a functional of trajectory. The resulting optimization problem with a differential constraint given by the multi-agent model is solved using the adjoint method where the solution to the optimal control problem is characterized by the solution of the optimality system that consists of the multi-agent model, the related adjoint equations, and an optimality condition.

The third part of this thesis is dedicated to numerical analysis of optimal control problem. The multi-agent optimality system is discretized with a Runge-Kutta scheme that is appropriate to compute an accurate gradient required in the implementation of an efficient conjugate gradient solution process [47, 50, 49]. We remark that this solution process solves an open-loop control problem in a finite time horizon. In order to construct a closed-loop control procedure, we consider a sequence of open-loop control problems on subsequent time intervals such that the final state of the multi-agent system at the end of one interval represents the initial state for the next interval.

Specifically, we implement an instance of the model predictive control (MPC) strategy [44, 62].

This thesis is organized as follows:
In **Chapter 2**, we provide an overview of multi-agent models that is central to the study in this thesis. Specifically, we illustrate Hegselmann-Krause opinion formation (HK) model in Section 2.1. We discuss the Heider social balance (HB) model in Section 2.2. In Section 2.3, we discuss a new flocking model that includes self-propelling, friction, attraction and repulsion, alignment features, and the presence of a leader. The main focus on this chapter is to present a description of multi-agent models together with theoretical concepts corresponding to the existence of solutions of these systems. Moreover, results of numerical simulation of each model are shown to investigate the behavior of the model and considering different ranges of values of the parameters that characterize the model.

In **Chapter 3**, we start with a discussion of essential concepts of controllability and stabilization for the general system (1.2), which are used in this thesis. In Section 3.2, we formulate a control problem for the HK model and a feedback control function is developed for purpose of global stabilization which is the main result of this chapter as seen in Theorem 7. Further, local controllability is investigated. In Section 3.3, we discuss local stability of a linearized HB system and then local controllability of the HB model is examined. In the last section of this chapter, we discuss the stability of flocking model. In particular, consensus in collective motions is investigated. This section is completed by investigating local controllability of our refined flocking model.

In **Chapter 4**, an optimal control of multi-agent systems is formulated. We discuss theoretical issues regarding existence of optimal controls and corresponding first-order necessary optimality systems, which are the main results of this chapter. In particular, the existence of an optimal control is proved in Theorem 8 and the corresponding first-order necessary optimality system is proved in Theorem 9. Optimal control problems for HK, HB, and our flocking models are discussed in Section 4.2, Section 4.3, and Section 4.4, respectively. Corresponding to different models, different objective functionals are considered. Existence of minimizers and first-order necessary conditions are derived by using the theoretical results proved in Section 4.1.

In **Chapter 5**, we discuss two main numerical issues. In Section 5.1, a Runge-Kutta discretization scheme is investigated that guarantees a high-order accuracy of the numerical solution to the optimality system. In Section 5.2, we discuss a model predictive control strategy and a nonlinear conjugate gradient optimization procedure.

In **Chapter 6**, results of numerical experiments are presented to validate the effectiveness of the leader-based control strategy. In Section 6.1, we start illustrating the numerical results of the HK system with a leader and global stabilizing feedback

control. Further, numerical solution obtained from MPC is presented. In Section 6.2, numerical results of optimal control problems for the HB model are illustrated. In Section 6.3, we present results of numerical experiments for a refined flocking model. An appendix with frequently used results is included in this thesis. A section of conclusion completes this thesis.

Parts of the results discussed in this thesis can be found in the following publications

1. Alfio Borzì and Suttida Wongkaew. *Modeling and control through leadership of a refined flocking system*, Mathematical Models and Methods in Applied Sciences, 25.02, (2015): 255-282.

2. Suttida Wongkaew, Marco Caponigro, and Alfio Borzì. *On the control through leadership of the Hegselmann Krause opinion formation model*, Mathematical Models and Methods in Applied Sciences, 25.03, (2015): 565-585.

3. Suttida Wongkaew, Marco Caponigro, Krzysztof Kułakowski and Alfio Borzì. *On the control of the Heider balance model*, accepted to the European Physical Journal Special Topics (EPJ-ST).

Chapter 2

Multi-agent models

In recent years, there has been a growing interest in the understanding and modeling of multi-agent systems that are observed in biology, ecology, physics, social sciences, and other occurrences of evolution systems; see, e.g., [10, 71] for reviews, and see [10, 14, 18, 34, 35, 40, 57, 73, 85] for specific examples of multi-agent systems. Furthermore, the investigation on multi-agent models has boosted recent technological developments in the construction of multi-agent systems as communication networks and swarming robots [61, 79]. These systems play an important role in the understanding of many natural collective phenomena that result from basic agent-to-agent interaction rules; see [23, 37] and references therein. A study of a set of agents interacting with a continuum can be seen in reference [31].

In this chapter, we introduce representative multi-agent models that are the focus of this thesis. In Section 2.1, we consider a model of opinion formation. Next, in Section 2.2 a nonlinear dynamic of social balance focused on Heider theory is discussed. For both models the problem of steering a group of agents to a desired common state by exploiting a leader is addressed in the next chapter. In Section 2.3, we give an overview of collective models and formulate a new feature of the flocking model that includes self-propelling, friction, attraction, repulsion and alignment features and specially the presence of a leader.

2.1 The Hegselmann-Krause opinion formation model

The fact that social networks have significant effect on people behavior and on their opinions motives the investigation of the dynamics of using mathematical models; see [11, 12, 67]. In general, systems describing a great variety of network-structured phenomena stem from agent-based models as seen in [12, 13, 14, 18, 20, 21]. In particular, one of the most representative classes of agent-based models explaining phenomena in social sciences is the class of the opinion formation models; see, e.g., [38, 51, 77] and [2, 11, 39, 59, 60, 82] for further developments.

In this thesis, we focus on the Hegselmann-Krause (HK) model [51] where the evolution of the opinion depends on interactions among agents taking place in a bounded domain of confidence. In this model, the system of N interacting agents whose opinions are located in $\mathbb{R}^d$ is given by

$$\dot{x}_b^{\text{of}}(t) = \sum_{\substack{j=1 \\ j\neq b}}^{N} a_{bj}(x_j^{\text{of}}(t) - x_b^{\text{of}}(t)), \qquad \text{for} \quad b = 1, ..., N, \tag{2.1}$$

with given initial positions $x_b^{\text{of}}(0) \in \mathbb{R}^d$, for $b = 1, \ldots, N$. The state of the system, representing the agents' opinions is denoted by $\mathbf{x}^{\text{of}} = (x_1^{\text{of}}, ..., x_N^{\text{of}}) \in \mathbb{R}^{dN}$.

In the dynamics (2.1), $\sum_{j=1}^{N} a_{bj}(x_b^{\text{of}} - x_j^{\text{of}})$ is the weighted value of confidence. The key idea of the HK model is that each agent updates his opinion by averaging the opinions of his neighborhoods with the following factor

$$a_{bj} = a(\|x_b^{\text{of}}(t) - x_j^{\text{of}}(t)\|),$$

given by a function $a(\rho) : [0, \infty) \to [0, 1]$ of the distance ρ between the position of his opinions and representing the interaction rate dependence on the limited confidence domain. The function $a = a(\rho)$ is given by the following smooth-cutoff function

$$a(\rho) = a(\rho; \delta, \varepsilon) := \begin{cases} 1, & 0 \leq \rho \leq \delta, \\ \varphi(\rho), & \delta < \rho < (\delta + \varepsilon), \\ 0, & (\delta + \varepsilon) \leq \rho, \end{cases} \tag{2.2}$$

where δ is the bounded confidence distance and the function

$$\varphi(\rho) : [\delta, \delta + \varepsilon] \to [0, 1], \quad \varphi(\delta) = 1, \quad \varphi(\delta + \varepsilon) = 0, \tag{2.3}$$

is a decreasing smooth function, and $\varepsilon > 0$ is a parameter of the HK model that defines the width of the region where the cutoff function decays to zero. An example of smooth-cutoff function is given as follows

Example 1. *The smooth-cutoff function for the HK model is given by*

$$a(\rho) = a(\rho; \delta, \varepsilon) = \begin{cases} 1, & 0 \leq \rho \leq \delta, \\ \frac{1}{2} + \frac{1}{2}\tanh\left(\frac{1}{\rho-\delta} + \frac{1}{\rho-(\delta+\varepsilon)}\right), & \delta < \rho < (\delta + \varepsilon), \\ 0, & (\delta + \varepsilon) \leq \rho. \end{cases}$$

where ρ is the distance between position of agent's opinion and δ is the confidence interval.

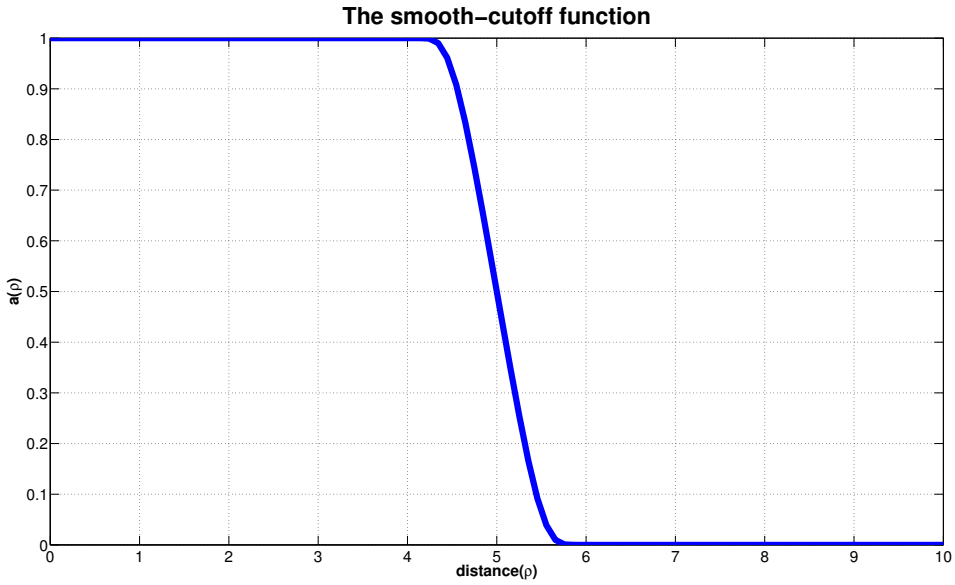

Figure 2.1: An example of the smooth-cutoff function with $\delta = 4$ and $\varepsilon = 2$.

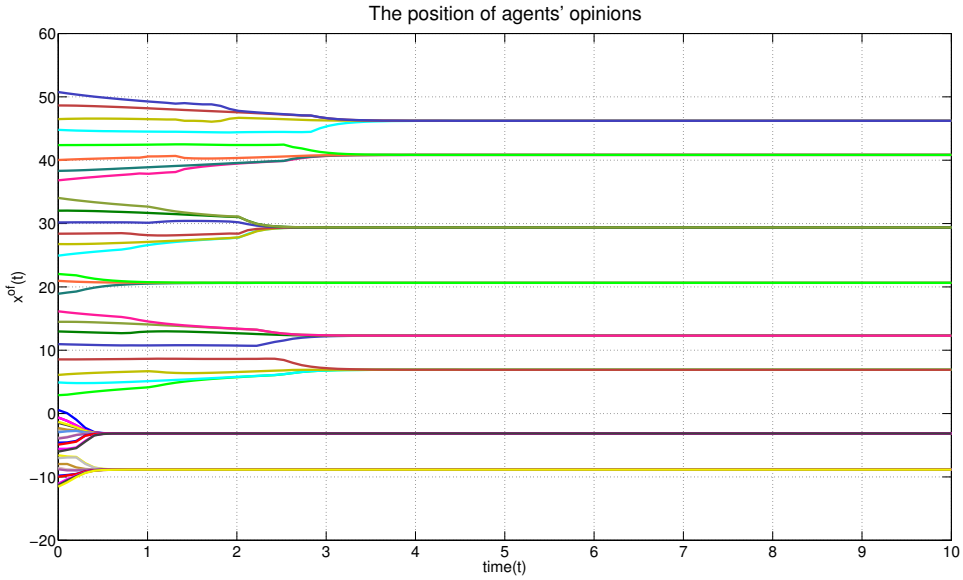

Figure 2.2: Numerical results with the opinion formation model with 50 interacting agents; $\delta = 2.5$ and $\varepsilon = 0.05$.

In Figure (2.2) we plot the time evolution of the HK model for given initial values $x_b^{\text{of}}(0)$, $b = 1, \ldots, N$, and we have δ is confident interval. The opinions $x_b^{\text{of}}(t), b = 1, \ldots, N$, converge to some limit opinion configuration, $x_b^{\text{of}*}$ in finite time, that is, for each agent b, there exists time $t_b > 0$ such that

$$x_b^{\text{of}}(t) = x_b^{\text{of}*}, \quad \forall t \geq t_b.$$

In the following, we introduce the control of the HK model where the control mechanism is implemented on the dynamics of the leader. The equations are governed by the following,

$$\begin{aligned} \dot{x}_0^{\text{of}}(t) &= u^{\text{of}}(t), \qquad (2.4) \\ \dot{x}_b^{\text{of}}(t) &= \sum_{j=1}^{N} a_{bj}(x_j^{\text{of}}(t) - x_b^{\text{of}}(t)) + c_b(x_0^{\text{of}}(t) - x_b^{\text{of}}(t)), \qquad \text{for} \quad b = 1, ..., N, \end{aligned}$$

with given initial positions $x_i^{\text{of}}(0) \in \mathbb{R}^d$, for $i = 0, 1, \ldots, N$. The state of the system, representing the agents' and the leader's opinions is $\mathbf{x}^{\text{of}} = (x_0^{\text{of}}, x_1^{\text{of}}, ..., x_N^{\text{of}}) \in (\mathbb{R}^d)^{N+1}$. We denote the leader by the index 0 and with the index $b = 1, \ldots, N$, we denote the N agents. The control $u^{\text{of}}(t)$ is a measurable function and belongs to the following set,

$$\mathbb{U}^{\text{of}} = \{u^{\text{of}} \in L^\infty([0, T]; \mathbb{R}^d) : \|u^{\text{of}}\|_\infty \leq M\}.$$

The first term in the dynamics (2.4), $\sum_{j=1}^{N} a_{bj}(x_b^{\text{of}} - x_j^{\text{of}})$ comes from the original HK model defined in (2.2). The second term in the dynamics (2.4) models the action of the leader on the b-th agent. A leader can be defined as one agent with a high level of confidence and self-esteem, that has the ability to withstand criticism, so that its dynamics is not influenced by the other agents' opinions. The influence of the opinion of the leader on the group opinion in decision making is given by the term $c_b(x_0^{\text{of}}(t) - x_b^{\text{of}}(t))$. The parameter

$$c_b := \gamma\phi(\|x_b^{\text{of}} - x_0^{\text{of}}\|), \qquad (2.5)$$

represents the rate of relationship between the leader and other agents, where $\phi : [0, \infty) \to (0, 1]$ is a smooth non-increasing positive function such that $\phi(0) = 1$ and $\lim_{d\to\infty} \phi(d) = 0$, and where the strength of the opinion leader is represented by the parameter $\gamma > 0$. In other words the leader has the ability to influence every agent with a factor that is inversely proportional to its distance from the agent.

2.2 The Heider social balance model

The social balance theory proposed by F. Heider [52, 53] attempts to model how people develop their relationships with other people and with objects in their environment based on a cognitive consistency motive that drives toward psychological balance. This motive urges to maintain one's values and beliefs over time resulting

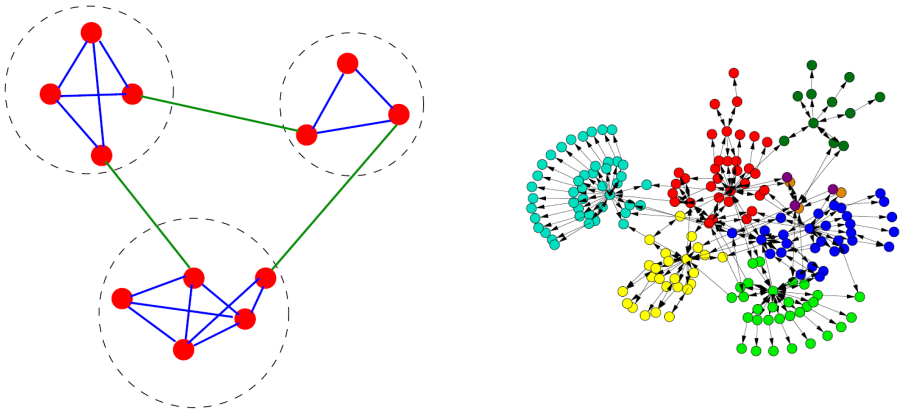

(a) A simple graph with three communities

(b) Community structure in technological networks

Figure 2.3: Figure(a) and Figure(b) show a social network and community structure in technological networks, respectively, [42].

in the preference to have a balanced state where the affect valence in the system multiplies out to a positive result. Specifically, in the relation of three people, balance state occurs when all sign multiplication of sentiment relations is positive. In this way, balance state will occur when there are sentiment relations with signs all positive or two negatives and one positive. We refer to sentiment relation between two people as a linking edge to which a positive value is associated in the case of friendship or otherwise a negative value in the case of hostility.

In a system of many people, the concept of social balance is related to the balance of each triad consisting of friendly and hostile edges. The resulting system can be investigated in the framework of network dynamics by using mathematical modeling based on agent-based simulation and in the framework of graph theory where nodes represent individuals and their links represent relationships; see [4, 5, 6, 63, 69] for a partial list of references on these approaches.

From a mathematical point of view, it is certainly advantageous to consider the continuous time Heider balance system [55]. In fact, in this case powerful tools for the investigation of the dynamics of this system can be applied; we refer to [55, 63] for some fundamental results and to [5, 6, 63, 83] for further development and applications.

The Heider social balance (HB) model involving N agents is proposed in [55]. This model is as follows

$$\dot{x}_{ij}^{\text{hb}} = c(x_{ij}^{\text{hb}}(t); R) \sum_{\substack{k=1 \\ k\neq i,j}}^{N} x_{ik}^{\text{hb}} x_{kj}^{\text{hb}}, \quad \text{for} \quad i,j = 1,...,N, \text{ and } \quad i \neq j, \tag{2.6}$$

with given initial conditions $x_{ij}^{\text{hb}}(t_0) = x_{0,ij}^{\text{hb}}$, and the indices i, j represent individuals in the network and $x_{ij}^{\text{hb}} \in \mathbb{R}$ denotes the relationship between the agents i and j. A positive value of x_{ij}^{hb} represents friendship; conversely, a negative value of x_{ij}^{hb} expresses hostility. We have

$$\text{sign}(x_{ij}^{\text{hb}}) := \begin{cases} 1, & \text{if i and j are friends,} \\ 0, & \text{if i and j have no relationship,} \\ -1, & \text{if i and j are enemies.} \end{cases} \tag{2.7}$$

We notice that in the dynamics given by (2.6), $x_{ii}^{\text{hb}} = 0$ and we assume that each agent is connected to all agents in the network, that is, the social structure can be seen as fully connected graph, and $x_{ij}^{\text{hb}} = x_{ji}^{\text{hb}}$ for any i and j.

The function $c : \mathbb{R} \to \mathbb{R}$ in (2.6) is defined as follows

$$c(x_{ij}^{\text{hb}}; R) = \frac{1}{N-2}\left(1 - \frac{(x_{ij}^{\text{hb}})^2}{R^2}\right), \quad R > 0. \tag{2.8}$$

A value $c(x_{ij}^{\text{hb}}; R) := c_{ij}$ is added to system for sake of avoiding the difficulty in numerical simulation. Without this term the value x_{ij}^{hb} would diverge much faster than others and leads the system to unbounded state.

Notice that in a fully connected network with N nodes, the total number of relations N_r and triads of relations $N_\triangle$ are given by

$$\begin{aligned} N_r &= \frac{N(N-1)}{2}, \\ N_\triangle &= \frac{N(N-1)(N-2)}{6}, \end{aligned} \tag{2.9}$$

respectively. In the following, we present the control of the HB model where the controlling agent is linked to all agents of the network. The resulting system of relationship of N interacting agents together with one reference agent is governed by the following set of differential equations

$$\begin{aligned} \dot{x}_{0i}^{\text{hb}}(t) &= u_i^{\text{hb}}(t) \\ \dot{x}_{ij}^{\text{hb}}(t) &= \frac{1}{N-2}\left(1 - \frac{(x_{ij}^{\text{hb}})^2}{R^2}\right) \sum_{\substack{k=1 \\ k\neq i,j}}^{N} x_{ik}^{\text{hb}} x_{kj}^{\text{hb}} + \gamma x_{0i}^{\text{hb}} x_{0j}^{\text{hb}}, \quad \text{for} \quad i,j = 1,...,N, \end{aligned} \tag{2.10}$$

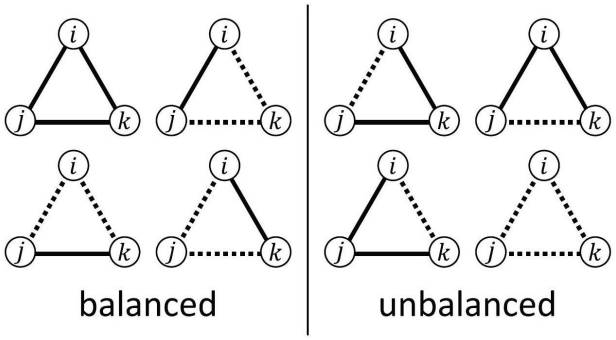

Figure 2.4: Balanced and unbalanced state of triads with full and dash lines represent friend and hostility, respectively, [69]

with given initial relationships $x_{ij}^{\text{hb}}(t_0) = x_{ij}^{\text{hb}}(0)$. The index 0 denotes the leader, and the index i denotes the i-th people in the network. The variables x_{0i}^{hb}, $i = 1, ..., N$, denote the relationships between leader and the other people, while the x_{ij}^{hb} represent the relationships between people in the community. The function $u_i^{\text{hb}}(t) \in L^2([0,T], \mathbb{R})$ represents the control and the parameter $\gamma > 0$ is added in order to avoid divergence of states. We notice that the model (2.10) now has $N_r = \dfrac{(N+1)N}{2}$ equations, whereas $N_c = N$ equations are related to the controlling links. Denote with $N_{uc} = N_r - N_c$.

2.3 Flocking models

Flocking models are well-known multi-agent models describing the collective behavior of a large aggregation of animals. The motion of the individuals in the group is the consequence of two natural behaviors. On the one hand, animals desire to stay close to the group. On the other hand, when they stay too close, they try to keep distance in order to avoid collision with other individuals. Reynolds observed these behaviors and developed the collective motion consisting of three fundamental characteristics of collective motion known as cohesion, separation, and alignment rules.

1. **Cohesion**: An agent attempts to stay close to others in the group,
2. **Separation**: Agents avoid collisions with neighbors,
3. **Alignment**: Each agent attempts to match its velocity with others.

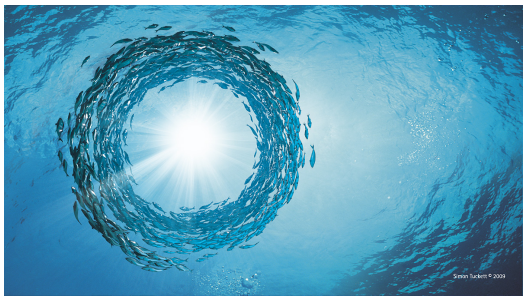

(a) A school of fishes

(b) A flock of birds

Figure 2.5: Collective motion observed in nature. Figure(a) shows mills in school of fishes. This picture is form [http://kanso.usc.edu/]. Figure(b) illustrates the flock of birds. This picture was taken by Christoffer A Rasmussen on 26 September 2007.

Recently, there has been a surge of interest in mathematical models of flocking systems based mainly on these three fundamental forces. These forces become predominant each on a different region, in other words, there are three fundamental regions of influence as follows:

Regions of influences,

1. **The repulsion region** this region is characterized by the tendency of an agent of moving apart from another agent within a certain distance in order to avoid collision.

2. **The alignment region** the agent tries to identify the possible direction of the group and matches its velocity with that of other individuals in the group.

3. **The attraction region** this is the outer region which models the influence of inherent socialization in agents. That is, when an agent feels itself too far apart from the group, it will try to join the group.

A three-zone model corresponding to these regions of influence contains three interaction mechanisms: short-range repulsion, alignment, and long-range attraction. This model draws primary references on [8, 9, 27, 56, 58, 78], and further continues refinement by numerous researchers by introducing additional interaction forces to explain different observed behaviors from real multi-agent systems in nature; see [1, 25, 24, 64].

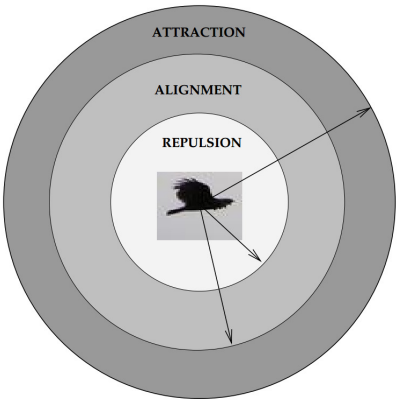

Figure 2.6: Regions of influences, Ref. [23]

Next, we present a brief description of a representative flocking model starting with self-propelling and friction mechanisms.

2.3.1 A self-propelling and friction model

Consider a group of agents with the following equations of motion

$$\begin{aligned} \dot{x}_b^{\mathrm{fm}} &= v_b^{\mathrm{fm}}, \\ \dot{v}_b^{\mathrm{fm}} &= (\alpha - \beta\|v_b^{\mathrm{fm}}\|^2)v_b^{\mathrm{fm}} + M_b, \qquad \text{for} \quad b = 1, ..., N. \end{aligned} \tag{2.11}$$

where $x_b^{\mathrm{fm}}, v_b^{\mathrm{fm}} \in \mathbb{R}^d$ represent the position and velocity of b-th agent, for $b = 1, ..., N$, where d is the space dimension. The notations $\dot{x}_b^{\mathrm{fm}}$ and $\dot{v}_b^{\mathrm{fm}}$ represent the derivatives of x_b^{fm} and v_b^{fm} with respect to time t. The index b stands for the b-th agent of the flocking system.

The term $(\alpha - \beta\|v_b^{\mathrm{fm}}\|^2)v_b^{\mathrm{fm}}$ represents self-propelling and friction force. A notation $\|\cdot\|$ stands for the Euclidean norm. The parameter $\alpha > 0$ models self-propulsion of agents, whereas the parameter $\beta > 0$ corresponds to the presence of friction given by Rayleigh's law. In the case that only the term $(\alpha - \beta\|v_b^{\mathrm{fm}}\|^2)v_b^{\mathrm{fm}}$ appears as a force acting to the system, then the motion of the agent develops towards a balance of the propelling and friction forces such that the asymptotic speed of each agent takes the value $\|v\| = \sqrt{\frac{\alpha}{\beta}}$, independently of the orientation.

The force $M_b : (\mathbb{R}^d)^N \to \mathbb{R}^d$ represents short-range and long-range interaction between agents. This force draws primarily on the work [37] and is given as follows

$$M_b = -\frac{1}{N}\sum_{j \neq b} \nabla_{x_b^{\mathrm{fm}}} U(\|x_b^{\mathrm{fm}} - x_j^{\mathrm{fm}}\|), \qquad \text{for} \quad b = 1, ..., N, \tag{2.12}$$

where $\nabla_x U(\|x-y\|)$ denotes the gradient of U with respect to x. The function $U : \mathbb{R}^d \times \mathbb{R}^d \to \mathbb{R}$ represents the following Morse potential

$$U_{bj} := U(\rho_{bj}) = -C_a e^{\frac{-\rho_{bj}}{l_a}} + C_r e^{\frac{-\rho_{bj}}{l_r}}, \tag{2.13}$$

where $\rho_{bj} = \|x_b^{\text{fm}} - x_j^{\text{fm}}\|$ is the Euclidean distance between the b-th agent and the j-th agent, the coefficients C_a and C_r define the attractive and repulsive strengths, respectively, and l_a, l_r are attractive and repulsive length scales, respectively.
The derivative of the Morse potential is evaluated as follows

$$\begin{aligned}
\sum_{j\neq b} \nabla_{x_b^{\text{fm}}} U(\rho_{bj}) &= \sum_{j\neq b} \nabla_{x_b^{\text{fm}}} \left(-C_a e^{\frac{-\rho_{ij}}{l_a}} + C_r e^{\frac{-\rho_{bj}}{l_r}} \right) \\
&= \sum_{j\neq b} \left(\frac{x_b^{\text{fm}} - x_j^{\text{fm}}}{\rho_{bj}} \right) \frac{\partial}{\partial \rho_{ij}} \left(-C_a e^{\frac{-\rho_{bj}}{l_a}} + C_r e^{\frac{-\rho_{bj}}{l_r}} \right) \\
&= \sum_{j\neq b} \left(\frac{x_b^{\text{fm}} - x_j^{\text{fm}}}{\rho_{bj}} \right) \left(\frac{C_a}{l_a} e^{\frac{-\rho_{bj}}{l_a}} - \frac{C_r}{l_r} e^{\frac{-\rho_{bj}}{l_r}} \right).
\end{aligned}$$

In the case of Morse potential, the patterns of aggregation depend on the values of the coefficients $C = C_r/C_a$ and $l = l_r/l_a$. The different behaviors of flocking observed in two dimensions are classified by using the concepts of H-stability phase diagram [37] corresponding to the choice of coefficients C and l. We have four cases discussed below.

1. $C_r > C_a$ and $l_r > l_a$.
   In this case, repulsion has greater magnitude than attraction. This means that repulsive force dominates and leads to the fact that agents are repelled from others at all distances. As a consequence, a social aggregate would not exist.

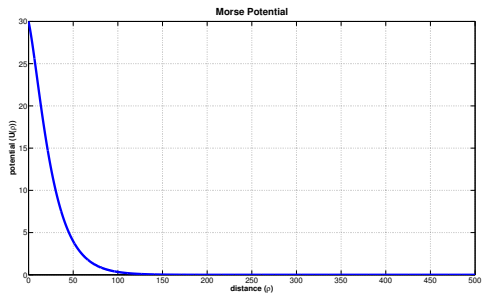

(a) Potential Function

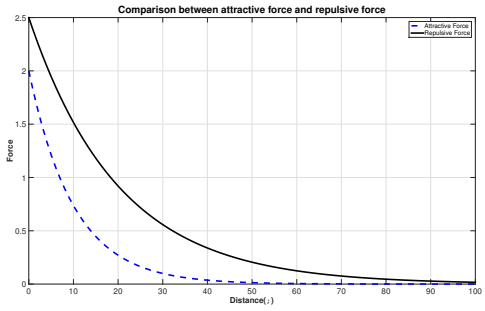

(b) Attractive and repulsive force

Figure 2.7: Figure(a) depicts a Morse potential function with $C_r = 50, C_a = 20, l_r = 20$ and $l_a = 10$. Figure(b) shows comparison between attractive and repulsive forces where dash and full lines represent attractive and repulsive force, respectively.

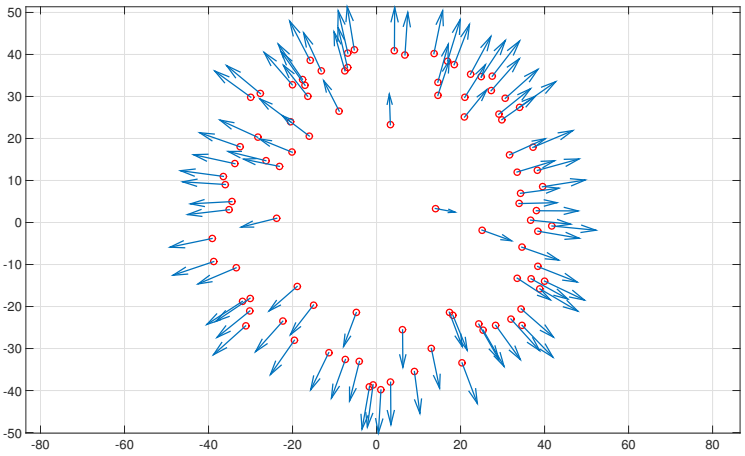

Figure 2.8: Motion representing with the choice $C_r > C_a$ and $l_r > l_a$.

2. $C_r < C_a$ **and** $l_r > l_a$
   It can be seen that attraction dominates close to the origin, conversely, repulsive force dominates at large distance. Consequently, agent would either flee away from each other or collapse to a point.

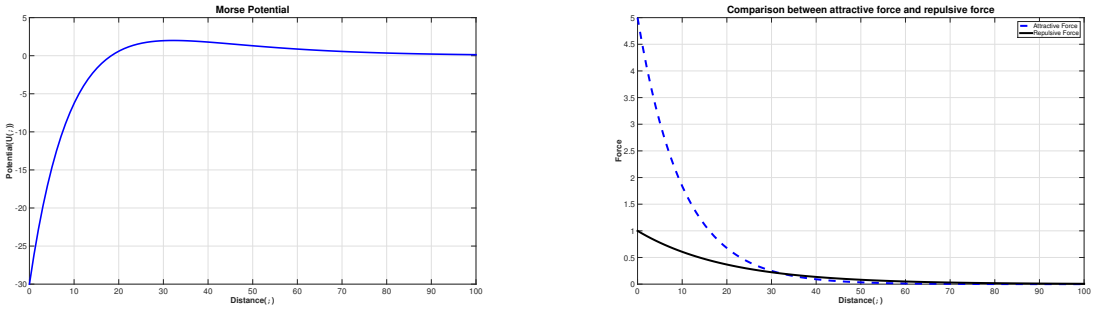

(a) Potential Function

(b) Attractive and repulsive force

Figure 2.9: Figure(a) shows a Morse potential function with $C_r = 20, C_a = 50, l_r = 20$ and $l_a = 10$. Figure(b) shows comparison between attractive and repulsive force where dash and full lines represent attractive and repulsive force, respectively.

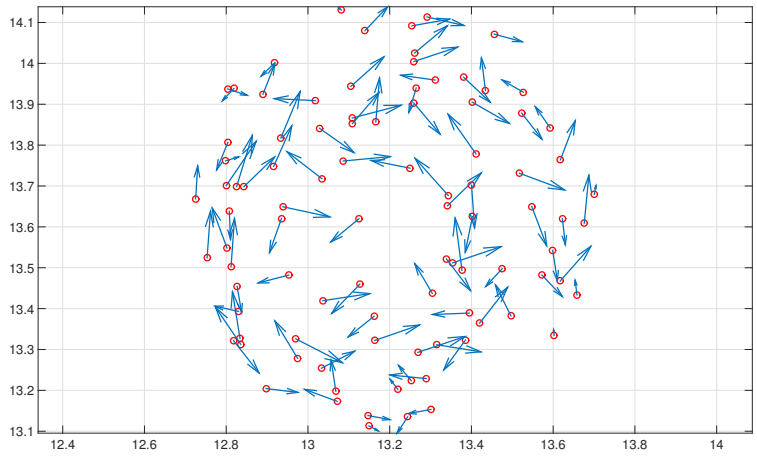

Figure 2.10: Motion representing with the choice $C_r < C_a$ and $l_r > l_a$.

3. $C_r < C_a$ **and** $l_r < l_a$
   In this case attraction is always stronger that repulsion. Therefore, agents always get closer to each other. Thus, we expect that the equilibrium state to be a tight cluster.

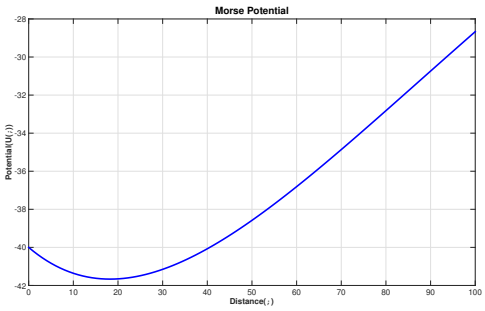

(a) Potential Function

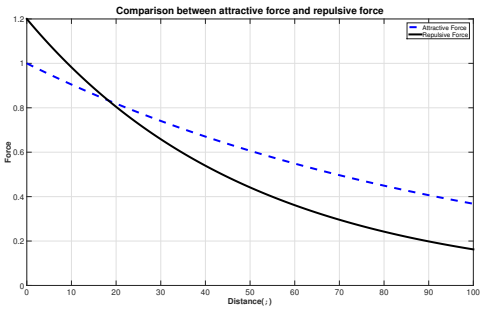

(b) Attractive and repulsive force

Figure 2.11: Figure(a) shows a Morse potential function with $C_r = 60, C_a = 100, l_r = 50$ and $l_a = 100$. Figure(b) shows comparison between attractive and repulsive force where dash and full lines represent attractive and repulsive forces, respectively.

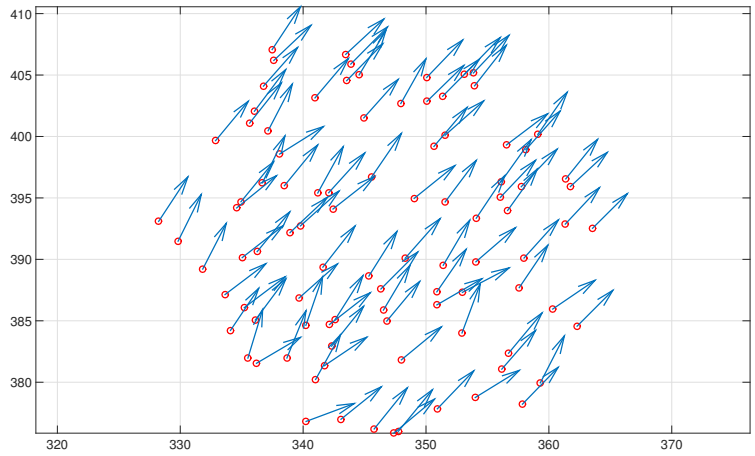

Figure 2.12: Motion representing with the choice $C_r < C_a$ and $l_r < l_a$.

4. $C_r > C_a$ **and** $l_r < l_a$
   This case results in short-range repulsion and long-range attraction. It is the most interesting case since short-range repulsion and long-range attraction are biologically relevant. Here, the potential has a global minimum and an equilibrium spacing (d_{min}) between two agents exists; therefore, the pattern of aggregation is formed.

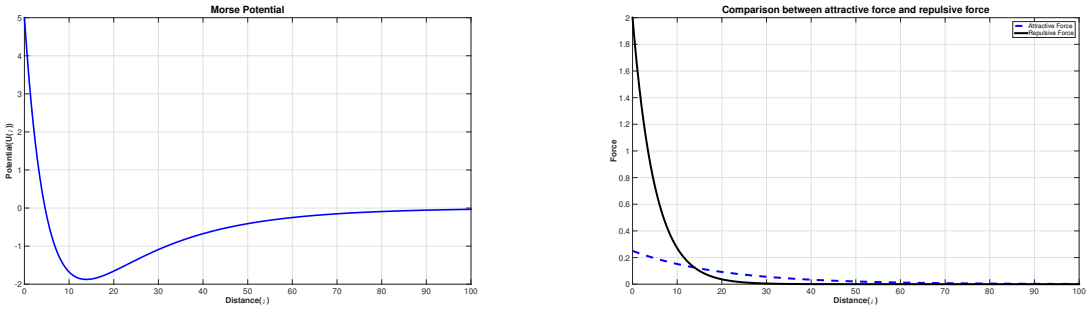

(a) Potential Function

(b) Attractive and repulsive force

Figure 2.13: Figure(a) shows a Morse potential function with $C_r = 10, C_a = 5, l_r = 5$ and $l_a = 20$. Figure(b) shows comparison between attractive and repulsive force where dash and full lines represent attractive and repulsive forces, respectively.

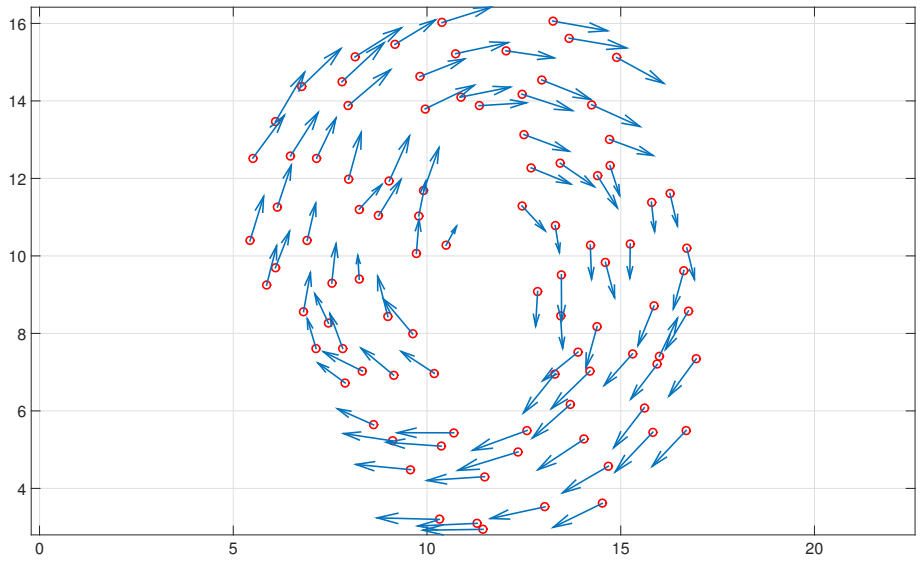

Figure 2.14: Motion representing with the choice $C_r > C_a$ and $l_r < l_a$.

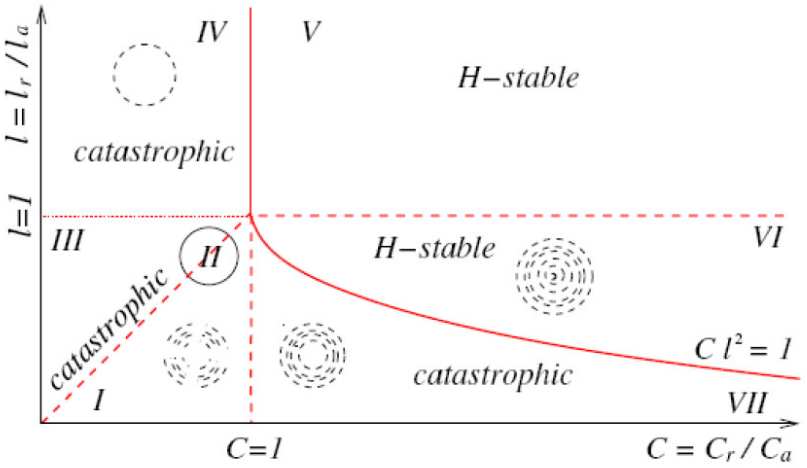

Figure 2.15: Classification of different regions of collective motion of (2.11), [37].

It can be seen in the stability diagram given in Figure 2.15 that regions are divided into two main parts. On the one hand, H-stable regions corresponding to parameters C and l where $Cl^d > 1$ are placed in region V and VI. In region V, the potential function has no local minimum at finite inter-agent distance. It is the case of net repulsive behavior and cohesive group structure is not observed. In regions VI, we find

the most interesting dynamics since short-range repulsion and long-range attraction are obtained. On the other hand, H-unstable or catastrophic region is related to $Cl^d < 1$. In this case, when agents stay initially well separated, then they tend to move rotationally with constant speed $\|v\| = \dfrac{\alpha}{\beta}$. Further, single or double mills are observed.

2.3.2 The Cucker-Smale model

The Cucker -Smale model (CS) concerns the orientation of the agents' velocities [35, 36]. It is the extension of the three-zone model. The key idea of this model stems from the observation that each agent adjusts its velocity based on a weighted average of the relative velocities of the other agents in the flock. The CS system has the following structure

$$\begin{aligned} \dot{x}_b^{\mathrm{fm}} &= v_b^{\mathrm{fm}}, \\ \dot{v}_b^{\mathrm{fm}} &= \frac{1}{N}\sum_{j=1}^{N} K(\|x_b^{\mathrm{fm}} - x_j^{\mathrm{fm}}\|)(v_j^{\mathrm{fm}} - v_b^{\mathrm{fm}}), \quad \text{for} \quad b = 1, ..., N, \end{aligned}$$

where $K(y) = \dfrac{\gamma}{(\alpha^2 + y^2)^\sigma}$ is a connectivity function depending on the distance between agents and parameters γ, α, and $\sigma \geq 0$.

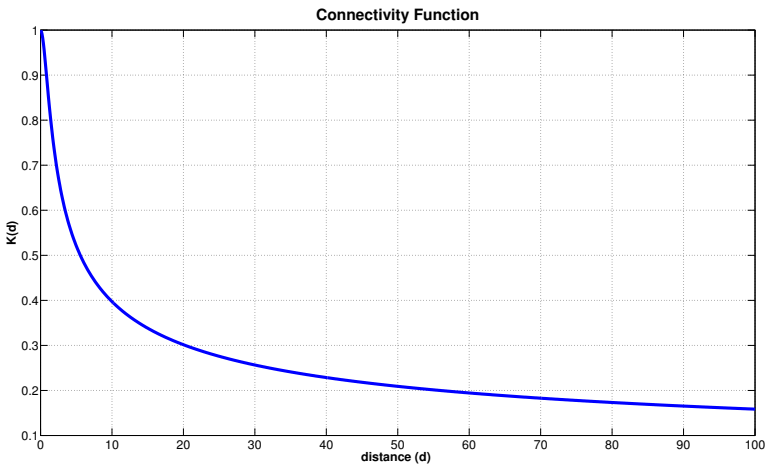

Figure 2.16: illustrates the connectivity function with parameters $\gamma = 1$, $\alpha = 1$, and $\sigma = 0.2$

With given initial conditions the solution to the Cucker-Smale (CS) model depends on the parameters γ, α and σ, that is, if $\sigma < \frac{1}{2}$, then the velocities v_b^{fm} tend asymptotically to a common limit v^* as can be seen in the following theorem; see also in references [19, 20, 35, 36, 45, 46].

Theorem 1. *(Unconditional consensus emergence)[20, 45]*
Let $(x^{\mathrm{fm}}(t), v^{\mathrm{fm}}(t)) \in C^1([0,\infty); \mathbb{R}^{d(2N)})$ *be the solution of the Cucker-Smale system and for* $b = 1, ..., N$, *we define*

$$\begin{aligned} X_{\max}(t) &= \max_b \|x_b^{\mathrm{fm}}(t) - x_b^{\mathrm{fm}}(0)\|, \qquad X_{\max}^0 = X(0), \\ V_{\max}(t) &= \max_b \|v_b^{\mathrm{fm}}(t)\|, \qquad V_{\max}^0 = V(0). \end{aligned}$$

Then one of the following holds,

- *if* $0 < \sigma < \frac{1}{2}$, *then*
$$V_{\max}(t) \leq V_{\max}^0 e^{-K(2\lambda)t}, \ \exists \lambda > 0,$$
- *if* $\sigma = \frac{1}{2}$, *then*
$$\lim_{t\to\infty} V_{\max}(t) = 0.$$

Consider the symmetric bilinear form

$$B(u,v) = \frac{1}{2N^2}\sum_{i,j}\langle u_i - u_j, v_i - v_j\rangle = \frac{1}{N}\sum_{i=1}^{N}\langle u_i, v_i\rangle - \langle \bar{u}, \bar{v}\rangle,$$

$$X(t) = B(x(t), x(t)), \quad V(t) = B(v(t), v(t)).$$

Theorem 2. *(Conditional consensus emergence)[20, 45].*
Let $(x_0^{\mathrm{fm}}, v_0^{\mathrm{fm}}) \in \mathbb{R}^{dN} \times \mathbb{R}^{dN}$ *be such that* $X_0 = B(x_0^{\mathrm{fm}}, x_0^{\mathrm{fm}})$ *and* $V_0 = B(v_0^{\mathrm{fm}}, v_0^{\mathrm{fm}})$ *satisfy*

$$\int_{\sqrt{NX_0}}^{\infty} a(\sqrt{2Nr})dr > \sqrt{V_0}.$$

Then the solution with initial data $(x_0^{\mathrm{fm}}, v_0^{\mathrm{fm}})$ *tends to consensus.*

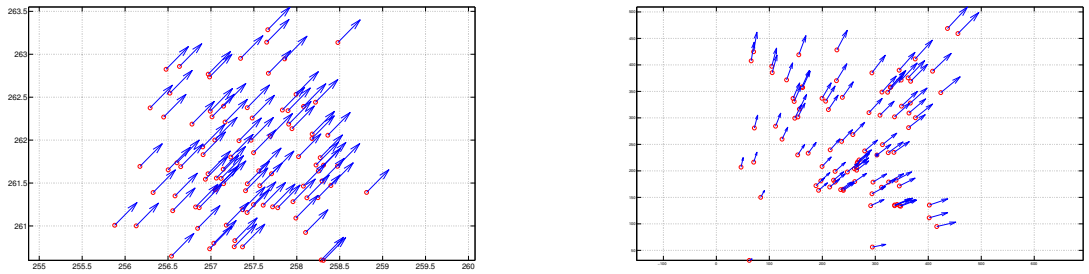

(a) $\sigma = 0.2$ (b) $\sigma = 5$

Figure 2.17: Results of numerical experiments with the CS model with different choice of the parameter σ. Figure(a) and Figure(b) show results with $\sigma = 0.2$ and $\sigma = 5$, respectively.

2.3.3 A refined flocking model

In this section, we present a modified flocking model which is a combination of three fundamental behaviors of interacting agents, that is self-propelling, friction, short-range repulsion and long-range attraction, and alignment. Furthermore, an external leader is included in the system. A refined flocking dynamical system of N interacting agents with one leader in $\mathbb{R}^d$, where d is the space dimension, is presented as follows

$$\begin{aligned} \dot{x}_b^{\text{fm}} &= v_b^{\text{fm}}, \\ \dot{v}_b^{\text{fm}} &= S_b + M_b + E_b, \qquad \text{for} \quad b = 1, ..., N, \end{aligned} \tag{2.14}$$

where $x_b^{\text{fm}}, v_b^{\text{fm}} \in \mathbb{R}^d$ represent the position and velocity of b-th agent, respectively, for $b = 1, ..., N$. The indices b denote the b-th agent of the flocking system. The first term in the dynamics system S_i represents self-propelling and friction force presented as

$$S_b = (\alpha - \beta \|v_b^{\text{fm}}\|^2) v_b^{\text{fm}}, \quad \text{for} \quad b = 1, ..., N. \tag{2.15}$$

The second terms, M_b is related to short-range repulsive and long-range attractive forces.

$$M_b = -\frac{1}{N} \sum_{j \neq i} \nabla_{x_b^{\text{fm}}} U(\|x_b^{\text{fm}} - x_j^{\text{fm}}\|), \quad \text{for} \quad b = 1, ..., N. \tag{2.16}$$

The force E_b is concerning the orientation of the agent's velocities based on the fact that a bird moving with sufficiently large velocity v will react only to birds observed within a conic-shaped observation domain. This force is modified version of the Cucker-Smale model. Notice that symmetry of the CS force leads to a conservation of momentum that is not observed in a flock of birds [1]. The reason is the existence of a blind zone. To explain this fact, consider the case of two agents such that the 1^{st} agent tries to follow the 2^{nd} agent who is unaware of this fact and thus it does not respond to the 1^{st} agent. To correct the CS model for this limitation, in [1] a vision cone is added. That is, an agent at position x moving with velocity v will react only to agents at position y observed within a conic-shaped domain defined by $\cos(y - x, v) \in (\delta_2, \delta_1)$, where the constants $\delta_1 > \delta_2$ are given. As a consequence, the CS connectivity function is replaced by the following

$$\widetilde{K}(x - y, v) = \frac{\gamma}{(1 + \|x - y\|^2)^\sigma} \cdot g\left(\frac{(y - x)}{\|y - x\|} \cdot \frac{v}{\|v\|} \right),$$

where the vision cutoff function g is given by

$$\begin{aligned} g(z) &= \begin{cases} 0, & \text{if} \quad z \leq \delta_2, \\ \frac{1}{2} - \frac{1}{2} \tanh\left(\frac{1}{z - \delta_2} + \frac{1}{z - \delta_1} \right), & \text{if} \quad \delta_2 < z < \delta_1, \\ 1, & \text{if} \quad z \geq \delta_1 \end{cases} \\ z &= \frac{\langle y - x, v \rangle}{\|y - x\| \|v\|}, \end{aligned}$$

where $\langle \cdot, \cdot \rangle$ is the scalar product in Euclidean space. The alignment forces are given by

$$E_b = \frac{1}{N} \sum_{j \neq b} \widetilde{K}(x_b^{\mathrm{fm}} - x_j^{\mathrm{fm}}, v_b^{\mathrm{fm}})(v_j^{\mathrm{fm}} - v_b^{\mathrm{fm}}), \qquad \text{for} \quad b = 1, ..., N. \tag{2.17}$$

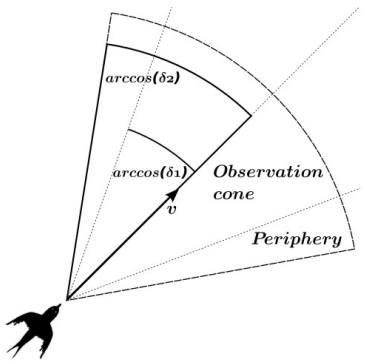

Figure 2.18: Cone of vision for a bird, Ref. [1]

Next, we present the control of the refined flocking system with the presence of leader given by

$$\begin{aligned} \dot{x}_0^{\mathrm{fm}}(t) &= v_0^{\mathrm{fm}}(t), \\ \dot{x}_b^{\mathrm{fm}}(t) &= v_b^{\mathrm{fm}}(t), \\ \dot{v}_0^{\mathrm{fm}}(t) &= S_0 + M_0 + E_0 + u^{\mathrm{fm}}(t), \\ \dot{v}_b^{\mathrm{fm}}(t) &= S_b + M_b + E_b + L_b, \qquad \text{for} \quad b = 1, ..., N, \end{aligned} \tag{2.18}$$

where $x_i^{\mathrm{fm}}, v_i^{\mathrm{fm}} \in \mathbb{R}^d$ represent the position and velocity of i-th agent, respectively, for $i = 0, 1, ..., N$. The index 0 refers to the leader and the indices b denote the b-th agent of the flocking system. The function $u^{\mathrm{fm}} : [0, T] \to \mathbb{R}^d$ is control function. In this case, the control strategy is implemented on the dynamics of velocity of leader for the purpose of force the flocking to reach the group pattern or follow the desired trajectory.

The first term in the dynamics system S_i represents self-propelling and friction forces defined in (2.15), that is,

$$S_i = (\alpha - \beta \|v_i^{\mathrm{fm}}\|^2) v_i^{\mathrm{fm}}, \quad \text{for} \quad i = 0, 1, ..., N. \tag{2.19}$$

The force M_i is related to short-range repulsive and long-range attractive forces as defined in (2.16). The force E_i corresponds to alignment and its structure was addressed

in (2.17). Now, our flocking system is included a leader; hence, we have

$$M_i = -\frac{1}{N+1}\sum_{j\neq i}\nabla_{x_i^{\mathrm{fm}}}U(\|x_i^{\mathrm{fm}}-x_j^{\mathrm{fm}}\|), \tag{2.20}$$

$$E_i = \frac{1}{N+1}\sum_{j\neq i}\widetilde{K}(x_i^{\mathrm{fm}}-x_j^{\mathrm{fm}},v_i^{\mathrm{fm}})(v_j^{\mathrm{fm}}-v_i^{\mathrm{fm}}), \quad \text{for} \quad i=0,1,...,N. \tag{2.21}$$

Finally, the force L_b in (2.18) models the action of the external leader. For this purpose, we consider the approach in [7] where the formula of the attraction-repulsion with the leader is given by

$$L_b = -\gamma_1\nabla_{x_b^{\mathrm{fm}}}U(\|x_b^{\mathrm{fm}}-x_0^{\mathrm{fm}}\|), \qquad \text{for} \quad b=1,...,N, \tag{2.22}$$

where the leader diversity with respect to the group is represented by the interaction-strength parameter $\gamma_1>0$, while a similar Morse potential U with different attractive and repulsive coefficients, C_a^0, C_r^0, l_a^0, and l_r^0, are used. Because of the different coefficients, we have different attractive and repulsive strengths and length scales between the leader and the agents in the flock.

Chapter 3

Controllability and stabilization of multi-agent systems

In this chapter, we study controllability and stabilization of multi-agent systems. The purpose of this study is to design control strategies for the group of agents in order to accomplish collective behaviors in some prescribed sense. In particular, in the multi-agent dynamical system under consideration the control input is assigned directly to the leader and for each agent is allowed to receive the influence of a controller through the interaction with a controlling leader.

In the first section of this chapter, we give a review of general theories corresponding to controllability and stabilization for a nonlinear system, that includes the dynamics of our multi- agent systems. This section is divided into two parts. In the first part, the definitions of local and global controllability are introduced and some theoretical concepts, conditions, and assumptions on the systems to be controllable are discussed. In the second part, the concept of stability is provided, together with the Lyapunov method that is a well-known tool to examine the stability of the system. Next, in Section 3.2, the control of the Hegselmann-Krause opinion formation system and the consensus problem are discussed. The concept of global and local stabilization are investigated. Furthermore, some theoretical conditions corresponding to controllability are proved. In Section 3.3, the stability of a social balance dynamical system is investigated considering the linearization of the Heider balance system. Furthermore, the local controllability is discussed. Finally, in Section 3.4, we introduce the definition of consensus for a flocking model, and in the subsequent section, we investigate the stability of flocking. We close this chapter with studying local controllability of our refined flocking model.

3.1 Controllability and stabilization

In this section, we are concerned with control problems with a structure that includes the multi-agent system. The system under consideration is control affine presented

as follows,

$$\begin{aligned} \dot{\mathbf{x}}(t) &= \mathbf{f}(\mathbf{x}(t)) + \sum_{j=1}^{nc} g_j(\mathbf{x}(t))u_j(t), \\ \mathbf{x}(0) &= \mathbf{x}_0, \end{aligned} \tag{3.1}$$

where $\mathbf{x}(t) = (x_1(t), x_2(t), ..., x_{nx}(t))^\top \in \mathbb{R}^{nx}$, is state of the system, which characterizes the system at time t, $t \in [0, T]$, $T > 0$ a terminal time. The number of state variables is denoted by nx and $\mathbf{x}_0$ is a given initial condition. A control variable $\mathbf{u} : [0, T] \to \mathbb{R}^{nc}$, $\mathbf{u} = (u_1, ..., u_{nc})^T$, represents an external input that is able to influence the future evolution of the state variable. In the vast majority of control problems, the controllers are restricted to a certain control region together with a class of control functions, called an admissible set $\mathbb{U}$. Throughout this chapter, the control function is specified to be an element of a normed linear space of real-vector valued function, which is in the class of piecewise continuous functions. The vector field $\mathbf{f} : \mathbb{R}^{nx} \to \mathbb{R}^{nx}$ describes the free dynamics and is assumed to be smooth. The vector fields $g_1(\mathbf{x}), \ldots, g_{nc}(\mathbf{x}) \in \mathbb{R}^{nx}$ are control vector fields. In our case, $g_j(\mathbf{x})$ are constant vector fields. For a sake of convenience, the control vector fields can be organized into an $nx \times nc$ matrix as follows

$$\mathbf{B} = \begin{pmatrix} g_1(\mathbf{x}) & g_2(\mathbf{x}) & \ldots & g_{nc}(\mathbf{x}). \end{pmatrix} \tag{3.2}$$

As a consequence, the system (3.1) can be equivalently written in the following form

$$\begin{aligned} \dot{\mathbf{x}}(t) &= \mathbf{f}(\mathbf{x}(t)) + \mathbf{B}\mathbf{u}(t), \\ \mathbf{x}(0) &= \mathbf{x}_0. \end{aligned} \tag{3.3}$$

Remark 1. *In our framework of control through leadership, the control function is implemented on leader. Therefore, without loss of generality, assuming that the state x_1 represents the leader, the matrix $\mathbf{B}$ takes the following form,*

$$\mathbf{B} = \begin{pmatrix} 1 \\ 0 \\ \vdots \\ 0 \end{pmatrix}$$

Notations 1. *We use the following notations,*

- $\langle \cdot, \cdot \rangle$ *denotes the Euclidean scalar product in* $\mathbb{R}^d$,
- $\| \cdot \|$ *is the Euclidean norm,*
- $\langle \cdot, \cdot \rangle_{L^2}$ *the* L^2*- inner product defined by*

$$\langle y, z \rangle_{L^2} := \int_0^T \langle y, z \rangle dt, \quad \textit{for every} \quad y, z \in L^2((0, T); \mathbb{R}^d),$$

- $\|\cdot\|_{L^2}$ *the* L^2*-norm defined by*

$$\|w\|_{L^2} := \left(\int_0^T \sum_{j=1}^{d} \|w_j\|^2 dt\right)^{\frac{1}{2}}, \quad \textit{for every } w \in L^2((0,T);\mathbb{R}^d).$$

Before investigating the controllability of the problem(3.3), we discuss first the existence and uniqueness of the solutions to (3.3) in the sense of Charathéodory; see Theorem A.1 in Appendix A.1 and the references [76, 81].

Proposition 1. *Consider the system (3.3) with* $\mathbf{x} \in D \subset \mathbb{R}^{nx}$ *and given* $\mathbf{u} \in L^2((0,T);\mathbb{R}^{nc})$*. Let* $D \subset \mathbb{R}^{nx}$ *and assume that* $\mathbf{f} : D \to \mathbb{R}^{nx}$ *is locally Lipschitz continuous on* D*. Then the system (3.3) admits the unique solution for any* $T > 0$ *and any initial condition.*

Proof. Let $\mathbf{u}$ be a given control function. Let us define $\mathbf{F} : [0,T] \times \mathbb{R}^{nx} \to \mathbb{R}^{nx}$ as

$$\mathbf{F}(t,\mathbf{x}) = \mathbf{f}(\mathbf{x}) + \mathbf{B}\mathbf{u}(t). \tag{3.4}$$

Since $\mathbf{u} \in L^2((0,T);\mathbb{R}^{nc})$ and $\mathbf{f}(\mathbf{x}) \in C^1(\mathbb{R}^{nx};\mathbb{R}^{nx})$, then $\mathbf{F}$ has the following properties,

- $\mathbf{F}(\cdot,\mathbf{x}) : [0,T] \to \mathbb{R}^{nx}$ is measurable, for each fixed $\mathbf{x}$,
- $\mathbf{F}(t,\cdot) : \mathbb{R}^{nx} \to \mathbb{R}^{nx}$ is continuous, for each fixed t.

Let $\mathbf{y}, \mathbf{z} \in \mathbb{X}$, we can see that

$$\begin{aligned} \|\mathbf{F}(t,\mathbf{y}) - \mathbf{F}(t,\mathbf{z})\| &= \|\mathbf{f}(\mathbf{y}) + \mathbf{B}\mathbf{u}(t) - \mathbf{f}(\mathbf{z}) - \mathbf{B}\mathbf{u}(t)\| \\ &\leq \|\mathbf{f}(\mathbf{y}) - \mathbf{f}(\mathbf{z})\| \\ &\leq c\|\mathbf{y} - \mathbf{z}\|, \quad c > 0. \end{aligned}$$

Consequently, $\mathbf{F}$ is Lipschitz in $\mathbf{x}$. Next, the locally integrable property of $\mathbf{F}$ is examined. For a given $\mathbf{x} \in \mathbb{X}$, we have that

$$\begin{aligned} \|\mathbf{F}(t,\mathbf{x})\| &= \|\mathbf{f}(\mathbf{x}) + \mathbf{B}\mathbf{u}(t)\| \\ &\leq \|\mathbf{f}(\mathbf{x})\| + \|\mathbf{B}\|\|\mathbf{u}(t)\| \\ &\leq \left(\sum_{n=1}^{nx} |f_n(x)|^2\right)^{1/2} + \|\mathbf{B}\|\|\mathbf{u}(t)\| \\ &\leq \left(\sum_{n=1}^{nx} |f_n(x)|_\infty^2\right)^{1/2} + \|\mathbf{B}\|\|\mathbf{u}(t)\| \\ &\leq \left(nx \cdot \max_n |f_n(x)|_\infty^2\right)^{1/2} + \|\mathbf{B}\|\|\mathbf{u}(t)\| \\ &\leq \alpha + \|\mathbf{B}\|\|\mathbf{u}(t)\|. \end{aligned}$$

Hence, by [76](Theorem 54), the system (3.3) admits a unique solution for any T and any initial condition. □

Remark 2. *We assume that the conditions stated in Proposition 1 hold, then we have*

$$\begin{aligned}
\mathbf{x}(T) &= \mathbf{x}_0 + \int_0^T (\mathbf{f}(\mathbf{x}(s)) + \mathbf{B}\mathbf{u}(s))ds, \\
\|\mathbf{x}(T)\| &\leq \|\mathbf{x}_0\| + \int_0^T \|\mathbf{f}(\mathbf{x}(s)) + \mathbf{B}\mathbf{u}(s)\|ds \\
&\leq \|\mathbf{x}_0\| + \int_0^T (\alpha + \|\mathbf{B}\|\|\mathbf{u}(s)\|)ds \\
&\leq \|\mathbf{x}_0\| + \alpha T + \|\mathbf{B}\| \int_0^T \|\mathbf{u}(s)\|ds \\
&\leq c(\|\mathbf{x}_0\|, \alpha, T) + \beta(\|\mathbf{B}\|)\|\mathbf{u}\|_{L^1(0,T)}.
\end{aligned}$$

3.1.1 The notions of controllability

In this section, the concepts of controllability for the system (3.3) are briefly provided; see e.g. [32, 54, 68, 76]. Given $\hat{\mathbf{x}} \in \mathbb{X} \subseteq \mathbb{R}^{nx}$, the general idea of controllability is that it is possible to find the set of points which can be reached from $\hat{\mathbf{x}}$ in finite time by a suitable choice of the input function $\mathbf{u}$. Before we arrive the definition of controllability, let us give a notation of the control and the trajectory or state corresponding to a control.

Definition 1. *Let a control $\mathbf{u} : [0, T] \to \mathbb{U}$ be a measurable function. A unique solution $\mathbf{x}(t, 0, \mathbf{x}_0, \mathbf{u})$ of (3.3) at time $t \geq 0$, is called a response of the system, or the state of the system, corresponding to the control $\mathbf{u}$ and to the initial condition $\mathbf{x}(0) = \mathbf{x}_0$.*

Definition 2. *The nonlinear system (3.3) is called controllable if for any two points $\mathbf{y}, \mathbf{z} \in \mathbb{X}$ there exists a finite time T and an admissible control function $\mathbf{u} : [0, T] \to \mathbb{U}$ such that $\mathbf{x}(T, 0, \mathbf{y}, \mathbf{u}) = \mathbf{z}$.*

Definition 3. *A point $(\mathbf{x}^*, \mathbf{u}^*)$ is called an equilibrium point of the control system (3.3), if*

$$\mathbf{f}(\mathbf{x}^*) + \mathbf{B}\mathbf{u}^* = 0.$$

Definition 4. *Let $(\mathbf{x}^*, \mathbf{u}^*)$ be an equilibrium point of the system (3.3). The linearized control system at $(\mathbf{x}^*, \mathbf{u}^*)$ of the control system (3.3) is the following linear control system*

$$\dot{\mathbf{x}} = \mathbf{A}\mathbf{x} + \mathbf{B}\mathbf{u}, \tag{3.5}$$

where $\mathbf{A}$ denotes the Jacobian matrix of $\mathbf{f}(\mathbf{x})$ with respect to $\mathbf{x}$ at $\mathbf{x}^*$, $\mathbf{A} = \nabla_{\mathbf{x}}\mathbf{f}(\mathbf{x}^*)$.

The next goal is to determine conditions for controllability in terms of the matrices $\mathbf{A}, \mathbf{B}$. For this, we define the Kalman controllability matrix,

$$\mathbf{K}(\mathbf{A}, \mathbf{B}) = \begin{bmatrix} \mathbf{B} & \mathbf{A}\mathbf{B} & \mathbf{A}^2\mathbf{B} & \cdots & \mathbf{A}^{nx-1}\mathbf{B} \end{bmatrix} \in \mathbb{R}^{nx \times (nx \cdot nc)}. \tag{3.6}$$

Theorem 3. *The linearized system (3.5) is controllable, if one of the following holds,*

1. $\mathbf{K}(\mathbf{A}, \mathbf{B})$ *has full rank.*
2. $[\lambda \mathbf{I}_{nx} - \mathbf{A}, \mathbf{B}]$ *has full rank, for each eigenvalue* λ *of* $\mathbf{A}$.

Theorem 4. *If the linearized control system (3.5) is controllable, then the system (3.3) is locally controllable.*

From the linearized system (3.5), one can easily check whether the linearized system is controllable or not by using Kalman rank condition. We remark that if the Kalman rank condition is not fulfilled, then it cannot be inferred any controllability property of system (3.3).

3.1.2 The notions of stabilization

In this section, we discuss the problem of designing nonlinear controls of feedback type in order to construct a closed-loop system having the desired behavior. Corresponding to this design objective, the tasks of control systems can be divided into two categories: stabilization and tracking problems.

- **Stabilization**
  In this problem, the control is designed so that the state of the closed-loop system will be stabilized around an equilibrium point. The control is called a stabilizer.
- **Tracking problem**
  the design objective is to construct a control so that the system output tracks a given desired trajectory.

In this thesis, both control problems for the multi-agent systems are studied. In the following, we provide some key concepts concerning stability that are main tools for investigating the stability properties of the multi-agent systems; see in [32, 54, 68, 76].

3.1.3 Linearization and local stability

Consider the system (3.3) without control.

$$\begin{aligned} \dot{\mathbf{x}} &= \mathbf{f}(\mathbf{x}), \\ \mathbf{x}(0) &= \mathbf{x}_0, \, , \quad t \in [0, T], \end{aligned} \tag{3.7}$$

where $\mathbf{f} : D \subset \mathbb{R}^{nx} \to \mathbb{R}^{nx}$ is a locally Lipschitz continuous on D. Let $\mathbf{x}^*$ be an equilibrium point of the system (3.7), that is, $\mathbf{f}(\mathbf{x}^*) = 0$. Our aim is studying the behavior of the dynamics in a neighborhood of an equilibrium point $\mathbf{x}^*$.

Definition 5. *The equilibrium point* $\mathbf{x}^*$ *of (3.7) is*

- ***locally stable****, if for any neighborhood* $B_0(\mathbf{x}^*)$ *, there exists a neighborhood* $B_1(\mathbf{x}^*)$ *such that*

$$\mathbf{x}_0 \in B_1(\mathbf{x}^*) \quad \Rightarrow \quad \text{the solution of (3.7)} \quad \mathbf{x}(t;\mathbf{x}_0) \in B_0(\mathbf{x}^*), \quad \forall t \geq 0.$$

- ***locally asymptotically stable****, if* $\mathbf{x}^*$ *is locally stable and there exists a neighborhood* $B_2(\mathbf{x}^*)$ *such that all solution* $\mathbf{x}(t;\mathbf{x}_0)$ *of (3.7) with* $\mathbf{x}_0 \in B_2(\mathbf{x}^*)$ *converges to* $\mathbf{x}^*$ *as* $t \to \infty$*.*

The above definition is provided in order to characterize the local behavior of the systems, in the sequel, we give a description of the Lyapunov's linearization method, which is the classical tool to check whether an equilibrium point $\mathbf{x}^*$ is locally stable or not. Assuming that $\mathbf{f}(\mathbf{x})$ is continuously differentiable, the system (3.7) can be written as follows

$$\dot{\mathbf{x}} = \mathbf{A}\mathbf{x}, \tag{3.8}$$

with $\mathbf{A} = \nabla_{\mathbf{x}}\mathbf{f}(\mathbf{x}^*)$. The following results state the relationship between the stability of the linear system (3.8) and that of the original nonlinear system.

Theorem 5. *(Lyapunov's linearization method)*

- *If all eigenvalue of* $\mathbf{A}$ *are strictly in the left-half complex plane, then for nonlinear system the equilibrium point is asymptotically stable, that is,*

$$Re(\lambda_k(\mathbf{A})) < 0, \quad \forall k \quad \Rightarrow \quad \mathbf{x}^* \text{ is locally asymptotically stable.}$$

- *If the linearized system is unstable, that is, at least one eigenvalue of* $\mathbf{A}$ *is strictly in the right-half complex plane, then the equilibrium point is unstable for nonlinear system.*

$$\exists k, \quad Re(\lambda_k(\mathbf{A})) > 0 \quad \Rightarrow \quad \mathbf{x}^* \text{ is unstable.}$$

Theorem 6. *(Lyapunov theorem for local stability)*
Let $\mathbf{x}^* \in B_r \subset \mathbb{R}^{nx}$ *be an equilibrium point of (3.7). Assume that* $V : B_r \to \mathbb{R}$ *is continuously differentiable function, and has the following properties*

1. $V(\mathbf{x}^*) = 0$.
2. $V(\mathbf{x}) > 0$*, for all* $\mathbf{x} \in D$ *,* $\mathbf{x} \neq \mathbf{x}^*$.
3. $\nabla_{\mathbf{x}} V \cdot \mathbf{f}(\mathbf{x}) \leq 0$ *along all trajectories of the system in* B_r.

Then the equilibrium point $\mathbf{x}^*$ *is locally stable. If* $\nabla_{\mathbf{x}} V \cdot \mathbf{f}(\mathbf{x}) < 0$ *in* B_r *, then* $\mathbf{x}^*$ *is asymptotically stable.*

3.2 Controllability of the Hegselmann-Krause opinion formation model

In this section, we investigate the controllability property of the HK system (2.4) where the control input is included in the system and acts only on the leader. The HK model with control through leadership is given by

$$\begin{aligned} \dot{x}_0^{\text{of}}(t) &= u^{\text{of}}(t), \\ \dot{x}_b^{\text{of}}(t) &= \sum_{j=1}^{N} a_{bj}(x_j^{\text{of}}(t) - x_b^{\text{of}}(t)) + c_b(x_0^{\text{of}}(t) - x_b^{\text{of}}(t)), \qquad \text{for} \quad b = 1, ..., N, \end{aligned} \tag{3.9}$$

with given initial positions $x_i^{\text{of}}(0) \in \mathbb{R}^d$ for $i = 0, 1, \ldots, N$.

From the above system (3.9), it can be written in general form as follows

$$\dot{\mathbf{x}}^{\text{of}}(t) = \mathbf{f}^{\text{of}}(\mathbf{x}^{\text{of}}) + \mathbf{B}^{\text{of}} u^{\text{of}}(t), \quad \mathbf{x}^{\text{of}}(t_0) = \mathbf{x}_0^{\text{of}}, \tag{3.10}$$

where $\mathbf{x}^{\text{of}} = (x_0^{\text{of}}, x_1^{\text{of}}, ..., x_N^{\text{of}}) \in \mathbb{R}^{d(N+1)}$, $u^{\text{of}} \in \mathbb{U}^{\text{of}}$, $\mathbf{f}^{\text{of}} : \mathbb{R}^{d(N+1)} \to \mathbb{R}^{d(N+1)}$,

$$\mathbf{f}^{\text{of}}(\mathbf{x}^{\text{of}}) := \begin{pmatrix} \mathbf{0}_{d,1} \\ \sum_{j=1}^{N} a_{1j}(x_j^{\text{of}} - x_1^{\text{of}}) + c_1(x_0^{\text{of}} - x_1^{\text{of}}) \\ \sum_{j=1}^{N} a_{2j}(x_j^{\text{of}} - x_2^{\text{of}}) + c_2(x_0^{\text{of}} - x_2^{\text{of}}) \\ \vdots \\ \sum_{j=1}^{N} a_{Nj}(x_j^{\text{of}} - x_N^{\text{of}}) + c_N(x_0^{\text{of}} - x_N^{\text{of}}) \end{pmatrix}, \quad \mathbf{B}^{\text{of}} = \begin{pmatrix} \mathbf{I}_d \\ \mathbf{0}_{d,d} \\ \mathbf{0}_{d,d} \\ \vdots \\ \mathbf{0}_{d,d} \end{pmatrix}, \tag{3.11}$$

where $\mathbf{I}_m$ denote $m \times m$ identity matrix and $\mathbf{0}_{m,n}$ stands for $m \times n$ zero matrix.

Consider the smooth function φ defined in (2.3). It can be seen that $\varphi \in C^1(\bar{D}; [0, 1])$; as a consequence, a_{bj} defined in (2.2) is locally Lipschitz continuous, for $b, j = 1, ..., N$. Moreover, the function c_b is also locally Lipschitz continuous, because of $\phi \in C^\infty([0, \infty); (0, 1)$. It is concluded that the function $\mathbf{f}^{\text{of}}$ defined in (3.11) is locally Lipschitz continuous and by Proposition 1, the system (3.11) admits the unique solution for any $T > 0$ and any initial conditions.

3.2.1 Global stabilization

The uncontrolled dynamics of system (2.4) is governed by local interactions and asymptotically leads to the formation of clusters. Although, from the mathematical point of view, clusters are a stable configuration for the system, we focus on the possibility to steer, using the leader's action on the group, all agents to the same unique opinion, that is, to consensus.

Definition 6 (**Consensus**).
We call consensus a configuration in which the states of all agents are equal, that is,

$$\mathbf{x}^{\mathrm{of}*} = (x_0^{\mathrm{of}}, x_1^{\mathrm{of}}, ..., x_N^{\mathrm{of}}) \in \mathbb{R}^{d(N+1)} \quad \textit{such that} \quad x_0^{\mathrm{of}} = x_1^{\mathrm{of}} = \cdots = x_N^{\mathrm{of}}. \tag{3.12}$$

We say that a solution $\mathbf{x}^{\mathrm{of}}$ *of system* (2.4) tends to consensus *if there exists a consensus configuration* $\mathbf{x}^{\mathrm{of}*} \in \mathbb{R}^{d(N+1)}$ *such that* $\lim_{t\to+\infty} \mathbf{x}^{\mathrm{of}}(t) = \mathbf{x}^{\mathrm{of}*}$.

Being consensus an equilibrium for system (2.4), the problem of steering asymptotically the system to consensus is, in fact, a stabilization problem.

Theorem 7. *For every initial condition* $\mathbf{x}^{\mathrm{of}}(0) \in \mathbb{R}^{d(N+1)}$ *and every* $M > 0$ *there exists a control* $t \mapsto u^{\mathrm{of}}(t) \in \mathbb{R}^d$ *satisfying* $\|u^{\mathrm{of}}\| \leq M$ *such that the associated solution* $\mathbf{x}^{\mathrm{of}}(t)$ *with initial data* $\mathbf{x}^{\mathrm{of}}(0)$ *tends to consensus.*

Proof. For every t let $\bar{n} = \bar{n}(t)$ be the smallest index in $\{1, \ldots, N\}$ such that

$$\|x_{\bar{n}}^{\mathrm{of}}(t) - x_0^{\mathrm{of}}(t)\| \geq \|x_b^{\mathrm{of}}(t) - x_0^{\mathrm{of}}(t)\|, \quad \text{for every } b = 1, \ldots, N.$$

Let

$$\alpha(t) = \frac{1}{2} \min \left\{ \frac{\phi(\|x_{\bar{n}}^{\mathrm{of}}(t) - x_0^{\mathrm{of}}(t)\|)}{N - \phi(\|x_{\bar{n}}^{\mathrm{of}}(t) - x_0^{\mathrm{of}}(t)\|)}, \frac{2M}{\gamma \sum_b \|x_b^{\mathrm{of}}(t) - x_0^{\mathrm{of}}(t)\|} \right\}.$$

Note that $\alpha(t) > 0$ for every $t \geq 0$. Consider the control law

$$u^{\mathrm{of}}(t) = \alpha(t)\gamma \sum_{b=1}^{N} \phi(\|x_b^{\mathrm{of}}(t) - x_0^{\mathrm{of}}(t)\|)(x_b^{\mathrm{of}}(t) - x_0^{\mathrm{of}}(t)). \tag{3.13}$$

The control u is admissible since

$$\|u^{\mathrm{of}}\| \leq \alpha\gamma \sum_{b=1}^{N} \phi(\|x_b^{\mathrm{of}} - x_0^{\mathrm{of}}\|)\|x_b^{\mathrm{of}} - x_0^{\mathrm{of}}\| \leq \alpha\gamma \sum_{b=1}^{N} \|x_b^{\mathrm{of}}(t) - x_0^{\mathrm{of}}(t)\| \leq M.$$

Consider $t \geq 0$ and assume, for simplicity of notation, that $\bar{n} = 1$,

$$c_b = \gamma\phi(\|x_b^{\mathrm{of}}(t) - x_0^{\mathrm{of}}(t)\|), \quad \text{and} \quad a_{bj} = a(\|x_b^{\mathrm{of}}(t) - x_j^{\mathrm{of}}(t)\|).$$

Then we have

$$\begin{aligned}
\frac{1}{2}\frac{d}{dt}\|x_1^{\mathrm{of}} - x_0^{\mathrm{of}}\|^2 &= \langle \dot{x}_1^{\mathrm{of}} - \dot{x}_0^{\mathrm{of}}, x_1^{\mathrm{of}} - x_0^{\mathrm{of}}\rangle \\
&= \langle \dot{x}_1^{\mathrm{of}}, x_1^{\mathrm{of}} - x_0^{\mathrm{of}}\rangle - \langle \dot{x}_0^{\mathrm{of}}, x_1^{\mathrm{of}} - x_0^{\mathrm{of}}\rangle \\
&= \sum_{j=2}^{N} a_{1j}\langle x_j^{\mathrm{of}} - x_1^{\mathrm{of}}, x_1^{\mathrm{of}} - x_0^{\mathrm{of}}\rangle - c_1\|x_1^{\mathrm{of}} - x_0^{\mathrm{of}}\|^2 \\
&\quad - \alpha\sum_{j=2}^{N} c_j\langle x_j^{\mathrm{of}} - x_0^{\mathrm{of}}, x_1^{\mathrm{of}} - x_0^{\mathrm{of}}\rangle - \alpha c_1\|x_1^{\mathrm{of}} - x_0^{\mathrm{of}}\|^2 \\
&= \sum_{j=2}^{N} a_{1j}\langle x_j^{\mathrm{of}} - x_0^{\mathrm{of}}, x_1^{\mathrm{of}} - x_0^{\mathrm{of}}\rangle - \sum_{j=2}^{N} a_{1j}\|x_1^{\mathrm{of}} - x_0^{\mathrm{of}}\|^2 - c_1\|x_1^{\mathrm{of}} - x_0^{\mathrm{of}}\|^2 \\
&\quad - \alpha\sum_{j=2}^{N} c_j\langle x_j^{\mathrm{of}} - x_0^{\mathrm{of}}, x_1^{\mathrm{of}} - x_0^{\mathrm{of}}\rangle - \alpha c_1\|x_1^{\mathrm{of}} - x_0^{\mathrm{of}}\|^2 \\
&\le \sum_{j=2}^{N} |a_{1j} - \alpha c_j|\|x_j^{\mathrm{of}} - x_0^{\mathrm{of}}\|\|x_1^{\mathrm{of}} - x_0^{\mathrm{of}}\| - \left(\sum_{j=2}^{N} a_{1j} + (1+\alpha)c_1\right)\|x_1^{\mathrm{of}} - x_0^{\mathrm{of}}\|^2 \\
&\le \left(\sum_{j=2}^{N}(|a_{1j} - \alpha c_j| - a_{1j}) - (1+\alpha)c_1\right)\|x_1^{\mathrm{of}} - x_0^{\mathrm{of}}\|^2.
\end{aligned}$$

Now if j is such that $a_{1j} - \alpha c_j \ge 0$ then $|a_{1j} - \alpha c_j| - a_{1j} = -\alpha c_j < 0$. Hence

$$\begin{aligned}
\sum_{j=2}^{N}(|a_{1j} - \alpha c_j| - a_{1j}) - (1+\alpha)c_1 &\le \sum_{j=2}^{N}(\alpha c_j - 2a_{1j}) - (1+\alpha)c_1 \\
&\le N\alpha - (1+\alpha)c_1 \\
&= (N - c_1)\alpha - c_1 \\
&\le -\frac{c_1}{2}.
\end{aligned}$$

In particular $\max_b \|x_b^{\mathrm{of}}(t) - x_0^{\mathrm{of}}(t)\|$ is decreasing for every t. Therefore, we have

$$\phi(\max_b \|x_b^{\mathrm{of}}(t) - x_0^{\mathrm{of}}(t)\|) \ge \phi(\max_b \|x_i^{\mathrm{of}}(0) - x_0^{\mathrm{of}}(0)\|),$$

and denoting by $I_0 = \max_b \|x_b^{\mathrm{of}}(0) - x_0^{\mathrm{of}}(0)\|$ we have that

$$\max_b \|x_b^{\mathrm{of}}(t) - x_0^{\mathrm{of}}(t)\|^2 \le \exp\left(-t\frac{\gamma\phi(I_0)}{2}\right) I_0,$$

which gives that

$$\|x_b^{\mathrm{of}}(t) - x_0^{\mathrm{of}}(t)\| \to 0, \qquad \text{as } t \to \infty, \qquad \text{for every } b = 1, \dots, N,$$

in other words the system tends to consensus. □

We discuss global stabilization of the HK model by using design tools of feedback control law based on an L^∞ approach; see Ref. [65] Section 2.

3.2.2 Local controllability

In this section, we discuss a local controllability strategy for the HK model. No information can be deduced on the local controllability around consensus from the linearized systems since, as the following example shows, it is not controllable.

Example 2. *Consider the linearization of system (3.9) around the consensus* $\mathbf{x}^{\mathrm{of}*}$. *The linearized system for the variable* $\widetilde{\mathbf{x}}^{\mathrm{of}} = \mathbf{x}^{\mathrm{of}} - \mathbf{x}^{\mathrm{of}*}$ *is given by*

$$\dot{\widetilde{\mathbf{x}}}^{\mathrm{of}} = \mathbf{A}^{\mathrm{of}}\widetilde{\mathbf{x}}^{\mathrm{of}} + \mathbf{B}^{\mathrm{of}}u^{\mathrm{of}}, \tag{3.14}$$

where $\mathbf{A}^{\mathrm{of}}$ *is a block matrix and* B *is a block vector as follows*

$$\mathbf{A}^{\mathrm{of}} = \begin{pmatrix} \mathbf{0}_{d,d} & \mathbf{0}_{d,d} & \cdots & \mathbf{0}_{d,d} \\ c_1\mathbf{I}_d & -(\sum_{j\neq 1} a_{1j} + c_1)\mathbf{I}_d & \cdots & a_{1N}\mathbf{I}_d \\ \vdots & \vdots & \ddots & \vdots \\ c_N\mathbf{I}_d & a_{N1}\mathbf{I}_d & \cdots & -(\sum_{j\neq N} a_{Nj} + c_N)\mathbf{I}_d \end{pmatrix}, \qquad \mathbf{B}^{\mathrm{of}} = \begin{pmatrix} \mathbf{I}_d \\ \mathbf{0}_{d,d} \\ \vdots \\ \mathbf{0}_{d,d} \end{pmatrix},$$

where $\mathbf{0}_{d,d}$ *is the* $d \times d$ *null matrix and* $\mathbf{I}_d$ *is the identity.*
Consider the simple case $N + 1 = 3$ *and* $d = 1$. *In this case the eigenvalues of* $\mathbf{A}^{\mathrm{of}}$ *are given by*

$$\begin{aligned} \lambda_1 &= 0, \\ \lambda_2 &= -1 - \frac{d_1}{2} - \frac{d_2}{2} - \frac{\sqrt{(d_1 - d_2)^2 + 4}}{2}, \\ \lambda_3 &= -1 - \frac{d_1}{2} - \frac{d_2}{2} + \frac{\sqrt{(d_1 - d_2)^2 + 4}}{2}, \end{aligned}$$

where $d_1 = \gamma\phi(\|x_1^{\mathrm{of}} - x_0^{\mathrm{of}}\|_2)$ *and* $d_2 = \gamma\phi(\|x_2^{\mathrm{of}} - x_0^{\mathrm{of}}\|_2)$. *The corresponding eigenvectors are*

$$w_1 = \begin{pmatrix} 1 \\ 1 \\ 1 \end{pmatrix}, \quad w_2 = \begin{pmatrix} 0 \\ \frac{d_2}{2} - \frac{d_1}{2} - \frac{\sqrt{(d_1 - d_2)^2 + 4}}{2} \\ 1 \end{pmatrix},$$

and

$$w_3 = \begin{pmatrix} 0 \\ \frac{d_2}{2} - \frac{d_1}{2} + \frac{\sqrt{(d_1 - d_2)^2 + 4}}{2} \\ 1 \end{pmatrix}.$$

In particular, by classical controllability results, such as the Hautus Lemma (see, for instance, Ref. [76] Lemma 3.3.7) system (3.21) *is not controllable since* $w_2^T\mathbf{B}^{\mathrm{of}} = 0$ *(and* $w_3^T\mathbf{B}^{\mathrm{of}} = 0$*).*

Following this example, it is possible to prove that if ϕ is constant on an interval $[0, \delta]$, then system (3.9) is not locally controllable. Indeed in this case, system (3.9) is linear whenever $\|\mathbf{x}^{\mathrm{of}} - \mathbf{x}^{\mathrm{of}*}\| < \delta$ for some consensus $\mathbf{x}^{\mathrm{of}*}$ and does not verify the rank

condition, necessary for controllability. For more general situation the local controllability depends on the communication rate ϕ between the leader and the agents and, a priori, we cannot infer the local controllability of the system. However the system verifies a very interesting local controllability property, that is the local controllability to consensus. As the following lemma states, if the agents are sufficiently close to each other they are attracted by the leader. The proof relies on the Lyapunov stability of the leader's state x_0^{of}.

Lemma 1. *Let $u(t) = 0$ for every $t \geq 0$. If $\|x_i^{\text{of}}(0) - x_0^{\text{of}}\| \leq \delta/N$ for every $i = 1, \dots, N$ then*

$$\lim_{t\to\infty} x_i^{\text{of}}(t) = x_0^{\text{of}}, \qquad \text{for every } i = 1, \dots, N.$$

Proof. Let $T \geq 0$ be the maximal time such that $\sum_i \|x_i^{\text{of}}(t) - x_0^{\text{of}}\|_2 \leq \delta$ on $t \in [0, T]$, with the convention that $T = +\infty$ if $\sum_i \|x_i^{\text{of}}(t) - x_0^{\text{of}}\|_2 \leq \delta$ for every $t \geq 0$. Then for every $t \in [0, T]$ the interaction coefficients between agents are

$$a_{ij} = a(\|x_i^{\text{of}} - x_j^{\text{of}}\|) = 1, \qquad \text{for every } i, j = 1, \dots, N.$$

For simplicity we set $c_i = \gamma\phi(\|x_i^{\text{of}}(t) - x_0^{\text{of}}(t)\|)$ and we drop the dependence on t. Hence

$$\begin{aligned}
\frac{d}{dt}\frac{1}{2N}\sum_{i=1}^{N}\|x_i^{\text{of}} - x_0^{\text{of}}\|^2 &= \frac{1}{N}\sum_{i=1}^{N}\langle \dot{x}_i^{\text{of}}, x_i^{\text{of}} - x_0^{\text{of}}\rangle \\
&= \frac{1}{N}\sum_i\sum_j\langle x_j^{\text{of}} - x_i^{\text{of}}, x_i^{\text{of}} - x_0^{\text{of}}\rangle - \frac{1}{N}\sum_i c_i\|x_i^{\text{of}} - x_0^{\text{of}}\|^2 \\
&= \frac{1}{N}\sum_i\sum_j\langle x_j^{\text{of}} - x_0^{\text{of}}, x_i^{\text{of}} - x_0^{\text{of}}\rangle - \sum_i\|x_i^{\text{of}} - x_0^{\text{of}}\|^2 \\
&\quad - \frac{1}{N}\sum_i c_i\|x_i^{\text{of}} - x_0^{\text{of}}\|^2 \\
&\leq \frac{1}{N}\sum_i\|x_i^{\text{of}} - x_0^{\text{of}}\|\sum_j\|x_j^{\text{of}} - x_0^{\text{of}}\| - \sum_i(1 + c_i/N)\|x_i^{\text{of}} - x_0^{\text{of}}\|^2 \\
&\leq \sum_i\|x_i^{\text{of}} - x_0^{\text{of}}\|^2 - \sum_i(1 + c_i/N)\|x_i^{\text{of}} - x_0^{\text{of}}\|^2 \\
&= -\sum_i c_i/N\|x_i^{\text{of}} - x_0^{\text{of}}\|^2 \\
&\leq -\gamma\phi(\delta/2)\frac{1}{N}\sum_i\|x_i^{\text{of}} - x_0^{\text{of}}\|^2. \qquad (3.15)
\end{aligned}$$

In particular the function $V(t) = \frac{1}{2N}\sum_{i=1}^{N}\|x_i^{\text{of}} - x_0^{\text{of}}\|^2$ is a Lyapunov function for the system. Moreover for every $t \geq 0$

$$\sum_i\|x_i^{\text{of}}(t) - x_0^{\text{of}}\| \leq \sum_i\|x_i^{\text{of}}(0) - x_0^{\text{of}}\| \leq \delta.$$

In particular the estimate (3.15) is valid for every $t \geq 0$ and

$$V(t) \leq \exp\left(-2\gamma\phi(\delta/2)t\right) V(0),$$

which gives that $x_i^{\rm of}(t) \to x_0^{\rm of}$ as $t \to +\infty$ for every $i = 1, \ldots, N$. □

As a consequence of this lemma and of Theorem 7, we have the following result of global stabilization and partial controllability.

Corollary 1. *For every initial condition* $\mathbf{x}^{\rm of}(0)$ *and for every consensus* $\mathbf{x}^{\rm of*}$ *there exists a control* u *such that the associated solution* $\mathbf{x}^{\rm of}(t)$ *of (2.4) with initial condition* $\mathbf{x}^{\rm of}(0)$ *tends to* $\mathbf{x}^{\rm of*}$.

Proof. Thanks to Theorem 7 there exist a consensus configuration $\bar{\mathbf{x}}^{\rm of} = (\bar{x}^{\rm of}, \ldots, \bar{x}^{\rm of})$ and a control u steering the solution $\mathbf{x}^{\rm of}(t)$ of (2.4) with initial condition $\mathbf{x}^{\rm of}(0)$ to $\bar{\mathbf{x}}^{\rm of}$. Let $t_1 > 0$ be a sufficiently large time such that

$$\|x_i^{\rm of}(t_1) - x_0^{\rm of}(t_1)\| \leq \frac{\delta}{2N}, \qquad \text{for every } i = 1, \ldots, N.$$

In particular,

$$\|x_i^{\rm of}(t_1) - \bar{x}_i^{\rm of}\| \leq \frac{\delta}{2N}, \qquad \text{for every } i = 0, \ldots, N.$$

Now consider the desired consensus configuration $\mathbf{x}^{\rm of*} = (x^{\rm of*}, \ldots, x^{\rm of*})$ and a finite sequence of points $z_0 = \bar{\mathbf{x}}^{\rm of}, z_1, \ldots, z_\ell, z_{\ell+1} = \mathbf{x}^{\rm of*}$ such that

$$\|z_k - z_{k+1}\| \leq \frac{\delta}{2N} \text{ for every } k = 0, \ldots, \ell.$$

Now, we apply iteratively Lemma 1 in order to construct a control steering the solution to every consensus configuration associated with the sequence $z_0, z_1, \ldots, z_\ell, z_{\ell+1}$. Assume, for $k \in \{0, \ldots, \ell\}$, that there exists $\tau > 0$ such that

$$\|x_i^{\rm of}(\tau) - z_k(\tau)\| \leq \frac{\delta}{2N}, \qquad \text{for every } i = 0, \ldots, N.$$

Then consider the control

$$u(t) = \begin{cases} M \dfrac{z_{k+1} - x_0^{\rm of}(t)}{\|z_{k+1} - x_0^{\rm of}(t)\|}, & \text{if } z_{k+1} \neq x_0^{\rm of} \\ 0, & \text{if } z_{k+1} = x_0^{\rm of}. \end{cases}$$

Hence

$$\frac{1}{2}\frac{d}{dt}\|x_0^{\rm of}(t) - z_{k+1}\|^2 = \langle u, x_0^{\rm of}(t) - z_{k+1}\rangle = -M\|x_0^{\rm of}(t) - z_{k+1}\|,$$

in particular $x_0^{\rm of}$ reaches z_{k+1} in finite time, say τ_k. Now $\|x_i^{\rm of}(\tau + \tau_k) - z_{k+1}\| \leq \delta/N$ for every $i = 1, \ldots, N$. Indeed for every $t \in [\tau, \tau + \tau_k]$ let $i = i(t)$ be such that

$\|x_i^{\rm of}(t) - z_{k+1}\|_2$ is maximal, then we have

$$\begin{aligned}\frac{d}{dt}\|x_i^{\rm of}(t) - z_{k+1}\|^2 &= \langle \dot{x}_i^{\rm of}(t), x_i^{\rm of}(t) - z_{k+1}\rangle \\ &= \sum_j \langle x_j^{\rm of}(t) - x_i^{\rm of}(t), x_i^{\rm of}(t) - z_{k+1}\rangle \\ &= \sum_j \langle x_j^{\rm of}(t) - z_{k+1}, x_i^{\rm of}(t) - z_{k+1}\rangle - N\|x_i^{\rm of}(t) - z_{k+1}\|^2 \\ &\le \sum_j \|x_j^{\rm of}(t) - z_{k+1}\|\|x_i^{\rm of}(t) - z_{k+1}\| - N\|x_i^{\rm of}(t) - z_{k+1}\|^2,\end{aligned}$$

which is smaller than or equal to 0 for the maximality of the index i. Therefore

$$\max_j \|x_j^{\rm of}(t) - z_{k+1}\| \le \max_j \|x_j^{\rm of}(0) - z_{k+1}\| \le \frac{\delta}{N},$$

or every $t \in [\tau, \tau + \tau_k]$. Then set the control $u(t) = 0$ for $t > \tau + \tau_k$ and by Lemma 1 we have that

$$\lim_{t\to\infty} x_i^{\rm of}(t) = z_{k+1}, \qquad \text{for every } i = 1, \dots, N.$$

The statement follows by induction on $k = 0, \dots, \ell$. □

3.3 Controllability of the Heider social balance model

Consider the following Heider social balance model

$$\dot{x}_{ij}^{\rm hb}(t) \;=\; \frac{1}{N-2}\left(1 - \frac{(x_{ij}^{\rm hb}(t))^2}{R^2}\right) \sum_{\substack{k=1\\ k\neq i,j}}^{N} x_{ik}^{\rm hb}(t) x_{kj}^{\rm hb}(t), \quad t \in [0, T], \tag{3.16}$$

for $i, j = 1, ..., N$, where $\mathbf{x}^{\rm hb} = (x_{12}^{\rm hb}, x_{13}^{\rm hb}, \dots, x_{1N}^{\rm hb}, x_{21}^{\rm hb}, \dots, x_{(N-1)N}^{\rm hb}) \in \mathbb{R}^{N_r}$ is the state of relationship of individual in the network. N and N_r represent the number of agents and the relation of people defined in (2.9). The parameter R is a given positive constant. Next, we discuss the stability of (3.16).

3.3.1 Stability of the Heider social balance model

In this section, we discuss stability of (3.16). In accordance to the Heider theory, the stable state of the HB model is defined as the balance in the triad of relation $\triangle_{ijk}$ between individuals i, j and k, and this balance is determined by the product of the values of the corresponding edges as follows

Definition 7. *The triad $\triangle_{ijk}$ of relationship between agents i, j and k is balanced if $x_{ij}^{\rm hb} x_{jk}^{\rm hb} x_{ki}^{\rm hb} > 0$, that is,*

$$sign(x_{ij}^{\rm hb} x_{jk}^{\rm hb} x_{ki}^{\rm hb}) = 1, \tag{3.17}$$

for any $i, j, k = 1, ..., N$ and i, j, k are not equal, otherwise the triad is imbalanced .

Concerning the evolution of the HB model towards a balanced state, we have the following result.

Proposition 2. *If $x_{ij}^{\rm hb}(0) \geq -R$, $i,j = 1,\ldots,N$, then there exits $T > 0$ such that all triads become balanced, that is, the product of links on triads $\triangle_{ijk}$ is positive*

$$x_{ij}^{\rm hb}(T)x_{jk}^{\rm hb}(T)x_{ki}^{\rm hb}(T) > 0 \quad \textit{for} \quad i,j,k = 1,...,N, \quad \textit{and} \quad i \neq j \neq k.$$

Proof. consider

$$\begin{aligned}
&\frac{d}{dt}\left(\sum_{\substack{i,j,k=1\\ i\neq j\neq k}}^{N} x_{ij}^{\rm hb}x_{jk}^{\rm hb}x_{ki}^{\rm hb}\right)\\
&= \sum_{\substack{i,j,k=1\\ i\neq j\neq k}}^{N}\left(\dot{x}_{ij}^{\rm hb}x_{jk}^{\rm hb}x_{ki}^{\rm hb} + x_{ij}^{\rm hb}\dot{x}_{jk}^{\rm hb}x_{ki}^{\rm hb} + x_{ij}^{\rm hb}x_{jk}^{\rm hb}\dot{x}_{ki}^{\rm hb}\right)\\
&= \sum_{i=1}^{N}\sum_{\substack{j=1\\ j\neq i}}^{N}\dot{x}_{ij}^{\rm hb}\left(\sum_{\substack{k=1\\ k\neq i,j}}^{N}x_{jk}^{\rm hb}x_{ki}^{\rm hb}\right) + \sum_{j=1}^{N}\sum_{\substack{k=1\\ k\neq j}}^{N}\dot{x}_{jk}^{\rm hb}\left(\sum_{\substack{i=1\\ i\neq k}}^{N}x_{ji}^{\rm hb}x_{ik}^{\rm hb}\right) + \sum_{i=1}^{N}\sum_{\substack{k=1\\ k\neq i}}^{N}\dot{x}_{ki}^{\rm hb}\left(\sum_{\substack{j=1\\ j\neq k}}^{N}x_{kj}^{\rm hb}x_{ji}^{\rm hb}\right)\\
&= \left(\frac{1}{N-2}\right)\left(\sum_{i=1}^{N}\sum_{\substack{j=1\\ j\neq i}}^{N}\left(1-\frac{(x_{ij}^{\rm hb})^2}{R^2}\right)\left(\sum_{\substack{k=1\\ k\neq i,j}}^{N}x_{ik}^{\rm hb}x_{kj}^{\rm hb}\right)^2 + \sum_{j=1}^{N}\sum_{\substack{k=1\\ j\neq j}}^{N}\left(1-\frac{(x_{jk}^{\rm hb})^2}{R^2}\right)\left(\sum_{\substack{i=1\\ i\neq j,k}}^{N}x_{ji}^{\rm hb}x_{ik}^{\rm hb}\right)^2\right)\\
&\quad + \left(\frac{1}{N-2}\right)\left(\sum_{i=1}^{N}\sum_{\substack{k=1\\ k\neq i}}^{N}\left(1-\frac{(x_{ik}^{\rm hb})^2}{R^2}\right)\left(\sum_{\substack{j=1\\ j\neq i,k}}^{N}x_{ij}^{\rm hb}x_{jk}^{\rm hb}\right)^2\right).
\end{aligned}$$

We have the following cases,

Case I : $|x_{ij}^{\rm hb}| < R$, for $i,j = 1,...,N$ and $i \neq j$.

In this case $\frac{d}{dt}\left(x_{ij}^{\rm hb}x_{jk}^{\rm hb}x_{ki}^{\rm hb}\right) > 0$, this implies that the product of links in each triads is increasing until $\exists T > 0$ such that $x_{ij}^{\rm hb} = R$ and it yields $\frac{d}{dt}\left(x_{ij}^{\rm hb}x_{jk}^{\rm hb}x_{ki}^{\rm hb}\right) = 0$.

Case II : $x_{ij}^{\rm hb} > R$, for $i,j = 1,...,N$ and $i \neq j$.

It is seen that $\frac{d}{dt}\left(x_{ij}^{\rm hb}x_{jk}^{\rm hb}x_{ki}^{\rm hb}\right) < 0$, this implies that the product of links in each triads is decreasing until $\exists T > 0$ such that $\frac{d}{dt}\left(x_{ij}^{\rm hb}x_{jk}^{\rm hb}x_{ki}^{\rm hb}\right) = 0$, that is $x_{ij}^{\rm hb} = R$.

Case III : $x_{ij}^{\rm hb} < -R$, for $i,j = 1,...,N$ and $i \neq j$.

In this case $\frac{d}{dt}\left(x_{ij}^{\rm hb}x_{jk}^{\rm hb}x_{ki}^{\rm hb}\right) < 0$, this implies that the product of links in

each triads is decreasing, this means that the value of x_{ij}^{hb} is decreasing and $\lim_{t\to\infty} x_{ij}^{\text{hb}}(t) = -\infty$.

□

The following Proposition establishes the asymptotic behavior of a balanced HB model.

Proposition 3. *If the HB model (3.16) is balanced, then*

$$\lim_{t\to\infty} x_{ij}^{\text{hb}}(t) = R \quad or \quad \lim_{t\to\infty} x_{ij}^{\text{hb}}(t) = -R, \tag{3.18}$$

for $i, j = 1, ..., N$ *and* $i \neq j$.

Proof. Consider

$$V(\mathbf{x}^{\text{hb}}) = \frac{1}{2}\sum_{i=1}^{N-1}\sum_{j=i+1}^{N}((x_{ij}^{\text{hb}})^2 - R^2)^2.$$

$$\begin{aligned}
\frac{dV(\mathbf{x}^{\text{hb}})}{dt} &= \sum_{i=1}^{N-1}\sum_{j=i+1}^{N}\frac{1}{2}\frac{d}{dt}((x_{ij}^{\text{hb}})^2 - R^2)^2 \\
&= \sum_{i=1}^{N-1}\sum_{j=i+1}^{N}((x_{ij}^{\text{hb}})^2 - R^2)\left(2x_{ij}^{\text{hb}}\dot{x}_{ij}^{\text{hb}}\right) \\
&= \sum_{i=1}^{N-1}\sum_{j=i+1}^{N}((x_{ij}^{\text{hb}})^2 - R^2)\left[2x_{ij}^{\text{hb}}\left(\frac{1}{N-2}\right)\left(1 - \frac{(x_{ij}^{\text{hb}})^2}{R^2}\right)\sum_{\substack{k=1\\k\neq i,j}}^{N} x_{ik}^{\text{hb}}x_{kj}^{\text{hb}}\right] \\
&= -\frac{2}{N-2}\sum_{i=1}^{N-1}\sum_{j=i+1}^{N}\left(\frac{((x_{ij}^{\text{hb}})^2 - R^2)^2}{R^2}\sum_{\substack{k=1\\k\neq i,j}}^{N} x_{ij}^{\text{hb}}x_{ik}^{\text{hb}}x_{kj}^{\text{hb}}\right).
\end{aligned}$$

Since (3.16) is balanced, every triads $\triangle_{ijk}$ is balanced, that is,

$$x_{ij}^{\text{hb}}x_{ik}^{\text{hb}}x_{kj}^{\text{hb}} > 0, \quad \text{for} \quad i, j, k = 1, ..., N, \text{and } i \neq j \neq k.$$

It yields $\dfrac{dV(x^{\text{hb}})}{dt} < 0.$ □

As a result of Proposition 2 and Proposition 3, if the relationship value of an edge starts with a value greater than or equal to $-R$, then the HB model reaches a balanced state where the trajectories of relationships may divide into two groups, one of them asymptotically reach the value R and the other the opposite value $-R$.

Next, we study the dynamics of (3.16) in the neighborhood of the equilibrium points $\mathbf{x}_1^{\text{hb}*} = \bar{R}$ and $\mathbf{x}_2^{\text{hb}*} = -\bar{R}$, where $\bar{R} = (R, ..., R) \in \mathbb{R}^{N_r}$. For this purpose, it is convenient to represent the HB model in the following form

$$\begin{aligned} \dot{\mathbf{x}}^{\text{hb}}(t) &= \mathbf{f}^{\text{hb}}(\mathbf{x}^{\text{hb}}), \\ \mathbf{x}^{\text{hb}}(0) &= \mathbf{x}_0^{\text{hb}}, \qquad t \in [0, T], \end{aligned} \tag{3.19}$$

where $\mathbf{x}^{\text{hb}} = (x_{12}^{\text{hb}}, x_{13}^{\text{hb}}, \ldots, x_{1N}^{\text{hb}}, x_{23}^{\text{hb}}, \ldots, x_{(N-1)N}^{\text{hb}}) \in \mathbb{R}^{Nr}$ and $\mathbf{f}^{\text{hb}}(\mathbf{x}^{\text{hb}})$ is the dynamics of the system.

The linearized HB model can be written as follows

$$\dot{\mathbf{x}}^{\text{hb}} = \mathbf{A}_n^{\text{hb}} \mathbf{x}^{\text{hb}},$$

where $\mathbf{A}_1^{\text{hb}}$ and $\mathbf{A}_2^{\text{hb}}$ denote the Jacobian matrix of $\mathbf{f}^{\text{hb}}$ with respect to $\mathbf{x}^{\text{hb}}$ at $\mathbf{x}_1^{\text{hb}*}$ and $\mathbf{x}_2^{\text{hb}*}$, respectively. They are given by

$$\mathbf{A}_n^{\text{hb}} = \begin{pmatrix} \frac{\partial f_{12}^{\text{hb}}}{\partial x_{12}^{\text{hb}}}(\mathbf{x}^{\text{hb}*}) & \frac{\partial f_{12}^{\text{hb}}}{\partial x_{13}^{\text{hb}}}(\mathbf{x}^{\text{hb}*}) & \cdots & \frac{\partial f_{12}^{\text{hb}}}{\partial x_{(N-1)N}^{\text{hb}}}(\mathbf{x}^{\text{hb}*}) \\ \frac{\partial f_{13}^{\text{hb}}}{\partial x_{12}^{\text{hb}}}(\mathbf{x}^{\text{hb}*}) & \frac{\partial f_{13}^{\text{hb}}}{\partial x_{13}^{\text{hb}}}(\mathbf{x}^{\text{hb}*}) & \cdots & \frac{\partial f_{13}^{\text{hb}}}{\partial x_{(N-1)N}^{\text{hb}}}(\mathbf{x}^{\text{hb}*}) \\ \vdots & \cdots & \cdots & \vdots \\ \frac{\partial f_{(N-1)N}^{\text{hb}}}{\partial x_{12}^{\text{hb}}}(\mathbf{x}^{\text{hb}*}) & \frac{\partial f_{(N-1)N}^{\text{hb}}}{\partial x_{13}^{\text{hb}}}(\mathbf{x}^{\text{hb}*}) & \cdots & \frac{\partial f_{(N-1)N}^{\text{hb}}}{\partial x_{(N-1)N}^{\text{hb}}}(\mathbf{x}^{\text{hb}*}) \end{pmatrix}.$$

$$\mathbf{A}_1^{\text{hb}} = \nabla_{\mathbf{x}^{\text{hb}}} \mathbf{f}^{\text{hb}}(\mathbf{x}_1^{\text{hb}*}) = \begin{pmatrix} -2R & 0 & \cdots & 0 \\ 0 & -2R & \cdots & 0 \\ \vdots & \cdots & \cdots & \vdots \\ 0 & 0 & \cdots & -2R \end{pmatrix}.$$

$$\mathbf{A}_2^{\text{hb}} = \nabla_{\mathbf{x}^{\text{hb}}} \mathbf{f}^{\text{hb}}(\mathbf{x}_2^{\text{hb}*}) = \begin{pmatrix} 2R & 0 & \cdots & 0 \\ 0 & 2R & \cdots & 0 \\ \vdots & \cdots & \cdots & \vdots \\ 0 & 0 & \cdots & 2R \end{pmatrix}.$$

Notice that with $\mathbf{A}_1^{\text{hb}}$, all eigenvalues of the linearized system are strictly less than zero and therefore the equilibrium point $\mathbf{x}_1^{\text{hb}*} = \bar{R}$ is asymptotically stable while the equilibrium point $\mathbf{x}_2^{\text{hb}*} = -\bar{R}$ is unstable since all eigenvalues of linearized system about $\mathbf{x}_2^{\text{hb}*} = -\bar{R}$ are strictly greater than zero.

To give experimental evidence of the theoretical results discussed above, in the Figures 3.1(a) and 3.1(b) we show numerical results of the Heider balance model with two different initial configurations. We chose $R = 5$. In Figure 3.1(a), at initial time

	initial time	final time
total triads($N_{\triangle}$)	1140	1140
balanced triads($N_{\triangle_b}$)	532	1140
unbalanced triads ($N_{\triangle_{ub}}$)	608	0

Table 3.1: The number of triads of relationship between people in group for Figure 3.1(a)

	initial time	final time
total triads($N_{\triangle}$)	1140	1140
balanced triads($N_{\triangle_b}$)	0	1140
unbalanced triads ($N_{\triangle_{ub}}$)	1140	0

Table 3.2: The number of triads of relationship between people in group for Figure 3.1(b)

$t_0 = 0$ the values of the relationships are distributed between $(-5, 5)$, while in Figure 3.1(b) all people in the network start with hostility. Additional details of the results of these experiments are given in Table 3.1 and Table 3.2, respectively.
We can see from the Figures 3.1(a) and 3.1(b) that people adjust their relationship so that the social group is balanced at final time. Moreover, as predicted by Proposition 2, when the HB model reaches the balance, the final states of relation are divided into two groups, one of them arrives to R, the other meets -R.
Next, we investigate numerically the stability properties of the HB model. Figure 3.2(a) shows that $\mathbf{x}_1^{\mathrm{hb}*} = R$ is asymptotically stable since the trajectories starting in a neighborhood of R asymptotically reach this point. Conversely, in Figure 3.2(b), taking a starting value close to the equilibrium point $\mathbf{x}_2^{\mathrm{hb}*} = -R$, we obtain trajectories that diverge from $-R$.

3.3.2 Local controllability of the Heider social balance model

In this section, we discuss a local controllability strategy for the HB system. As addressed in (2.10), we recall that the control of the HB system is governed by the following set of differential equations

$$\begin{aligned} \dot{\mathbf{x}}_{0i}^{\mathrm{hb}}(t) &= u_i^{\mathrm{hb}}(t), \\ \dot{\mathbf{x}}_{ij}^{\mathrm{hb}}(t) &= \frac{1}{N-2}\left(1 - \frac{(x_{ij}^{\mathrm{hb}})^2}{R^2}\right) \sum_{\substack{k=1 \\ k\neq i,j}}^{N} x_{ik}^{\mathrm{hb}} x_{kj}^{\mathrm{hb}} + \gamma x_{0i}^{\mathrm{hb}} x_{0j}^{\mathrm{hb}}, \quad \text{for} \quad i,j = 1,...,N, \end{aligned} \tag{3.20}$$

with given initial relationships $x_{ij}^{\mathrm{hb}}(t_0) = x_{ij}^{\mathrm{hb}}(0)$. The number of relations , the number of controls and the number of uncontrols are given by

$$N_r = \frac{(N+1)N}{2}, \quad N_c = N, \quad N_{uc} = N_r - N_c.$$

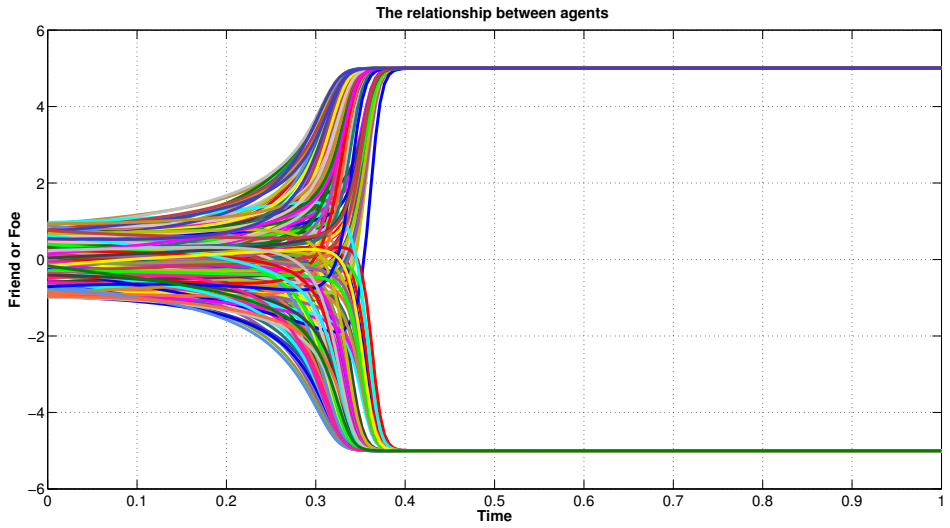

(a) $x_{ij}^{\mathrm{hb}}(0) \in (-5, 5)$

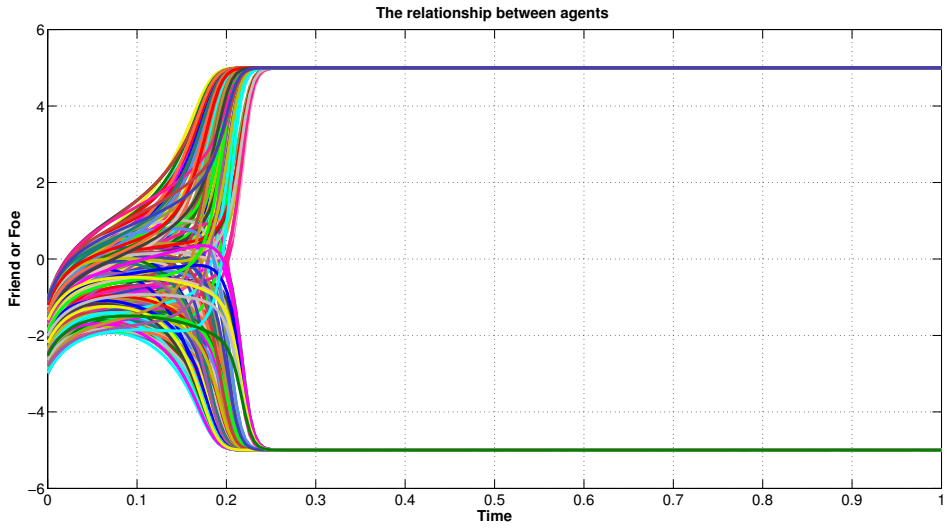

(b) $x_{ij}^{\mathrm{hb}}(0) \in (-5, 0)$

Figure 3.1: Simulation with $N = 20$ agents. The status of relation of individuals in figure(a) are started with friendship and hostility. Figure (b) show the relation of all agents begin with hostility.

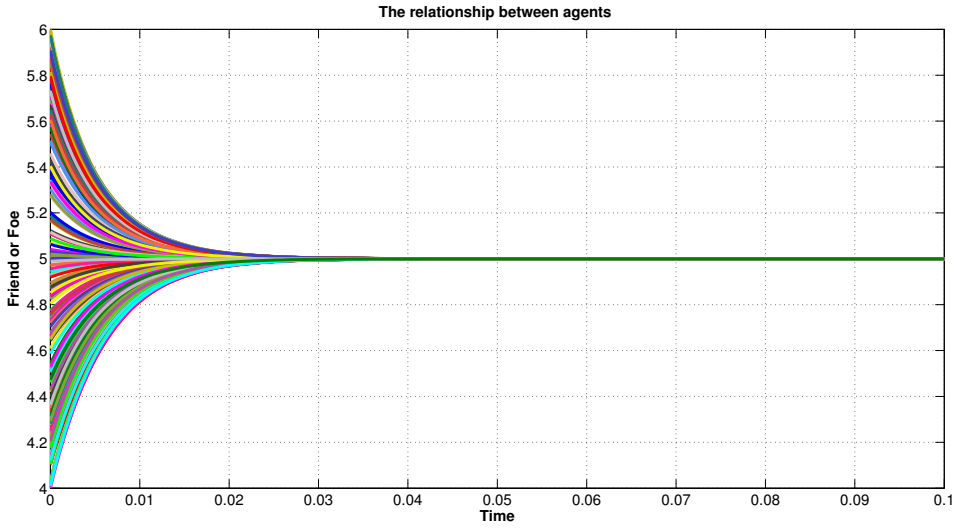

(a) $x_{ij}^{\mathrm{hb}}(0) \in [4, 6]$

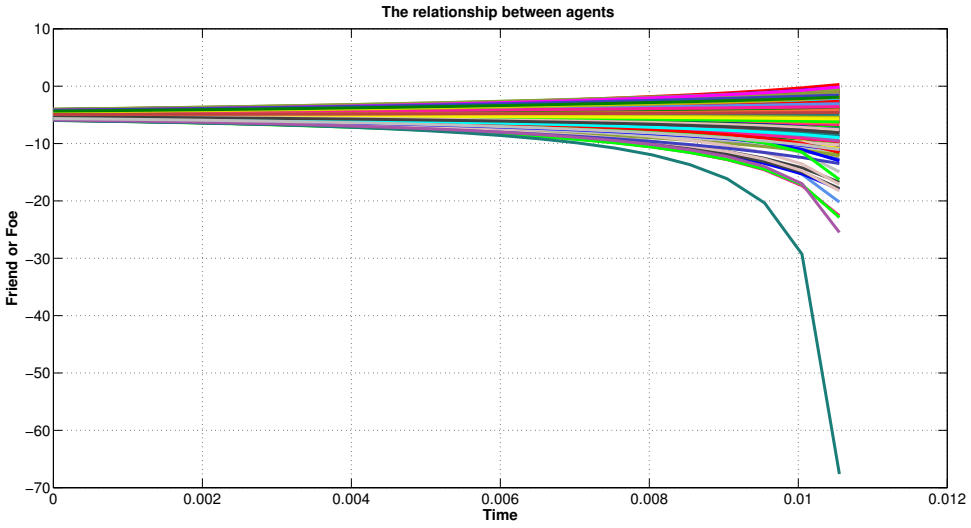

(b) $x_{ij}^{\mathrm{hb}}(0) \in [-6, -4]$

Figure 3.2: Simulation with $N = 20$ agents. Figure(a) show solution . Figure (b) show the relation of all agents begin with hostility.

Next, we consider the linearization of this system around the equilibrium points $\mathbf{x}_1^{\mathrm{hb}*} = R$ and $\mathbf{x}_2^{\mathrm{hb}*} = -R$. The linearized system for the variable $\widetilde{\mathbf{x}}^{\mathrm{hb}} = \mathbf{x}^{\mathrm{hb}} - \mathbf{x}^{\mathrm{hb}*}$ is given by

$$\dot{\widetilde{\mathbf{x}}}^{\mathrm{hb}} = \widetilde{\mathbf{A}}^{\mathrm{hb}}\widetilde{\mathbf{x}}^{\mathrm{hb}} + \mathbf{B}^{\mathrm{hb}}\mathbf{u}^{\mathrm{hb}}, \tag{3.21}$$

where $\widetilde{\mathbf{A}}^{\mathrm{hb}}$ is a block matrix and $\mathbf{B}^{\mathrm{hb}}$ is a block vector as follows

$$\widetilde{\mathbf{A}}^{\mathrm{hb}} = \begin{pmatrix} \mathbf{0}_{N_c,N_c} & \mathbf{0}_{N_c,N_{uc}} \\ \mathbf{L}^{\mathrm{hb}} & \mathbf{D}^{\mathrm{hb}} \end{pmatrix}, \qquad \mathbf{B}^{\mathrm{hb}} = \begin{pmatrix} \mathbf{I}_{N_c} \\ \mathbf{0}_{N_{uc},N_{uc}} \end{pmatrix}, \tag{3.22}$$

where $\mathbf{L}^{\mathrm{hb}} \in \mathbb{R}^{N_{uc}\times N_c}$ and $\mathbf{D}^{\mathrm{hb}} \in \mathbb{R}^{N_{uc}\times N_{uc}}$ are presented as follows

$$\begin{aligned} \mathbf{L}^{\mathrm{hb}} &= \gamma \begin{pmatrix} \mathbf{x}^{\mathrm{hb}*} & \mathbf{x}^{\mathrm{hb}*} & 0 & \cdots & 0 \\ \mathbf{x}^{\mathrm{hb}*} & 0 & \mathbf{x}^{\mathrm{hb}*} & \cdots & 0 \\ \vdots & \vdots & \vdots & \ddots & \vdots \\ \mathbf{x}^{\mathrm{hb}*} & 0 & 0 & \cdots & \mathbf{x}^{\mathrm{hb}*} \\ 0 & \mathbf{x}^{\mathrm{hb}*} & \mathbf{x}^{\mathrm{hb}*} & \cdots & 0 \\ \vdots & \vdots & \vdots & \ddots & \vdots \\ 0 & 0 & 0 & \mathbf{x}^{\mathrm{hb}*} & \mathbf{x}^{\mathrm{hb}*} \end{pmatrix}_{N_{uc},N_c}, \\ \mathbf{D}^{\mathrm{hb}} &= \begin{pmatrix} -2\mathbf{x}^{\mathrm{hb}*} & 0 & \cdots & 0 \\ 0 & -2\mathbf{x}^{\mathrm{hb}*} & \cdots & 0 \\ \vdots & \vdots & \ddots & 0 \\ 0 & 0 & 0 & -2\mathbf{x}^{\mathrm{hb}*} \end{pmatrix}_{N_{uc},N_{uc}}. \end{aligned}$$

We can see that rank of the Kalmann matrix $K(A,B)$

$$\begin{aligned} \mathbf{K}(\widetilde{\mathbf{A}}^{\mathrm{hb}}, \mathbf{B}^{\mathrm{hb}}) &= \begin{bmatrix} \mathbf{B}^{\mathrm{hb}} & \widetilde{\mathbf{A}}^{\mathrm{hb}}\mathbf{B}^{\mathrm{hb}} & (\widetilde{\mathbf{A}}^{\mathrm{hb}})^2\mathbf{B}^{\mathrm{hb}} & ... & (\widetilde{\mathbf{A}}^{\mathrm{hb}})^{N_r-1}\mathbf{B}^{\mathrm{hb}} \end{bmatrix} \\ &= \begin{bmatrix} \begin{pmatrix} \mathbf{I}_{N_c} \\ \mathbf{0}_{N_{uc},N_c} \end{pmatrix} & \begin{pmatrix} \mathbf{0}_{N_c,N_c} \\ \mathbf{L}^{\mathrm{hb}} \end{pmatrix} & \begin{pmatrix} \mathbf{0}_{N_c,N_c} \\ \mathbf{L}^{\mathrm{hb}}\mathbf{D}^{\mathrm{hb}} \end{pmatrix} & \cdots & \begin{pmatrix} \mathbf{0}_{N_c,N_c} \\ \mathbf{L}^{\mathrm{hb}}(\mathbf{D}^{\mathrm{hb}})^{N_r-2} \end{pmatrix} \end{bmatrix}. \end{aligned} \tag{3.23}$$

is equal to $2N_c$, that is, it has full rank if $N_{uc} = N_c$, otherwise not. If the Kalman rank condition is fulfilled then the model (3.20) is locally controllable, otherwise one cannot infer any controllability property for this model. An example for a locally controllable system is given in the case of three agents and one leader such that $N_r = 6$, $N_c = 3$, and $N_{uc} = 3$.

3.4 Controllability of the refined flocking model

In this section, we investigate stability and local controllability of the refined flocking model with leadership presented in (2.18). Recall this system given by

$$\begin{aligned} \dot{x}_0^{\mathrm{fm}} &= v_0^{\mathrm{fm}}, \\ \dot{x}_b^{\mathrm{fm}} &= v_b^{\mathrm{fm}}, \\ \dot{v}_0^{\mathrm{fm}} &= S_0 + M_0 + E_0 + u^{\mathrm{fm}}(t), \\ \dot{v}_b^{\mathrm{fm}} &= S_b + M_b + E_b + L_b, \qquad \text{for} \quad b = 1, ..., N. \end{aligned} \tag{3.24}$$

It can be written in the general form,

$$\dot{\mathbf{x}}^{\mathrm{fm}} = \mathbf{f}^{\mathrm{fm}}(\mathbf{x}^{\mathrm{fm}}) + \mathbf{B}^{\mathrm{fm}} u^{\mathrm{fm}}(t), \tag{3.25}$$

where the vector $\mathbf{x}^{\mathrm{fm}} := (x^{\mathrm{fm}}, v^{\mathrm{fm}})^\top = (x_0^{\mathrm{fm}}, x_1^{\mathrm{fm}}, \ldots, x_N^{\mathrm{fm}}, v_0^{\mathrm{fm}}, v_1^{\mathrm{fm}}, \ldots, v_N^{\mathrm{fm}})^\top \in \mathbb{R}^{2d(N+1)}$ is the state variable. The vector-value function $\mathbf{f}^{\mathrm{fm}} : \mathbb{R}^{2d(N+1)} \to \mathbb{R}^{2d(N+1)}$ and the constant matrix $\mathbf{B}^{\mathrm{fm}}$ are given as follows

$$\mathbf{f}^{\mathrm{fm}}(\mathbf{x}^{\mathrm{fm}}) = \begin{pmatrix} v_0^{\mathrm{fm}} \\ v_1^{\mathrm{fm}} \\ \vdots \\ v_N^{\mathrm{fm}} \\ S_0 + M_0 + E_0 \\ S_1 + M_1 + E_1 + L_1^0 \\ \vdots \\ S_N + M_N + E_N + L_N^0 \end{pmatrix}, \qquad \mathbf{B}^{\mathrm{fm}} = \begin{pmatrix} \mathbf{0}_{d,d} \\ \mathbf{0}_{d,d} \\ \vdots \\ \mathbf{0}_{d,d} \\ \mathbf{I}_d \\ \mathbf{0}_{d,d} \\ \vdots \\ \mathbf{0}_{d,d} \end{pmatrix}. \tag{3.26}$$

We write $\mathbf{f}^{\mathrm{fm}}(\mathbf{x}^{\mathrm{fm}})$ in the simple form,

$$\mathbf{f}^{\mathrm{fm}}(\mathbf{x}^{\mathrm{fm}}) = \begin{pmatrix} \mathbf{f}_x \\ \mathbf{f}_v \end{pmatrix}, \tag{3.27}$$

where the function $\mathbf{f}_x \in \mathbb{R}^{d(N+1)}$ and $\mathbf{f}_v \in \mathbb{R}^{d(N+1)}$ represent the dynamics of flocking corresponding to the position and velocity, respectively. They are given by

$$\mathbf{f}_x := \begin{pmatrix} v_0 \\ v_1 \\ \vdots \\ v_N \end{pmatrix}, \qquad \mathbf{f}_v := \begin{pmatrix} S_0 + M_0 + E_0 \\ S_0 + M_1 + E_1 + L_1 \\ \vdots \\ S_N + M_N + E_N + L_N \end{pmatrix}. \tag{3.28}$$

The existence and uniqueness of the solution of the refined flocking system require Lipschitz continuity of the function $\mathbf{f}^{\mathrm{fm}}$, which is a combination of several functions, namely, S_i, M_i, E_i and L_i, for $i = 0, 1, ..., N$. In the following Propositions we discuss Lipschitz continuity of S_i, M_i, E_i, and L_b, for $i = 0, 1, ..., N$ and $b = 1, ..., N$.

Let us define

$$\begin{aligned} D_x &= \{y \in \mathbb{R}^d : \epsilon \le \|x - y\| \le c, \quad y \ne x, \text{ and } \epsilon, c > 0\} \subset \mathbb{R}^d, \\ D_v &= \{v \in \mathbb{R}^d : \|v\| \le c_1, \quad c_1 > 0\} \subset \mathbb{R}^d. \end{aligned}$$

Proposition 4. *The function $\widetilde{s} : D_v \to \mathbb{R}^d$ given by*

$$\widetilde{s}(w) := (\alpha - \beta\|w\|^2)w, \quad \alpha, \beta > 0,$$

is locally Lipschitz on D_v

Proof. Since $\widetilde{s}$ is a product of two locally Lipschitz continuous function defined on D_v, namely,

$$s_1(w) = \alpha - \beta\|w\|^2 \quad \text{and} \quad s_2(w) = w.$$

Therefore $\widetilde{s}$ is locally Lipschitz continuous on D. Moreover, its derivative

$$\frac{d}{dw}\widetilde{s}(w) = (\alpha - \beta\|w\|^2)\mathbf{I}_d - 2\beta ww^\top \tag{3.29}$$

is also continuous. It follows that $\widetilde{s}$ is continuously differentiable, $\widetilde{s} \in C^1(D_v, \mathbb{R}^d)$. □

Proposition 5. *Let the function $m : D_x \times D_x \to \mathbb{R}^d$ is defined as*

$$m(x,y) := \left(\frac{C_a}{l_a}e^{-\frac{\|x-y\|}{l_a}} - \frac{C_r}{l_r}e^{-\frac{\|x-y\|}{l_r}}\right)\frac{x-y}{\|x-y\|}, \quad C_a, C_r, l_a, l_r > 0, \quad x \neq y.$$

Then m is locally Lipschitz on $D_x \times D_x$.

Proof. For a sake of simplification, we write $m(x,y)$ as the production of m_1 and m_2 given by

$$m_1(x,y) = \frac{C_a}{l_a}e^{-\frac{\|x-y\|}{l_a}} - \frac{C_r}{l_r}e^{-\frac{\|x-y\|}{l_r}}, \quad \text{and} \quad m_2(x,y) = \frac{x-y}{\|x-y\|}, \quad x \neq y.$$

It can be seen that m_1 has the following properties

- m_1 is continuous on $D_x \times D_x$,
- $\|m_1(x,y)\| \leq |\frac{C_a}{l_a}| + |\frac{C_r}{l_r}|$,
- the derivative of m_1 with respect to x and y is continuous,

$$\begin{aligned} \frac{\partial m_1}{\partial x} &= \frac{(x-y)^\top}{\|x-y\|}\left(\frac{C_r}{l_r^2}e^{-\frac{\|x-y\|}{l_r}} - \frac{C_a}{l_a^2}e^{-\frac{\|x-y\|}{l_a}}\right) = -\frac{\partial m_1}{\partial y}, \\ \|\frac{\partial m_1}{\partial x}\| &\leq |\frac{C_a}{l_a^2}| + |\frac{C_r}{l_r^2}|. \end{aligned}$$

In addition, m_2 is continuous on $D_x \times D_x$. We notice that

$$\frac{\partial m_2}{\partial x} = \frac{1}{\|x-y\|}\mathbf{I}_d - \frac{(x-y)(x-y)^\top}{\|x-y\|^2}, \quad \frac{\partial m_2}{\partial y} = -\frac{\partial m_2}{\partial x}.$$

Hence m is locally Lipschitz continuous on $D_x \times D_x$. □

Proposition 6. *Let the functions $\omega : D_x \times D_x \to \mathbb{R}$, $\hbar : D_x \times D_x \times D_v \to \mathbb{R}$, and $g : \mathbb{R} \to \mathbb{R}$ are defined as follows,*

$$\begin{aligned} \omega(x,y) &= \frac{\gamma}{(1+\|x-y\|^2)^\sigma}, \\ r = \hbar(x,y,v) &= \frac{\langle y-x, v\rangle}{\|y-x\|\|v\|}, \quad x \neq y, v \neq 0, \\ g(r) &= \begin{cases} 1, & \text{if} \quad r \geq \delta_1, \\ \frac{1}{2} - \frac{1}{2}\tanh\left(\frac{1}{r-\delta_2} + \frac{1}{r-\delta_1}\right), & \text{if} \quad \delta_2 < r < \delta_1, \\ 0, & \text{if} \quad r \leq \delta_2. \end{cases} \end{aligned} \tag{3.30}$$

Let $D \subseteq (D_x)^2 \times (D_v)^2$. The function $\varpi : D \to \mathbb{R}^d$ is defined as

$$\varpi(x,y,v,z) := \omega(x,y) \cdot g(r) \cdot (z-v). \tag{3.31}$$

Then ϖ is locally Lipschitz continuous on D.

Proof. It can be seen that ϖ has the following properties

- ϖ is continuous on D, due to continuity of ω on $D_x \times D_x$ and g on $\mathbb{R}$,
- $\|\varpi(x,y,v,z)\| \leq (1 + \|x\|+\|y\|+\|v\|+\|z\|)$, since $\|\omega(x,y)\| \leq \gamma$, $|g(r)| \leq 1$, and $|r| \leq 1$.

The derivative of $\varpi(x,v)$ with respect to x, y, v, and z are given as the following,

$$\begin{aligned} \frac{\partial \varpi}{\partial x} &= \left(\frac{\partial \omega(x,y)}{\partial x} g(r) + \omega(x,y)\frac{\partial g(r)}{\partial r}\frac{\partial r}{\partial x}\right)(v-z), \\ \frac{\partial \varpi}{\partial y} &= \left(\frac{\partial \omega(x,y)}{\partial y} g(r) + \omega(x,y)\frac{\partial g(r)}{\partial r}\frac{\partial r}{\partial y}\right)(v-z), \\ \frac{\partial \varpi}{\partial v} &= \left(\omega(x,y)\frac{\partial g(r)}{\partial r}\frac{\partial r}{\partial v}\right)(v-w) - \omega(x,y)g(r)I_{d,d}, \\ \frac{\partial \varpi}{\partial z} &= \omega(x,y)g(r)I_{d,d}, \end{aligned}$$

where

$$\begin{aligned} \frac{\partial \omega(x,y)}{\partial x} &= \frac{2\sigma(x-y)^\top}{(1+\|x-y\|_2^2)^{\sigma+1}}, \quad \text{and} \quad \frac{\partial \omega(x,y)}{\partial y} = -\frac{\partial \omega(x,y)}{\partial x}, \\ \frac{d}{dr}g(r) &= \begin{cases} -\frac{1}{2}\left(\tanh^2\left(\frac{1}{r-\delta_2} + \frac{1}{r-\delta_1}\right) - 1\right)\left(\frac{1}{(r-\delta_1)^2} + \frac{1}{(r-\delta_2)^2}\right), & \text{if} \quad \delta_2 < r < \delta_1, \\ 0, & \text{else} \end{cases} \\ \frac{\partial r}{\partial x} &= \frac{\langle y-x, v\rangle}{\|y-x\|^3\|v\|}(y-x)^\top - \frac{v^\top}{\|y-x\|\|v\|}, \quad \text{and} \quad \frac{\partial r}{\partial y} = -\frac{\partial r}{\partial x}, \\ \frac{\partial r}{\partial v} &= -\frac{\langle y-x, v\rangle}{\|y-x\|^2\|v\|^3}v^\top + \frac{(y-x)^\top}{\|y-x\|\|v\|}. \end{aligned}$$

We see that ϖ is Locally Lipschitz on D following from the fact that ϖ,$\dfrac{\partial \varpi}{\partial x}$, $\dfrac{\partial \varpi}{\partial y}$,$\dfrac{\partial \varpi}{\partial v}$, and $\dfrac{\partial \varpi}{\partial z}$ are all continuous on D. □

Remark 3. *Let* $x = (x_1, x_2, \ldots, x_d) \in \mathbb{R}^d$,

$$xx^\top = \begin{pmatrix} x_1^2 & x_1x_2 & \ldots & x_1x_{d-1} & x_1x_d \\ x_1x_2 & x_2^2 & \ldots & x_2x_{d-1} & x_2x_d \\ \vdots & \vdots & \ddots & \vdots & \vdots \\ x_dx_1 & x_dx_2 & \ldots & x_dx_{d-1} & x_d^2 \end{pmatrix}.$$

It can be seen that $\|xx^\top\| = \|x\|^2$, *since*

$$\begin{aligned} \|xx^\top\|^2 &= tr\left((xx^\top)^\top(xx^\top)\right) \\ &= tr\left((x^\top x)(xx^\top)\right) \\ &= tr\left(\langle x, x\rangle(xx^\top)\right) \\ &= \langle x, x\rangle tr\left(xx^\top\right) \\ &= \langle x, x\rangle\langle x, x\rangle \\ &= \|x\|^4. \\ \Rightarrow \|xx^\top\| &= \|x\|^2, \end{aligned}$$

where $tr(A) = \sqrt{A^\top A}$, *for matrix* $A \in \mathbb{R}^{n\times m}$.

3.4.1 Stability of the refined flocking system

Consider the refined flocking system including a leader and without control, as follows

$$\dot{\mathbf{x}}^{\mathrm{fm}} = \mathbf{f}^{\mathrm{fm}}(\mathbf{x}^{\mathrm{fm}}), \tag{3.32}$$

with given initial conditions. Let $(\mathbf{x}^{\mathrm{fm}}(t), \mathbf{v}^{\mathrm{fm}}(t))^\top \in C^1([0,\infty); \mathbb{R}^{2d(N+1)})$ be a solution of the refined flocking system (3.32). The next step is to introduce notation for discussing stability of flocking states.

Notations 2. *For every* $\mathbf{x}^{\mathrm{fm}}(t), \mathbf{v}^{\mathrm{fm}}(t) \in \mathbb{R}^{d(N+1)}$, *we define the quantities*

- *The mean position and the mean velocity are denoted by*

$$\bar{\mathbf{x}}^{\mathrm{fm}}(t) = \frac{1}{N+1}\sum_{i=0}^{N} x_i^{\mathrm{fm}}(t), \quad \bar{\mathbf{v}}^{\mathrm{fm}}(t) = \frac{1}{N+1}\sum_{i=0}^{N} v_i^{\mathrm{fm}}(t), \tag{3.33}$$

  respectively, for $i = 0, 1, ..., N$.

- *The dispersion is denoted by*

$$\Gamma(\mathbf{x}^{\mathrm{fm}}) = \frac{1}{2(N+1)^2}\sum_{i,j=0}^{N} \|x_i^{\mathrm{fm}}(t) - x_j^{\mathrm{fm}}(t)\|^2. \tag{3.34}$$

- *The disagreement is defined as*

$$\Lambda(\mathbf{v}^{\mathrm{fm}}) = \frac{1}{2(N+1)^2} \sum_{i,j=0}^{N} \|v_i^{\mathrm{fm}}(t) - v_j^{\mathrm{fm}}(t)\|^2. \tag{3.35}$$

Our aim is to investigate collective behavior of our flocking model under the influence of leadership. A control design objective is concerned with the stabilization problem, that is, to find control functions that drive all states to the consensus state. From mathematical point of view, consensus is defined as follows

Definition 8. *(Consensus point) [20]*
Let $\mathcal{V}_e$ be a set defined as follows

$$\mathcal{V}_e = \{w = (w_0, w_1, \ldots, w_N) \in \mathbb{R}^{d(N+1)} | \quad w_0 = w_1 = \ldots = w_N \in \mathbb{R}^d\}. \tag{3.36}$$

A steady configuration of the system (3.32) $(\mathbf{x}^{\mathrm{fm}}, \mathbf{v}^{\mathrm{fm}}) \in (\mathbb{R}^d)^{N+1} \times \mathcal{V}_e$ is called a ***consensus point*** *in the sense that the dynamics originating from $(\widetilde{\mathbf{x}}, \widetilde{\mathbf{v}})$ is simply given by rigid translation $\mathbf{x}^{\mathrm{fm}}(t) = \widetilde{\mathbf{x}} + t\bar{\mathbf{v}}^{\mathrm{fm}}$.*

Definition 9. *(Consensus)[20]*
We say that a solution $(\mathbf{x}^{\mathrm{fm}}(t), \mathbf{v}^{\mathrm{fm}}(t))$ of the system (3.32) tends to consensus e mean the consensus parameters vector tends to the mean $\bar{\mathbf{v}}^{\mathrm{fm}}$, that is, if

$$\lim_{t\to\infty} \|v_i^{\mathrm{fm}}(t) - \bar{v}^{\mathrm{fm}}\| = 0, \quad \textit{for} \quad i = 0, ..., N. \tag{3.37}$$

Remark 4. *The following definitions of consensus are equivalent:*

1. $\lim_{t\to\infty} v_i^{\mathrm{fm}}(t) = \bar{\mathbf{v}}^{\mathrm{fm}}$ *for every* $i = 0, 1, ..., N$,
2. $\lim_{t\to\infty} \Lambda(\mathbf{v}^{\mathrm{fm}}(t)) = 0$.

A consensus state in our sense is known as a flocking state having the following properties,

1. **Cohesion**
   Cohesion is the situation that agents stay on the bounded domain. In our case, we observe that flock configuration corresponding to annulus with a radius given by the minimum of the Morse potential, that is,

$$\nabla_x U(\|x_i^{\mathrm{fm}} - x_j^{\mathrm{fm}}\|) = 0 \quad \text{and} \quad \nabla_x U^0(\|x_0^{\mathrm{fm}} - x_b^{\mathrm{fm}}\|) = 0, \tag{3.38}$$

   for all $i, j = 0, 1, \ldots, N$ and $b = 1, \ldots, N$, that is, in the situation that

$$\left(\frac{x_i^{\mathrm{fm}} - x_j^{\mathrm{fm}}}{\|x_i^{\mathrm{fm}} - x_j^{\mathrm{fm}}\|}\right)\left(\frac{C_a}{l_a} e^{-\frac{\|x_i^{\mathrm{fm}} - x_j^{\mathrm{fm}}\|}{l_a}} - \frac{C_r}{l_r} e^{-\frac{\|x_i^{\mathrm{fm}} - x_j^{\mathrm{fm}}\|}{l_r}}\right) = 0,$$

$$\left(\frac{x_0^{\mathrm{fm}} - x_b^{\mathrm{fm}}}{\|x_b^{\mathrm{fm}} - x_0^{\mathrm{fm}}\|}\right)\left(\frac{C_a^0}{l_a^0} e^{-\frac{\|x_0^{\mathrm{fm}} - x_b^{\mathrm{fm}}\|}{l_a^0}} - \frac{C_r^0}{l_r^0} e^{-\frac{\|x_0^{\mathrm{fm}} - x_b^{\mathrm{fm}}\|}{l_r^0}}\right) = 0,$$

for all $i, j = 0, 1, \ldots, N$. Since we assume that no collision occurs, $x_i^{\text{fm}} \neq x_j^{\text{fm}}$. As a consequence, we obtain that

$$\begin{aligned}\left(\frac{C_a}{l_a}e^{-\frac{\|x_i^{\text{fm}}-x_j^{\text{fm}}\|}{l_a}} - \frac{C_r}{l_r}e^{-\frac{\|x_i^{\text{fm}}-x_j^{\text{fm}}\|}{l_r}}\right) &= 0, \\ \left(\frac{C_a^0}{l_a^0}e^{-\frac{\|x_0^{\text{fm}}-x_b^{\text{fm}}\|}{l_a^0}} - \frac{C_r^0}{l_r^0}e^{-\frac{\|x_0^{\text{fm}}-x_b^{\text{fm}}\|}{l_r^0}}\right) &= 0.\end{aligned} \tag{3.39}$$

When the swarm reaches the flocking state, the approximated distance between agents is obtained as follows

$$\begin{aligned}\lim_{t\to\infty}\left(\frac{1}{2(N+1)^2}\sum_{i,j=0}^{N}\sum_{i,j=0}^{N}\|x_i^{\text{fm}}(t)-x_j^{\text{fm}}(t)\|\right) &= \ln\left(\frac{C_r}{l_r}\frac{l_a}{C_a}\right)\cdot\frac{l_a l_r}{(l_a-l_r)}, \\ \lim_{t\to\infty}\left(\frac{1}{N}\sum_{i,j=0}^{N}\sum_{b=1}^{N}\|x_0^{\text{fm}}(t)-x_b^{\text{fm}}(t)\|\right) &= \ln\left(\frac{C_r^0}{l_r^0}\frac{l_a^0}{C_a^0}\right)\cdot\frac{l_a^0 l_r^0}{(l_a^0-l_r^0)},\end{aligned} \tag{3.40}$$

with given parameters $C_a, C_r, C_a^0, C_r^0, l_a, l_r, l_a^0, l_r^0 > 0$.

2. **Alignment**
   Alignment is the process such that each agent tries to match its velocity to that of other agents in the group. In a flocking state all agents move with the same velocity given by
$$v_0^{\text{fm}} = v_1^{\text{fm}} = \ldots = v_N^{\text{fm}}. \tag{3.41}$$

In order to explain stability of the flocking model, it is convenient to define the following quantities,

$$\begin{aligned}q_{ij}(t) &:= \frac{\gamma}{(1+\|x_i^{\text{fm}}(t)-x_j^{\text{fm}}(t)\|^2)^{\sigma}}S\left(\frac{\langle x_j^{\text{fm}}-x_i^{\text{fm}}, v_i^{\text{fm}}\rangle}{\|x_j^{\text{fm}}(t)-x_i^{\text{fm}}(t)\|\|v_i^{\text{fm}}\|}\right), \\ c_{ij}(t) &:= \frac{1}{\|x_i^{\text{fm}}(t)-x_j^{\text{fm}}(t)\|}\left(\frac{C_a}{l_a}e^{-\frac{\|x_i^{\text{fm}}-x_j^{\text{fm}}\|}{l_a}} - \frac{C_r}{l_r}e^{-\frac{\|x_i^{\text{fm}}-x_j^{\text{fm}}\|}{l_r}}\right), \\ c_b^0(t) &:= \frac{\gamma_1}{\|x_0^{\text{fm}}(t)-x_b^{\text{fm}}(t)\|}\left(\frac{C_a^0}{l_a^0}e^{-\frac{\|x_0^{\text{fm}}-x_b^{\text{fm}}\|}{l_a^0}} - \frac{C_r^0}{l_r^0}e^{-\frac{\|x_0^{\text{fm}}-x_b^{\text{fm}}\|}{l_r^0}}\right),\end{aligned} \tag{3.42}$$

for $i, j = 0, \ldots, N$, $b = 1, \ldots, N$.

Proposition 7. *Let $V_{\max}(t) = \max_i\|v_i^{\text{fm}}(t)\|$ and assume that $V_{\max}(0) \geq \sqrt{\frac{\alpha}{\beta}}$. If the swarm reaches the cohesive state, then the velocity of the swarm stays bounded by $V_{\max}(0)$.*

Proof. Since $t \mapsto \|v_i(t)\|^2$ are C^1 functions, we can for each t find a time interval $[a, b]$ which contains t and an index $\bar{n}$ such that $V_{\max}(\tau) = \|v_{\bar{n}}^{\text{fm}}\|$ for all $\tau \in [a, b]$. Since dynamics of leader agent and followers has different features; firstly, we assume that

$$V_{\max}(t) = \|v_0^{\text{fm}}(t)\|, \quad \text{and} \quad \|v_0^{\text{fm}}(t)\| \geq \sqrt{\frac{\alpha}{\beta}}.$$

Then by Cauchy's inequality,

$$\langle v_b^{\text{fm}}, v_0^{\text{fm}} \rangle \leq \|v_b^{\text{fm}}\| \|v_0^{\text{fm}}\| \leq \|v_0^{\text{fm}}\|^2, \qquad \text{for} \quad b = 1, ..., N. \tag{3.43}$$

Consider

$$\begin{aligned}
\frac{1}{2}\frac{d}{dt}V_{\max}^2(t) &= \frac{1}{2}\frac{d}{dt}\|v_0^{\text{fm}}(t)\|^2 \\
&= \langle \dot{v}_0^{\text{fm}}, v_0^{\text{fm}} \rangle \\
&= \langle (\alpha - \beta\|v_0^{\text{fm}}\|^2)v_0^{\text{fm}}, v_0^{\text{fm}} \rangle + \frac{1}{N+1}\left\langle \sum_{j\neq 0} c_{0j}(t)(x_0^{\text{fm}} - x_j^{\text{fm}}), v_0^{\text{fm}} \right\rangle \\
&\quad + \frac{1}{N+1}\left\langle \sum_{j\neq 0} q_{0j}(t)(v_j^{\text{fm}} - v_0^{\text{fm}}), v_0^{\text{fm}} \right\rangle.
\end{aligned}$$

Due to $\|v_0^{\text{fm}}\|^2 \geq \dfrac{\alpha}{\beta}$, it yields $\langle (\alpha - \beta\|v_0^{\text{fm}}\|^2)v_0^{\text{fm}}, v_0^{\text{fm}} \rangle = \alpha\|v_0^{\text{fm}}\|^2 - \beta\|v_0^{\text{fm}}\|^4 < 0$. Moreover, $q_{0j}(t) \geq 0$, for $j = 1, 2, \ldots, N$ and from (3.43), we get

$$\frac{1}{N+1}\left\langle \sum_{j\neq 0} q_{0j}(t)(v_j^{\text{fm}} - v_0^{\text{fm}}), v_0^{\text{fm}} \right\rangle \leq 0.$$

Since when swarms reaches the cohesive state, we have that $c_{0j} = 0$, for $j = 1, \ldots, N$. Then

$$\frac{1}{2}\frac{d}{dt}V_{\max}^2(t) \leq 0. \tag{3.44}$$

If $V_{\max}(t) = \|v_b^{\text{fm}}(t)\|, \quad$ for some $k \in \{1, 2, \ldots, N\}$, we get the same result as above because $c_b^0(t) = 0$, that is,

$$\begin{aligned}
\frac{1}{2}\frac{d}{dt}V_{\max}^2(t) &= \langle (\alpha - \beta\|v_k^{\text{fm}}\|^2)v_k^{\text{fm}}, v_k^{\text{fm}} \rangle - \frac{1}{N+1}\left\langle \sum_{j\neq 0} c_{kj}(t)(x_k^{\text{fm}} - x_j^{\text{fm}}), v_k^{\text{fm}} \right\rangle \\
&\quad + \frac{1}{N+1}\left\langle \sum_{j\neq 0} q_{kj}(t)(v_j^{\text{fm}} - v_k^{\text{fm}}), v_k^{\text{fm}} \right\rangle - \langle c_b^0(t)(x_b^{\text{fm}} - x_0^{\text{fm}}), v_k^{\text{fm}} \rangle \\
&\leq 0.
\end{aligned}$$

It can be concluded that when the swarm reaches the flocking state, its velocity is bounded.

□

From Proposition 7, we claim that when the group of agent reaches the flocking state, we have

$$\lim_{t\to\infty}\|v_i^{\mathrm{fm}}(t)\| = \sqrt{\frac{\alpha}{\beta}}. \tag{3.45}$$

3.4.2 Local controllability of a refined flocking system

The linearization of the flocking system (3.24) at consensus $\mathbf{x}^{\mathrm{fm}*} = (x^{\mathrm{fm}*}, v^{\mathrm{fm}*})$ can be written as follows

$$\dot{\mathbf{x}}^{\mathrm{fm}} = \mathbf{A}^{\mathrm{fm}}\mathbf{x}^{\mathrm{fm}} + \mathbf{B}^{\mathrm{fm}}u, \tag{3.46}$$

where $\mathbf{A}^{\mathrm{fm}}$ denote the Jacobian matrix of $\mathbf{f}^{\mathrm{fm}}$ with respect to $\mathbf{x}^{\mathrm{fm}}$ at consensus presented as

$$\mathbf{A}^{\mathrm{fm}} := \nabla\mathbf{f}^{\mathrm{fm}}(\mathbf{x}^{\mathrm{fm}*}) = \begin{pmatrix}\nabla_x\mathbf{f}_x & \nabla_v\mathbf{f}_x\\ \nabla_x\mathbf{f}_v & \nabla_v\mathbf{f}_v\end{pmatrix}(\mathbf{x}^{\mathrm{fm}*}), \tag{3.47}$$

with $\nabla_x\mathbf{f}_x$, $\nabla_x\mathbf{f}_x$, $\nabla_x\mathbf{f}_v$, and $\nabla_v\mathbf{f}_v$ given by

$$\begin{aligned}\nabla_x\mathbf{f}_x &= \mathbf{0}_{d(N+1),d(N+1)},\\ \nabla_v\mathbf{f}_x &= \mathbf{I}_{d(N+1)},\\ \nabla_x\mathbf{f}_v &= \nabla_x\mathbf{M} + \nabla_x\mathbf{E} + \nabla_x\mathbf{L},\\ \nabla_v\mathbf{f}_v &= \nabla_v\mathbf{S} + \nabla_v\mathbf{E},\end{aligned} \tag{3.48}$$

where

$$\nabla_x\mathbf{M} = [\partial M_{ij}], \quad \partial M_{ij} := \left(\frac{\partial M_i}{\partial x_j^{\mathrm{fm}}}\right); \qquad \nabla_x\mathbf{E} = [\partial E_{ij}^x], \quad \partial E_{ij}^x := \left(\frac{\partial E_i}{\partial x_j^{\mathrm{fm}}}\right);$$

$$\nabla_v\mathbf{E} = [\partial E_{ij}^v], \quad \partial E_{ij}^v := \left(\frac{\partial E_i}{\partial v_j^{\mathrm{fm}}}\right); \qquad \nabla_x\mathbf{L} = [\partial L_{ij}], \quad \partial L_{ij} := \left(\frac{\partial L_i}{\partial x_j^{\mathrm{fm}}}\right);$$

$$\nabla_v\mathbf{S} = [\partial S_{ij}], \quad \partial S_{ij} := \left(\frac{\partial S_i}{\partial v_j^{\mathrm{fm}}}\right),$$

with

$$\begin{aligned}\left(\frac{\partial M_i}{\partial x_i^{\mathrm{fm}}}\right) &= \frac{1}{N+1}\sum_{j\neq i}^{N}\left[\frac{(x_i^{\mathrm{fm}}-x_j^{\mathrm{fm}})(x_i^{\mathrm{fm}}-x_j^{\mathrm{fm}})^\top}{\|(x_i^{\mathrm{fm}}-x_j^{\mathrm{fm}})\|^2}\right]\left[\frac{C_a}{(l_a)^2}e^{-\frac{\|x_i^{\mathrm{fm}}-x_j^{\mathrm{fm}}\|}{l_a}} - \frac{C_r}{(l_r)^2}e^{-\frac{\|x_i^{\mathrm{fm}}-x_j^{\mathrm{fm}}\|}{l_r}}\right]\\ &- \frac{1}{N+1}\sum_{j\neq i}^{N}\left[\frac{C_a}{l_a}e^{-\frac{\|x_i^{\mathrm{fm}}-x_j^{\mathrm{fm}}\|}{l_a}} - \frac{C_r}{l_r}e^{-\frac{\|x_i^{\mathrm{fm}}-x_j^{\mathrm{fm}}\|}{l_r}}\right]\left[\frac{\|x_i^{\mathrm{fm}}-x_j^{\mathrm{fm}}\|^2\mathbf{I}_d - (x_i^{\mathrm{fm}}-x_j^{\mathrm{fm}})(x_i^{\mathrm{fm}}-x_j^{\mathrm{fm}})^\top}{\|x_i^{\mathrm{fm}}-x_j^{\mathrm{fm}}\|^3}\right],\\ \left(\frac{\partial M_i}{\partial x_j^{\mathrm{fm}}}\right) &= -\frac{1}{N+1}\left[\frac{(x_i^{\mathrm{fm}}-x_j^{\mathrm{fm}})(x_i^{\mathrm{fm}}-x_j^{\mathrm{fm}})^\top}{\|(x_i^{\mathrm{fm}}-x_j^{\mathrm{fm}})\|^2}\right]\left[\frac{C_a}{l_a^2}e^{-\frac{\|x_i^{\mathrm{fm}}-x_j^{\mathrm{fm}}\|}{l_a}} - \frac{C_r}{l_r^2}e^{-\frac{\|x_i^{\mathrm{fm}}-x_j^{\mathrm{fm}}\|}{l_r}}\right]\\ &+ \frac{1}{N+1}\left[\frac{C_a}{l_a}e^{-\frac{\|x_i^{\mathrm{fm}}-x_j^{\mathrm{fm}}\|}{l_a}} - \frac{C_r}{l_r}e^{-\frac{\|x_i^{\mathrm{fm}}-x_j^{\mathrm{fm}}\|}{l_r}}\right]\left[\frac{\|x_i^{\mathrm{fm}}-x_j^{\mathrm{fm}}\|^2\mathbf{I}_d - (x_i^{\mathrm{fm}}-x_j^{\mathrm{fm}})(x_i^{\mathrm{fm}}-x_j^{\mathrm{fm}})^\top}{\|x_i^{\mathrm{fm}}-x_j^{\mathrm{fm}}\|^3}\right],\end{aligned}$$

$$
\begin{aligned}
\left(\frac{\partial L_i}{\partial x_i^{\mathrm{fm}}}\right) &= \gamma_1\left[\frac{(x_i^{\mathrm{fm}}-x_0^{\mathrm{fm}})(x_i^{\mathrm{fm}}-x_0^{\mathrm{fm}})^\top}{\|(x_i^{\mathrm{fm}}-x_0^{\mathrm{fm}})\|^2}\right]\left[\frac{C_a^0}{(l_a^0)^2}e^{-\frac{\|x_i^{\mathrm{fm}}-x_0^{\mathrm{fm}}\|}{l_a^0}}-\frac{C_r^0}{(l_r^0)^2}e^{-\frac{\|x_i^{\mathrm{fm}}-x_0^{\mathrm{fm}}\|}{l_r^0}}\right]\\
&- \gamma_1\left[\frac{C_a^0}{l_a^0}e^{-\frac{\|x_i^{\mathrm{fm}}-x_0^{\mathrm{fm}}\|}{l_a^0}}-\frac{C_r^0}{l_r^0}e^{-\frac{\|x_i^{\mathrm{fm}}-x_0^{\mathrm{fm}}\|}{l_r^0}}\right]\left[\frac{\|x_i^{\mathrm{fm}}-x_0^{\mathrm{fm}}\|^2\mathbf{I}_d-(x_i^{\mathrm{fm}}-x_0^{\mathrm{fm}})(x_i^{\mathrm{fm}}-x_0^{\mathrm{fm}})^\top}{\|x_i^{\mathrm{fm}}-x_0^{\mathrm{fm}}\|^3}\right],\\
\left(\frac{\partial L_i}{\partial x_0^{\mathrm{fm}}}\right) &= -\gamma_1\left[\frac{(x_i^{\mathrm{fm}}-x_0^{\mathrm{fm}})(x_i^{\mathrm{fm}}-x_0^{\mathrm{fm}})^\top}{\|(x_i^{\mathrm{fm}}-x_0^{\mathrm{fm}})\|^2}\right]\left[\frac{C_a^0}{(l_a^0)^2}e^{-\frac{\|x_i^{\mathrm{fm}}-x_0^{\mathrm{fm}}\|}{l_a^0}}-\frac{C_r^0}{(l_r^0)^2}e^{-\frac{\|x_i^{\mathrm{fm}}-x_0^{\mathrm{fm}}\|}{l_r^0}}\right]\\
&+\gamma_1\left[\frac{C_a^0}{l_a^0}e^{-\frac{\|x_i^{\mathrm{fm}}-x_0^{\mathrm{fm}}\|}{l_a^0}}-\frac{C_r^0}{l_r^0}e^{-\frac{\|x_i^{\mathrm{fm}}-x_0^{\mathrm{fm}}\|}{l_r^0}}\right]\left[\frac{\|x_i^{\mathrm{fm}}-x_0^{\mathrm{fm}}\|^2\mathbf{I}_d-(x_i^{\mathrm{fm}}-x_0^{\mathrm{fm}})(x_i^{\mathrm{fm}}-x_0^{\mathrm{fm}})^\top}{\|x_i^{\mathrm{fm}}-x_0^{\mathrm{fm}}\|^3}\right],\\
\left(\frac{\partial L_i}{\partial x_j^{\mathrm{fm}}}\right) &= 0,\\
\left(\frac{\partial E_i}{\partial x_i^{\mathrm{fm}}}\right) &= \frac{1}{N+1}\sum_{j\neq i}^{N}\left[(v_j^{\mathrm{fm}}-v_i^{\mathrm{fm}})\left(\frac{\partial\omega(\|x_i^{\mathrm{fm}}-x_j^{\mathrm{fm}}\|)}{\partial x_i^{\mathrm{fm}}}\right)g(r)\right]\\
&+\frac{1}{N+1}\sum_{j\neq i}^{N}\left[(v_j^{\mathrm{fm}}-v_i^{\mathrm{fm}})\left(\omega(\|x_i^{\mathrm{fm}}-x_j^{\mathrm{fm}}\|)\frac{\partial g(r)}{\partial g}\frac{\partial r}{\partial x_i^{\mathrm{fm}}}\right)\right],\\
\left(\frac{\partial E_i}{\partial x_j^{\mathrm{fm}}}\right) &= \frac{1}{N+1}\left[(v_j^{\mathrm{fm}}-v_i^{\mathrm{fm}})\left(\frac{\partial\omega(\|x_i^{\mathrm{fm}}-x_j^{\mathrm{fm}}\|)}{\partial x_j^{\mathrm{fm}}}\right)g(r)\right]\\
&+\frac{1}{N+1}\left[(v_j^{\mathrm{fm}}-v_i^{\mathrm{fm}})\left(\omega(\|x_i^{\mathrm{fm}}-x_j^{\mathrm{fm}}\|)\frac{\partial g(r)}{\partial r}\frac{\partial r}{\partial x_j^{\mathrm{fm}}}\right)\right],\\
\left(\frac{\partial E_i}{\partial v_i^{\mathrm{fm}}}\right) &= \frac{1}{N+1}\sum_{j\neq i}^{N}\left[(v_j^{\mathrm{fm}}-v_i^{\mathrm{fm}})\omega(\|x_i^{\mathrm{fm}}-x_j^{\mathrm{fm}}\|)\frac{\partial g(r)}{\partial r}\frac{\partial r}{\partial v_i^{\mathrm{fm}}}\right],\\
\left(\frac{\partial E_i}{\partial v_j^{\mathrm{fm}}}\right) &= \frac{1}{N+1}\omega(\|x_i^{\mathrm{fm}}-x_j^{\mathrm{fm}}\|)g(r)\mathbf{I}_d,\\
\left(\frac{\partial S_i}{\partial v_i^{\mathrm{fm}}}\right) &= -2\beta v_i^{\mathrm{fm}}(v_i^{\mathrm{fm}})^\top+(\alpha-\beta\|v_i^{\mathrm{fm}}\|^2)\mathbf{I}_d,\\
\left(\frac{\partial S_i}{\partial v_j^{\mathrm{fm}}}\right) &= 0.
\end{aligned}
$$

Remark 5. *The quantities* $\dfrac{\partial\omega(\|x_i^{\mathrm{fm}}-x_j^{\mathrm{fm}}\|)}{\partial x_i^{\mathrm{fm}}}$, $\dfrac{\partial g(r)}{dr}$, $\dfrac{\partial r}{\partial x_i^{\mathrm{fm}}}$, $\dfrac{\partial r}{\partial v_i^{\mathrm{fm}}}$ *can be calculated by following Proposition 6.*

At consensus $\mathbf{x}^{\mathrm{fm}*}$, the following constraints hold

$$\left(\frac{C_a}{l_a}e^{-\frac{\|x_i^{\mathrm{fm}*}-x_j^{\mathrm{fm}*}\|}{l_a}}-\frac{C_r}{l_r}e^{-\frac{\|x_i^{\mathrm{fm}*}-x_j^{\mathrm{fm}*}\|_2}{l_r}}\right)=0,\quad \left(\frac{C_a^0}{l_a^0}e^{-\frac{\|x_0^{\mathrm{fm}*}-x_b^{\mathrm{fm}*}\|_2}{l_a^0}}-\frac{C_r^0}{l_r^0}e^{-\frac{\|x_0^{\mathrm{fm}*}-x_b^{\mathrm{fm}*}\|}{l_r^0}}\right)=0,$$

and $\quad v_0^{\mathrm{fm}*}=v_1^{\mathrm{fm}*}=\ldots=v_N^{\mathrm{fm}*}.$

As a consequence, we have that

$$\begin{aligned}
\left(\frac{\partial M_i}{\partial x_i^{\mathrm{fm}}}\right)(\mathbf{x}^{\mathrm{fm}*}) &= \frac{1}{N+1}\sum_{j\neq i}^{N}\left[\frac{(x_i^{\mathrm{fm}*}-x_j^{\mathrm{fm}*})(x_i^{\mathrm{fm}*}-x_j^{\mathrm{fm}*})^\top}{\|(x_i^{\mathrm{fm}*}-x_j^{\mathrm{fm}*})\|^2}\right]\left[\frac{C_a}{(l_a)^2}e^{-\frac{\|x_i^{\mathrm{fm}*}-x_j^{\mathrm{fm}}\|}{l_a}}-\frac{C_r}{(l_r)^2}e^{-\frac{\|x_i^{\mathrm{fm}*}-x_j^{\mathrm{fm}*}\|}{l_r}}\right],\\
\left(\frac{\partial M_i}{\partial x_j^{\mathrm{fm}}}\right)(\mathbf{x}^{\mathrm{fm}*}) &= -\frac{1}{N+1}\left[\frac{(x_i^{\mathrm{fm}*}-x_j^{\mathrm{fm}})(x_i^{\mathrm{fm}*}-x_j^{\mathrm{fm}*})^\top}{\|(x_i^{\mathrm{fm}*}-x_j^{\mathrm{fm}*})\|^2}\right]\left[\frac{C_a}{l_a^2}e^{-\frac{\|x_i^{\mathrm{fm}*}-x_j^{\mathrm{fm}*}\|}{l_a}}-\frac{C_r}{l_r^2}e^{-\frac{\|x_i^{\mathrm{fm}*}-x_j^{\mathrm{fm}*}\|}{l_r}}\right],\\
\left(\frac{\partial L_i}{\partial x_i^{\mathrm{fm}}}\right)(\mathbf{x}^{\mathrm{fm}*}) &= \gamma_1\left[\frac{(x_i^{\mathrm{fm}*}-x_0^{\mathrm{fm}*})(x_i^{\mathrm{fm}*}-x_0^{\mathrm{fm}*})^\top}{\|(x_i^{\mathrm{fm}*}-x_0^{\mathrm{fm}*})\|^2}\right]\left[\frac{C_a^0}{(l_a^0)^2}e^{-\frac{\|x_i^{\mathrm{fm}*}-x_0^{\mathrm{fm}*}\|}{l_a^0}}-\frac{C_r^0}{(l_r^0)^2}e^{-\frac{\|x_i^{\mathrm{fm}*}-x_0^{\mathrm{fm}*}\|}{l_r^0}}\right],\\
\left(\frac{\partial L_i}{\partial x_0^{\mathrm{fm}}}\right)(\mathbf{x}^{\mathrm{fm}*}) &= -\gamma_1\left[\frac{(x_i^{\mathrm{fm}*}-x_0^{\mathrm{fm}*})(x_i^{\mathrm{fm}*}-x_0^{\mathrm{fm}*})^\top}{\|(x_i^{\mathrm{fm}*}-x_0^{\mathrm{fm}*})\|^2}\right]\left[\frac{C_a^0}{(l_a^0)^2}e^{-\frac{\|x_i^{\mathrm{fm}*}-x_0^{\mathrm{fm}*}\|}{l_a^0}}-\frac{C_r^0}{(l_r^0)^2}e^{-\frac{\|x_i^{\mathrm{fm}*}-x_0^{\mathrm{fm}*}\|}{l_r^0}}\right],\\
\left(\frac{\partial L_i}{\partial x_j^{\mathrm{fm}}}\right)(\mathbf{x}^{\mathrm{fm}*}) &= 0,\quad \left(\frac{\partial E_i}{\partial x_i^{\mathrm{fm}}}\right)(\mathbf{x}^{\mathrm{fm}*})=0,\quad \left(\frac{\partial E_i}{\partial x_j^{\mathrm{fm}}}\right)(\mathbf{x}^{\mathrm{fm}*})=0,\\
\left(\frac{\partial E_i}{\partial v_i^{\mathrm{fm}}}\right)(\mathbf{x}^{\mathrm{fm}*}) &= \frac{1}{N+1}\sum_{j\neq i}\left(\omega(\|x_i^{\mathrm{fm}*}-x_j^{\mathrm{fm}*}\|)g(r)\mathbf{I}_d\right),\\
\left(\frac{\partial E_i}{\partial v_j^{\mathrm{fm}}}\right)(\mathbf{x}^{\mathrm{fm}*}) &= \frac{1}{N+1}\omega(\|x_i^{\mathrm{fm}*}-x_j^{\mathrm{fm}*}\|)g(r)\mathbf{I}_d,\\
\left(\frac{\partial S_i}{\partial v_i^{\mathrm{fm}}}\right)(\mathbf{x}^{\mathrm{fm}*}) &= -2\beta v_i^{\mathrm{fm}*}(v_i^{\mathrm{fm}*})^\top+(\alpha-\beta\|v_i^{\mathrm{fm}*}\|^2)\mathbf{I}_d,\\
\left(\frac{\partial S_i}{\partial v_j^{\mathrm{fm}}}\right)(\mathbf{x}^{\mathrm{fm}*}) &= 0.
\end{aligned}$$

We observe that the linearized system (3.46) is controllable if the following Kalman operator

$$\mathbf{K}(\mathbf{A}^{\mathrm{fm}},\mathbf{B}^{\mathrm{fm}})=\begin{bmatrix}\mathbf{B}^{\mathrm{fm}} & \mathbf{A}^{\mathrm{fm}}\mathbf{B}^{\mathrm{fm}} & (\mathbf{A}^{\mathrm{fm}})^2\mathbf{B}^{\mathrm{fm}} & \ldots & (\mathbf{A}^{\mathrm{fm}})^{(2d(N+1)-1)}\mathbf{B}^{\mathrm{fm}}\end{bmatrix} \tag{3.49}$$

has full rank.

Chapter 4

Optimal control of multi-agent systems

In the previous chapter, we discussed the properties of controllability for constructing a control in order to steer the multi-agent systems to reach a desired state. In this chapter, we formulate optimal control problems governed by multi-agent systems. Our aim is to determine the leader-based open-loop control that drives a multi-agent system to attain a given objective. However, we use our open-loop control framework to construct an effective closed-loop control strategy using the model predictive control scheme. To formulate our optimal control problems, the following components are considered,

- A cost functional or the performance criteria,
- A multi-agent dynamical system,
- A control mechanism based on leadership.

This chapter is organized as follows: In Section 4.1, we start by describing a general optimal control problem with the multi-agent system. The existence of our optimal control is discussed and an optimality criteria is addressed. We discuss a set of conditions that optimal control the satisfies. In Section 4.2, our optimal control problem for the HK opinion formation model is formulated and analyzed. The HB social balance model and our refined flocking model is discussed in Section 4.3 and in Section 4.4, respectively.

4.1 Formulation of optimal control problems

We consider a class of optimal control problems for multi-agent systems. A general formulation is given by

$$\min_{\mathbf{x},\mathbf{u}} \quad J(\mathbf{x},\mathbf{u}) := \frac{1}{2}\|\mathbf{x}(T)-\mathbf{x}_{\text{des}}(T)\|_2^2 + \int_0^T l(\mathbf{x})dt + \frac{\nu}{2}\|\mathbf{u}(t)\|_{L^2}^2, \tag{4.1}$$

$$\begin{aligned} \text{subject to} \quad \dot{\mathbf{x}} &= \mathbf{f}(\mathbf{x}) + \mathbf{B}\mathbf{u}(t), \quad t \in [0,T] \\ \mathbf{x} \in \mathbb{X}, &\qquad \mathbf{u} \in \mathbb{U} = L^2((0,T);\mathbb{R}^{nc}), \end{aligned} \tag{4.2}$$

where the variable $\mathbf{x}$ is the state of the system and belonging to in the following set

$$\mathbb{X} := \{\mathbf{x} \in H^1((0,T);\mathbb{R}^{nx}) : \mathbf{x}(0) = \mathbf{x}_0\},$$

where $\mathbf{x}_0 \in \mathbb{R}^{nx}$ is a given initial state. The control function $\mathbf{u} : [0,T] \to \mathbb{R}^{nc}$ belongs to the admissible set $\mathbb{U} := L^2((0,T);\mathbb{R}^{nc})$. The function $\mathbf{f} : \mathbb{R}^{nx} \to \mathbb{R}^{nx}$ in the dynamics of the system is assumed to be a smooth vector-valued function, $\mathbf{f} \in C^1(\mathbb{R}^{nx};\mathbb{R}^{nx})$ and $\mathbf{B} \in \mathbb{R}^{nx\times nc}$ is a constant matrix. The function $J : \mathbb{R}^{nx} \times \mathbb{R}^{nc} \to \mathbb{R}$ is called the objective function. The function $\mathbf{x}_{\text{des}} : [0,T] \to \mathbb{R}^{nx}$ in the objective function is a given desired trajectory. The function $l : \mathbb{R}^{nx} \to \mathbb{R}$ is real-valued function and we assume that l is continuous and continuously differentiable, bounded from below and convex, $l \in C^1(\mathbb{R}^{nx};\mathbb{R})$. In particular, l may corresponds to a tracking problem. In this case, the cost functional is designed in order to steer the state $\mathbf{x}(t)$ as close as possible to a desired $\mathbf{x}_{\text{des}}(t)$. We have

$$l(\mathbf{x};\mathbf{x}_{\text{des}}) = \sum_{i=0}^{N} \|\mathbf{x}_i(t) - \mathbf{x}_{\text{des}}(t)\|^2.$$

By Proposition 1, the solution $\mathbf{x}$ of the dynamical system (4.2) is uniquely determined by $\mathbf{u} \in \mathbb{U}$. In the following, our aim is to prove that the mapping $\mathbf{u} \mapsto \mathbf{x}(\mathbf{u})$ is sequentially weakly semi-continuous. Notice that a similar result can be found in [28, 29].

Proposition 8. *Let $(\mathbf{u}^m)_{m=1}^{\infty}$ be a sequence of controls such that*

$$\mathbf{u}^m \rightharpoonup \widetilde{\mathbf{u}} \quad \textit{in} \quad L^2((0,T);\mathbb{R}^{nc}).$$

Then the corresponding solution to (4.2) has the following property

$$\mathbf{x}^m := \mathbf{x}(\mathbf{u}^m) \quad \textit{satisfies} \quad \mathbf{x}^m \to \widetilde{\mathbf{x}} = \mathbf{x}(\widetilde{\mathbf{u}}) \quad \textit{in} \quad C([0,T];\mathbb{R}^{nx}). \tag{4.3}$$

Proof. Consider a sequence of controls $\mathbf{u}^m = (u_1^m, \ldots, u_{nc}^m) \in L^2((0,T);\mathbb{R}^{nc})$ such that $u_j^m \rightharpoonup \widetilde{u}_j$ in $L^2((0,T);\mathbb{R})$.
Let $(\mathbf{x}^m)_{m=1}^{\infty}$ be a sequence in $H^1((0,T);\mathbb{R}^{nx})$ defined as $\mathbf{x}^m := \mathbf{x}(\mathbf{u}^m)$.
By Proposition 1, we know that $\mathbf{x}^m$ is bounded together with the reflexive property of

$H^1((0,T);\mathbb{R}^{nx})$, hence by using Banach-Eberlein-Šmulian Theorem A.4 (see Appendix A.2), we can extract a weakly convergent subsequence that

$$\mathbf{x}^{m_l} \rightharpoonup \widetilde{\mathbf{x}} \quad \text{in} \quad H^1((0,T);\mathbb{R}^{nx}) \quad \text{as} \quad l \to \infty.$$

We know that the embedding $H^1(0,T) \to C[0,T]$ is compact; consequently,

$$\mathbf{x}^{m_l} \to \widetilde{\mathbf{x}} \quad \text{in} \quad C([0,T];\mathbb{R}^{nx}).$$

Next, we shall prove that $\widetilde{\mathbf{x}}$ is the solution to $\widetilde{\mathbf{u}}$, i.e, $\widetilde{\mathbf{x}} = \mathbf{x}(\widetilde{\mathbf{u}})$. Consider the dynamical system corresponding to $(\mathbf{x}^{m_l}, \mathbf{u}^{m_l})$.
By multiplying from the right-hand side with a test function $\mathbf{v} \in H^1((0,T);\mathbb{R}^{nx})$, we have

$$\langle\, \dot{\mathbf{x}}^{m_l} - \mathbf{f}(\mathbf{x}^{m_l}) - \mathbf{B}\mathbf{u}^{m_l}, \mathbf{v} \,\rangle_{L^2} = 0. \tag{4.4}$$

Since $\mathbf{x}^{m_l} \to \widetilde{\mathbf{x}}$ in $C([0,T];\mathbb{R}^{nx})$ and $\mathbf{f} \in C^\infty([0,T];\mathbb{R}^{nx})$, it yields $\mathbf{f}(\mathbf{x}^{m_l}) \to \mathbf{f}(\widetilde{\mathbf{x}})$.
Furthermore, we know that $\mathbf{u}^{m_l} \rightharpoonup \widetilde{\mathbf{u}}$; consequently,

$$\langle\, \dot{\mathbf{x}}^{m_l} - \mathbf{f}(\mathbf{x}^{m_l}) - \mathbf{B}\mathbf{u}^{m_l}, \mathbf{v} \,\rangle_{L^2} \to \left\langle\, \dot{\widetilde{\mathbf{x}}} - \mathbf{f}(\widetilde{\mathbf{x}}) - \mathbf{B}\widetilde{\mathbf{u}}, \mathbf{v} \,\right\rangle_{L^2}, \tag{4.5}$$

for all $\mathbf{v} \in H^1((0,T);\mathbb{R}^{nx})$. Since the above limit is true for all subsequences, and the limit $\mathbf{x}(\widetilde{\mathbf{u}})$ is unique, we have that $\mathbf{x}(\mathbf{u}^m) \to \widetilde{\mathbf{x}} = \mathbf{x}(\widetilde{\mathbf{u}})$ in $C([0,T];\mathbb{R}^{nx})$.

□

By Proposition 1, the state $\mathbf{x}$ is uniquely determined by the initial condition and the controls, the mapping $\mathbf{u} \mapsto \mathbf{x} = \mathbf{x}(\mathbf{u})$ is well-defined; therefore, the structure of the considered optimal control problem allows to consider the state as a function of the control, that is, $\mathbf{x} = \mathbf{x}(\mathbf{u})$. For this reason, it is possible to introduce the so-called reduced cost functional, given by the following

$$\min_{\mathbf{u}\in\mathbb{U}} J_r(\mathbf{u}), \tag{4.6}$$

where $J_r(\mathbf{u}) := J(\mathbf{x}(\mathbf{u}), \mathbf{u})$. Our aim is to find a control $\widetilde{\mathbf{u}} \in \mathbb{U}$ that results in a state $\mathbf{x}$ that minimizes the objective function J.

$$J(\mathbf{x}(\widetilde{\mathbf{u}}), \widetilde{\mathbf{u}}) \leqslant J(\mathbf{x}(\mathbf{u}), \mathbf{u}), \quad \forall \mathbf{u} \in \mathbb{U}.$$

In this reduced problem only the control $\mathbf{u}$ appears as an unknown. In the following, we discuss the existence of solution to the optimal control problem (4.6). Furthermore, for such problem, we present assumptions such that at least one optimal solution exists.

Definition 10. *A vector $\widetilde{\mathbf{u}} \in \mathbb{U}$ is called an optimal control for problem (4.6), if $J_r(\widetilde{\mathbf{u}}) \leq J_r(\mathbf{u})$ for all $\mathbf{u} \in \mathbb{U}$, then $\widetilde{\mathbf{x}} = \mathbf{x}(\widetilde{\mathbf{u}})$ is called the optimal state associated with $\widetilde{\mathbf{u}}$.*

In general, an optimal control problem considered in finite-dimension has at least one solution if the cost functional is continuous and the admissible set is nonempty, bounded and closed. In fact, the continuity of the cost function implies that the reduce cost is also continuous. Moreover, as a bounded and closed set in finite-dimensional space, the admissible set is compact. By the Weierstrass theorem, which says that every continuous function attains its minimum on a compact set, the cost functional attains its minimum in the set of admissible controls. Consequently, an optimal control exists.

However, in our case $\mathbb{U}$ is a set of an infinite-dimensional space, therefore closeness and boundedness do not guarantee compactness. In this case the proof of the existence of the solution becomes more involved. In fact, possible conditions concerning J and $\mathbb{U}$, which ensure the existence of optimal solution of problem (4.6), are that the admissible set is weakly sequentially compact and the functional J is weakly lower semi-continuous. The proof of weakly sequential semi-continuity only make use of the fact that the objective functional J is continuous and convex. The following Proposition state the properties of J.

Proposition 9. *Let $\mathbf{x} \in \mathbb{X}$ and $\mathbf{u} \in \mathbb{U}$. The function $l : \mathbb{R}^{nx} \to \mathbb{R}$ is continuously differentiable and convex. Then the objective function*

$$J(\mathbf{x}, \mathbf{u}) = \frac{1}{2}\|\mathbf{x}(T) - \mathbf{x}_{\text{des}}(T)\|_2^2 + \int_0^T l(\mathbf{x}(t))dt + \frac{\nu}{2}\|\mathbf{u}(t)\|_{L^2}^2 \tag{4.7}$$

is continuous, convex and weakly coercive on u

Proof. Let X be normed vector space and $a \in X$. We know that the functional

$$f_a : X \to \mathbb{R}, \quad x \mapsto \|x - a\|,$$

is continuous and convex; see Appendix A.2. In addition, the function $l : \mathbb{R}^{nx} \to \mathbb{R}$ in our case is also defined as the distance functional. This implies that the cost functional J is continuous and convex. Due to continuity and convexity of J, it implies that J is weakly sequentially semi-continuous from below. Moreover, it can be seen that when $\|\mathbf{u}\|_{L^2} \to \infty$, implies $\lim J(\mathbf{x}, \mathbf{u}) = \infty$, that is, J is weakly coercive on $\mathbf{u}$. □

The following Theorem shows that there exists an optimal control solution to (4.6). The reflexivity of the Banach space plays an important role for proving it.

Theorem 8. *Assume that $\nu > 0$ and $\mathbb{U} = L^2((0,T);\mathbb{R}^{nc})$, then the minimization problem (4.2) admits a solution.*

Proof. From Proposition 1, $(\mathbf{x}, \mathbf{u}) \mapsto J(\mathbf{x}, \mathbf{u})$ is weakly lower semi-continuous. According to coercivity of J, by Proposition A.1, we have that the minimizing sequence $(\mathbf{u}^m)_{m=1}^{\infty}$ in $L^2((0,T);\mathbb{R}^{nc})$ is bounded. By Banach-Eberlein-Šmulian theorem, we can extract a weak convergent subsequence $\mathbf{u}^{m_l} \rightharpoonup \widetilde{\mathbf{u}}$ in $L^2((0,T);\mathbb{R}^{nc})$.

By Proposition 8, we have that $\mathbf{x}^{m_l}(t) \to \widetilde{\mathbf{x}}(t)$, $t \in [0,T]$. With these properties, we obtain $(\tilde{\mathbf{x}}, \tilde{\mathbf{u}})$ of the minimization problem as follows

$$\begin{aligned}
\liminf_{l\to\infty} J(\mathbf{x}^{m_l}, \mathbf{u}^{m_l}) &= \lim_{l\to\infty} \frac{1}{2}\|\mathbf{x}^{m_l}(T) - \mathbf{x}_{\text{des}}(T)\|^2 + \lim_{l\to\infty} \int_0^T l(\mathbf{x}^{m_l})dt + \liminf_{l\to\infty} \frac{\nu}{2}\|\mathbf{u}^{m_l}\|_{L^2}^2 \\
&\geq \frac{1}{2}\|\widetilde{\mathbf{x}}(T) - \mathbf{x}_{\text{des}}(T)\|^2 + \int_0^T l(\widetilde{\mathbf{x}})dt + \frac{\nu}{2}\|\widetilde{\mathbf{u}}(t)\|_{L^2}^2 \\
&= J(\widetilde{\mathbf{x}}, \widetilde{\mathbf{u}}).
\end{aligned}$$

□

Now, we consider the operator

$$\begin{aligned}
c(\cdot,\cdot) : \mathbb{X} \times \mathbb{U} \to \mathbb{P}, \qquad & c(\mathbf{x},\mathbf{u}) := \dot{\mathbf{x}} - \mathbf{f}(\mathbf{x}) - \mathbf{B}\mathbf{u}, \\
Dc(\cdot,\cdot) : \mathbb{X} \times \mathbb{U} \to \mathbb{P}, \qquad & Dc(\mathbf{x},\mathbf{u}) := \dot{\delta\mathbf{x}} - \nabla_x \mathbf{f}(\mathbf{x})\delta\mathbf{x} - \mathbf{B}\delta\mathbf{u},
\end{aligned} \tag{4.8}$$

where $\mathbb{P} = L^2((0,T);\mathbb{R}^{nx})$.

In the following Proposition, the concept of the Fréchet derivative of c is investigated in oder to ensure that the differentiable mapping c is continuous and then we are able to deduce necessary optimality conditions from these derivatives.

Proposition 10. *The operator c is Fréchet differentiable and invertible for fixed $\mathbf{u}$.*

Proof. We start proving Fréchet differentiability of $(\mathbf{x},\mathbf{u}) \mapsto c(\mathbf{x},\mathbf{u})$.

Consider $c(\mathbf{x},\mathbf{u}) = \dot{\mathbf{x}} - \mathbf{f}(\mathbf{x}) - \mathbf{B}\mathbf{u}$, and $Dc(\delta\mathbf{x},\delta\mathbf{u}) := \dot{\delta\mathbf{x}} - \nabla_x \mathbf{f}(\mathbf{x})\delta\mathbf{x} - \mathbf{B}\delta\mathbf{u}$.

$$\begin{aligned}
& c(\mathbf{x}+\delta\mathbf{x}, \mathbf{u}+\delta\mathbf{u}) - c(\mathbf{x},\mathbf{u}) - Dc(\delta\mathbf{x},\delta\mathbf{u}) \\
= \; & \frac{d}{dt}(\mathbf{x}+\delta\mathbf{x}) - \mathbf{f}(\mathbf{x}+\delta\mathbf{x}) - \mathbf{B}(\mathbf{u}+\delta\mathbf{u}) - \frac{d}{dt}\mathbf{x} + \mathbf{f}(\mathbf{x}) + \mathbf{B}\mathbf{u} - \frac{d}{dt}\delta\mathbf{x} + \nabla_x\mathbf{f}(\mathbf{x})\delta\mathbf{x} + \mathbf{B}\delta\mathbf{u} \\
= \; & \frac{d}{dt}\mathbf{x} + \frac{d}{dt}\delta\mathbf{x} - \mathbf{f}(\mathbf{x}+\delta\mathbf{x}) - \mathbf{B}\mathbf{u} - \mathbf{B}\delta\mathbf{u} - \frac{d}{dt}\mathbf{x} + \mathbf{f}(\mathbf{x}) + \mathbf{B}\mathbf{u} - \frac{d}{dt}\delta\mathbf{x} + \nabla_x\mathbf{f}(\mathbf{x})\delta x + \mathbf{B}\delta\mathbf{u} \\
= \; & \mathbf{f}(\mathbf{x}) - \mathbf{f}(\mathbf{x}+\delta\mathbf{x}) + \nabla_x\mathbf{f}(\mathbf{x})\delta\mathbf{x}.
\end{aligned}$$

Consider $\dfrac{d}{dt}\mathbf{f}(\mathbf{x}+t\delta\mathbf{x}) = \nabla\mathbf{f}(\mathbf{x}+t\delta\mathbf{x})$. Therefore we have

$$\mathbf{f}(\mathbf{x}+\delta\mathbf{x}) - \mathbf{f}(\mathbf{x}) = \int_0^1 \nabla_x\mathbf{f}(\mathbf{x}+h\delta\mathbf{x})\delta\mathbf{x}\, dh, \quad \text{and} \quad \nabla_x\mathbf{f}(\mathbf{x})\delta\mathbf{x} = \int_0^1 \nabla_x\mathbf{f}(\mathbf{x})\delta\mathbf{x}\, dh.$$

As a consequence, we get the following

$$\mathbf{f}(\mathbf{x}+\delta\mathbf{x}) - \mathbf{f}(\mathbf{x}) - \nabla_x\mathbf{f}(\mathbf{x})\delta\mathbf{x} = \int_0^1 (\nabla_x\mathbf{f}(\mathbf{x}+h\delta\mathbf{x})\delta\mathbf{x} - \nabla_x\mathbf{f}(\mathbf{x})\delta\mathbf{x})\, dh$$

Since $\mathbf{x}, \delta\mathbf{x} \in H^1((0,T);\mathbb{R}^{nx})$ and $H^1((0,T)) \hookrightarrow C((0,T))$, then

$$\sup_{t\in(0,T)} \|\mathbf{x}(t)\| < \infty \quad \text{and} \sup_{t\in(0,T)} \|\delta\mathbf{x}(t)\| < \infty$$

In addition, $\mathbf{f} \in C^1(\mathbb{R}^{nx};\mathbb{R}^{nx}) \Rightarrow \nabla_x \mathbf{f} \in C(\mathbb{R}^{nx};\mathbb{R}^{nx})$.

Let $K = \|\mathbf{x}\|_{L^\infty(0,T)}$ and $\epsilon > 0$. Due to uniform continuity of $\nabla_x \mathbf{f}$, we have

$$\begin{aligned} \exists \delta > 0 : \quad & \|\nabla_x \mathbf{f}(y+\delta y) - \nabla_x \mathbf{f}(y)\| < \epsilon, \\ & \forall y \in \{z \in H^1((0,T);\mathbb{R}^{nx}) : \|z\|_{L^\infty(0,T)} < 2K\}, \\ \text{and} \quad & \forall \delta y \in \{z \in H^1((0,T);\mathbb{R}^{nx}) : \|z\|_{L^\infty(0,T)} < \delta\}. \end{aligned}$$

Therefore, if we choose $\|\delta\mathbf{x}\|_{L^\infty(0,T)} < \delta$, then

$$\begin{aligned} \int_0^T \|\mathbf{f}(\mathbf{x}+\delta\mathbf{x}) - \mathbf{f}(\mathbf{x}) - \nabla_x \mathbf{f}(\mathbf{x})\delta\mathbf{x}\|^2 dt &\leq \int_0^T \int_0^1 \|\nabla_x \mathbf{f}(\mathbf{x}+h\delta\mathbf{x}) - \nabla_x \mathbf{f}(\mathbf{x})\|^2 \|\delta\mathbf{x}\|^2 \, dh dt \\ &\leq \|\delta\mathbf{x}\|^2_{L^\infty(0,T)} \int_0^T \int_0^1 \|\nabla_x \mathbf{f}(\mathbf{x}+h\delta\mathbf{x}) - \nabla_x \mathbf{f}(\mathbf{x})\|^2 \, dh dt \\ &\leq T\epsilon^2\delta^2. \end{aligned} \tag{4.9}$$

Hence, from (4.9) we get that

$$\lim_{\|\delta\mathbf{x}\|_{\mathbb{X}}\to 0} \frac{\|\mathbf{f}(\mathbf{x}) - \mathbf{f}(\mathbf{x}+\delta\mathbf{x}) + \nabla_x \mathbf{f}(\mathbf{x})\delta\mathbf{x}\|}{\|\delta\mathbf{x}\|} \to 0.$$

This means that $(\mathbf{x},\mathbf{u}) \mapsto c(\mathbf{x},\mathbf{u})$ is Fréchet derivative of c and $Dc(\mathbf{x},\mathbf{u})$ is the Fréchet derivative of c.
To prove that c is invertible for fixed $\mathbf{u}$, we recall that Proposition 1 proves the existence of a solution and the same holds for $c(\mathbf{x},\mathbf{u}) = b, b \in \mathbb{P}$. Hence c is invertible. Using the same argument, we obtain that $Dc(\mathbf{x},\mathbf{u})$ is invertible for fixed $\mathbf{x}$, $\mathbf{u}$, and $\delta\mathbf{u}$, hence surjective. □

Using the operator defined in (4.8), problem (4.2) can be equivalently written in the following compact form

$$\min_{\mathbf{u}\in\mathbb{U}} \quad J_r(\mathbf{u}) = J(\mathbf{x}(\mathbf{u}),\mathbf{u}) \tag{4.10}$$

where $\mathbf{x}(\mathbf{u})$ is the soultion to $c(\mathbf{x},\mathbf{u}) = 0$. A solution to (4.10) is characterized in the terms of first-order necessary optimality conditions, $\nabla_{\mathbf{u}} J_r(\mathbf{u}) = 0$. By Proposition 10 the linearized constraint is surjective, then there exists a Lagrange multiplier $\mathbf{p} \in \mathbb{P}^* = L^2((0,T);\mathbb{R}^{nx})$, where $\mathbb{P}^*$ denotes the dual space of $\mathbb{P}$.

Proposition 11. *Consider the system*

$$-\dot{\mathbf{p}} = -(\nabla_{\mathbf{x}} l(\mathbf{x}))^\top + (\nabla_{\mathbf{x}} \mathbf{f}(\mathbf{x}))^\top \mathbf{p}, \quad \mathbf{p}(T) = -(\mathbf{x}(T) - \mathbf{x}_{\text{des}}(T)) \tag{4.11}$$

with $\mathbf{x}, \mathbf{p} \in H^1((0,T);\mathbb{R}^{nx})$. *Let* $D \subset \mathbb{R}^{nx}$ *and assume that* $\mathbf{f} : D \to \mathbb{R}^{nx}$ *is locally Lipschitz continuous on* D. *Moreover, the function* $l : \mathbb{R}^{nx} \to \mathbb{R}$ *is continuous and continuously differentiable, bounded from below and convex. Then the system (4.11) admits the unique solution for any* $T > 0$ *and any initial condition.*

Proof. Given $\mathbf{x} \in H^1((0,T);\mathbb{R}^{nx})$. Let us define $\mathbf{f}_p : [0,T] \times \mathbb{R}^{nx} \to \mathbb{R}^{nx}$ as

$$\mathbf{f}_p(t, \mathbf{p}) = -(\nabla_{\mathbf{x}} l(\mathbf{x}))^\top + (\nabla_{\mathbf{x}} \mathbf{f}(\mathbf{x}))^\top \mathbf{p} \tag{4.12}$$

Since $\mathbf{x} \in H^1((0,T);\mathbb{R}^{nx})$, $l \in C^1(\mathbb{R}^{nx};\mathbb{R})$, and $\mathbf{f} \in C^1(\mathbb{R}^{nx};\mathbb{R}^{nx})$, $\mathbf{f}_p$ has the following properties,

- $\mathbf{f}_p(\cdot, \mathbf{p}) : [0,T] \to \mathbb{R}^{nx}$ is measurable, for each fixed $\mathbf{p}$.
- $\mathbf{f}_p(t, \cdot) : \mathbb{R}^{nx} \to \mathbb{R}^{nx}$ is continuous, for each fixed t.

Let $\mathbf{p}_1, \mathbf{p}_2 \in D$, we can see that

$$\begin{aligned} \|\mathbf{f}_p(t, \mathbf{p}_1) - \mathbf{f}_p(t, \mathbf{p}_2)\| &= \|(\nabla_{\mathbf{x}} \mathbf{f}(\mathbf{x}))^\top\| \|\mathbf{p}_1 - \mathbf{p}_2\| \\ &\leq L\|\mathbf{p}_1 - \mathbf{p}_2\|, \quad L > 0. \end{aligned}$$

Consequently, $\mathbf{f}_p$ is Lipschitz in $\mathbf{p}$. Next, the locally integrable property of $\mathbf{f}_p$ is examined. For given $\mathbf{p} \in D$ we have that

$$\begin{aligned} \|\mathbf{f}_p(t, \mathbf{p})\| &= \|-(\nabla_{\mathbf{x}} l(\mathbf{x}))^\top + (\nabla_{\mathbf{x}} \mathbf{f}(\mathbf{x}))^\top \mathbf{p}\| \\ &\leq \|(\nabla_{\mathbf{x}} l(\mathbf{x}))^\top\| + \|(\nabla_{\mathbf{x}} \mathbf{f}(\mathbf{x}))^\top\| \|\mathbf{p}\| \\ &= \left(\sum_{i=1}^{nx} |\frac{\partial l(\mathbf{x})}{\partial x_i}|^2 \right)^{1/2} + \left(\sum_{i=1}^{nx} \sum_{j=1}^{nx} |\frac{\partial f_i(\mathbf{x})}{\partial x_j}|^2 \right)^{1/2} \|\mathbf{p}\| \\ &\leq \left(\sum_{i=1}^{nx} |\frac{\partial l(\mathbf{x})}{\partial x_i}|_\infty^2 \right)^{1/2} + \left(\sum_{i=1}^{nx} \sum_{j=1}^{nx} |\frac{\partial f_i(\mathbf{x})}{\partial x_j}|_\infty^2 \right)^{1/2} \|\mathbf{p}\| \\ &\leq \left(nx \cdot \max_i |\frac{\partial l(\mathbf{x})}{\partial x_i}|_\infty^2 \right)^{1/2} + \left((nx)^2 \cdot \max_i \left\{ \max_j |\frac{\partial f_i(\mathbf{x})}{\partial x_j}|_\infty^2 \right\} \right)^{1/2} \|\mathbf{p}\| \\ &\leq \alpha + \beta\|\mathbf{p}\|, \quad \alpha, \beta > 0 \end{aligned}$$

Hence, by [76](Theorem 54), the system (4.11) admits a unique solution for any T and any initial conditions. □

Proposition 12. *The gradient of the reduced system (4.10) is given by*

$$\nabla_{\mathbf{u}} J_r(\mathbf{u}) = \nu \mathbf{u} - \mathbf{B}^\top \mathbf{p}, \tag{4.13}$$

where $\mathbf{p} \in H^1((0,T);\mathbb{R}^{nx})$ *is the unique solution to the following problem*

$$-\dot{\mathbf{p}} = -(\nabla_{\mathbf{x}} l(\mathbf{x}))^\top + (\nabla_{\mathbf{x}} \mathbf{f}(\mathbf{x}))^\top \mathbf{p}, \quad \mathbf{p}(T) = -(\mathbf{x}(T) - \mathbf{x}_{\text{des}}(T)). \tag{4.14}$$

Proof. Let $\mathbf{p}$ be the unique solution of (4.14). From the Proposition 11, we have $\mathbf{p} \in H^1((0,T);\mathbb{R}^{nx})$. Consider the cost functional $(\mathbf{x},\mathbf{u}) \mapsto J(\mathbf{x},\mathbf{u})$ and $\delta\mathbf{x}$ satisfying the linearized constraint (4.8) allow to compute $\nabla_{\mathbf{u}} J_r(\mathbf{u})$ as follows

$$\begin{aligned}
\langle \nabla_{\mathbf{u}} J_r(\mathbf{u}), \delta\mathbf{x}\rangle_{L^2} &= \left\langle \frac{\partial J(\mathbf{x},\mathbf{u})}{\partial \mathbf{x}}, \delta\mathbf{x} \right\rangle_{L^2} + \left\langle \frac{\partial J(\mathbf{x},\mathbf{u})}{\partial \mathbf{u}}, \delta\mathbf{u} \right\rangle_{L^2} \\
&= \langle \mathbf{x}(T) - \mathbf{x}_{\mathrm{des}}(T), \delta\mathbf{x}(T)\rangle + \langle (\nabla_{\mathbf{x}} l(\mathbf{x}))^\top, \delta\mathbf{x}\rangle_{L^2} + \langle \nu\mathbf{u}, \delta\mathbf{u}\rangle_{L^2} \\
&= \langle -\mathbf{p}(T), \delta\mathbf{x}(T)\rangle + \langle (\nabla_{\mathbf{x}} l(\mathbf{x}))^\top, \delta\mathbf{x}\rangle_{L^2} + \langle \nu\mathbf{u}, \delta\mathbf{u}\rangle_{L^2} \qquad (4.15)
\end{aligned}$$

By means of the integration -by-parts rule, we have

$$\begin{aligned}
\langle -\mathbf{p}(T), \delta\mathbf{x}(T)\rangle &= \langle \mathbf{p}(0), \delta\mathbf{x}(0)\rangle + \langle -\dot{\mathbf{p}}, \delta\mathbf{x}\rangle_{L^2} - \langle \mathbf{p}, \dot{\delta\mathbf{x}}\rangle_{L^2} \\
&= \langle -\dot{\mathbf{p}}, \delta\mathbf{x}\rangle_{L^2} - \langle \mathbf{p}, \dot{\delta\mathbf{x}}\rangle_{L^2} \\
&= \langle -(\nabla_{\mathbf{x}} l(\mathbf{x}))^\top + (\nabla_{\mathbf{x}}\mathbf{f}(\mathbf{x}))^\top\mathbf{p}, \delta\mathbf{x}\rangle_{L^2} - \langle \mathbf{p}, \nabla_x \mathbf{f}(\mathbf{x})\delta\mathbf{x} + \mathbf{B}\delta\mathbf{u}\rangle_{L^2} \\
&= \langle -(\nabla_{\mathbf{x}} l(\mathbf{x}))^\top + (\nabla_{\mathbf{x}}\mathbf{f}(\mathbf{x}))^\top\mathbf{p}, \delta\mathbf{x}\rangle_{L^2} - \langle (\nabla_x \mathbf{f}(\mathbf{x}))^\top\mathbf{p}, \delta\mathbf{x}\rangle_{L^2} - \langle \mathbf{B}^\top\mathbf{p}, \delta\mathbf{u}\rangle_{L^2} \\
&= \langle -(\nabla_{\mathbf{x}} l(\mathbf{x}))^\top, \delta\mathbf{x}\rangle_{L^2} - \langle \mathbf{B}^\top\mathbf{p}, \delta\mathbf{u}\rangle_{L^2} \qquad (4.16)
\end{aligned}$$

Substituting (4.16) into (4.15), we get

$$\langle \nabla_{\mathbf{u}} J_r(\mathbf{u}), \delta\mathbf{x}\rangle_{L^2} = \langle \nu\mathbf{u}, \delta\mathbf{u}\rangle_{L^2} - \langle \mathbf{B}^\top\mathbf{p}, \delta\mathbf{u}\rangle_{L^2}$$

Therefore, we obtain that $\nabla_{\mathbf{u}} J_r(\mathbf{u}) = \nu\mathbf{u} - \mathbf{B}^\top\mathbf{p}$. □

A way to obtain the first-order optimality system is to consider the Lagrange function L defined as follows

$$\begin{aligned}
L(\mathbf{x},\mathbf{u},\mathbf{p}) &= J(\mathbf{x},\mathbf{u}) + \langle \dot{\mathbf{x}} - \mathbf{f}(\mathbf{x}) - \mathbf{B}\mathbf{u}, \mathbf{p}\rangle_{L^2} \qquad (4.17) \\
&= \frac{1}{2}\|\mathbf{x}(T) - \mathbf{x}_{\mathrm{des}}(T)\|^2 + \int_0^T l(\mathbf{x})dt + \frac{\nu}{2}\|\mathbf{u}(t)\|^2_{L^2} \\
&\quad + \langle \dot{\mathbf{x}} - \mathbf{f}(\mathbf{x}) - \mathbf{B}\mathbf{u}, \mathbf{p}\rangle_{L^2}\,.
\end{aligned}$$

Using the Lagrange function L, by Theorem 2.13 in [15] we find that necessary conditions for optimality are equivalent to

$$\begin{aligned}
\nabla_{\mathbf{x}} L(\mathbf{x},\mathbf{u},\mathbf{p}) &= 0, \qquad (4.18) \\
\nabla_{\mathbf{p}} L(\mathbf{x},\mathbf{u},\mathbf{p}) &= 0, \\
\nabla_{\mathbf{u}} L(\mathbf{x},\mathbf{u},\mathbf{p}) &= 0,
\end{aligned}$$

where the notations $\nabla_{\mathbf{x}} L$, $\nabla_{\mathbf{u}} L$, and $\nabla_{\mathbf{p}} L$ represent the derivative of L with respect to $\mathbf{x}$, $\mathbf{u}$, and $\mathbf{p}$, respectively.

Theorem 9. *Assume that the pair $(\mathbf{x},\mathbf{u}) \in \mathbb{X}\times\mathbb{U}$ is a minimizer for the problem (4.1). Then there exists a unique Lagrange multiplier $\mathbf{p} \in H^1((0,T);\mathbb{R}^{nx})$ such that the triple $(\mathbf{x},\mathbf{u},\mathbf{p})$ solves the following system,*

$$\begin{aligned}
&\dot{\mathbf{x}} = \mathbf{f}(\mathbf{x}) + \mathbf{B}\mathbf{u}, \quad \mathbf{x}(0) = \mathbf{x}_0, \qquad (4.19) \\
&-\dot{\mathbf{p}} = -(\nabla_{\mathbf{x}} l(\mathbf{x}))^\top + (\nabla_{\mathbf{x}}\mathbf{f}(\mathbf{x}))^\top\mathbf{p}, \quad \mathbf{p}(T) = -(\mathbf{x}(T) - \mathbf{x}_{\mathrm{des}}(T)), \\
&\nu\mathbf{u} - \mathbf{B}^\top\mathbf{p} = 0.
\end{aligned}$$

The system(4.19) is called the first- order optimality system for Problem(4.1).

Proof. By applying Proposition 11 and 12. □

4.2 Optimal control of the Hegselmann-Krause opinion formation model

In this section, we study how to enforce consensus in the "best" possible way. First, the formulation of optimal control problems with the HK model and the presence of a leader are formulated and the corresponding optimality systems are obtained. From now on, we set the problem in a more general framework in which we allow the communication rate of the leader with the followers to be zero. To this purpose, we introduce two functions: c_i^1 and c_i^2. In the first case, $c_i^1 : \mathbb{R} \to [0,1]$ represents a cut-off smooth function of the bounded confidence δ_0 as follows

$$c_i^1(r) = c_i^1(r;\delta_0,\varepsilon_0) \;=\; \begin{cases} 1, & 0 \le r \le \delta_0, \\ \widetilde{\varphi}(r_{i0}), & \delta_0 < r < (\delta_0+\varepsilon_0), \\ 0, & (\delta_0+\varepsilon_0) \le r, \end{cases} \tag{4.20}$$

for a smooth decreasing function $\widetilde{\varphi}(r)$ between $(\delta_0, \delta_0+\varepsilon_0]$. We then denote by $c_i^2(r) = \phi(r)$ the function of the distance between the leader and the followers as in the previous sections, i.e. a non-increasing positive function such that $\phi(0) = 1$ and $\lim_{r\to\infty}\phi(r) = 0$.

Our optimal control problem is stated as follows

$$\begin{aligned} \min_{\mathbf{x}^{\rm of},u^{\rm of}} J^{\rm of}(\mathbf{x}^{\rm of},u^{\rm of}) \;:=\; & \frac{\mu}{2}\|x_0^{\rm of}(T) - x_{des}^{\rm of}(T)\|^2 + \frac{1}{2N^2}\int_0^T \sum_{i,j=1}^N \|x_i^{\rm of}(t) - x_j^{\rm of}(t)\|^2 dt \\ & + \frac{1}{2}\int_0^T \sum_{i=1}^N \|x_0^{\rm of}(t) - x_i^{\rm of}(t)\|^2 dt + \frac{\nu}{2}\int_0^T \|u^{\rm of}(t)\|^2 dt, \end{aligned} \tag{4.21}$$

$$\begin{aligned} \text{subject to} \quad \dot{x}_0^{\rm of}(t) &= u^{\rm of}(t), \\ \dot{x}_i^{\rm of}(t) &= \sum_{j\neq 0,i} a_{ij}(x_j^{\rm of} - x_i^{\rm of}) + c_i^{\widetilde{n}}(x_0^{\rm of} - x_i^{\rm of}), \quad \text{for} \quad i = 1,...,N, \end{aligned}$$

with given initial conditions and for $\widetilde{n} = 1, 2$. The positive parameters μ and ν in the cost function are weight constants. Notice that, the second and third term in the cost functional corresponds to consensus problem. In addition, the tracking functional at final time requires the leader to approach a desired target opinion $x_{des}^{\rm of}$. This term has also the property to stabilize the MPC scheme [44]. The last term in the functional represents the cost of the control. The problem stated in (4.21) can be written in the

general form presented in (4.2) as follows

$$\begin{aligned} \min_{x^{\text{of}},u^{\text{of}}} J^{\text{of}}(x^{\text{of}},u^{\text{of}}) &= \frac{\mu}{2}\|x_0^{\text{of}}(T)-x_{des}^{\text{of}}(T)\|^2+\int_0^T l^{\text{of}}(x^{\text{of}})dt+\frac{\nu}{2}\int_0^T\|u(t)\|^2dt, \\ \text{s.t} \quad \dot{\mathbf{x}}^{\text{of}}(t) &= \mathbf{f}^{\text{of}}(\mathbf{x}^{\text{of}})+\mathbf{B}^{\text{of}}u^{\text{of}}(t), \\ \mathbf{x}^{\text{of}}\in\mathbb{X}^{\text{of}}, &\quad u^{\text{of}}\in\mathbb{U}^{\text{of}}=L^2((0,T);\mathbb{R}^d), \end{aligned} \tag{4.22}$$

where the vector $\mathbf{x}^{\text{of}}=(x_0^{\text{of}},x_1^{\text{of}},...,x_N^{\text{of}})$ is the state of the system and belongs to

$$\mathbb{X}^{\text{of}}=\{\mathbf{x}^{\text{of}}\in H^1((0,T);\mathbb{R}^{d(N+1)}):\mathbf{x}^{\text{of}}(0)=\mathbf{x}_0^{\text{of}}\}. \tag{4.23}$$

The function $u^{\text{of}}:[0,T]\to\mathbb{R}^d$ is the control function. The functional $l^{\text{of}}:\mathbb{R}^{d(N+1)}\to\mathbb{R}$ is defined as

$$l^{\text{of}}(\mathbf{x}^{\text{of}}):=\frac{1}{2N^2}\sum_{i,j=1}^N\|x_i^{\text{of}}(t)-x_j^{\text{of}}(t)\|^2+\frac{1}{2}\sum_{i=1}^N\|x_0^{\text{of}}(t)-x_i^{\text{of}}(t)\|^2. \tag{4.24}$$

The vector-valued function $\mathbf{f}^{\text{of}}:\mathbb{R}^{d(N+1)}\to\mathbb{R}^{d(N+1)}$ in the first term of the dynamics of the system and the constant matrix $\mathbf{B}^{\text{of}}\in\mathbb{R}^{d(N+1)\times d}$ are given by

$$\mathbf{f}^{\text{of}}=\begin{pmatrix} 0 \\ \sum_{j\neq 0,1}a_{1j}(x_j^{\text{of}}-x_1^{\text{of}})+c_1^{\tilde{n}}(x_0^{\text{of}}-x_1^{\text{of}}) \\ \sum_{j\neq 0,2}a_{2j}(x_j^{\text{of}}-x_2^{\text{of}})+c_2^{\tilde{n}}(x_0^{\text{of}}-x_2^{\text{of}}) \\ \vdots \\ \sum_{j\neq 0,N}a_{Nj}(x_j^{\text{of}}-x_N^{\text{of}})+c_N^{\tilde{n}}(x_0^{\text{of}}-x_N^{\text{of}}) \end{pmatrix}, \quad \mathbf{B}^{\text{of}}=\begin{pmatrix} \mathbf{I}_d \\ \mathbf{0}_{d,d} \\ \mathbf{0}_{d,d} \\ \vdots \\ \mathbf{0}_{d,d} \end{pmatrix}. \tag{4.25}$$

Remark 6.

1. *The gradient of the functional l^{of} is given by*

$$\nabla_x l^{\text{of}}=\begin{pmatrix}\frac{\partial l^{\text{of}}}{\partial x_0^{\text{of}}} & \frac{\partial l^{\text{of}}}{\partial x_1^{\text{of}}} & \cdots & \frac{\partial l^{\text{of}}}{\partial x_N^{\text{of}}}\end{pmatrix}^\top, \tag{4.26}$$

where its components are given by the following

$$\begin{aligned} \frac{\partial l^{\text{of}}}{\partial x_0^{\text{of}}} &= \sum_{i=1}^N(x_0^{\text{of}}-x_i^{\text{of}}), \\ \frac{\partial l^{\text{of}}}{\partial x_i^{\text{of}}} &= \frac{2}{N^2}\sum_{j\neq i}(x_i^{\text{of}}-x_j^{\text{of}})-(x_0^{\text{of}}-x_i^{\text{of}}). \end{aligned}$$

2. *The jacobian matrix $\mathbf{f}^{\text{of}}$ is presented as follows*

$$\nabla_x\mathbf{f}^{\text{of}}=\begin{pmatrix}\frac{\partial f_0^{\text{of}}}{\partial x_0^{\text{of}}} & \frac{\partial f_0^{\text{of}}}{\partial x_1^{\text{of}}} & \cdots & \frac{\partial f_0^{\text{of}}}{\partial x_N^{\text{of}}} \\ \frac{\partial f_1^{\text{of}}}{\partial x_0^{\text{of}}} & \frac{\partial f_1^{\text{of}}}{\partial x_1^{\text{of}}} & \cdots & \frac{\partial f_1^{\text{of}}}{\partial x_N^{\text{of}}} \\ \vdots & \vdots & \ddots & \vdots \\ \frac{\partial f_N^{\text{of}}}{\partial x_0^{\text{of}}} & \frac{\partial f_N^{\text{of}}}{\partial x_1^{\text{of}}} & \cdots & \frac{\partial f_N^{\text{of}}}{\partial x_N^{\text{of}}}\end{pmatrix}, \tag{4.27}$$

where its components are as follows

$$
\begin{aligned}
\frac{\partial f_0^{\text{of}}}{\partial x_i^{\text{of}}} &= 0, \qquad (4.28)\\
\frac{\partial f_b^{\text{of}}}{\partial x_0^{\text{of}}} &= c_i^{\tilde{n}}(\|x_i^{\text{of}} - x_0^{\text{of}}\|) + \frac{\partial c_i^{\tilde{n}}}{\partial x_0^{\text{of}}}(x_0^{\text{of}} - x_i^{\text{of}}),\\
\frac{\partial f_b^{\text{of}}}{\partial x_b^{\text{of}}} &= -\sum_{j=1}^{N} a_{bj}(\|x_b^{\text{of}} - x_j^{\text{of}}\|)(x_j^{\text{of}} - x_b^{\text{of}}) + \frac{\partial a_{bj}}{\partial x_b^{\text{of}}}(x_j^{\text{of}} - x_b^{\text{of}}) - c_b^{\tilde{n}}(\|x_b^{\text{of}} - x_0^{\text{of}}\|)\\
&\quad + \frac{\partial c_b^{\tilde{n}}}{\partial x_b^{\text{of}}}(x_0^{\text{of}} - x_b^{\text{of}}),\\
\frac{\partial f_b^{\text{of}}}{\partial x_j^{\text{of}}} &= a_{bj}(\|x_b^{\text{of}} - x_j^{\text{of}}\|) + \frac{\partial a_{bj}}{\partial x_j^{\text{of}}}(x_j^{\text{of}} - x_b^{\text{of}}), \quad for \quad i = 0, ..., N, b = 1, ..., N.
\end{aligned}
$$

We assume that the pair $(\mathbf{x}^{\text{of}}, u^{\text{of}}) \in \mathbb{X}^{\text{of}} \times \mathbb{U}^{\text{of}}$ is a minimizer for the problem (4.21). By Theorem 9, there exists a unique Lagrange multiplier $\mathbf{p}^{\text{of}} \in H^1((0,T);\mathbb{R}^{d(N+1)})$ such that the triple $(\mathbf{x}^{\text{of}}, u^{\text{of}}, \mathbf{p}^{\text{of}})$ solves the following system,

$$\begin{array}{ll} \dot{\mathbf{x}}^{\text{of}} = \mathbf{f}^{\text{of}}(\mathbf{x}^{\text{of}}) + \mathbf{B}^{\text{of}} u^{\text{of}}, & \mathbf{x}^{\text{of}}(0) = \mathbf{x}_0^{\text{of}}, \\ -\dot{\mathbf{p}}^{\text{of}} = -(\nabla_x l^{\text{of}}(\mathbf{x}^{\text{of}}))^\top + (\nabla_x \mathbf{f}^{\text{of}}(\mathbf{x}^{\text{of}}))^\top \mathbf{p}^{\text{of}}, & \mathbf{p}^{\text{of}}(T) = -(\mathbf{x}^{\text{of}}(T) - \mathbf{x}_{des}^{\text{of}}(T)), \\ \nu u^{\text{of}} - (\mathbf{B}^{\text{of}})^\top \mathbf{p}^{\text{of}} = 0, & \end{array} \tag{4.29}$$

where $\nabla_x l^{\text{of}}$ is defined in (4.26) and $\nabla_x \mathbf{f}^{\text{of}}(\mathbf{x}^{\text{of}})$ is given in (4.27) and final condition for adjoint equation is given by

$$\mathbf{x}^{\text{of}}(T) - \mathbf{x}_{des}^{\text{of}}(T) = (x_0^{\text{of}}(T) - x_{des}^{\text{of}}(T), \mathbf{0}_{d,1}, \mathbf{0}_{d,1}, ..., \mathbf{0}_{d,1})^\top. \tag{4.30}$$

The system (4.29) is called the first- order optimality system for Problem(4.22).

4.3 Optimal control of the Heider social balance model

In this section, we formulate an optimal control problem of the Heider balance model with the presence of a leader. We have

$$\min_{\mathbf{x}^{\text{hb}}, \mathbf{u}^{\text{hb}}} J^{\text{hb}}(\mathbf{x}^{\text{hb}}, \mathbf{u}^{\text{hb}}) = \frac{1}{2} \sum_{i,j=1}^{N} (x_{ij}^{\text{hb}}(T) - x_{des}^{\text{hb}})^2 + \frac{\nu}{2} \|\mathbf{u}^{\text{hb}}(t)\|_{L^2}^2, \tag{4.31}$$

subject to the differential constraint given by

$$\begin{aligned} \dot{x}_{0i}^{\text{hb}}(t) &= u_i^{\text{hb}}(t), \\ \dot{x}_{ij}^{\text{hb}}(t) &= \frac{1}{N-2} \left(1 - \frac{(x_{ij}^{\text{hb}})^2}{R^2}\right) \sum_{k=0}^{N} x_{ik}^{\text{hb}} x_{kj}^{\text{hb}} + \gamma x_{i0}^{\text{hb}} x_{j0}^{\text{hb}}, \quad \text{for} \quad i,j = 1, ..., N, \end{aligned} \tag{4.32}$$

with given initial conditions. This optimal control problem requires to find a vector of controls $u_i^{\text{hb}} : (0,T) \to \mathbb{R}$, $i = 1, \ldots, N$, such that the HB model evolves from the given initial condition to a final state $x_{ij}^{\text{hb}}(T)$ that is as close as possible to the given friendship state $x_{des}^{\text{hb}} \in \mathbb{R}$ while minimizing the cost of the control given by the second term of the cost functional J^{hb}, where $\nu > 0$ represents the weight of the cost of the control. The problem stated in (4.31) and (4.32) can be written in the general form presented in (4.2) as the following,

$$\begin{aligned} \min_{\mathbf{x}^{\text{hb}}, \mathbf{u}^{\text{hb}}} J^{\text{hb}}(\mathbf{x}^{\text{hb}}, \mathbf{u}^{\text{hb}}) &= \frac{1}{2} \sum_{i,j=0}^{N} (x_{ij}^{\text{hb}}(T) - x_{des}^{\text{hb}})^2 + \frac{\nu}{2} \|\mathbf{u}^{\text{hb}}(t)\|_{L^2}^2, \\ \text{subject to} \quad \dot{\mathbf{x}}^{\text{hb}}(t) &= \mathbf{f}^{\text{hb}}(\mathbf{x}^{\text{hb}}) + \mathbf{B}^{\text{hb}} \mathbf{u}^{\text{hb}}(t), \end{aligned} \tag{4.33}$$

where the state variable $\mathbf{x}^{\text{hb}} = (x_{01}^{\text{hb}}, x_{02}^{\text{hb}}, ..., x_{(N-1)N}^{\text{hb}})$ has the dimension

$$N_r = \frac{N(N+1)}{2},$$

N_r denoted the number of relationship in the social group. The state $\mathbf{x}^{\text{hb}}$ belongs to

$$\mathbb{X}^{\text{hb}} = \{\mathbf{x}^{\text{hb}} \in H^1((0,T);\mathbb{R}^{N_r}) : \mathbf{x}^{\text{hb}}(0) = \mathbf{x}_0^{\text{hb}}\},$$

with x_0^{hb} a given initial condition. The function $\mathbf{u}^{\text{hb}} = (u_1^{\text{hb}}, u_2^{\text{hb}}, \ldots, u_N^{\text{hb}}) \in \mathbb{R}^N$, $u_i^{\text{hb}} : [0,T] \to \mathbb{R}$, is the control function. Notice that in the HB model the number of controllers is equal to the number of links connecting the leader to individuals. The vector-valued function $\mathbf{f}^{\text{hb}} : \mathbb{R}^{N_r} \to \mathbb{R}^{N_r}$ in the first term of the dynamics of the system and the constant matrix $\mathbf{B}^{\text{hb}} \in \mathbb{R}^{N_r \times N}$ are given by

$$\begin{aligned}
\mathbf{f}^{\text{hb}}(\mathbf{x}^{\text{hb}}) &= \frac{1}{N-2}\begin{pmatrix}
\mathbf{0}_{N,1} \\
\left(1 - \frac{(x_{12}^{\text{hb}})^2}{R^2}\right)\sum_{k=1}^{N} x_{1k}^{\text{hb}} x_{k2}^{\text{hb}} + \gamma x_{01}^{\text{hb}} x_{02}^{\text{hb}} \\
\left(1 - \frac{(x_{13}^{\text{hb}})^2}{R^2}\right)\sum_{k=1}^{N} x_{1k}^{\text{hb}} x_{k3}^{\text{hb}} + \gamma x_{01}^{\text{hb}} x_{03}^{\text{hb}} \\
\vdots \\
\left(1 - \frac{(x_{(N-1)N}^{\text{hb}})^2}{R^2}\right)\sum_{k=1}^{N} x_{(N-1)k}^{\text{hb}} x_{kN}^{\text{hb}} + \gamma x_{0(N-1)}^{\text{hb}} x_{0N}^{\text{hb}}
\end{pmatrix}, \\
\mathbf{B}^{\text{hb}} &= \begin{pmatrix} \mathbf{I}_{N,N} \\ \mathbf{0}_{N_{uc},N} \end{pmatrix},
\end{aligned}$$

where N_{uc} is the number of the uncontrolled variables, in our case $N_{uc} = N_r - N$.

Remark 7. *The Jacobian matrix $\nabla_x \mathbf{f}^{\text{hb}}$ is as follows*

$$\nabla_x \mathbf{f}^{\text{hb}} = \begin{pmatrix}
\frac{\partial f_{01}^{\text{of}}}{\partial x_{01}^{\text{hb}}} & \cdots & \frac{\partial f_{01}^{\text{of}}}{\partial x_{0N}^{\text{hb}}} & \frac{\partial f_{01}^{\text{of}}}{\partial x_{12}^{\text{hb}}} & \cdots & \frac{\partial f_{01}^{\text{of}}}{\partial x_{1N}^{\text{hb}}} & \cdots & \frac{\partial f_{01}^{\text{of}}}{\partial x_{(N-1)N}^{\text{hb}}} \\
\vdots & \cdots & \vdots & \vdots & \cdots & \vdots & \cdots & \vdots \\
\frac{\partial f_{0N}^{\text{of}}}{\partial x_{01}^{\text{hb}}} & \cdots & \frac{\partial f_{0N}^{\text{of}}}{\partial x_{0N}^{\text{hb}}} & \frac{\partial f_{0N}^{\text{of}}}{\partial x_{12}^{\text{hb}}} & \cdots & \frac{\partial f_{0N}^{\text{of}}}{\partial x_{1N}^{\text{hb}}} & \cdots & \frac{\partial f_{0N}^{\text{of}}}{\partial x_{(N-1)N}^{\text{hb}}} \\
\frac{\partial f_{12}^{\text{of}}}{\partial x_{01}^{\text{hb}}} & \cdots & \frac{\partial f_{12}^{\text{of}}}{\partial x_{0N}^{\text{hb}}} & \frac{\partial f_{12}^{\text{of}}}{\partial x_{12}^{\text{hb}}} & \cdots & \frac{\partial f_{12}^{\text{of}}}{\partial x_{1N}^{\text{hb}}} & \cdots & \frac{\partial f_{12}^{\text{of}}}{\partial x_{(N-1)N}^{\text{hb}}} \\
\vdots & \cdots & \vdots & \vdots & \cdots & \vdots & \cdots & \vdots \\
\frac{\partial f_{(N-1)N}^{\text{of}}}{\partial x_{01}^{\text{hb}}} & \cdots & \frac{\partial f_{(N-1)N}^{\text{of}}}{\partial x_{0N}^{\text{hb}}} & \frac{\partial f_{(N-1)N}^{\text{of}}}{\partial x_{12}^{\text{hb}}} & \cdots & \frac{\partial f_{(N-1)N}^{\text{of}}}{\partial x_{1N}^{\text{hb}}} & \cdots & \frac{\partial f_{(N-1)N}^{\text{of}}}{\partial x_{(N-1)N}^{\text{hb}}}
\end{pmatrix},$$

where its elements are given by

$$
\begin{aligned}
\frac{\partial f_{0b}^{\text{of}}}{\partial x_{ij}^{\text{hb}}} &= 0, \qquad \textit{for} \quad i = 0, 1, ..., N, \\
\frac{\partial f_{bj}^{\text{of}}}{\partial x_{0b}^{\text{hb}}} &= \gamma x_{0j}^{\text{hb}}, \\
\frac{\partial f_{bj}^{\text{of}}}{\partial x_{0j}^{\text{hb}}} &= \gamma x_{0b}^{\text{hb}}, \\
\frac{\partial f_{bj}^{\text{of}}}{\partial x_{bj}^{\text{hb}}} &= -\frac{2x_{bj}^{\text{hb}}}{(N-2)R^2}\left(\sum_{k\neq 0,b,j}^{N} x_{bk}^{\text{hb}} x_{kj}^{\text{hb}}\right), \\
\frac{\partial f_{bj}^{\text{of}}}{\partial x_{bk}^{\text{hb}}} &= \frac{x_{kj}^{\text{hb}}}{N-2}\left(1 - \frac{(x_{bj}^{\text{hb}})^2}{R^2}\right), \\
\frac{\partial f_{bj}^{\text{of}}}{\partial x_{kj}^{\text{hb}}} &= \frac{x_{bk}^{\text{hb}}}{N-2}\left(1 - \frac{(x_{bj}^{\text{hb}})^2}{R^2}\right), \quad \textit{for} \quad b, j, k = 1, 2, \ldots, N, \quad \textit{and} \quad k \neq b \neq j.
\end{aligned} \tag{4.34}
$$

Let us assume that the pair $(\mathbf{x}^{\text{hb}}, \mathbf{u}^{\text{hb}}) \in \mathbb{X}^{\text{hb}} \times L^2((0,T);\mathbb{R}^N)$ is a minimizer for the problem (4.33). Then there exists a unique Lagrange multiplier $\mathbf{p}^{\text{hb}} \in H^1((0,T);\mathbb{R}^{N_r})$ such that the triple $(\mathbf{x}^{\text{hb}}, \mathbf{u}^{\text{hb}}, \mathbf{p}^{\text{hb}})$ solves the following system,

$$
\begin{aligned}
&\dot{\mathbf{x}}^{\text{hb}} = \mathbf{f}^{\text{hb}} + \mathbf{B}^{\text{hb}}\mathbf{u}^{\text{hb}}, && \mathbf{x}^{\text{hb}}(0) = \mathbf{x}_0^{\text{hb}}, \\
&-\dot{\mathbf{p}}^{\text{hb}} = \nabla_x \mathbf{f}^{\text{hb}}(\mathbf{x}^{\text{hb}}))^\top \mathbf{p}^{\text{hb}}, && \mathbf{p}^{\text{hb}}(T) = -(\mathbf{x}^{\text{hb}}(T) - \mathbf{x}^{\text{hb}}des(T)), \\
&\nu\mathbf{u}^{\text{hb}} - (\mathbf{B}^{\text{hb}})^\top \mathbf{p}^{\text{hb}} = 0,
\end{aligned} \tag{4.35}
$$

where $\nabla_x \mathbf{f}^{\text{hb}}(\mathbf{x}^{\text{hb}})$ is defined as in Remark. 7 and the final condition for the adjoint equation is given by

$$
\mathbf{x}^{\text{hb}}(T) - \mathbf{x}_{des}^{\text{hb}}(T) = \begin{pmatrix} x_{01}^{\text{hb}}(T) - x_{des}^{\text{hb}} \\ x_{02}^{\text{hb}}(T) - x_{des}^{\text{hb}} \\ \vdots \\ x_{12}^{\text{hb}}(T) - x_{des}^{\text{hb}} \\ \vdots \\ x_{(N-1)N}^{\text{hb}}(T) - x_{des}^{\text{hb}} \end{pmatrix}, \tag{4.36}
$$

The system (4.35) is called the first- order optimality system for (4.33).

4.4 Optimal control of a refined flocking model

In this section, we consider our flocking model in the presence of an external leader that is subject to a control function that aims at driving the leader and the group to reach a target position or to follow a desired trajectory, $\mathbf{x}_{des}^{\text{fm}}$. In the following, we discuss these two optimal control problems for our refined flocking model with leadership. For the case where the objective is a target position at a final time, we have

Problem P1. Reach a target position at final time T.

$$\begin{aligned}
\min_{\mathbf{x}^{\mathrm{fm}},u^{\mathrm{fm}}} \quad J_1^{\mathrm{fm}}(\mathbf{x}^{\mathrm{fm}},u^{\mathrm{fm}}) &= \frac{1}{2}\|x_0^{\mathrm{fm}}(T)-x_{des}^{\mathrm{fm}}(T)\|^2+\frac{\mu}{2}\sum_{b=1}^{N}\int_0^T\|x_0^{\mathrm{fm}}(t)-x_b^{\mathrm{fm}}(t)\|^4\,dt \\
&\quad +\frac{\nu}{2}\|\mathbf{u}^{\mathrm{fm}}(t)\|_{L^2}^2, \qquad (4.37)\\
\text{subject to} \quad \dot{x}_0^{\mathrm{fm}}(t) &= v_0^{\mathrm{fm}}(t),\\
\dot{x}_b^{\mathrm{fm}}(t) &= v_b^{\mathrm{fm}}(t), \qquad (4.38)\\
\dot{v}_0^{\mathrm{fm}}(t) &= S_0+M_0+E_0+u^{\mathrm{fm}}(t),\\
\dot{v}_b^{\mathrm{fm}}(t) &= S_b+M_b+E_b+L_b, \qquad \text{for} \quad b=1,...,N,
\end{aligned}$$

with given initial conditions for the positions and velocities of the agents of the flock.

Problem P2. Follow a desired trajectory.

$$\begin{aligned}
\min_{\mathbf{x}^{\mathrm{fm}},u^{\mathrm{fm}}} \quad J_2^{\mathrm{fm}}(\mathbf{x}^{\mathrm{fm}},u^{\mathrm{fm}}) &= \frac{1}{2}\|x_0^{\mathrm{fm}}(T)-x_{des}^{\mathrm{fm}}(T)\|^2+\frac{\mu}{2}\sum_{b=1}^{N}\int_0^T\|x_0^{\mathrm{fm}}(t)-x_b^{\mathrm{fm}}(t)\|^4dt, \\
&\quad +\frac{\eta}{2}\int_{t_0}^{t_f}\|x_0^{\mathrm{fm}}(t)-x_{des}^{\mathrm{fm}}(t)\|^2dt+\frac{\nu}{2}\|u^{\mathrm{fm}}(t)\|_{L^2}^2 \qquad (4.39)\\
\text{subject to} \quad \dot{x}_0^{\mathrm{fm}}(t) &= v_0^{\mathrm{fm}}(t),\\
\dot{x}_b^{\mathrm{fm}}(t) &= v_b^{\mathrm{fm}}(t), \qquad (4.40)\\
\dot{v}_0^{\mathrm{fm}}(t) &= S_0+M_0+E_0+u^{\mathrm{fm}}(t),\\
\dot{v}_b^{\mathrm{fm}}(t) &= S_b+M_b+E_b+L_b, \qquad \text{for} \quad b=1,...,N,
\end{aligned}$$

with given initial conditions for the positions and velocities of the agents of the flock.

In the problems P1 and P2, $\mathbf{x}^{\mathrm{fm}}=(x_0^{\mathrm{fm}},\ldots,x_N^{\mathrm{fm}},v_0^{\mathrm{fm}},\ldots,v_N^{\mathrm{fm}})\in\mathbb{R}^{2d(N+1)}$ represents state variables and belongs to the following set

$$\mathbb{X}^{\mathrm{fm}}=\{\mathbf{x}^{\mathrm{fm}}\in H^1((0,T);\mathbb{R}^{2d(N+1)}):\quad \mathbf{x}^{\mathrm{fm}}(0)=\mathbf{x}_0^{\mathrm{fm}}\}. \qquad (4.41)$$

The control function $u^{\mathrm{fm}}(t)\in L^2((0,T);\mathbb{R}^d)$ represent the control force. The parameters μ, ν, and η in the cost functions are positive constants. Notice that in both problems, the second term in the functionals has the purpose to minimize the distance between the leader and the other agents in flock. The power four of this distance results from numerical experience. The last term in the functionals represents the cost of the control. In problem P2, the tracking functional implements the additional objective of minimizing the distance between the trajectory of the leader and a desired path.

We reformulate our optimal control such that it is in the form (4.1) and (4.2). Corresponding to problem P1, we obtain the following system

Problem P1. Reach a target position at final time T

$$\begin{aligned} \min_{\mathbf{x}^{\mathrm{fm}},u^{\mathrm{fm}}} \quad J_1^{\mathrm{fm}}(\mathbf{x}^{\mathrm{fm}},u^{\mathrm{fm}}) &= \frac{1}{2}\|x_0^{\mathrm{fm}}(T)-x_{des}^{\mathrm{fm}}(T)\|^2+\int_0^T l_1^{\mathrm{fm}}(\mathbf{x}^{\mathrm{fm}})dt+\frac{\nu}{2}\|u^{\mathrm{fm}}\|_{L^2}^2, \\ \text{subject to} \quad \dot{\mathbf{x}}^{\mathrm{fm}} &= \mathbf{f}^{\mathrm{fm}}(\mathbf{x}^{\mathrm{fm}})+\mathbf{B}^{\mathrm{fm}}u^{\mathrm{fm}} \end{aligned} \tag{4.42}$$

where the function $l_1^{\mathrm{fm}}:\mathbb{R}^{2d(N+1)}\to\mathbb{R}$ is defined as

$$l_1^{\mathrm{fm}}(\mathbf{x}^{\mathrm{fm}})=\frac{\mu}{2}\sum_{b=1}^{N}\|x_0^{\mathrm{fm}}(t)-x_b^{\mathrm{fm}}(t)\|^4. \tag{4.43}$$

Problem P2. Follow a desired trajectory

$$\begin{aligned} \min_{\mathbf{x}^{\mathrm{fm}},u^{\mathrm{fm}}} \quad J_2^{\mathrm{fm}}(\mathbf{x}^{\mathrm{fm}},u^{\mathrm{fm}}) &= \frac{1}{2}\|x_0^{\mathrm{fm}}(T)-x_{des}^{\mathrm{fm}}(T)\|^2+\int_0^T l_2^{\mathrm{fm}}(\mathbf{x}^{\mathrm{fm}})dt+\frac{\nu}{2}\|u^{\mathrm{fm}}(t)\|_{L^2}^2 \\ \text{subject to} \quad \dot{\mathbf{x}}^{\mathrm{fm}} &= \mathbf{f}^{\mathrm{fm}}(\mathbf{x}^{\mathrm{fm}})+\mathbf{B}^{\mathrm{fm}}u^{\mathrm{fm}} \end{aligned} \tag{4.44}$$

with given initial conditions. The function $l_2^{\mathrm{fm}}:\mathbb{R}^{2d(N+1)}\to\mathbb{R}$ is given by

$$l_2^{\mathrm{fm}}(\mathbf{x}^{\mathrm{fm}})=\frac{\mu}{2}\sum_{b=1}^{N}\|x_0^{\mathrm{fm}}(t)-x_b^{\mathrm{fm}}(t)\|^4+\frac{\eta}{2}\|x_0^{\mathrm{fm}}(t)-x_{des}^{\mathrm{fm}}(t)\|^2. \tag{4.45}$$

Both problems P1 and P2 can be written in compact form as follows

$$\begin{aligned} \min \quad J_{\widetilde{n}}^{\mathrm{fm}}(\mathbf{x}^{\mathrm{fm}},u^{\mathrm{fm}}) &= \frac{1}{2}\|x_0^{\mathrm{fm}}(T)-x_{des}^{\mathrm{fm}}(T)\|^2+\int_0^T l_{\widetilde{n}}^{\mathrm{fm}}(\mathbf{x}^{\mathrm{fm}})dt+\frac{\nu}{2}\|u^{\mathrm{fm}}\|_{L^2}^2, \\ \text{subject to} \quad \dot{\mathbf{x}}^{\mathrm{fm}} &= \mathbf{f}^{\mathrm{fm}}(\mathbf{x}^{\mathrm{fm}})+\mathbf{B}^{\mathrm{fm}}u^{\mathrm{fm}}(t), \end{aligned} \tag{4.46}$$

where $\widetilde{n}=1,2$ denotes the problem. In both problem, the function $\mathbf{f}^{\mathrm{fm}}:\mathbb{R}^{2d(N+1)}\to\mathbb{R}^{2d(N+1)}$ and the constant matrix $\mathbf{B}^{\mathrm{fm}}$ are given by

$$\mathbf{f}^{\mathrm{fm}}(\mathbf{x}^{\mathrm{fm}})=\begin{pmatrix} v_0^{\mathrm{fm}} \\ v_1^{\mathrm{fm}} \\ \vdots \\ v_N^{\mathrm{fm}} \\ S_0+M_0+A_0 \\ S_1+M_1+A_1+L_1 \\ \vdots \\ S_N+M_N+A_N+L_N \end{pmatrix}, \qquad \mathbf{B}^{\mathrm{fm}}=\begin{pmatrix} \mathbf{0}_{d,d} \\ \mathbf{0}_{d,d} \\ \vdots \\ \mathbf{0}_{d,d} \\ \mathbf{I}_d \\ \mathbf{0}_{d,d} \\ \vdots \\ \mathbf{0}_{d,d} \end{pmatrix}. \tag{4.47}$$

Remark 8.

1. *The gradient of* $l_1^{\mathrm{fm}}(\mathbf{x}^{\mathrm{fm}})$ *with respect to* $\mathbf{x}^{\mathrm{fm}}$ *is given by*

$$\nabla_x l_1^{\mathrm{fm}}(\mathbf{x}^{\mathrm{fm}}) = \left(\frac{\partial l_1^{\mathrm{fm}}}{\partial x_0^{\mathrm{fm}}} \quad \frac{\partial l_1^{\mathrm{fm}}}{\partial x_1^{\mathrm{fm}}} \quad \cdots \quad \frac{\partial l_1^{\mathrm{fm}}}{\partial x_N^{\mathrm{fm}}} \quad \frac{\partial l_1^{\mathrm{fm}}}{\partial v_0^{\mathrm{fm}}} \quad \cdots \quad \frac{\partial l_1^{\mathrm{fm}}}{\partial v_N^{\mathrm{fm}}} \right)^\top, \tag{4.48}$$

where its elements are given by

$$\begin{aligned} \frac{\partial l_1^{\mathrm{fm}}}{\partial x_0^{\mathrm{fm}}} &= 2\mu \sum_{b=1}^{N} \|(x_0^{\mathrm{fm}} - x_b^{\mathrm{fm}})\|^2, \\ \frac{\partial l_1^{\mathrm{fm}}}{\partial x_b^{\mathrm{fm}}} &= -2\mu (x_0^{\mathrm{fm}} - x_b^{\mathrm{fm}}) \|\|^2, \\ \frac{\partial l_1^{\mathrm{fm}}}{\partial v_i^{\mathrm{fm}}} &= 0, \quad for \quad i = 0, ..., N. \end{aligned} \tag{4.49}$$

2. *The gradient of* $l_2^{\mathrm{fm}}(\mathbf{x}^{\mathrm{fm}})$ *with respect to* $\mathbf{x}^{\mathrm{fm}}$ *is given by*

$$\nabla_x l_2^{\mathrm{fm}}(\mathbf{x}^{\mathrm{fm}}) = \left(\frac{\partial l_2^{\mathrm{fm}}}{\partial x_0^{\mathrm{fm}}} \quad \frac{\partial l_2^{\mathrm{fm}}}{\partial x_1^{\mathrm{fm}}} \quad \cdots \quad \frac{\partial l_2^{\mathrm{fm}}}{\partial x_N^{\mathrm{fm}}} \quad \frac{\partial l_2^{\mathrm{fm}}}{\partial v_0^{\mathrm{fm}}} \quad \cdots \quad \frac{\partial l_2^{\mathrm{fm}}}{\partial v_N^{\mathrm{fm}}} \right)^\top, \tag{4.50}$$

where its elements are given by

$$\begin{aligned} \frac{\partial l_2^{\mathrm{fm}}}{\partial x_0^{\mathrm{fm}}} &= 2\mu \sum_{b=1}^{N} \|(x_0^{\mathrm{fm}} - x_b^{\mathrm{fm}})\|^2 + \eta (x_0^{\mathrm{fm}} - x_{des}^{\mathrm{fm}}), \\ \frac{\partial l_2^{\mathrm{fm}}}{\partial x_b^{\mathrm{fm}}} &= -2\mu \|(x_0^{\mathrm{fm}} - x_b^{\mathrm{fm}})\|^2, \\ \frac{\partial l_2^{\mathrm{fm}}}{\partial v_i^{\mathrm{fm}}} &= 0, \quad for \quad i = 0, ..., N. \end{aligned} \tag{4.51}$$

We assume that the pair $(\mathbf{x}^{\mathrm{fm}}, \mathbf{u}^{\mathrm{fm}}) \in \mathbb{X}^{\mathrm{fm}} \times L^2((0,T); \mathbb{R}^d)$ are minimizer for the problem (4.46). Then there exists a unique Lagrange multiplier $\mathbf{p}^{\mathrm{fm}} \in H^1((0,T); \mathbb{R}^{2d(N+1)})$ such that the triple $(\mathbf{x}^{\mathrm{fm}}, u^{\mathrm{fm}}, \mathbf{p}^{\mathrm{fm}})$ solves the following system,

$$\begin{array}{ll} \dot{\mathbf{x}}^{\mathrm{fm}} = \mathbf{f}^{\mathrm{fm}}(\mathbf{x}^{\mathrm{fm}}) + \mathbf{B}^{\mathrm{fm}} u^{\mathrm{fm}}, & \mathbf{x}^{\mathrm{fm}}(0) = \mathbf{x}_0^{\mathrm{fm}}, \\ -\dot{\mathbf{p}}^{\mathrm{fm}} = -(\nabla_x l_{\widetilde{n}}^{\mathrm{fm}}(\mathbf{x}^{\mathrm{fm}}))^\top + (\nabla_x \mathbf{f}^{\mathrm{fm}}(\mathbf{x}^{\mathrm{fm}}))^\top \mathbf{p}^{\mathrm{fm}}, & \mathbf{p}^{\mathrm{fm}}(T) = -(\mathbf{x}^{\mathrm{fm}}(T) - \mathbf{x}_{des}^{\mathrm{fm}}(T)), \\ \nu u^{\mathrm{fm}} - (\mathbf{B}^{\mathrm{fm}})^\top \mathbf{p}^{\mathrm{fm}} = 0, & \end{array}$$

where $\nabla_x l_{\widetilde{n}}^{\mathrm{fm}}(\mathbf{x}^{\mathrm{fm}})$ are defined in (4.48) and (4.50). The Jacobian matrix of function $\mathbf{f}^{\mathrm{fm}}$ with respect to $\mathbf{x}^{\mathrm{fm}}$, $\nabla \mathbf{f}^{\mathrm{fm}}(\mathbf{x}^{\mathrm{fm}})$, is defined in (3.47) and final condition for adjoint equation is given by

$$\mathbf{x}^{\mathrm{fm}}(T) - \mathbf{x}_{des}^{\mathrm{fm}}(T) = (x_0^{\mathrm{fm}}(T) - x_{des}^{\mathrm{fm}}(T), \mathbf{0}_{d,d}, \mathbf{0}_{d,d}, ..., \mathbf{0}_{d,d})^\top. \tag{4.52}$$

This system is called the first- order optimality system for Problem (4.46).

Chapter 5

Numerical discretization and optimization

In this chapter, we address two important issues for implementing our control strategies: The first one is an accurate discretization scheme for the forward multi-agent models and for the optimality systems. The second is a numerical optimization procedure that allows to construct a feedback control mechanism by exploiting the solution of the open-loop optimal control problems discussed in the previous chapter.

5.1 A Runge-Kutta discretization scheme

In this section, we discuss the Runge-Kutta (RK) discretization scheme proposed in [47, 49]. We extend this numerical framework to the case of multi-agent systems and a leadership-based control. One of the motivation for focusing on this scheme [47, 49] is the ability of this method to provide high-order RK schemes for the optimality system equations that are particularly suitable for implementing numerical optimization schemes. Specifically, the scheme in [47, 49] guarantees very accurate gradients that are essential for a successful optimization procedure. For ease of illustration of approximation scheme, we discuss the following optimal control problem

$$\begin{aligned} \min_{x^{\mathrm{rk}},u^{\mathrm{rk}}} \quad & J^{\mathrm{rk}}(x^{\mathrm{rk}},u^{\mathrm{rk}}) &&= \phi(x^{\mathrm{rk}}(T)) \\ \text{subject to} \quad & \dot{x}^{\mathrm{rk}}(t) &&= f^{\mathrm{rk}}(x^{\mathrm{rk}}(t),u^{\mathrm{rk}}(t)), \quad t\in[0,T] \\ & x^{\mathrm{rk}}(t_0) &&= x_0^{\mathrm{rk}}, \end{aligned} \tag{5.1}$$

where $x^{\mathrm{rk}}(t) \in H^1((0,T);\mathbb{R}^{nx})$ and $u^{\mathrm{rk}}(t) \in \mathbb{R}^{nc}$ are called the state and control variables, respectively. We choose $u^{\mathrm{rk}} \in \mathbb{U}^{\mathrm{rk}} = L^2((0,T);\mathbb{R}^{nc})$. The function $\phi : \mathbb{R}^{nx} \to \mathbb{R}$ represents the objective and the dynamics of the model given by $f^{\mathrm{rk}} : \mathbb{R}^{nx} \times \mathbb{R}^{nc} \to \mathbb{R}^{nx}$. We assume that, for a given u^{rk}, the dynamical model in (5.1) admits a unique solution $x^{\mathrm{rk}} = x^{\mathrm{rk}}(u^{\mathrm{rk}})$ and the map $u^{\mathrm{rk}} \mapsto x^{\mathrm{rk}}(u^{\mathrm{rk}})$ is differentiable. Therefore, the problem (5.1) can be written in the following equivalent reduced form.

$$\min_{u^{\mathrm{rk}}\in\mathbb{U}^{\mathrm{rk}}} J_r^{\mathrm{rk}}(u^{\mathrm{rk}}), \tag{5.2}$$

where $J_r^{\mathrm{rk}}(u^{\mathrm{rk}}) := J^{\mathrm{rk}}(x^{\mathrm{rk}}(u^{\mathrm{rk}}), u^{\mathrm{rk}})$. Our aim is to find a control $\widetilde{u}^{\mathrm{rk}}$ such that for all admissible controls u^{rk}, we have

$$J^{\mathrm{rk}}(x^{\mathrm{rk}}(\widetilde{u}^{\mathrm{rk}}), \widetilde{u}^{\mathrm{rk}}) \leqslant J^{\mathrm{rk}}(x^{\mathrm{rk}}(u^{\mathrm{rk}}), u^{\mathrm{rk}}).$$

Suppose that there exists an open set $\Omega \subset \mathbb{R}^{nx} \times \mathbb{R}^{nc}$ such that the neighborhood of $(\tilde{x}^{\mathrm{rk}}, \tilde{u}^{\mathrm{rk}})$ with radius $\epsilon > 0$, $B_\epsilon(\tilde{x}^{\mathrm{rk}}, \tilde{u}^{\mathrm{rk}}) \subset \Omega$ for every $t \in [0, T]$. Moreover, the first partial derivatives of f^{rk} with respect to x^{rk} and u^{rk} are Lipschitz continuous in Ω and the first partial derivatives of J^{rk} with respect to x^{rk} are Lipschitz continuous in $B_\epsilon(\tilde{x}^{\mathrm{rk}}(T))$.
Under these assumptions, there exists an associated Lagrange multiplier $\tilde{p}^{\mathrm{rk}} \in H^1((0, T); \mathbb{R}^{nx})$ for which the following first-order optimality conditions are satisfied at $(\tilde{x}^{\mathrm{rk}}, \tilde{p}^{\mathrm{rk}}, \tilde{u}^{\mathrm{rk}})$ as follows

$$\begin{aligned}
\nabla_p^{\mathrm{rk}} L(\tilde{x}^{\mathrm{rk}}, \tilde{p}^{\mathrm{rk}}, \tilde{u}^{\mathrm{rk}}) &= 0, \\
\nabla_x L(\tilde{x}^{\mathrm{rk}}, \tilde{p}^{\mathrm{rk}}, \tilde{u}^{\mathrm{rk}}) &= 0, \\
\nabla_u L(\tilde{x}^{\mathrm{rk}}, \tilde{p}^{\mathrm{rk}}, \tilde{u}^{\mathrm{rk}}) &= 0,
\end{aligned}$$

where L is the Lagrange function $L : \mathbb{R}^{nx} \times \mathbb{R}^{nx} \times \mathbb{R}^{nc} \to \mathbb{R}$ given by

$$\begin{aligned}
L(x^{\mathrm{rk}}, p^{\mathrm{rk}}, u^{\mathrm{rk}}) &= J^{\mathrm{rk}}(x^{\mathrm{rk}}, u^{\mathrm{rk}}) + \langle \dot{x}^{\mathrm{rk}} - f^{\mathrm{rk}}(x^{\mathrm{rk}}, u^{\mathrm{rk}}), p^{\mathrm{rk}} \rangle_{L^2}, \\
&= \phi(x^{\mathrm{rk}}(T)) + \langle \dot{x}^{\mathrm{rk}} - f^{\mathrm{rk}}(x^{\mathrm{rk}}, u^{\mathrm{rk}}), p^{\mathrm{rk}} \rangle_{L^2}.
\end{aligned}$$

By calculation of the derivation of Lagrange function we obtain the optimality system as presented as following,

$$\begin{array}{ll}
\dot{x}^{\mathrm{rk}}(t) = f^{\mathrm{rk}}(x^{\mathrm{rk}}(t), u^{\mathrm{rk}}(t)), & x^{\mathrm{rk}}(0) = x_0^{\mathrm{rk}}, \\
\dot{p}^{\mathrm{rk}}(t) = -(\nabla_x f^{\mathrm{rk}}(x^{\mathrm{rk}}))^\top p^{\mathrm{rk}}, & p^{\mathrm{rk}}(T) = -(\nabla_x \phi(x^{\mathrm{rk}}(T)))^\top, \\
-(\nabla_u f^{\mathrm{rk}})^\top p^{\mathrm{rk}} = 0, & t \in [0, T].
\end{array} \tag{5.3}$$

We call the first equation of (5.3) the state equation, the second equation is the adjoint equation with the terminal condition $p^{\mathrm{rk}}(T) = \nabla_x \phi(x^{\mathrm{rk}}(T))$. The third condition is referred to as the optimality condition equation.

An essential aspect in the numerical solution of optimal control problems is the discretization of the reduced gradient. In order to derive an adequate discrete reduced gradient, we consider the so-called first-discretize-then optimize strategy, that is, one follows the following procedures. First, one discretize the optimal control problem, that means to discretize the cost functional and the differential constraints . Second, one constructs the corresponding discrete Lagrangian function. Third, one derives the first-order discrete optimality system.
We consider the discretization of the optimality system (5.3) by a RK scheme on a uniform time mesh and the following time-step size

$$h = \frac{T}{n},$$

where n is the total number of discrete time intervals in $(0,T)$ and the value of $x^{\mathrm{rk}}(t)$ at the discrete time t_k is denoted with

$$x_k^{\mathrm{rk}} = x^{\mathrm{rk}}(t_k), \quad t_k = kh \quad \text{for} \quad k = 0, \ldots, n.$$

We consider a s-stage Runge-Kutta discretization scheme that is defined by setting the values of the coefficients a_{ij} and $b_i, 1 \leq i, j \leq s$, such that they satisfy the conditions given in Table 5.1. In the same table on the left-hand column, the order of accuracy resulting from the given conditions on the coefficients is given.

Table 5.1: Order of accuracy Runge-Kutta discretization for different choices of the discrete parameters.

Order	Conditions ($c_i = \sum_{j=1}^{s} a_{ij}, \quad d_j = \sum_{i=1}^{s} b_i a_{ij}$)
1	$\sum b_i = 1$
2	$\sum d_i = \frac{1}{2}$
3	$\sum c_i d_i = \frac{1}{6}, \quad \sum b_i c_i^2 = \frac{1}{3}, \quad \sum d_i^2/b_i = \frac{1}{3}$
4	$\sum b_i c_i^3 = \frac{1}{4}, \quad \sum b_i c_i a_{ij} c_j = \frac{1}{8}, \quad \sum d_i^2 c_i^2 = \frac{1}{12}, \quad \sum d_i a_{ij} c_j = \frac{1}{24}$,
	$\sum c_i d_i^2/b_i = \frac{1}{12}, \quad \sum d_i^3/b_i^2 = \frac{1}{4}, \quad \sum b_i c_i a_{ij} d_j/b_j = \frac{5}{24}, \quad \sum d_i a_{ij} d_j/b_j = \frac{1}{8}$

Corresponding to the RK discretization setting, the optimal control problem (5.3) with s-stage RK scheme becomes the following

$$\begin{aligned} \min_{x^{\mathrm{rk}}, u^{\mathrm{rk}}} \quad J^{\mathrm{rk}}(x_k^{\mathrm{rk}}, u_k^{\mathrm{rk}}) &= \phi(x_n^{\mathrm{rk}}) \\ \text{subject to} \quad x_{k+1}^{\mathrm{rk}} &= x_k^{\mathrm{rk}} + h \sum_{i=1}^{s} b_i f(y_i^{\mathrm{rk}}, u_{ki}^{\mathrm{rk}}), \quad x^{\mathrm{rk}}(0) = x_0^{\mathrm{rk}}, \\ y_i^{\mathrm{rk}} &= x_k^{\mathrm{rk}} + h \sum_{j=1}^{s} a_{ij} f^{\mathrm{rk}}(y_j^{\mathrm{rk}}, u_{kj}^{\mathrm{rk}}), \end{aligned} \tag{5.4}$$

for $1 \leq i, j \leq s$, and $0 \leq k \leq n-1$.
where the vector y_j and u_{kj} are intermediate state and control variables on the interval $[t_k, t_{k+1}]$. Notice that $u_k \in \mathbb{R}^{nc \cdot s}$ represents the s-stages of the RK discrete control vector at time step k. We have

$$u_k^{\mathrm{rk}} = (u_{k1}^{\mathrm{rk}}, u_{k2}^{\mathrm{rk}}, \ldots, u_{ks}^{\mathrm{rk}}) \in \mathbb{R}^{nc \cdot s}.$$

Moreover, we consider the discrete $L^2((0,T); \mathbb{R}^{nx})$ -scalar-product as follows

$$\langle x, y \rangle_h := h \sum_{k=0}^{n-1} \langle x_k, y_k \rangle. \tag{5.5}$$

For $x_k^{\rm rk}$ near $x(t_k)$ and u_{kj} near $u(t_k)$, for $j = 1, \ldots, s$, by smoothness and the implicit theorem, when h is small enough, the intermediate variables y_i are uniquely determined; see [47], [17][Thm.303A].

Theorem 10. ***State Uniqueness property***
There exist positive constants h_1 and ϵ_1 such that for $h \le h_1$ and $(x^{\rm rk}, u_j^{\rm rk}) \in B_{\epsilon_1}(\tilde{x}^{\rm rk}, \tilde{u}^{\rm rk})$ for some $t \in [0, T]$, for $j = 1, \ldots, s$. Then

$$y_i^{\rm rk} = x^{\rm rk} + h \sum_{j=1}^{s} a_{ij} f^{\rm rk}(y_j^{\rm rk}, u_j^{\rm rk}), \quad 1 \le i \le s, \tag{5.6}$$

has a unique solution $y_i^{\rm rk} \in B_\epsilon(\tilde{x}^{\rm rk}, \tilde{u}^{\rm rk})$, for $i = 1, \ldots, s$. If $y^{\rm rk}(x^{\rm rk}, u^{\rm rk})$ denotes the solution of (5.6) corresponding to given $(x, u) \in \mathbb{R}^{nx} \times \mathbb{R}^{s \cdot nc}$, then $y^{\rm rk}(x^{\rm rk}, u^{\rm rk})$ is continuously differentiable in x and u.

Next, consider the discrete Lagrange function corresponding to (5.4). We have

$$\begin{aligned} L^h(x^{\rm rk}, y^{\rm rk}, u^{\rm rk}, p^{\rm rk}, \psi^{\rm rk}) &= \phi(x_n^{\rm rk}) + \left\langle \frac{x_{k+1}^{\rm rk} - x_k^{\rm rk}}{h} - \sum_{i=0}^{s} b_i f^{\rm rk}(y_{ki}^{\rm rk}, u_{ki}^{\rm rk}), p_{k+1}^{\rm rk} \right\rangle_{L^2} \\ &+ \left\langle \frac{y_{ki}^{\rm rk} - x_k^{\rm rk}}{h} - \sum_{j=1}^{s} a_{ij} f^{\rm rk}(y_{kj}^{\rm rk}, u_{kj}^{\rm rk}), \psi_{ki}^{\rm rk} \right\rangle_{L^2} \\ &= \phi(x_n^{\rm rk}) + h \sum_{k=0}^{n-1} \left\langle \frac{x_{k+1}^{\rm rk} - x_k^{\rm rk}}{h} - \sum_{i=1}^{s} b_i f^{\rm rk}(y_{ki}^{\rm rk}, u_{ki}^{\rm rk}), p_{k+1}^{\rm rk} \right\rangle \\ &+ h \sum_{k=0}^{n-1} \sum_{i=1}^{s} b_i \left\langle \frac{y_{ki}^{\rm rk} - x_k^{\rm rk}}{h} - \sum_{j=1}^{s} a_{ij} f^{\rm rk}(y_{kj}^{\rm rk}, u_{kj}^{\rm rk}), \psi_{ki}^{\rm rk} \right\rangle, \end{aligned}$$

where $p_k^{\rm rk} \in \mathbb{R}^{nx}$, for $0 \le k \le n-1$. We compute the gradient of the objective functional $J^{\rm rk}$ with respect to the discrete control. The adjoint equation corresponding to the optimality condition results as follows

$$p_k^{\rm rk} = p_{k+1}^{\rm rk} + \sum_{i=1}^{s} b_i \psi_{ki}^{\rm rk}, \qquad p_n^{\rm rk} = -\nabla_x \phi(x_n^{\rm rk}),$$

where

$$\psi_{ki}^{\rm rk} = (\nabla_x f^{\rm rk}(y_{ki}^{\rm rk}, u_{ki}^{\rm rk}))^\top \left(p_{k+1} + \sum_{j=1}^{s} \frac{b_j a_{ij}}{b_i} \psi_{kj}^{\rm rk} \right).$$

for $1 \le i, j \le s, \quad 0 \le k \le n-1$.

Summarizing, the discrete optimality system corresponding to (5.1) is given by

$$\begin{aligned} x_{k+1}^{\mathrm{rk}} &= x_k^{\mathrm{rk}} + h\sum_{i=1}^{s} b_i f^{\mathrm{rk}}(y_{ki}^{\mathrm{rk}}, u_{ki}^{\mathrm{rk}}), \qquad x^{\mathrm{rk}}(t_0) = x_0^{\mathrm{rk}}, \\ y_{ki}^{\mathrm{rk}} &= x_k^{\mathrm{rk}} + h\sum_{j=1}^{n} a_{ij} f^{\mathrm{rk}}(y_{kj}^{\mathrm{rk}}, u_{kj}^{\mathrm{rk}}), \\ p_k^{\mathrm{rk}} &= p_{k+1}^{\mathrm{rk}} + \sum_{i=1}^{s} b_i \psi_{ki}^{\mathrm{rk}}, \qquad p_n^{\mathrm{rk}} = -\nabla_x \phi(x_n^{\mathrm{rk}}), \\ \psi_{ki}^{\mathrm{rk}} &= (\nabla_x f^{\mathrm{rk}}(y_{ki}^{\mathrm{rk}}, u_{ki}^{\mathrm{rk}}))^\top \left(p_{k+1}^{\mathrm{rk}} + \sum_{j=1}^{s} \tfrac{b_j a_{ij}}{b_i} \psi_{kj}^{\mathrm{rk}} \right). \end{aligned} \tag{5.7}$$

From this system, the following gradient results

$$\nabla_{u_{ki}} J^{\mathrm{rk}}(u^{\mathrm{rk}}) = -(\nabla_{u^{\mathrm{rk}}} f^{\mathrm{rk}}(y_{ki}^{\mathrm{rk}}, u_{ki}^{\mathrm{rk}}))^\top \left(p_{k+1}^{\mathrm{rk}} + \sum_{j=1}^{s} \frac{b_j a_{ij}}{b_i} \psi_{kj}^{\mathrm{rk}} \right), \tag{5.8}$$

for $\widetilde{n} = 1, 2$, $1 \le i, j \le s$, and $0 \le k \le n-1$.

The well-posedness of the optimal control problem (5.4) and the estimation of error in the discrete approximation can be investigated by the following Theorem. This result can be found in [47].

Theorem 11. *If the smoothness and coercivity properties hold, $b_i > 0$ for each i, the Runge -Kutta scheme is of order κ for the optimal control, and $U = \mathbb{R}^{nc}$, then for all sufficiently small h, there exists a strict local minimizer (x^h, u^h) of the discrete optimal control problem (5.4) and an associated adjoint variable p^h satisfying the optimality system such that*

$$\begin{aligned} \max_{0\le k\le n} \|(x_k^{\mathrm{rk}})^h - \tilde{x}^{\mathrm{rk}}(t_k)\|_2 &+ \|(p_k^{\mathrm{rk}})^h - \tilde{p}^{\mathrm{rk}}(t_k)\|_2 + \|(u_k^{\mathrm{rk}})^h - \tilde{u}^{\mathrm{rk}}(t_k)\|_2 \\ &\le c h^{\kappa-1} \left(h + \tau \left(\frac{d^{\kappa-1}}{dt^{\kappa-1}} \widetilde{u}; h \right) \right), \end{aligned} \tag{5.9}$$

where $u(x_k^h, \psi_k^h)$ is a local minimizer corresponding to $x = x_k$ and $p = p_k$.

For convenience in application of Runge-Kutta schemes to our optimal control problem, we reformulate our optimal control problem (4.1) into the form (5.1) by introducing an additional state variable $\hat{x}$, with the additional differential equation

$$\dot{\hat{x}}(t) = l(\mathbf{x}) + \frac{\nu}{2}\|\mathbf{u}\|_2^2, \quad \hat{x}(0) = 0. \tag{5.10}$$

Therefore the new state variables can be written as

$$X := (\mathbf{x}, \hat{x})^\top = (x_1, \ldots, x_{nx}, \hat{x})^\top,$$

and the dynamics of transformed system is given by

$$\mathbf{F}(\mathbf{x}, \mathbf{u}) = \begin{pmatrix} \mathbf{f}(\mathbf{x}) + \mathbf{B}\mathbf{u}(t) \\ l(\mathbf{x}) + \dfrac{\nu}{2}\|\mathbf{u}\|^2 \end{pmatrix} \in \mathbb{R}^{nx+1}. \tag{5.11}$$

As a consequence, the optimal control problem (4.1) is equivalently transformed into

$$\begin{aligned} \min \quad J(\mathbf{X},\mathbf{u}) &= \phi(X(T)) && (5.12)\\ \text{subject to} \quad \dot{X}(t) &= \mathbf{F}(X,\mathbf{u}), \qquad t\in[0,T], \\ X\in\mathbb{X}, &\quad \mathbf{u}\in\mathbb{U}. && (5.13)\end{aligned}$$

We also denote

$$\phi(X(T)) = \frac{1}{2}\|x(T)-x_{des}(T)\|^2 + \hat{x}(T).$$

In the following, we discuss this setting in detail for our multi-agent models.

1. **The Hegselmann-Krause opinion formation model**
   The cost functional is given by

$$\begin{aligned} J^{\text{of}}(\mathbf{x}^{\text{of}},\mathbf{u}^{\text{of}}) &= \frac{\mu}{2}\|x_0^{\text{of}}(T)-x_{des}^{\text{of}}(T)\|_2^2 + \frac{1}{2N^2}\int_0^T \sum_{i,j=1}^N \|x_i^{\text{of}}(t)-x_j^{\text{of}}(t)\|^2 dt \\ &\quad + \frac{1}{2}\int_0^T \sum_{i=1}^N \|x_0^{\text{of}}(t)-x_i^{\text{of}}(t)\|_2^2 dt + \frac{\nu}{2}\int_0^T \|u^{\text{of}}(t)\|^2 dt \end{aligned}$$

   Corresponding to this cost function, we introduce the variable $\hat{x}$ and the following setting,

$$\begin{aligned} \dot{\hat{x}}^{\text{of}} &= \frac{1}{2N^2}\sum_{i,j=1}^N \|x_i^{\text{of}}(t)-x_j^{\text{of}}(t)\|^2 + \frac{1}{2}\sum_{i=1}^N \|x_0^{\text{of}}(t)-x_i^{\text{of}}(t)\|^2 + \frac{\nu}{2}\|u^{\text{of}}(t)\|^2 \\ \hat{x}^{\text{of}}(0) &= 0. \qquad (5.14)\end{aligned}$$

   Therefore our optimal control problem governed by HK system can be written in compact form as follows

$$\begin{aligned} \min_{\mathbf{X}^{\text{of}},u^{\text{of}}} \quad J^{\text{of}}(\mathbf{X}^{\text{of}},u^{\text{of}}) &= \frac{\mu}{2}\|x_0^{\text{of}}(T)-x_{des}^{\text{of}}(T)\|^2 + \hat{x}^{\text{of}}(T) && (5.15)\\ \text{subject to} \quad \dot{\mathbf{x}}^{\text{of}} &= \mathbf{f}^{\text{of}}(\mathbf{x}^{\text{of}}) + \mathbf{B}^{\text{of}}u^{\text{of}}(t) \\ \dot{\hat{x}}^{\text{of}} &= \frac{1}{2N^2}\sum_{i,j=1}^N \|x_i^{\text{of}}(t)-x_j^{\text{of}}(t)\|^2 + \frac{1}{2}\sum_{i=1}^N \|x_0^{\text{of}}(t)-x_i^{\text{of}}(t)\|^2 \\ &\quad + \frac{\nu}{2}\|u^{\text{of}}(t)\|^2, \end{aligned}$$

   where $X^{\text{of}} = (\mathbf{x}^{\text{of}},\hat{x}^{\text{of}})^\top = (x_0^{\text{of}},x_1^{\text{of}},\ldots,x_N^{\text{of}},\hat{x}^{\text{of}}) \in \mathbb{R}^{d(N+1)+1}$ are new state variable. In compact form, the optimal control problem with the HK model is equivalently transformed into

$$\begin{aligned} \min \quad J^{\text{of}}(X^{\text{of}}, u^{\text{of}}) &= \phi^{\text{of}}(X^{\text{of}}(T)) \\ \text{subject to} \quad \dot{X}^{\text{of}}(t) &= \mathbf{F}^{\text{of}}(X^{\text{of}}, u^{\text{of}}), \qquad t \in [0,T] \\ X^{\text{of}} \in \mathbb{X}^{\text{of}}, &\qquad u^{\text{of}} \in \mathbb{U}^{\text{of}}, \end{aligned} \tag{5.16}$$

where

$$\phi^{\text{of}}(X^{\text{of}}(T)) = \frac{1}{2}\|x^{\text{of}}(T) - x^{\text{of}}_{des}(T)\|^2 + \hat{x}^{\text{of}}(T).$$

2. **The Heider social balance model**
the cost functional is given by

$$J^{\text{hb}}(\mathbf{x}^{\text{hb}}, \mathbf{u}^{\text{hb}}) = \frac{1}{2}\sum_{i,j=1}^{N}(x^{\text{hb}}_{ij}(T) - x^{\text{hb}}_{des}(T))^2 + \frac{\nu}{2}\|\mathbf{u}^{\text{hb}}(t)\|^2_{L^2}$$

We introduce the following problem,

$$\begin{aligned} \dot{\hat{x}}^{\text{hb}} &= \frac{\nu}{2}\|\mathbf{u}^{\text{hb}}(t)\|^2 \\ \hat{x}^{\text{hb}}(0) &= 0. \end{aligned}$$

Thus we get the transformed system

$$\begin{aligned} \min_{X^{\text{hb}}, \mathbf{u}^{\text{hb}}} \quad J^{\text{hb}}(X^{\text{hb}}, \mathbf{u}^{\text{hb}}) &= \frac{\mu}{2}\|x^{\text{hb}}_0(T) - x^{\text{hb}}_{des}(T)\|^2 + \hat{x}^{\text{hb}}(T) \\ \text{subject to} \quad \dot{\mathbf{x}}^{\text{hb}} &= \mathbf{f}^{\text{hb}}(\mathbf{x}^{\text{hb}}) + \mathbf{B}^{\text{hb}}\mathbf{u}^{\text{hb}}(t) \\ \dot{\hat{x}}^{\text{hb}} &= \frac{\nu}{2}\|\mathbf{u}^{\text{hb}}(t)\|, \end{aligned} \tag{5.17}$$

where $X^{\text{hb}} = (x^{\text{hb}}_{01}, x^{\text{hb}}_{02}, \ldots, x^{\text{hb}}_{(N-1)N}, \hat{x}^{\text{hb}}) \in \mathbb{R}^{N_r+1}$.

On compact form, our HK optimal control problem is equivalently transformed into

$$\begin{aligned} \min \quad J^{\text{hb}}(X^{\text{hb}}, \mathbf{u}^{\text{hb}}) &= \phi^{\text{hb}}(X^{\text{hb}}(T)) \\ \text{subject to} \quad \dot{X}^{\text{hb}}(t) &= F^{\text{hb}}(X^{\text{hb}}, \mathbf{u}^{\text{hb}}), \qquad t \in [0,T] \\ X^{\text{hb}} \in \mathbb{X}^{\text{hb}}, &\qquad \mathbf{u}^{\text{of}} \in \mathbb{U}^{\text{hb}}, \end{aligned} \tag{5.18}$$

where

$$\phi^{\text{hb}}(X^{\text{hb}}(T)) = \frac{1}{2}\sum_{i,j=1}^{N}(x^{\text{hb}}_{ij}(T) - x^{\text{hb}}_{des}(T))^2 + \hat{x}^{\text{hb}}(T).$$

3. **The refined flocking system**
We reformulate our optimal control such that it is in the form (5.1). Corresponding to problem P1, the cost function is given by

$$J_1^{\mathrm{fm}}(\mathbf{x}^{\mathrm{fm}}, u^{\mathrm{fm}}) = \frac{1}{2}\|x_0^{\mathrm{fm}}(T) - x_{des}^{\mathrm{fm}}(T)\|^2 + \frac{\mu}{2}\sum_{b=1}^{N}\int_0^T \|x_0^{\mathrm{fm}}(t) - x_b^{\mathrm{fm}}(t)\|^4\, dt + \frac{\nu}{2}\|u^{\mathrm{fm}}\|_{L^2}^2.$$

We introduce the following equation

$$\begin{aligned} \dot{\hat{x}}_1^{\mathrm{fm}}(t) &= \frac{\mu}{2}\sum_{b=1}^{N}\|x_0^{\mathrm{fm}}(t) - x_b^{\mathrm{fm}}(t)\|^4 + \frac{\nu}{2}\|u^{\mathrm{fm}}(t)\|^2. \\ \hat{x}_1^{\mathrm{fm}}(0) &= 0. \end{aligned}$$

In the case of problem P2, the cost functional is as follows

$$\begin{aligned} J_2^{\mathrm{fm}}(\mathbf{x}^{\mathrm{fm}}, \mathbf{u}^{\mathrm{fm}}) &= \frac{1}{2}\|x_0^{\mathrm{fm}}(T) - x_{des}^{\mathrm{fm}}(T)\|^2 + \frac{\mu}{2}\sum_{b=1}^{N}\int_0^T \|x_0^{\mathrm{fm}}(t) - x_b^{\mathrm{fm}}(t)\|^4 dt \\ &\quad + \frac{\eta}{2}\int_{t_0}^T \|x_0^{\mathrm{fm}}(t) - x_{des}^{\mathrm{fm}}(t)\|_2^2 dt + \frac{\nu}{2}\|u^{\mathrm{fm}}(t)\|_{L^2}^2 \end{aligned}$$

We define the following problem

$$\begin{aligned} \dot{\hat{x}}_2^{\mathrm{fm}}(t) &= \frac{\mu}{2}\sum_{b=1}^{N}\|x_0^{\mathrm{fm}}(t) - x_b^{\mathrm{fm}}(t)\|^4 + \frac{\eta}{2}\|x_0^{\mathrm{fm}}(t) - x_{des}^{\mathrm{fm}}(t)\|^2 + \frac{\nu}{2}\|u^{\mathrm{fm}}(t)\|^2. \\ \hat{x}_2^{\mathrm{fm}}(0) &= 0. \end{aligned}$$

Therefore our optimal control problems P1 and P2 are transformed into the following Pt1 and Pt2 problems.

Problem Pt1. Reach a target position at final time T

$$\begin{aligned} \min \quad J_1^{\mathrm{fm}}(X_1^{\mathrm{fm}}, u^{\mathrm{fm}}) &= \frac{1}{2}\|x_0^{\mathrm{fm}}(T) - x_{des}^{\mathrm{fm}}(T)\|^2 + \hat{x}_1^{\mathrm{fm}}(T) \qquad (5.19) \\ \text{subject to} \quad \dot{x}_0^{\mathrm{fm}} &= v_0^{\mathrm{fm}} \\ \dot{x}_b^{\mathrm{fm}} &= v_b^{\mathrm{fm}} \\ \dot{v}_0^{\mathrm{fm}} &= S_0 + M_0 + E_0 + u^{\mathrm{fm}} \\ \dot{v}_b^{\mathrm{fm}} &= S_b + E_b + L_b \\ \dot{\hat{x}}_1^{\mathrm{fm}} &= \frac{\mu}{2}\sum_{b=1}^{N}\|x_0^{\mathrm{fm}}(t) - x_b^{\mathrm{fm}}(t)\|^4 + \frac{\nu}{2}\|u^{\mathrm{fm}}(t)\|^2. \end{aligned}$$

Problem Pt2. Follow a desired trajectory

$$\begin{aligned}
\min \quad J_2^{\mathrm{fm}}(X_2^{\mathrm{fm}}, u^{\mathrm{fm}}) &= \frac{1}{2}\|x_0^{\mathrm{fm}}(T) - x_{des}^{\mathrm{fm}}(T)\|^2 + \hat{x}_2^{\mathrm{fm}}(T) \qquad (5.20)\\
\text{subject to} \quad \dot{x}_0^{\mathrm{fm}} &= v_0^{\mathrm{fm}}\\
\dot{x}^{\mathrm{fm}} &= v_b^{\mathrm{fm}}\\
\dot{v}_0^{\mathrm{fm}} &= S_0 + M_0 + E_0 + u^{\mathrm{fm}}\\
\dot{v}_b^{\mathrm{fm}} &= S_b + M_b + E_b + L_b\\
\dot{\hat{x}}_2^{\mathrm{fm}} &= \frac{\mu}{2}\sum_{b=1}^{N}\|x_0^{\mathrm{fm}}(t) - x_b^{\mathrm{fm}}(t)\|^4 + \frac{\eta}{2}\|x_0^{\mathrm{fm}}(t) - x_{des}^{\mathrm{fm}}(t)\|^2\\
&\quad + \frac{\nu}{2}\|u^{\mathrm{fm}}(t)\|^2.
\end{aligned}$$

with given initial conditions.

Both problems Pt1 and Pt2 can be formulated in compact form as follows

$$\begin{aligned}
\min \quad J_{\widetilde{n}}^{\mathrm{fm}}(X_{\widetilde{n}}^{\mathrm{fm}}, u^{\mathrm{fm}}) &= \frac{1}{2}\|x_0^{\mathrm{fm}}(T) - x_{des}^{\mathrm{fm}}(T)\|^2 + \hat{x}_{\widetilde{n}}^{\mathrm{fm}}(T)\\
\text{subject to} \quad \dot{X}_{\widetilde{n}}^{\mathrm{fm}} &= \mathbf{F}_{\widetilde{n}}^{\mathrm{fm}}(X_{\widetilde{n}}^{\mathrm{fm}}, u^{\mathrm{fm}}). \qquad (5.21)
\end{aligned}$$

where $\widetilde{n} = 1, 2$ denotes the problem, and the state variable $X_{\widetilde{n}}^{\mathrm{fm}} = (x_0^{\mathrm{fm}}, x_1^{\mathrm{fm}}, ..., x_N^{\mathrm{fm}}, v_0^{\mathrm{fm}}, v_1^{\mathrm{fm}}, ..., v_N^{\mathrm{fm}}, \hat{x}_{\widetilde{n}}^{\mathrm{fm}})^T$ and $\mathbf{F}_{\widetilde{n}}^{\mathrm{fm}}(X_{\widetilde{n}}^{\mathrm{fm}}, \mathbf{u}^{\mathrm{fm}})$ denote the state and the dynamics of the transformed flocking systems. We also denote

$$\phi^{\mathrm{fm}}(X_{\widetilde{n}}^{\mathrm{fm}}) = \frac{1}{2}\|x_0^{\mathrm{fm}}(T) - x_{des}^{\mathrm{fm}}(T)\|^2 + \hat{x}_{\widetilde{n}}^{\mathrm{fm}}(T).$$

Next, we present results of numerical experiments to validate the accuracy of reduced gradient (5.8), corresponding to the RK approximation to the optimal control problem (5.21). We consider a time interval and a one dimensional problem with one leader and 3 agents. Therefore, the number of state and control variables are $nx = 9$ and $nc = 1$, respectively. The initial positions and velocity of the individuals are chosen randomly in $(0, 1)$ whereas the initial position of the leader is $x_0 = 2$. The target position for problem Pt1 is $x_{des} = 15$, while the desired trajectory for problem Pt2 is $x_{des} = \cos(t)$. The parameter values corresponding to our flocking model are given in Table 5.2.

The motivation for choosing the RK scheme is the high accuracy of the resulting optimization gradient. We validate this property by comparing the optimization gradient resulting from the RK optimality system applied to a given direction with the corresponding numerical directional derivative approximated by centered differences. In this experiment, the control function and the direction δu are chosen randomly in the interval $(0, 1)$. Results for this experiment are reported in Table 5.3. We see in Table 5.3 that the error in the computation of the gradient is of order $O(\alpha^2)$. However, we remark that the good accuracy observed in this experiment requires sufficiently small time-step sizes. This fact also motivates the use of the MPC control strategy discussed in the following section, since we can choose small time windows in combination with moderate values of n to guarantee accurate gradients.

Parameters		
initial time	t_0	0
final time	T	10.0
time step size	h	0.05
cost function	μ	0.5
	η	0.5
	ν	0.001
self-propelling force	α	0.07
	β	0.05
Morse Potential	C_r	0.2
	C_a	0.5
	l_r	0.5
	l_a	1
Attractive force by leader	C_r^0	0.002
	C_a^0	0.5
	l_r^0	0.5
	l_a^0	1
	γ_1	10
Attractive force	γ	1
	σ	0.5
	δ_1	cos(1.047)
	δ_2	cos(1.57)

Table 5.2: Parameters values the refined flocking model and for the objectives.

α	$\left(\frac{J^{\text{fm}}(u+\alpha\delta u) - J^{\text{fm}}(u-\alpha\delta u)}{2\alpha}\right)$	$(\nabla_u J^{\text{fm}}, \delta u)_{L^2}$	Error
1	-7.210251e+000	-7.540379e+000	3.301283e-001
0.1	-8.017659e+000	-8.020856e+000	3.196608e-003
0.01	-8.083906e+000	-8.083939e+000	3.283014e-005
0.001	-7.293766e+000	-7.293766e+000	2.546723e-007
0.0001	-7.313259e+000	-7.313259e+000	2.641321e-009

Table 5.3: Values of the directional derivative of the objective with different time mesh sizes and corresponding values of the optimization gradient applied to the same direction. The last column reports the values of their norm differences.

5.2 The model predictive control scheme

In this section, we discuss a model predictive control (MPC) scheme, see e.g. [44, 62], that implements a closed-loop control strategy for the multi-agent model to track a given sequence of desired positions in time.

Model predictive control is an optimal control strategy based on numerical optimization for the feedback control that can be applied to stabilization and tracking problems. The general idea of model predictive control is that future control inputs and future state are predicted using the system model and optimized at regular intervals with respect to a performance index. Specially, let $(0, T)$ be the time interval where the evolution of the multi-agent system is considered. We assume time windows of size $\Delta t = T/M$ with M a positive integer. Let $t_k = k\Delta t$, $k = 0, 1, \ldots, M$. Furthermore, at time t_0, we have given initial conditions denoted with $x(0) = x_0$. Our MPC strategy for tracking problems starts at time t_0 and solves the open-loop control problem defined in the interval $(0, t_1)$. Then, with the response x_1 resulting at $t = t_1$, we have the initial condition for the subsequent optimization problem defined in the interval (t_1, t_2). This procedure is repeated by receding the time horizon until the last time window is reached. We implement a MPC scheme where the time horizon used to evaluate the control coincides with the time horizon where the control is used. We notice that the closed-loop system with the MPC scheme is nominally asymptotically stable [70]. We remark that our control system belongs to the class of MPC schemes discussed in Ch. 6 and 7 of [44]; see in particular Section 7.2.
The MPC procedure is summarized in the following algorithm.

Algorithm 1 : Model predictive control (MPC)

Set $k = 0$, X_0;
1. Assign the initial condition, $X(t_k) = X_k$ and the target $x_{des}(t_{k+1})$;
2. In (t_k, t_{k+1}), solve (5.12), thus obtain the optimal pair (X, u);
3. If $t_{k+1} < T$, set $k := k + 1$, $X_k = X(t_k)$, go to 1.

End.

Next, we discuss the second step of Algorithm 1, that consists in solving the optimal control problem (5.12). Notice that the solution of the state equation in (5.12) gives the mapping $u \to X(u)$, that allows to transform the constrained optimization problem in an unconstrained one as follows

$$\min_{u \in \mathbb{U}_{ad}} J_r(u) := J(x(u), u). \tag{5.22}$$

We solve these problems implementing a nonlinear conjugate gradient strategy. The evaluation of the corresponding gradient is given in (5.8): For a given u, we solve first the forward flocking equation and then the adjoint flocking equation. This procedure is implemented with the RK scheme and is summarized in the following

Algorithm 2: Evaluation of the gradient

1. Solve the discrete multi-agent model in the optimality system (5.7) with the given initial conditions;
2. Solve the discrete adjoint multi-agent equation in 5.7 with the computed terminal condition;
3. Compute the gradient $\nabla_u \hat{J}(u)$ using (5.8);

End

We solve the optimization problem (5.12) by computing the gradient using Algorithm 2 and implementing it in a nonlinear conjugate gradient (NCG) scheme; see, e.g., [43, 74]. The NCG scheme is as follows.

Algorithm 1 : Nonlinear Conjugate Gradient

Input initial approx. u_0, $d_0 = -\nabla \hat{J}(u_0)$, $g_0 = -d_0$ index $k = 0$, maximum k_{max}, tolerance tol.

While ($k < k_{max}$ and $\|g_k\|_{\mathbb{R}^\ell} > tol$) do

1. Apply a linesearch to determine steplength $\alpha_k > 0$ along
2. d_k satisfying (5.23);
3. Set $u_{k+1} = u_k + \alpha_k\, d_k$;
4. Compute $g_{k+1} = \nabla \hat{J}(u_{k+1})$ using Algorithm 2;
5. Compute β_k given by (5.24);
6. Let $d_{k+1} = -g_{k+1} + \beta_k^{HZ}\, d_k$;
7. Set $k = k + 1$;

End while

In this NCG scheme $\alpha_k > 0$ is a step-length obtained with a linesearch algorithm [84], that satisfies the following Armijo condition of sufficient decrease

$$\hat{J}(u_k + \alpha_k\, d_k) \leq \hat{J}(u_k) + \delta\, \alpha_k\, (\nabla \hat{J}(u_k), d_k), \tag{5.23}$$

where $0 < \delta < 1/2$; see [84]. Notice that we use the inner product of the U space. The parameter β_k resembles the one appearing in the well-known linear CG scheme. There are many different formula for β_k which result in different performance depending on the nonlinear optimization problem. We use the formulation due to Hager and Zhang [48], as follows

$$\beta_k = \beta_k^{HZ} := \frac{(\sigma_k, g_{k+1})}{(d_k, y_k)}, \qquad \sigma_k = y_k - 2 d_k \frac{(y_k, y_k)}{(y_k, d_k)}, \tag{5.24}$$

where $y_k = g_{k+1} - g_k$. Our choice is motivated by our numerical experience. In fact, the Hager-Zhang NCG formula results to be the most efficient among the known formulas [84] .

Chapter 6

Numerical experiments

In this chapter, we present results of numerical experiments with our multi-agent models. These results demonstrate the control performance of our leader-based control strategies.

6.1 The Hegselmann-Krause opinion formation model

In this section, we present numerical simulations with system (2.4) in the one dimensional case $d = 1$. First, we consider the uncontrolled HK model where the control $u^{\text{of}} = 0$. This model is solved using the explicit fourth-order Runge-Kutta method illustrated in previous section. In our experiments, the connectivity functions $a_{ij} = a(\|x_i^{\text{of}} - x_j^{\text{of}}\|)$ are given by

$$a(r) = a(r;\delta,\varepsilon) \;=\; \begin{cases} 1, & 0 \le r \le \delta, \\ \frac{1}{2} + \frac{1}{2}\tanh\left(\frac{1}{r-\delta} + \frac{1}{r-(\delta+\varepsilon)}\right), & \delta < r < (\delta+\varepsilon). \\ 0, & (\delta+\varepsilon) \le r. \end{cases}$$

The connectivity coefficient accounting for the relationship between the leader and the other agents is chosen as follows

$$c_i^1(r) = c_i^1(r;\delta_0,\varepsilon_0) \;=\; \begin{cases} 1, & 0 \le r \le \delta_0, \\ \frac{1}{2} + \frac{1}{2}\tanh\left(\frac{1}{r-\delta_0} + \frac{1}{r-(\delta_0+\varepsilon_0)}\right), & \delta_0 < r < (\delta_0+\varepsilon_0), \\ 0, & (\delta_0+\varepsilon_0) \le r, \end{cases}$$

where r is the distance from the leader and δ_0 is the bounded confidence. Alternatively, we take

$$c_i^2(r_{i0}) = e^{-\frac{|x_i^{\text{of}} - x_0^{\text{of}}|^2}{l_x}},$$

where $l_x = 20$ is a parameter that scales the region of attraction. The comparison of the connectivity function is shown in Figure 6.1.
Figure 6.2 shows numerical results with the HK model and an uncontrolled external leader. The initial positions of the agent's opinion are distributed randomly in

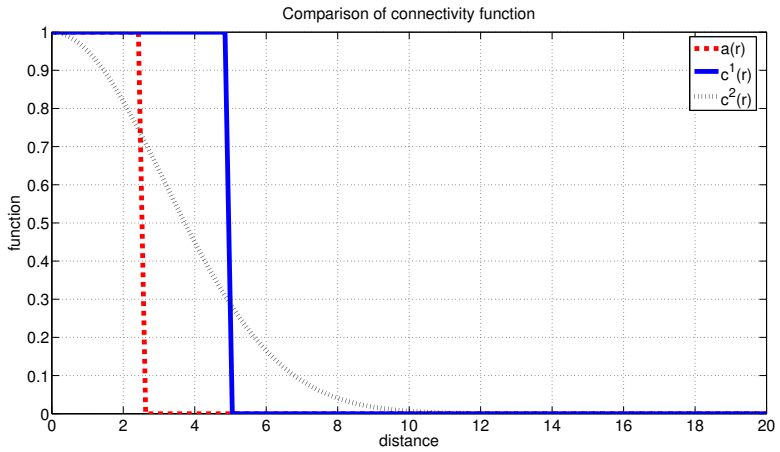

Figure 6.1: Comparison of the connectivity function a_{ij} , c_i^1 ,c_i^2

Table 6.1: Parameters for the HK model with leadership.

connectivity function (a_{ij})	δ	2.5
	ε	0.05
connectivity function (c_i^1)	δ_0	5
	ε_0	0.05
connectivity function $(c_i^2$)	l_a	20
strength of leader power	γ	10

$[-20, 20]$ while the leader's initial opinion is $\mathbf{x}_0^{\text{of}}(0) = 30$. For these initial conditions $\mathbf{x}^{\text{of}}(0) = (x_0^{\text{of}}(0), x_1^{\text{of}}(0), ..., x_N^{\text{of}}(0))$, $N = 19$, and bounded confidence $\delta = 2.5, \delta_0 = 5$, it can be seen that the opinions $x_i^{\text{of}}(t)$, for $i = 0, ..., N$, converge to an opinion $\mathbf{x}^{\text{of}*}$. Moreover, due to the limitation of confidence, clusters of agents' opinions are formed. That is, agent groups are formed with different opinions, $x_i^{\text{of}*} \neq x_j^{\text{of}*}$ when i and j are not in the same group, while in the other case, $x_i^{\text{of}*} = x_j^{\text{of}*}$ whenever i and j are in the same cluster.

Next, we investigate the HK model with a leader subject to the global stabilizing feedback control given by Theorem 7. We allow the connectivity function with the leader ϕ to be zero in the bounded confidence case (that is with connectivity functions c_1^i). We consider two test cases, corresponding to two different initial conditions. In the bounded confidence case, for some initial configuration, this feedback fails to be a global stabilizer (see Figure 6.4(a)). For all tests, the parameters related to the model are set up as stated in Table 6.1.

Case I The initial conditions are taken as above, that is, a group of 20 agents including the leader are examined where the opinion leader is at $\mathbf{x}_0^{\mathrm{fm}}(0) = 30$, while the other opinions are chosen randomly in [-20,20]. In the Figures 6.3(a), we report the results with the HK system with c_i^1, and in Figure 6.3(b), we report results obtained with c_i^2, when the control with different functions c_i^1 and c_i^2 is applied. We see that by applying the input control to the HK system, the leader forces the agent's opinions to achieve consensus.

Case II The initial position of the leader opinion is placed at the center of the group of agents, while the opinions of the other agents are randomly distributed in a neighborhood of the leader's position where the distance between the leader opinion and the next nearest agent opinion is greater than the length of bounded confidence δ_0. With this set of initial conditions, we get the results as shown in Figure6.4, where Figure 6.4(a) and 6.4(b) show the solution of the HK system with the c_i^1 function and Figure 6.5(a) and 6.5(b) show results using c_i^2. As we see in Figure 6.4(a), because the value of c_i^1 is initially zero, the feedback control u is equal to zero. Therefore the leader has no influence on the other agents and fails in steering the agent to consensus. On the other hand, with the c_i^2 function consensus is obtained.

To complete this section, we present results of numerical experiments obtained with the optimal control problem (5.16) in the time interval $[0, 10]$. First, we consider two series of experiments; in the first one, we consider the consensus problem and the second one, we focus on the tracking problem, In both tests, we solve the optimal control problem (5.16) with $N + 1 = 10$. The parameters related to the model are given as shown in Table 6.1. In addition, the parameters in the objective function are given by $\mu = 1, \nu = 0.001$. The initial opinions of the agents are randomly chosen in [-5,10] and the opinion of the leader is at $x_0(t_0) = 20$. Furthermore, the target is $x_{des} = \cos([0, 10])$. To apply the MPC strategy to the first and the second series of experiments, the time horizon is divided into subintervals of size $\Delta t = 0.25$. From Figure 6.6 and Figure 6.7 we see that the resulting optimal control is able to steer the system to achieve the objective.

Next, we consider the tracking problem of the system (5.16) in the time interval $[0, 10]$. The corresponding parameters in objective functional and the target x_{des} are chosen as same as the previous experiments. To apply MPC, time horizon is again divided into subintervals with the same time window size, $\Delta t = 0.25$. Our MPC strategy for this experiment starts at the time $t_0 = 0$ and solves the open-loop of the control problem defined in $(0, t_1)$ with $\Delta t = 0.25$. In general cases, the response x_1 resulting at $t = t_1$ is chosen to be the initial condition for the subsequent optimization problem defined in the next interval (t_1, t_2). However, in this experiment, the response $\widetilde{x}_1$ resulting at $\widetilde{t}_1 = \frac{t_1}{2}$ is chosen as the initial condition for the next time interval with the same window size, i.e., $(\widetilde{t}_1, \widetilde{t}_1 + \Delta t)$. This procedure is repeated by receding the time horizon until the last time window is reached. Comparison with results in Figure

Table 6.2: Comparison of total running time

The number of time window (n)	Δt	total running time (s)
20	0.5	2,066.50
40	0.25	312.13
80	0.125	204.14

6.7, it is seen that the evolution of leader's opinion in Figure 6.8 has no jump at final time of each time window.

Finally, we verify the ability of leader to track the desired trajectory. In these series of experiments, we consider the tracking problem with the different sizes of time window Δt. In the Figures 6.9, we compare the distance between leader's opinion and the desired trajectory corresponding to different values of Δt where the results with line-circle , line-square, and line- diamond are related to $\Delta t = 0.5$, $\Delta t = 0.25$ and $\Delta t = 0.125$, respectively. It is seen that the smaller sizes of time window, the closer the desired trajectory can be obtained. Moreover, by comparison of total time running shown in Table 6.2, it can be seen that length of time window has impact on the total running time. The smaller length of Δt, the smaller total running time is spent. One of reasons for these consequences is that the optimal control problem is solved accurately with small time window.

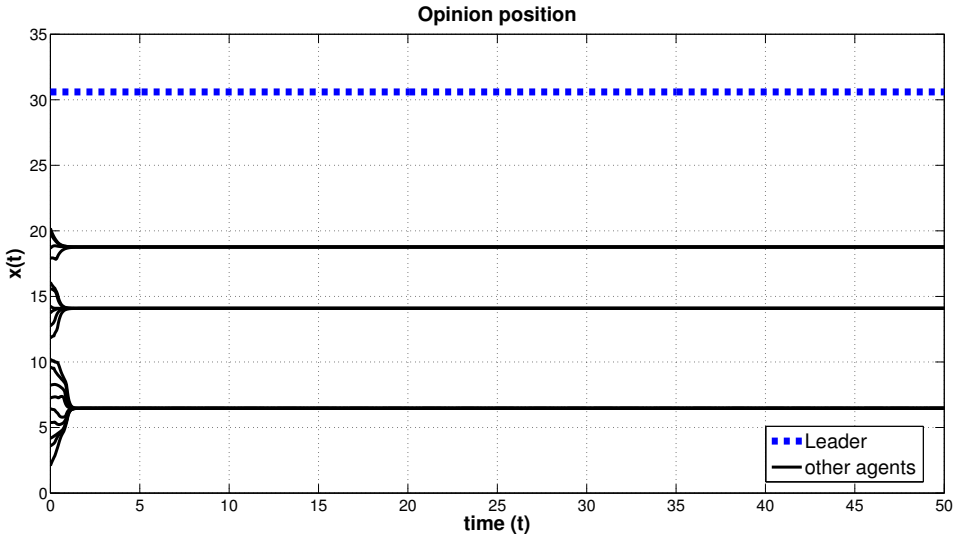

(a) t=50 with c_i^1

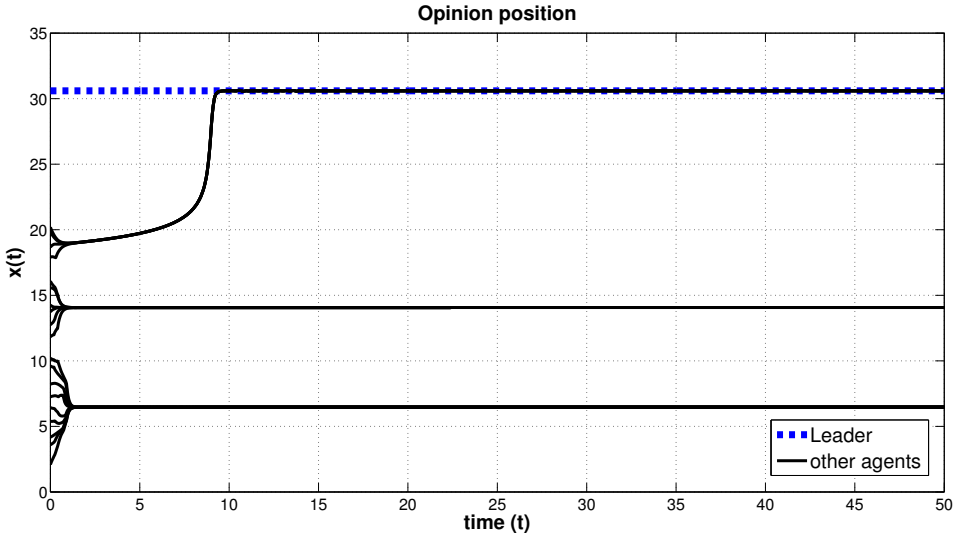

(b) t=50 with c_i^2

Figure 6.2: Free evolution of the system (uncontrolled case). Simulation with $N+1 = 20$ agents. The initial position values are chosen randomly in $[-20, 20]$ and leader opinion is at $x_0(0) = 30$. Figure (a) shows with c_i^1. Figure (b) result is with c_i^2. The evolution of the opinion is denoted by a line and the dashed line represent the opinion of the leader.

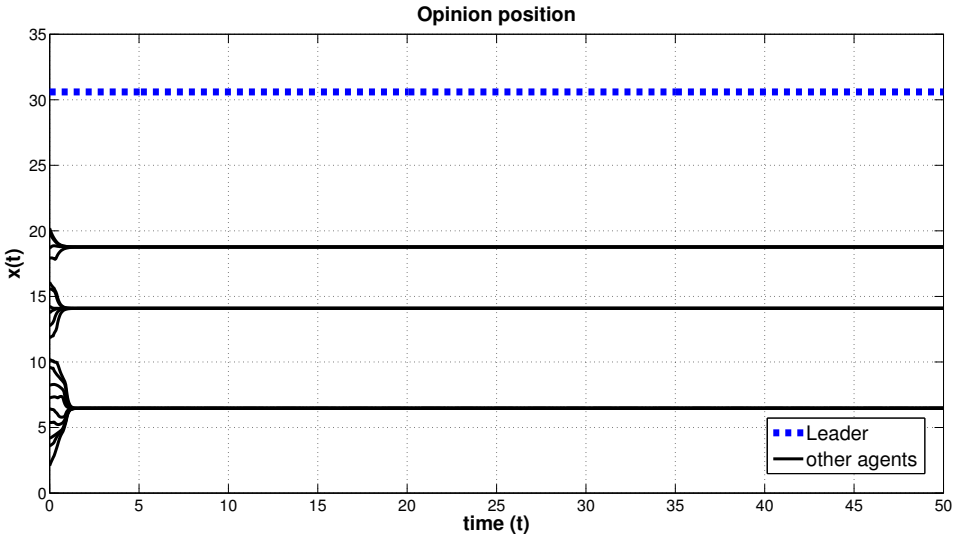

(a) t=50 with c_i^1

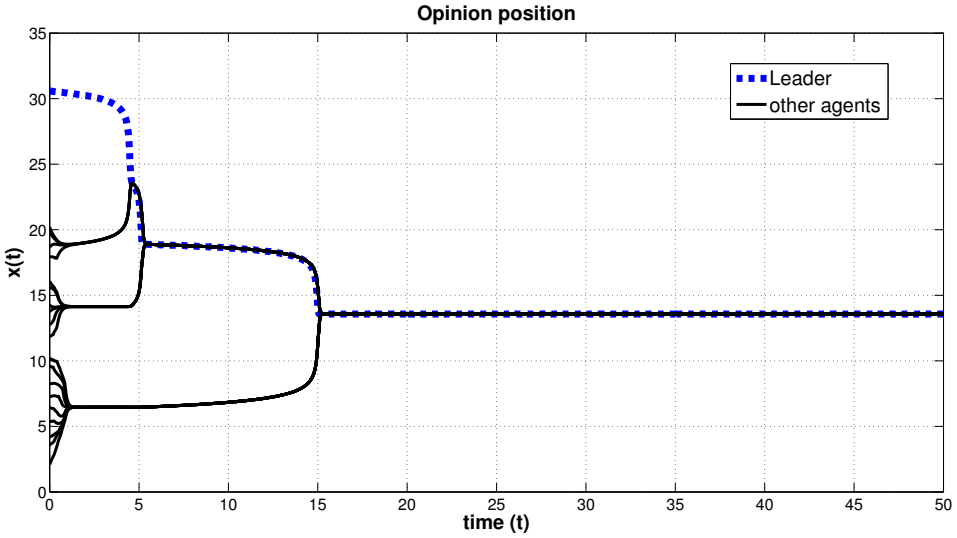

(b) t=50 with c_i^2

Figure 6.3: Stabilizing control. Simulation with $N + 1 = 20$ agents. The initial position values are chosen randomly in $[-20, 20]$ and leader opinion is at $\mathbf{x}_0^{\text{fm}}(0) = 30$. Figure(a) show results with c_i^1, results (b) with c_i^2. The opinion evolution of each agent is denoted by a continuous line and the dashed line presents the opinion of the leader.

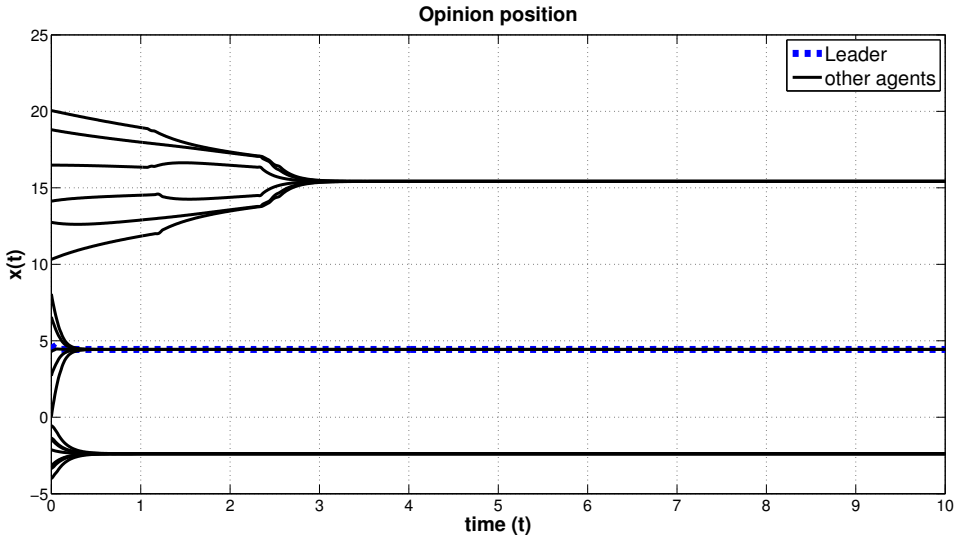

(a) t=10 with c_i^1

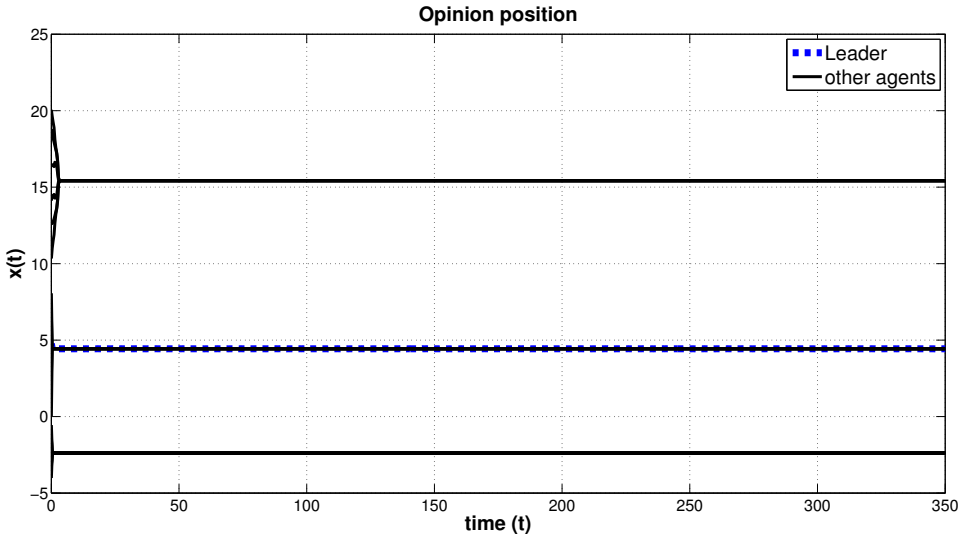

(b) t=350 with c_i^1

Figure 6.4: Stabilizing control. Simulation with $N + 1 = 20$ agents. The leader's initial opinion is at center of group, other initial positions are randomly distributed on both sides of leader's position. Figure (a) and (b) show the results with c_i^1. The opinion evolution of each agent is denoted by a continuous line and the dashed line presents the opinion leader.

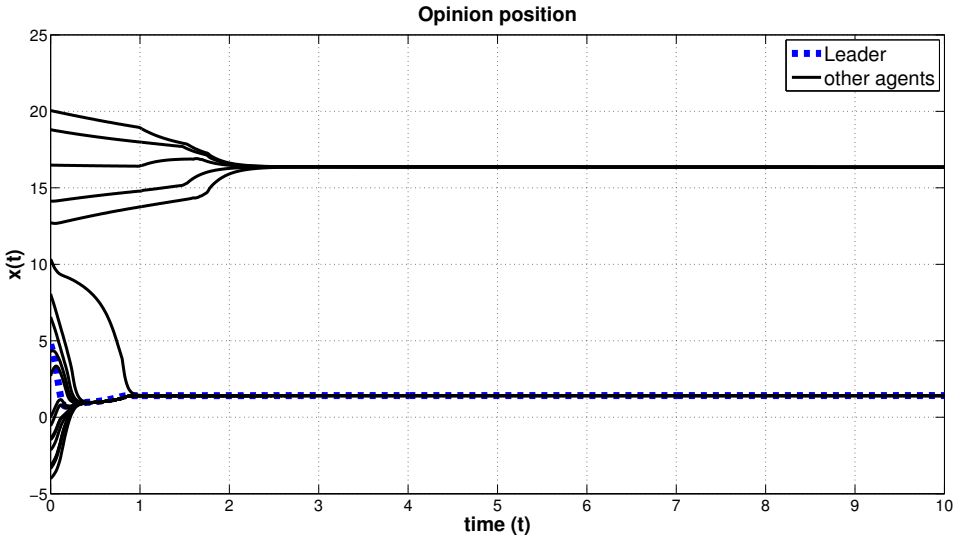

(a) t=10 with c_i^2

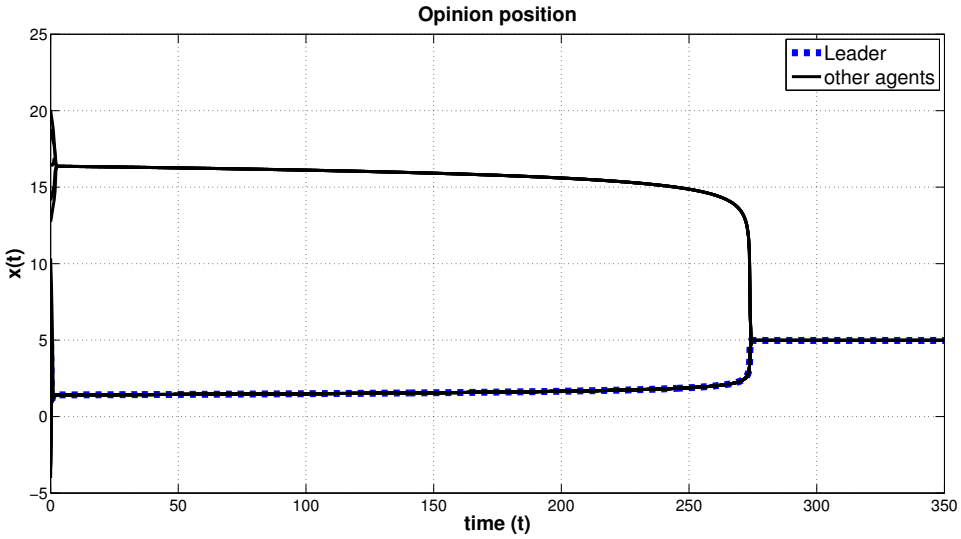

(b) t=350 with c_i^2

Figure 6.5: Stabilizing control. Simulation with $N + 1 = 20$ agents. The leader's initial opinion is at center of group, other initial positions are randomly distributed on both sides of leader's position. Figure (a) and (b) show the results with c_i^2. The opinion evolution of each agent is denoted by a continuous line and the dashed line presents the opinion leader.

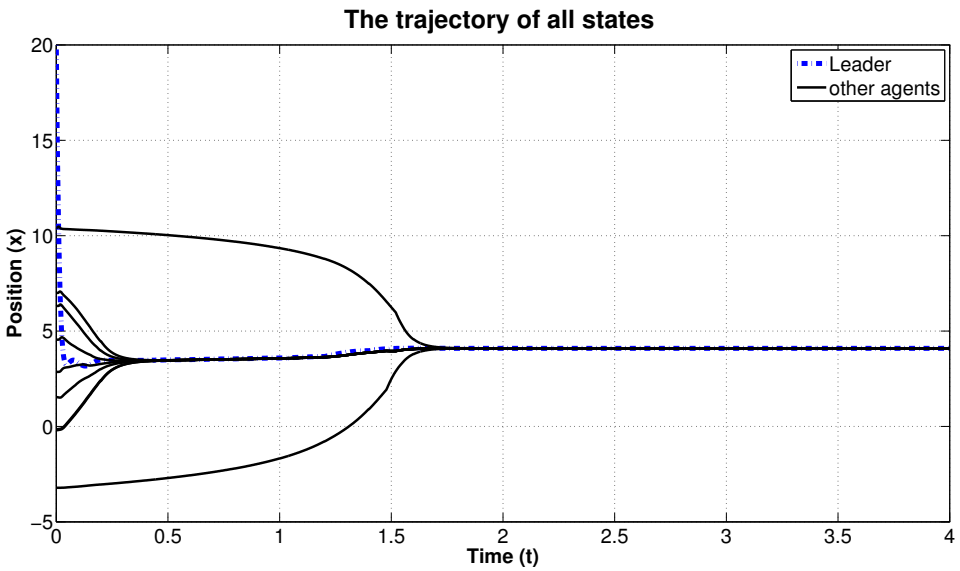

(a) t=[0,4]

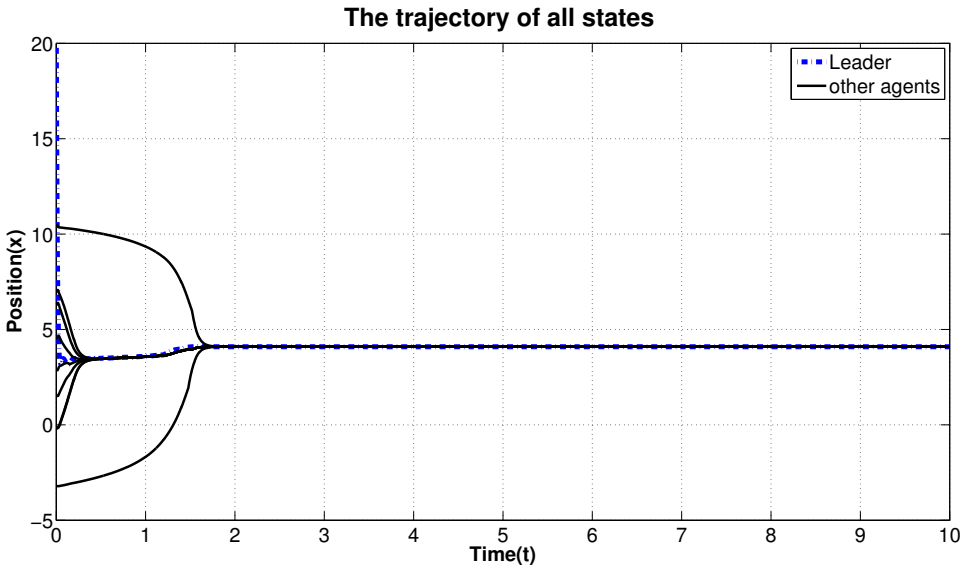

(b) t=[0,10]

Figure 6.6: Optimal control. Simulation with $N+1=10$ agents. Figures (a) and (b) represent the optimal results of the HK with leadership for $\mu=0$. The objective is to force all agents to reach the consensus $\mathbf{x}^{\text{of}*}$. The opinion evolution of each agent is denoted by a continuous line and the dashed line represents the opinion of the leader.

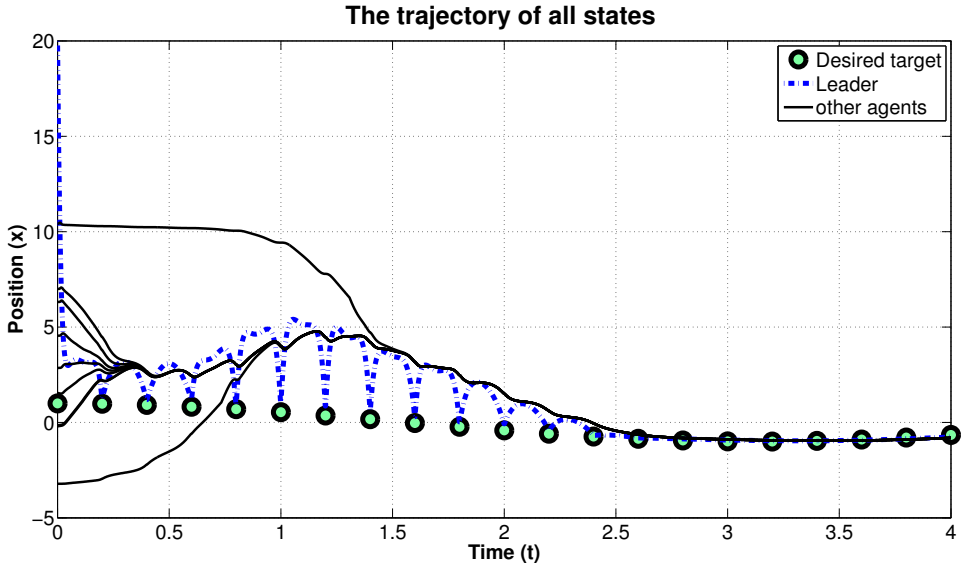

(a) t=[0,4]

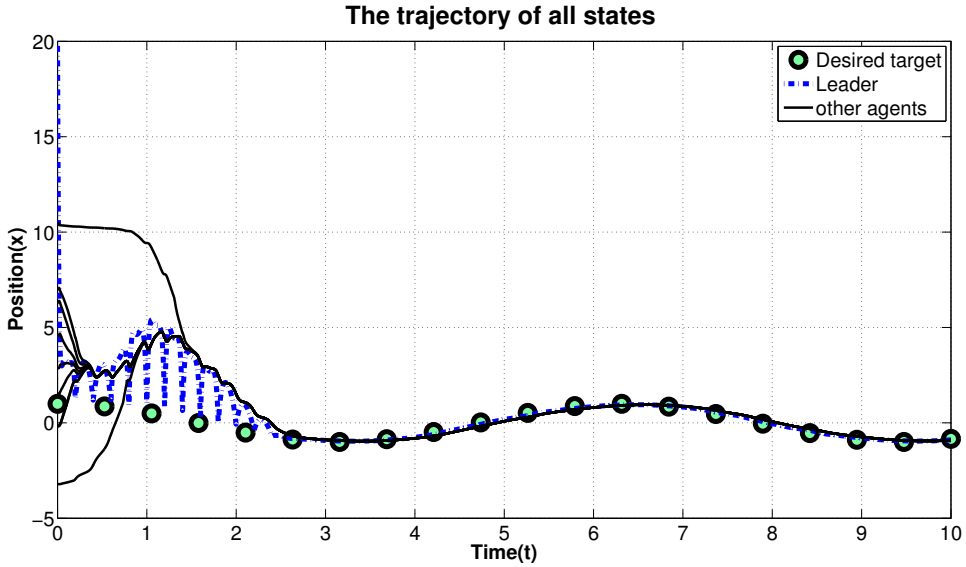

(b) t=[0,10]

Figure 6.7: Optimal control. Simulation with $N+1=10$ agents. In figures (a) and (b) the optimal results of HK with leadership for $\mu=1$. The objective is to force all agents to reach the desired position $\mathbf{x}_{des}^{\text{of}}=\cos([0,10])$. The opinion evolution of each agent is denoted by a continuous line and the dashed line represents the opinion of the leader.

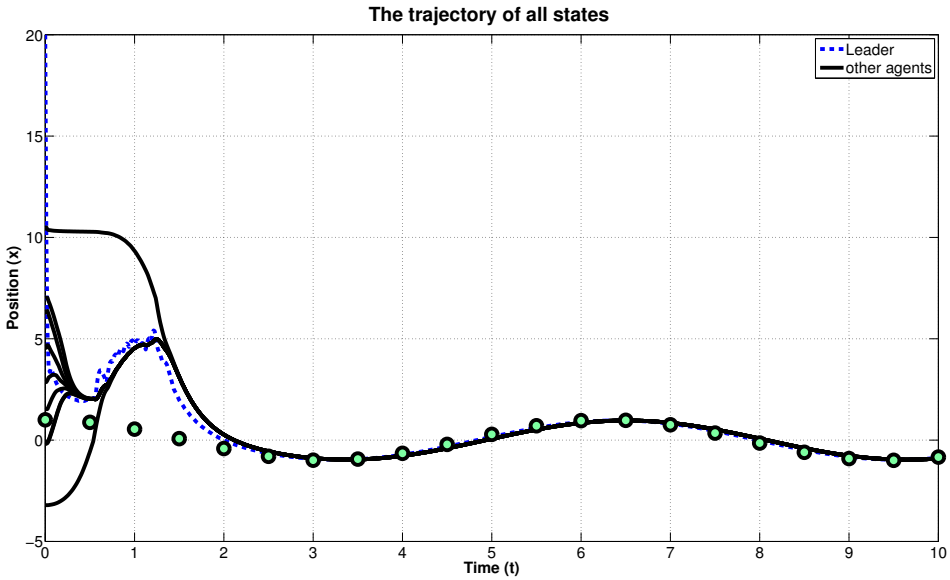

Figure 6.8: shows the results of optimal control by means of MPC.

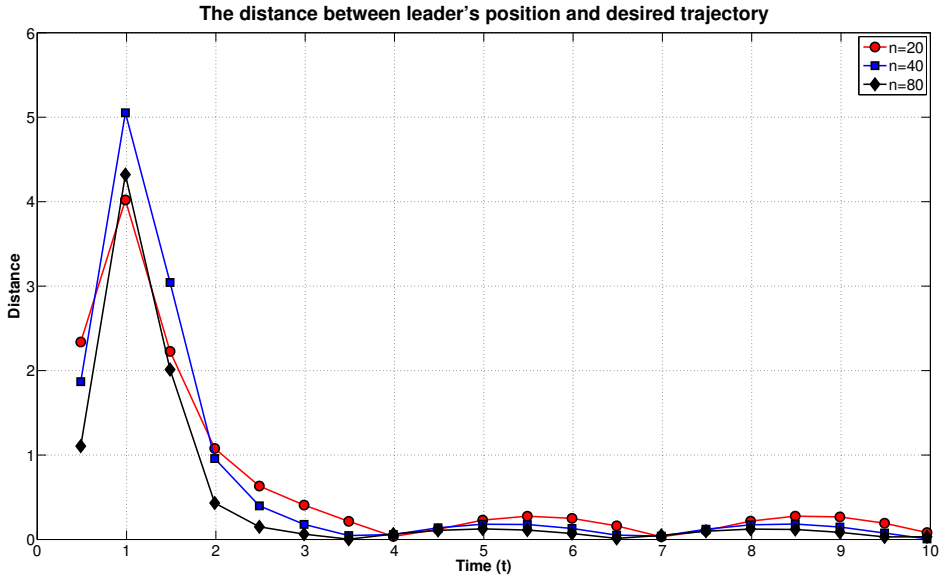

Figure 6.9: shows comparison of the distance between leader's opinion and desired trajectory where line-circle, line-square, and line-diamond are the results corresponding to $n = 20$, $n = 40$, and $n = 80$, respectively.

6.2 The Heider social balance model

The purpose of this section is to present results of numerical experiments with our HB optimal control problem. We chose the time horizon $T = 2$. The objective is to find the optimal control in order to drive the HB system to reach a friendship state where $x_{ij}^{\text{hb}} = R$ for all $i, j = 0, ..., N,\ i \neq j$. We consider two series of experiments; in the first one, the initial conditions $x_{ij}^{\text{hb}}(0) \in (-5, 5)$. In the second one, the state of relations starts with hostility that is characterized by values in a neighborhood of the unstable equilibrium point $\mathbf{x}^{\text{hb}*} = -\bar{R}$. In both cases, we solve the optimal control problem (5.18) with $N = 9$ people and one leader, with $R = 5$. In the objective functional we take $\nu = 0.001$. Furthermore, the target is $\mathbf{x}_{des}^{\text{hb}} = R$. To apply the MPC strategy, the time horizon is divided into subintervals of size $\Delta t = 0.25$.

Case I The initial state of relationships of the agents in our network is randomly chosen with friendly and hostility values. With this set of initial conditions, we get the results shown in Figure 6.10, where Figure 6.10(a) shows the solution of the HB model with zero control $u_{0i} = 0$, for $i = 1, ..., N$, and in Figure 6.10(b) the controllers are activated into the HB system. As we see in Figure 6.10(a), the HB model evolves towards the equilibrium states as it is expected because the value of the controls u_{0i} is equal to zero. Therefore the leader has no influence on the other agents and fails in steering the agents to a friendship state. On the other hand, as we see in Figure 6.10(b), as soon as the control is active friendship is obtained.

Case II In this case, the initial state of relationships of the agents in our network are randomly placed in a neighborhood of the unstable hostility equilibrium point $\mathbf{x}^{\text{hb}*} = -R$. With this set of initial conditions, we get the results as shown in Figure 6.11. Specifically, in Figure 6.11(a) we see that the solution of the HB model without active control is unstable. On the other hand, whenever the leader is actively controlling the system, the HB model successfully reaches the desired friendship state; see Figure 6.11(b).

We remark that results of further numerical experiments show that our control strategy is ineffective in driving the HB model to hostility.

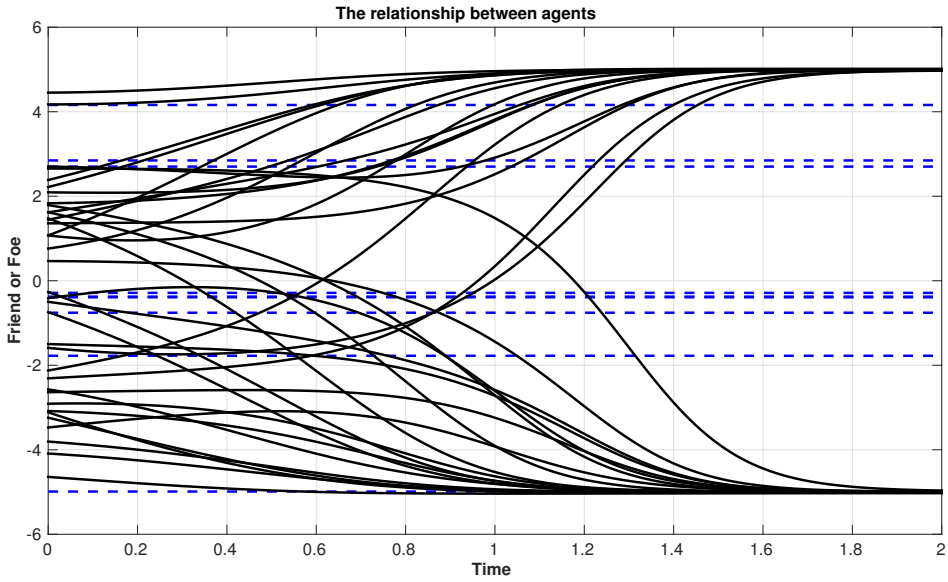

(a) $x_{ij}^{\text{hb}}(0) \in [-5, 5]$ with no controller

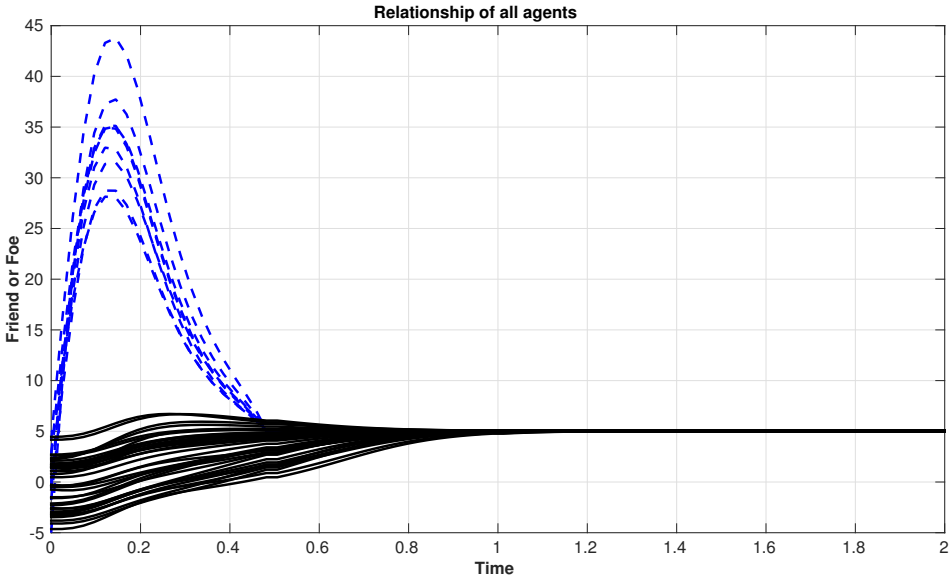

(b) $x_{ij}^{\text{hb}}(0) \in [-5, 5]$ with controllers

Figure 6.10: Simulation with $N+1 = 10$ agents. The status of relation of individuals in figure (a) are started randomly with friendship and hostility $x_{ij}^{\text{hb}} \in (-5, 5)$. Figure (a) shows the results where no controller is included the system while in Figure (b) controllers are included in the HB system. The dot-lines represent state of the relationship of leader and normal people, otherwise are of normal people.

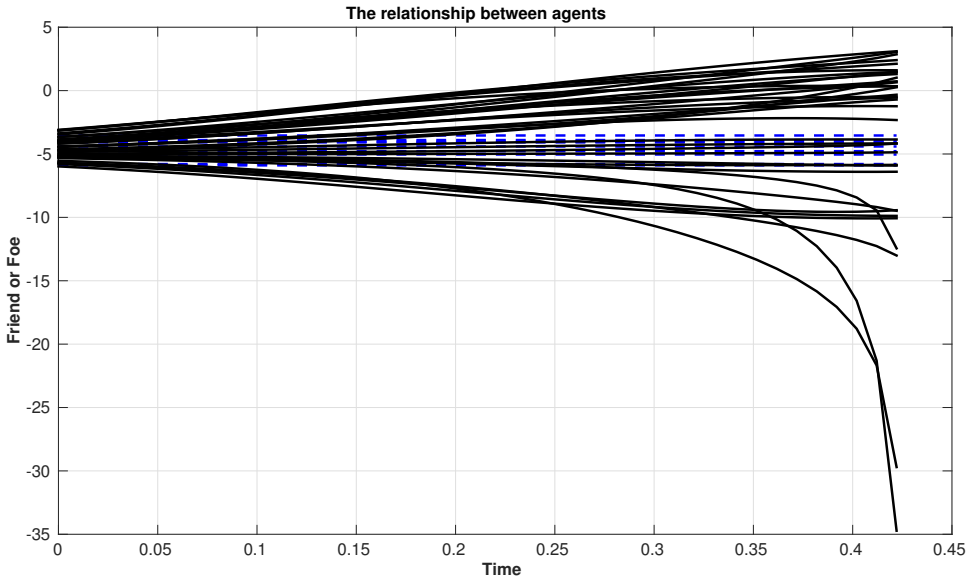

(a) $x_{ij}^{\text{hb}}(0) \in [-6, 3]$ with no controller

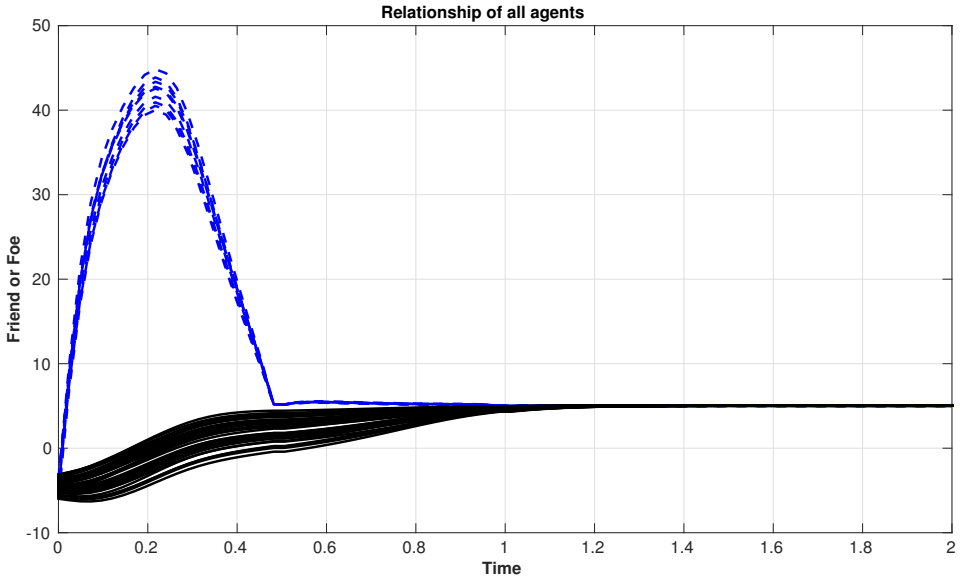

(b) $x_{ij}^{\text{hb}}(0) \in [-6, -3]$ with controllers

Figure 6.11: Simulation with $N+1 = 10$ agents. The status of relation of individuals in figure (a) are started with hostility $x_{ij}^{\text{hb}} \in (-6, 3)$. Figure (a) shows the results where no controller is included the system while in Figure (b) controllers are included in the HB system. The dot-lines represent state of the relationship of leader and normal people, otherwise are of normal people.

6.3 A refined flocking model

In this section, we discuss results of numerical simulation with our refined flocking model.These numerical experiments are organized into two parts. In the first part, we discuss the numerical tests regarding the investigation of the stability of the flocking system. In the second part numerical experiments with the optimal control governed by the flocking model is discussed.

For our experiments, the parameters are chosen based on biological concerns $C > 1, l < 1$ and in the catastrophic region $Cl^d < 1, d = 2$. Corresponding to our experiments, the values of the parameters of the flocking model are given in Table 6.3.

Table 6.3: Parameters values for the refined flocking model.

Parameters		
self-propelling force	α	0.07
	β	0.05
Morse Potential	C_r	50
	C_a	20
	l_r	2
	l_a	100
Attractive force by leader	C_r^0	25
	C_a^0	10
	l_r^0	1
	l_a^0	50
	γ_1	10
Attractive force	γ	1
	σ	0.5
	δ_1	cos(1.047)
	δ_2	cos(1.57)

Next we discuss stability of the refined flocking model with leadership. The Figures 6.12, 6.13, and 6.16 show numerical results of the refined flocking model with external leader and two different initial configurations. In Figure 6.12, two flocks of agents are distributed uniformly on circle configurations with initial velocities $v = \sqrt{\frac{\alpha}{\beta}}\frac{x^\perp}{\|x\|}$, while a leader is situated outside the groups as shown in Figure 6.12(a). In the Figures 6.12(b), 6.12(c) and 6.12(d) results of simulation are reported where the leader is not included in the swarming system. After $t = 100$, it can be seen that the flock develops into a chaotic configuration (Figure 6.12(b)) before it starts self-organizing in a single mill that is observed after $t = 800$ (Figure 6.12(c)). Figure 6.12(d) demonstrates the result of flocking that is a combination of alignment and Morse potential. It can

be seen that agents form the pattern configuration and move in the same direction. However, when the leader is present in the system, we can see that the agents react to the presence of the leader adjusting the orientation of the velocity in order to align with the leader and follow it after some time as shown in Figure 6.13. Similar results with leader are shown in Figures 6.16, where the coefficients C, l are chosen in a H-stable region ($C > 1, l > 1$) but C^0, l^0 are set in catastrophic region $C^0 > 1, l^0 < 1$. To discuss this case, we consider 62 agents with leadership starting with an initial configuration that forms as a uniformly circle and each individual moves initially with random velocities, see Figure 6.16. For this case, the coefficients corresponding to the Morse potential are given as follows

$$\begin{array}{llll} C_r = 20 & C_a = 50 & l_r = 2 & l_a = 10 \\ C_r^0 = 25 & C_a^0 = 10 & l_r^0 = 1 & l_a^0 = 50. \end{array}$$

After $t = 20$, the group of agents breaks down and tries to move towards the leader as shown in Figure 6.16(b) and 6.16(c). After some time, the group organizes itself to follow and adjust its alignment in the direction of the leader; see Figure 6.16(d).

To examine the asymptotic behavior of the refined flocking system, we calculate the dispersion $\Gamma(x^{\mathrm{fm}}(t))$ and disagreement $\Lambda(t)$ as discussed in [22].

$$\begin{aligned} \Gamma(t) &= \frac{1}{2(N+1)^2} \sum_{i,j}^{N+1} \|x_i^{\mathrm{fm}}(t) - x_j^{\mathrm{fm}}(t)\|, \qquad (6.1) \\ \Lambda(t) &= \frac{1}{2(N+1)^2} \sum_{i,j}^{N+1} \|v_i^{\mathrm{fm}}(t) - v_j^{\mathrm{fm}}(t)\| \end{aligned}$$

where $(x^{\mathrm{fm}}(t), v^{\mathrm{fm}}(t))$ represent the solution of the system (2.14) with the given initial conditions. Furthermore, it is reasonable to expect that asymptotically this solution becomes a minimizer of the Morse potential U, U^0 and the zeros of $(\alpha - \beta\|v_i^{\mathrm{fm}}\|^2)$. That is when the swarm reaches the asymptotic state, the distance between followers and leader tends to the value

$$\lim_{t\to\infty} \frac{1}{N} \sum_{b=1}^{N} \|x_b^{\mathrm{fm}} - x_0^{\mathrm{fm}}\| = \ln\left(\frac{C_r^0}{l_r^0}\frac{l_a^0}{C_a^0}\right) \frac{l_a^0 l_r^0}{(l_a^0 - l_r^0)} \quad \text{and} \quad \lim_{t\to\infty} \|v_i^{\mathrm{fm}}\| = \sqrt{\frac{\alpha}{\beta}}$$

It can be seen from Figure 6.14 and 6.15 that when $t \to \infty$, the value of $\Gamma(t)$ is becoming constant and the value $\Lambda(t)$ tends to zero, that is, the group attains a stable configuration where each individual in the group moves with the same velocity, and the relative distance remains constant.

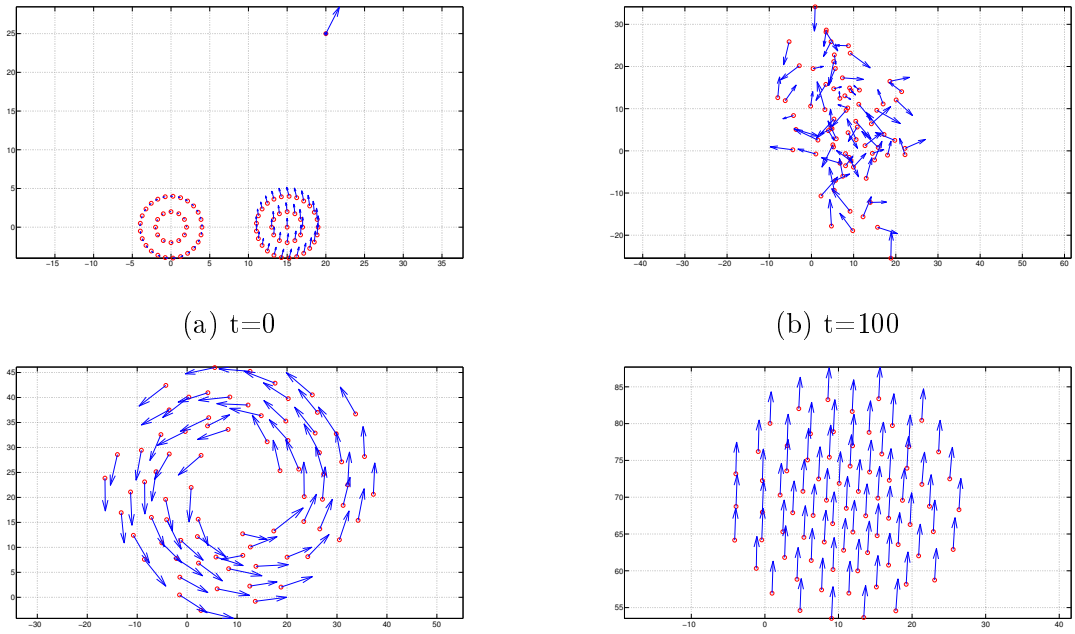

(a) t=0

(b) t=100

(c) t=800

(d) Morse potential and alignment

Figure 6.12: Simulation with $N+1 = 76$ agents. The initial configuration of swarming is displayed in Figure (a). Figure (b) and (c) show the position and the velocities of the agents at time $t = 100$ and $t = 800$ where the leader is not included in the dynamical system. Figure (d) shows results for the swarming system after t= 200 where Morse potential and alignment force are included in the model. The position of each individual is denoted by a circle and the shaded circle represents the leader.

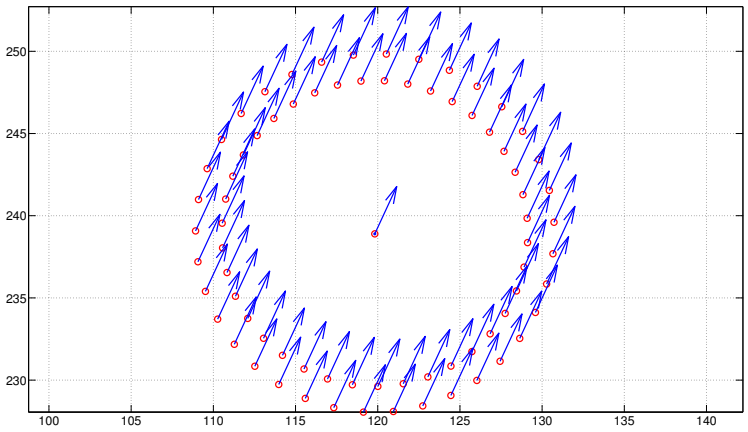

Figure 6.13: shows results for the swarming system after t= 200 when the leader is presented. The initial configuration of swarming is displayed in Figure 6.12(a).

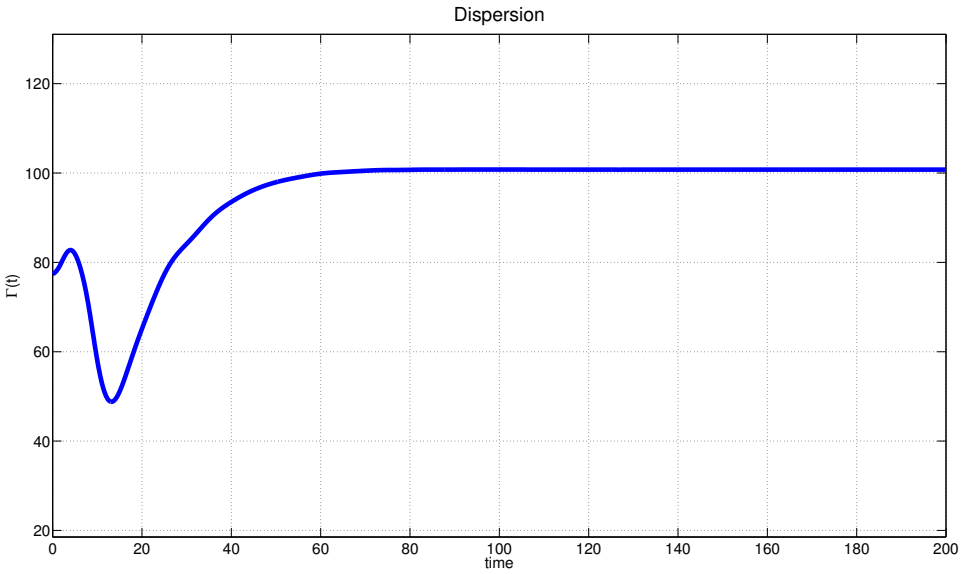

(a) $\Gamma(t)$

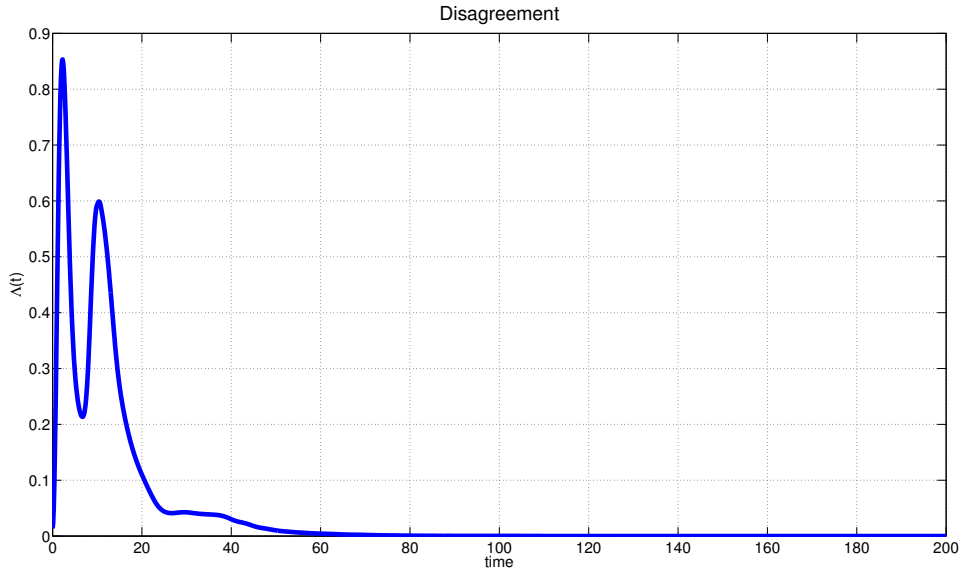

(b) $\Lambda(t)$

Figure 6.14: Figure (a) and (b) show the dispersion $\Gamma(t)$ and disagreement $\Lambda(t)$ for the system including leadership in time interval $[0, 200]$ where the initial configuration of swarming is displayed in Figure 6.12(a).

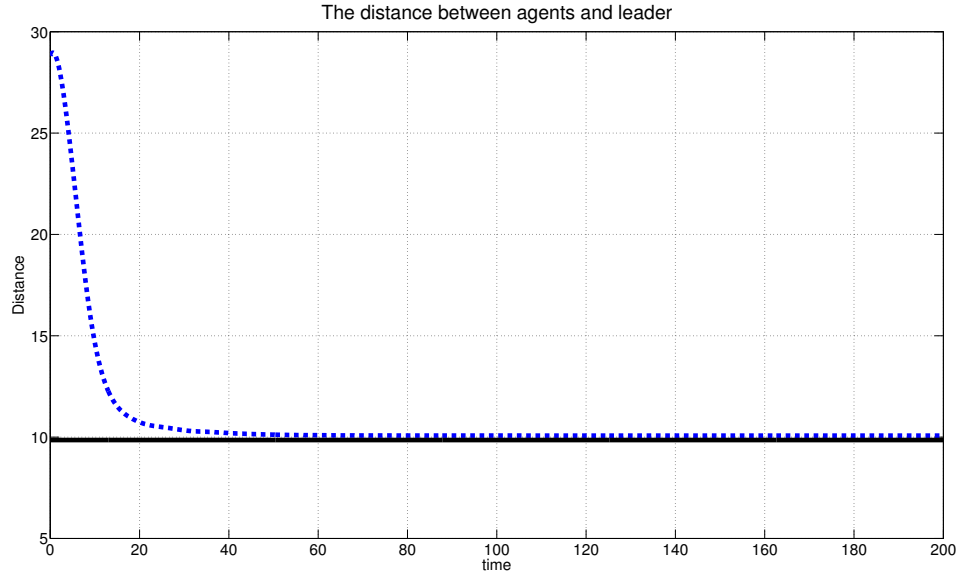

(a) $\frac{1}{N}\sum_{b=1}^{N}\|x_b^{\mathrm{fm}} - x_0^{\mathrm{fm}}\|$

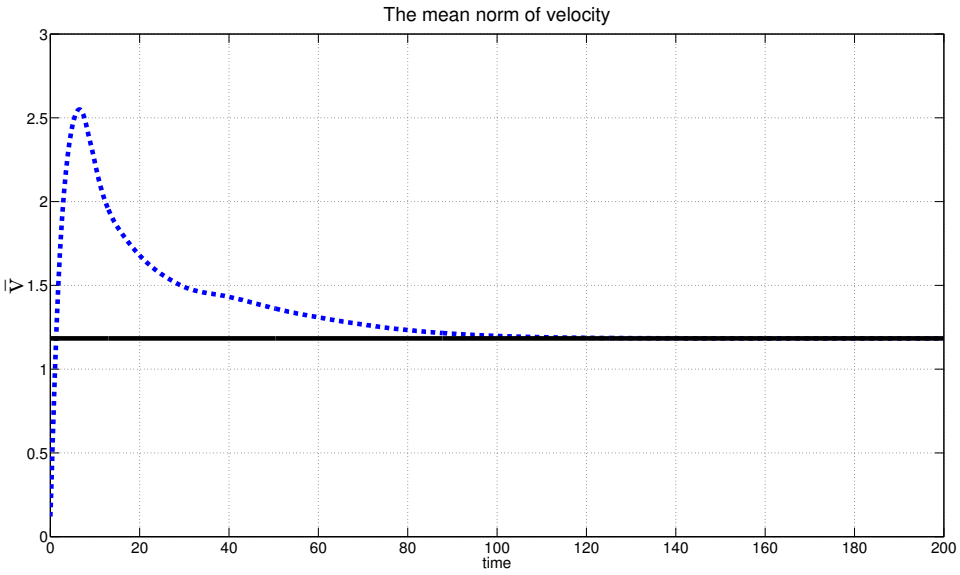

(b) $\frac{1}{N+1}\sum_{i=0}^{N}\|v_i^{\mathrm{fm}}\|$

Figure 6.15: Figure (a) show the distance between leader and follower compared with the value $\ln\left(\frac{C_r^0}{l_r^0}\frac{l_a^0}{C_a^0}\right)\frac{l_a^0 l_r^0}{(l_a^0 - l_r^0)}$. Figure(b) presents the comparison of the quantity of agents'velocities and the value $\sqrt{\frac{\alpha}{\beta}}$.

.

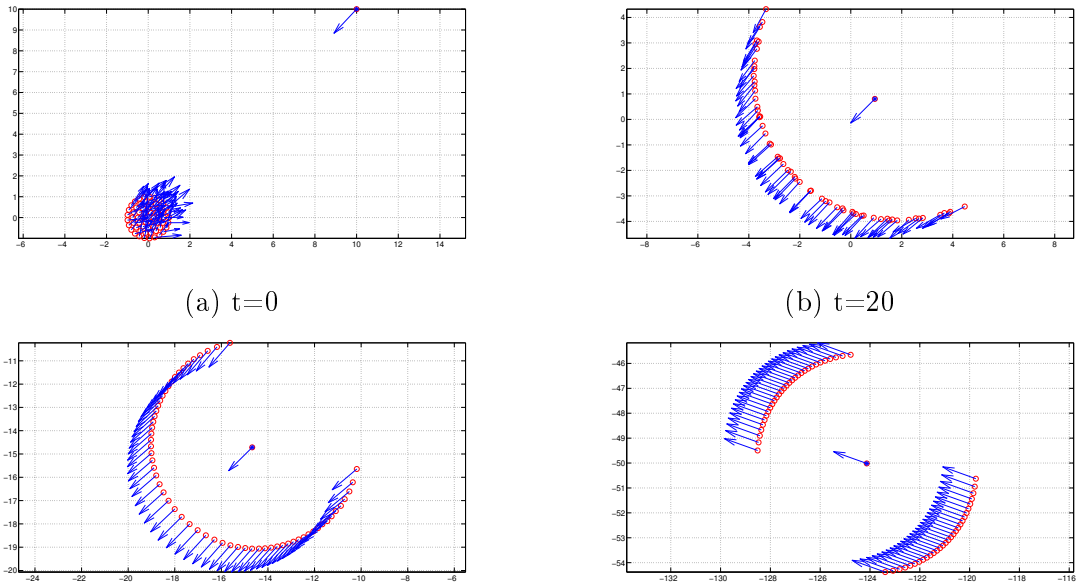

(a) t=0

(b) t=20

(c) t=50

(d) t=[0,100]

Figure 6.16: The numerical simulation of the dynamical system of $N+1 = 62$ agents. The initial velocity values are chosen randomly and the initial position of individuals are distributed into circle region as shown in Figure (a). Figure (b)-(d) show the position and velocities of the agents from time $t = 0$ to $t = 100$. The position of each individual is denoted by a circle and the shaded circle represents the leader.

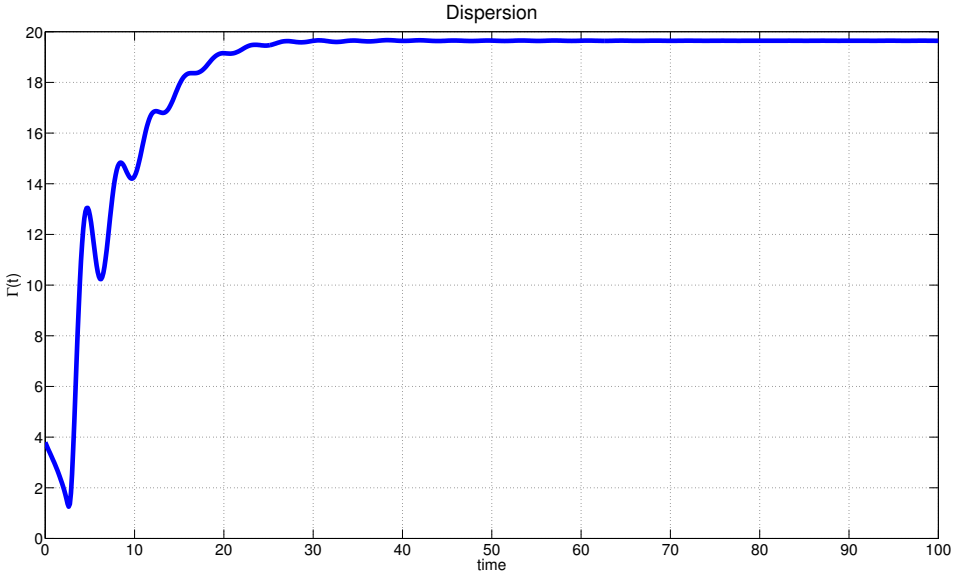

(a) $\Gamma(t)$

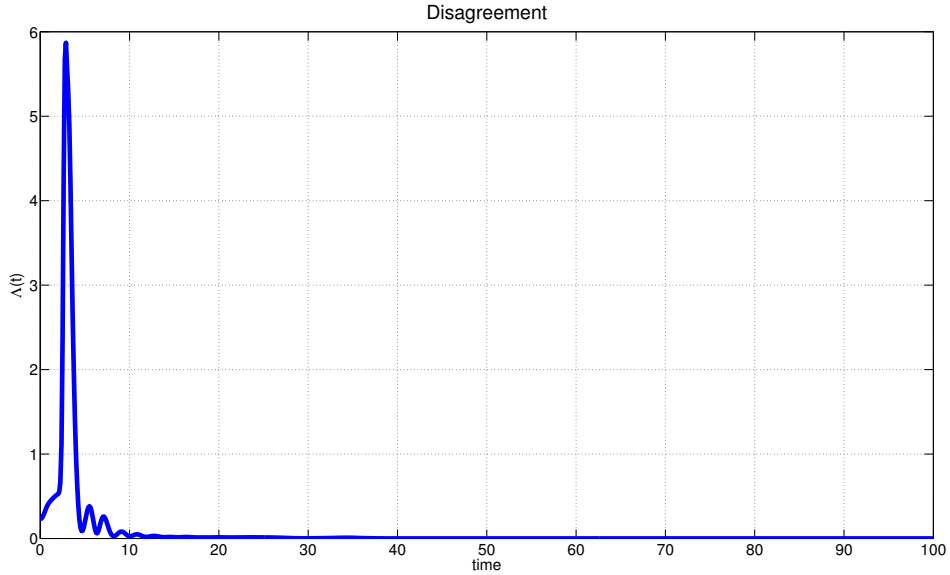

(b) $\Lambda(t)$

Figure 6.17: Figure (a) and (b) show the value dispersion $\Gamma(t)$ and disagreement $\Lambda(t)$ for the system including leadership in time interval $[0, 100]$ where the initial configuration of swarming is displayed in Figure 6.16(a).

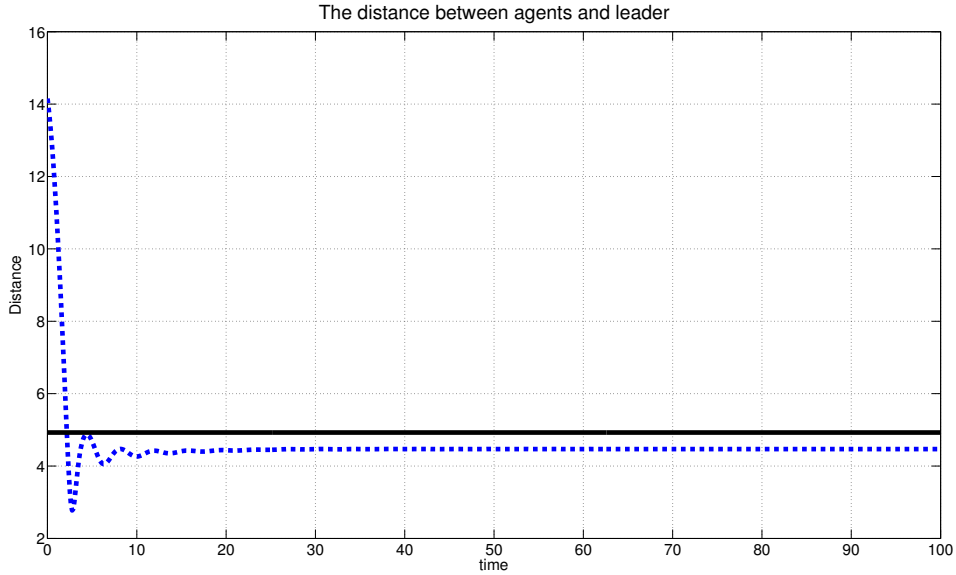

(a) $\frac{1}{N}\sum_{b=1}^{N}\|x_b^{\mathrm{fm}} - x_0^{\mathrm{fm}}\|$

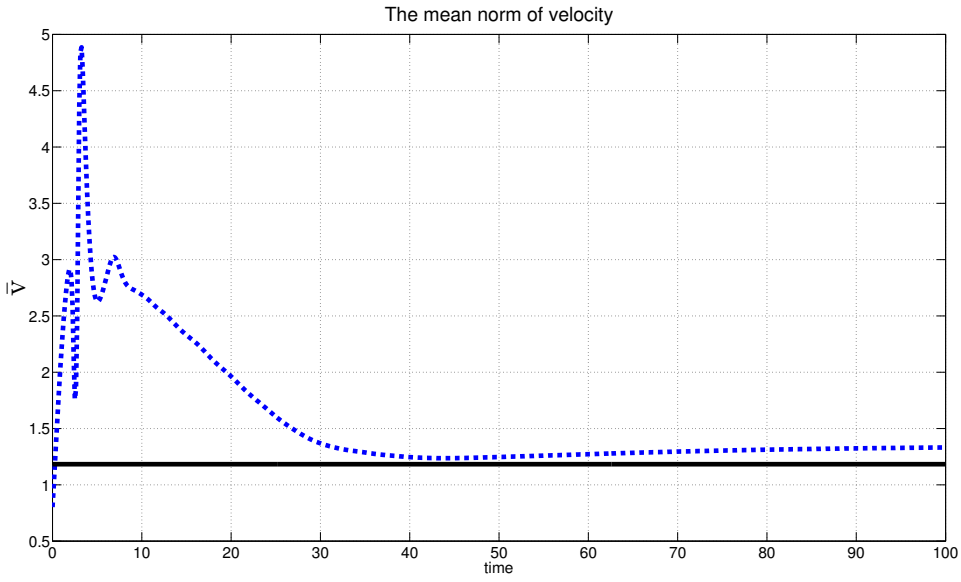

(b) $\frac{1}{N+1}\sum_{i=0}^{N}\|v_i^{\mathrm{fm}}\|$

Figure 6.18: Figure (a) and Figure (b) illustrate the results of the system including leadership in time interval $[0, 100]$ where the initial configuration of swarming is displayed in Figure 6.16(a). Figure (a) shows the distance between leader and follower compared with the value $\ln\left(\frac{C_r^0}{l_r^0}\frac{l_a^0}{C_a^0}\right)\frac{l_a^0 l_r^0}{(l_a^0 - l_r^0)}$. Figure (b) presents the comparison of the quantity of agents'velocities and the value $\sqrt{\frac{\alpha}{\beta}}$.

In the final part of this section, we discuss results of numerical tests with our control scheme. In the first experiment, we investigate problem (5.12) in one dimension considering a system with one leader and 9 agents, as already discussed in part in Section 5.1. The number of state and control variables are $nx = 21$ and $nc = 1$, respectively. The initial positions and velocity of the individuals are chosen randomly in $(0, 1)$ whereas the initial position of the leader is $x_0^{\text{fm}} = 10$. The desired trajectory for problem Pt2 is $\mathbf{x}_{des}^{\text{fm}} = \cos(t)$. The parameter values corresponding to our flocking model are given in Table 5.2. In this test, we consider a time horizon with $T = 20$ and time windows of size $\Delta t = 0.5$ and $\Delta t = 0.25$.

In Figure 6.19 we compare results obtained with different time windows. On the left-hand side, $\Delta t = 0.50$ is chosen whereas the results shown on the right-hand side of Figure 6.19 are obtained with $\Delta t = 0.25$. We can see that the smaller the length of the time window, the closer the objective can be obtained. These results are confirmed also when solving problem Pt2; see Figure 6.20. We remark that in all cases, the effectiveness of our control strategy is demonstrated.

Next, we discuss experiments in two space dimensions in the time horizon $T = 10$. In this case, the refined flocking model is composed of 10 agents including the leader and we choose the following parameters' values

$$\begin{array}{cccc} C_a = 2 & C_r = 5 & l_a = 0.2 & l_r = 2 \\ C_a^0 = 1 & C_r^0 = 0.5 & l_a^0 = 0.2 & l_r^0 = 10 \ . \end{array}$$

In this case, we use the MPC scheme with 20 time windows and the number of time-discretization points is $n = 100$ in each window. The desired trajectory is a circle $\mathbf{x}_{des}^{\text{fm}} = [\cos(t), \sin(t)]$ on the plane. At the initial time, the leader is outside of the flock while the other agents in the flock stay together within a small region. The leader and the agents are initialized with random velocities. In Figure 6.21, we depict the controlled evolution of the flocking model to follow the desired circular trajectory. We see that the leader is able to follow the desired circular trajectory and to lead the flock along this path.

The dispersion $\Gamma(t)$ and the disagreement $\Lambda(t)$ defined in (6.2) are presented in Figure (6.22). As a consequence of the optimization process, it can be concluded that after a transient time, the value of $\Gamma(t)$ is almost constant and the value of $\Lambda(t)$ tends to zero. Therefore each individual in the group moves with the same velocity and stays close together following the leader.

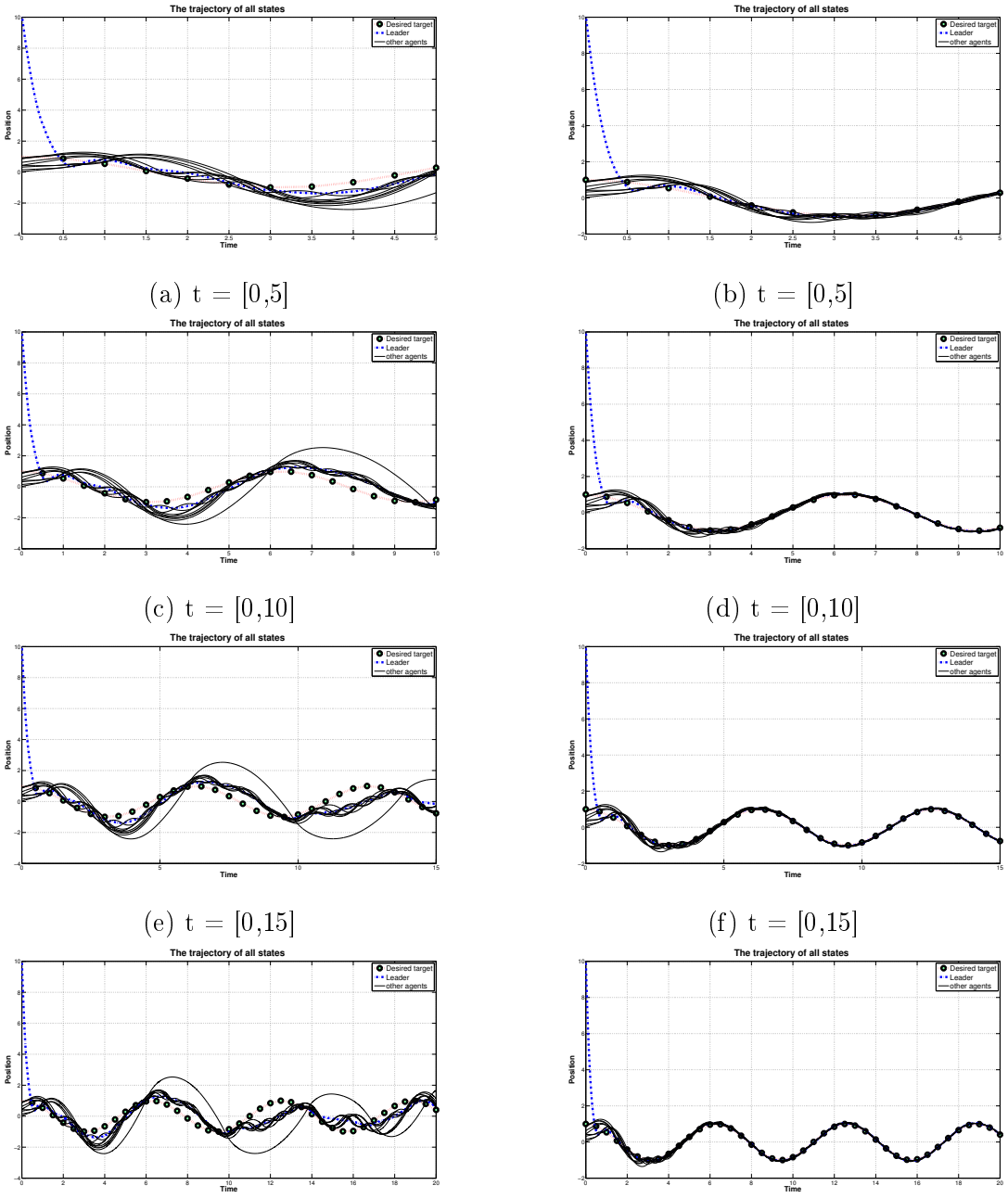

(a) t = [0,5] (b) t = [0,5]

(c) t = [0,10] (d) t = [0,10]

(e) t = [0,15] (f) t = [0,15]

(g) t = [0,20] (h) t = [0,20]

Figure 6.19: The figures show the trajectories of $N + 1 = 10$ individuals in the interval $[0, 20]$ for problem Pt1 by using different sizes of the MPC time windows. The figures in the left-hand side show the trajectories where the length of each time window is $[t_{k-1}, t_k] = 0.50$, while the figures in the right-hand side show the solution for time length $[t_{k-1}, t_k] = 0.25$. The same time-step size $n = 500$ is used in each window. The dotted line, dotted with shaded circle line, and straight line display the state trajectory of leader, desired target and other agents in the flock, respectively. The shaded circle presents the desired position for optimization problem in each time length.

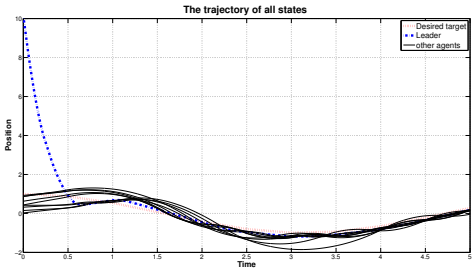

(a) t = [0,5]

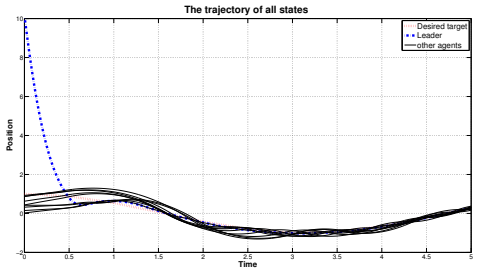

(b) t = [0,5]

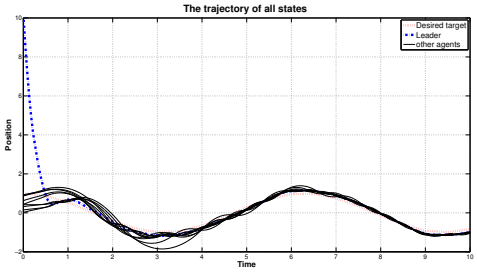

(c) t = [0,10]

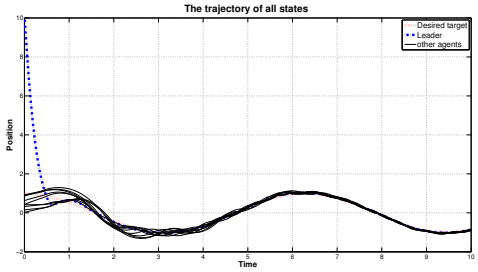

(d) t = [0,10]

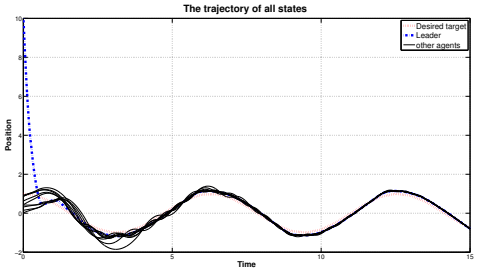

(e) t = [0,15]

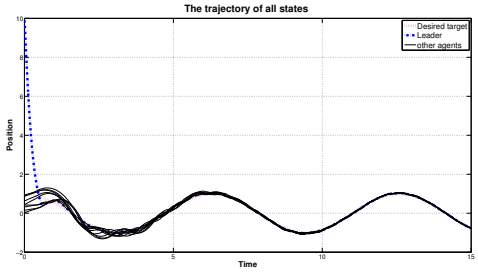

(f) t = [0,15]

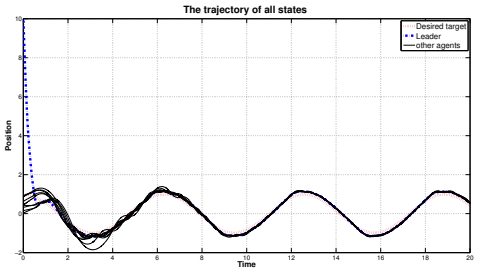

(g) t = [0,20]

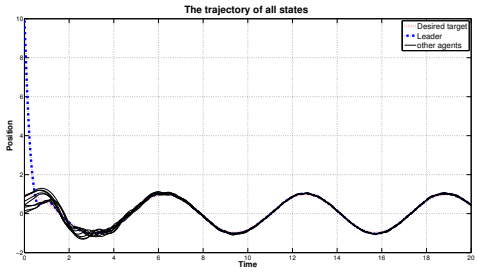

(h) t = [0,20]

Figure 6.20: The figures show results for the problem Pt2 of tracking a desired trajectory by using different sizes of the time windows. The dash-dotted line, dotted-dotted line and straight line display the state trajectory of leader, desired path and other agents in flocking, respectively. The figures in the left-hand side show the state trajectories computed with $[t_{k-1}, t_k] = 0.50$, while the figures in the right-hand side show the solution for time length $[t_{k-1}, t_k] = 0.25$. The same time-step size $n = 500$ is used in each window.

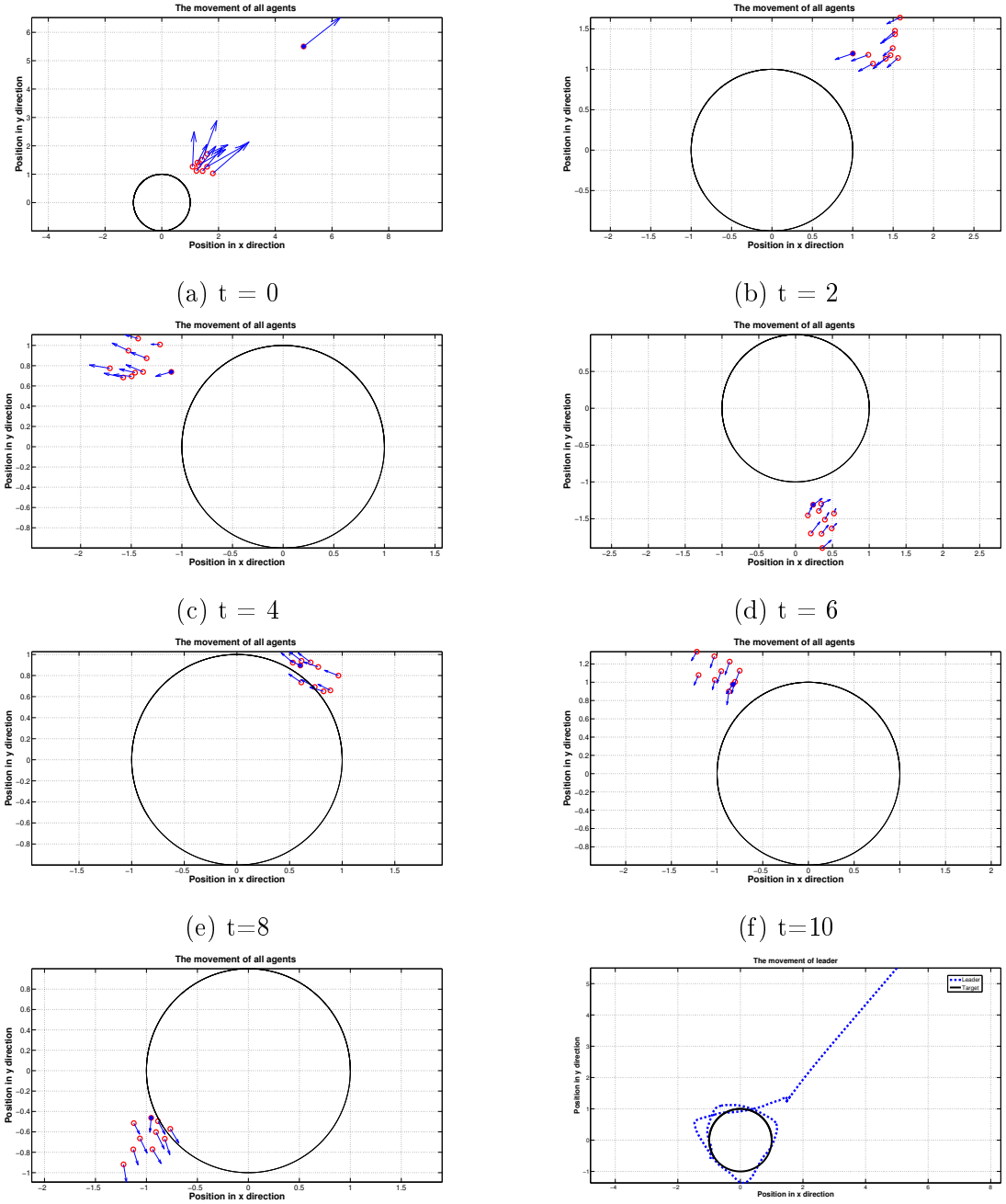

(a) t = 0

(b) t = 2

(c) t = 4

(d) t = 6

(e) t=8

(f) t=10

(g) at t=0 and at t=10

(h) t = [0,10]

Figure 6.21: Two-dimensional case: snapshots of 10 agents and the leader tracking a desired circular path. The position of each individual is denoted by a circle and the shaded circle represents the leader. The velocity is represented by a vector at the agent position. The Figures (a)-(f) illustrate the position at different times along the evolution. The last figure shows the path followed by the leader together with the desired path.

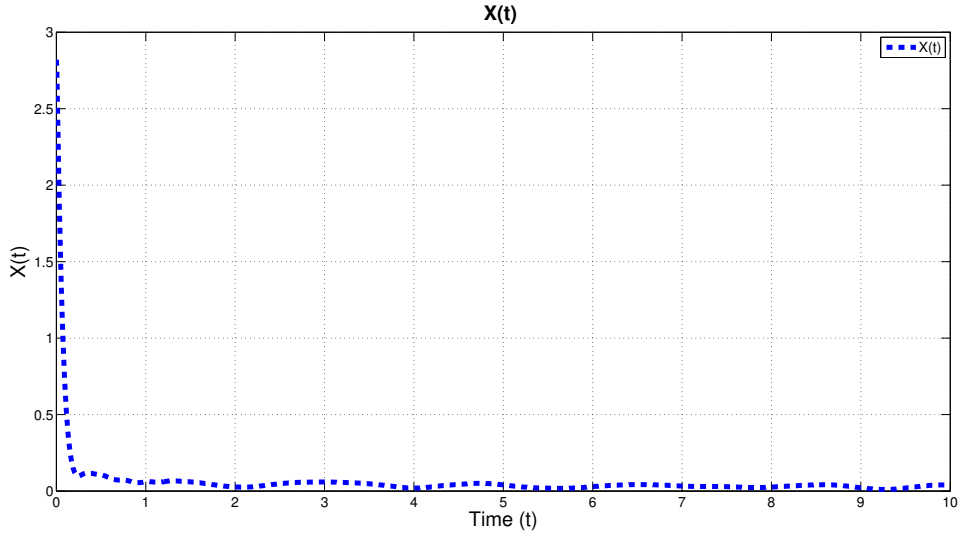

(a) $\Gamma(t)$

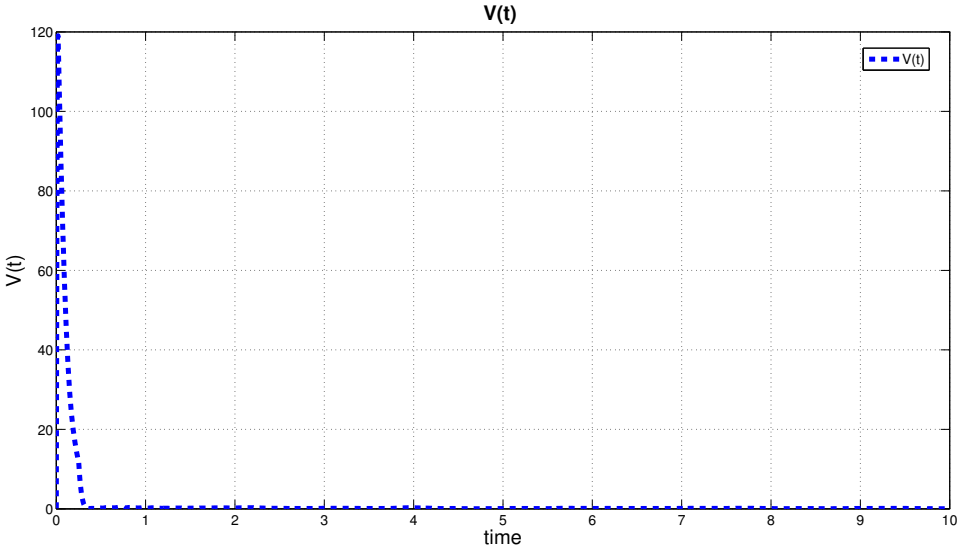

(b) $\Lambda(t)$

Figure 6.22: Figure (a) and (b) show the evolution of the values $\Gamma(t)$ and $\Lambda(t)$ of the solution $(\mathbf{x}^{\mathrm{fm}}(t), \mathbf{v}^{\mathrm{fm}}(t))$ to the refined flocking system with leadership; the time interval is $[0, 10]$. The initial configuration is displayed in Figure 6.21(a).

Chapter 7

Conclusions

In this thesis, we studied controllability of representative multi-agent models with the presence of a leader focusing on the Hegselmann- Krause opinion formation (HK) model, on the Heider social balance (HB) model and on our refined flocking model. For these three models different control strategies were investigated. On the one hand, the stabilizing control function was explicitly determined by application of control theoretical tools. On the other hand, optimal controls were obtained using a model predictive control (MPC) strategy. This control strategy requires the solution of a sequence of open-loop optimality systems. The corresponding discretized optimization problems were solved with an accurate Runge-Kutta method that guaranteed accurate gradients of the reduced objectives. These gradients were implemented in a nonlinear conjugate gradient solution procedure. In all cases, the control function was implemented in the leader dynamics.

For the HK model, the analysis of the stabilization in the case of bounded confidence and leader was provided. In addition, local controllabilty near consensus was investigated. One of the novelties of this study is that we have explored the possibility to control the evolution of agent's opinion to reach agreement. In particular, a global stabilization was achieved by feedback control implemented on the dynamics of leader's opinion. Further, a tracking problem was discussed via optimal control problems and feedback control was obtained by using MPC.

Second, we have studied the continuous time Heider balance model. This model describes the evolution of relationship in a social network. It was shown that in the absences of controls, this model evolves towards equilibrium states of friendship and hostility. In correspondence to these states the local stability of the linearized system was discussed. Furthermore, an optimal strategy, based on leadership, that steers the relationships in the network to friendship state was investigated. The corresponding optimization problems were solved with an appropriated Runge-Kutta method that guaranteed accurate gradients of the objectives. These gradients were implemented in a nonlinear conjugate gradient solution procedure and MPC.

Finally, we presented a new flocking model including self-propelling, friction, attraction and repulsion, and alignment features. The presence of a leader in the system has been exploited in oder to develop a control strategy for our flocking model to accomplish desired objectives. In this model, we investigated the pattern formation or consensus of flocking. In correspondence to this state, the local controllability of linearized system was discussed. Further, optimal control problems governed by a refined flocking systems were considered.

Results of numerical experiments with these three models demonstrated the ability of the proposed control through leadership strategy to steer the multi-agent systems convergence to consensus.

Appendix A

Appendix

In this chapter, we provide some essential concepts and precise mathematical results related to real functional analysis that are used in this thesis. Our main references for the first section are [54, 76, 81] and [18, 30, 26, 41, 72, 80] for the second section.

A.1 Initial-value problems

In this section, we present the general results on nonlinear dynamical systems characterized by differential equations of the form

$$\dot{x} = f(t, x) \tag{A.1}$$

Theorem A.1. *Assume that $f : [0, T] \times X \to \mathbb{R}^n$ is a vector function, where X is open subset of $\mathbb{R}^n$ and f has the following properties*

- *$f(\cdot, x) : [0, T] \to \mathbb{R}^n$ is measurable for each fixed x.*
- *$f(t, \cdot) : \mathbb{R}^n \to \mathbb{R}^n$ is continuous for each fixed t.*

Moreover, the following two conditions also hold:

1. *f is locally Lipschitz on x; that is, there are for each $x^0 \in X$ a real number $\rho > 0$ and a locally integrable function $\alpha : [0, T] \to \mathbb{R}^+$ such that $B_\rho(x^0)$ is contained in X and*

$$\|f(t, x) - f(t, y)\|_2 \leq \alpha(t)\|x - y\|_2 \tag{A.2}$$

   for each $t \in [0, T]$ and $x, y \in B_\rho(x^0)$

f is locally integrable on t; that is, for each fixed x^0 there is a locally integrable function $\beta : [0, T] \to \mathbb{R}^+$ such that

$$\|f(t, x^0)\| \leq \beta(t) \tag{A.3}$$

for almost all t.

Then, for each pair $(t, x^0) \in [0,T] \times X$ there is some nonempty subinterval $J \subseteq [0,T]$ open relative to $[0,T]$ and there exists a solution $x(t)$ of (A.1) on J, with the following property: If $\xi : \tilde{J} \to X$ is any other solution of (A.1) where $\tilde{J} \subseteq [0,T]$, then necessarily

$$\tilde{J} \subseteq J \quad \text{and} \quad x = \xi \quad \text{on} \quad \tilde{J}. \tag{A.4}$$

The solution x is called the maximal solution of the initial-value problem in the interval $[0,T]$.

A.2 Results of functional analysis

Definition A.1. *Let X be a normed vector space and let X^* denote its dual. A sequence $\{x_n\}_{n=1}^{\infty}$ of elements $x_n \in X$ is said to converge weakly in X if there exists $x \in X$ such that*

$$\text{for each } x^* \in X^*, \quad x^*(x_n) \to x^*(x) \quad \text{as } n \to \infty$$

and such an x is called the weak limit of the sequence $\{x_n\}_{n=1}^{\infty}$. Weak convergence is usually denoted by $x_n \rightharpoonup x$

Theorem A.2. *Let X and Y be normed vector spaces over the same field $\mathbb{K}$. It holds:*

- *let $A \in \mathcal{L}(X,Y)$, then*

$$x_n \rightharpoonup x \quad \text{in} \quad X \quad \text{implies} \quad Ax_n \rightharpoonup Ax \quad \text{in} \quad Y;$$

- *let $B \in \mathcal{L}(X \times Y, \mathbb{K})$, then*

$$x_n \rightharpoonup x \quad \text{in} \quad X \quad \text{and} \quad y_n \to y \quad \text{in} \quad Y \quad \text{implies} \quad B(x_n, y_n) \to B(x,y) \quad \text{in} \quad \mathbb{K}$$

Theorem A.3. *(Banach-Saks-Mazur)*
Let X be a real normed vector space. Let C be a nonempty, convex, and closed subset of X, and let $\{x_k\}_{k=1}^{\infty}$ be a sequence of points $x_k \in C$ that weakly converges to $x \in X$ as $k \to \infty$. Then the weak limit x belongs to C

Theorem A.4. *(Banach-Eberlein- Šmulian).*

1. *Any bounded sequence in a reflexive Banach space contains a weakly convergent subsequence.*
2. *A Banach space in which every bounded sequence contains a weakly convergent subsequence is reflexive.*

Theorem A.5. *Let X be a reflexive Banach space. Let C be a nonempty, convex, closed and bounded subset of X. Then C is weakly sequentially compact, that is every sequence contains a subsequence that weakly converges to some $x \in C$.*

Theorem A.6. *The following Banach spaces are reflexive*

1. *Any finite-dimensional normed vector space*
2. *Any Hilbert space*
3. *Any closed subspace of reflexive Banach space*
4. *The dual space of any reflexive Banace space*
5. *The space l^p, $1 < p < \infty$, and the Lebesgue spaces $L^p(\Omega)$, $1 < p < \infty$, with Ω any subset of $\mathbb{R}^n$.*

Definition A.2. *Let X be a normed vector space and let X^* denote its dual. A function $J : X \to \mathbb{R} \cup \{\infty\}$ is said sequentially lower semicontinuous if*

$$\lim_{k\to\infty} x_k = x \quad in \quad X \quad implies \quad J(x) = \lim_{k\to\infty} \inf J(x_k).$$

Furthermore, let $U \subset X$ be nonempty, then $J : U \to \mathbb{R} \cup \{\infty\}$ is said sequentially weakly lower semicontinuous if

$$x_k \in U \rightharpoonup x \in U \quad as \quad k \to \infty \quad implies \quad J(x) = \lim_{k\to\infty} \inf J(x_k).$$

Theorem A.7. *Let X be a normed space. Then a convex and continuous function $J : X \to \mathbb{R} \cup \{\infty\}$ is sequentially weakly lower semicontinuous on X*

We are now going to provide some results that are used to guarantee the boundedness property of the sequence by the application of coercivity.

Proposition A.1. *Let U be a nonempty unbounded subset of a reflexive Banach space. Let $\psi : U \to \mathbb{R} \cup \{\infty\}$ be a functional that is sequentially weakly lower semicontinuous and coercive on U. Let $(u^m)_{m=1}^{\infty}$ be an minimizing sequence of the functional ψ, that is, a sequence $(u^k)_{k=1}^{\infty}$ that satisfies*

$$u^m \in U \quad and \quad \lim_{m\to\infty} \psi(u^m) = \inf_{\tilde{u}\in U} \psi(\tilde{u}). \tag{A.5}$$

Then the sequence $(u^m)_{m=1}^{\infty}$ is bounded.

Proof. Let $(u^m)_{m=1}^{\infty}$ be a minimizing sequence for the functional ψ, that is,

$$u^m \in U \quad \text{and} \quad \lim_{m\to\infty} \psi(u^m) = \inf_{\tilde{u}\in U} \psi(\tilde{u}). \tag{A.6}$$

Suppose that $(u^m)_{m=1}^{\infty}$ is unbounded, then there exists a subsequence $(u^{m_l})_{l=1}^{\infty}$ of the sequence $(u^m)_{m=1}^{\infty}$ such that $\|u^{m_l}\| \to \infty$. Thanks to coercivity of ψ,

$$\psi(u^{m_l}) \to \infty \quad \text{as} \quad m_l \to \infty$$

That is a contradiction. □

Proposition A.2. *Let X be normed vector space and $a \in X$. The functional*

$$f_a : X \to \mathbb{R}, \quad x \mapsto \|x - a\|,$$

is continuous and convex

Proof.

- Continuity
  Let $(\mathbf{x}_n)_{n\in\mathbb{N}}$ be a sequence in X such that $\lim_{n\to\infty} x_n = x \in X$. Then we get,

$$\begin{aligned} \|x_n - a\| - \|x - a\| &\leq \|(x_n - a) - (x - a)\| = \|x_n - x\| \\ \lim_{n\to\infty} \|x_n - a\| - \|x - a\| &\leq \lim_{n\to\infty} \|x_n - x\| \to 0 \end{aligned}$$

  It yields , $\lim_{n\to\infty}\|x_n - a\| = \|x - a\|$.

- Convexity
  For each $x, y \in X$ and $\lambda \in [0, 1]$, consider

$$\begin{aligned} f_a(\lambda x + (1-\lambda)y) &= \|\lambda x + (1-\lambda)y - a\| \\ &= \|\lambda x - \lambda a + (1-\lambda)y + \lambda a - a\| \\ &= \|\lambda(x-a) + (1-\lambda)(y-a)\| \\ &\leq \lambda\|x-a\| + (1-\lambda)\|y-a\| \end{aligned}$$

  That is, f_a is convex.

□

Bibliography

[1] Martial Agueh, Reinhard Illner, and Ashlin Richardson. Analysis and simulations of a refined flocking and swarming model of cucker-smale type. *Kinetic and Related Models*, 4(1):1–16, 2011.

[2] Giacomo Albi, Michael Herty, and Lorenzo Pareschi. Kinetic description of optimal control problems and applications to opinion consensus. *arXiv preprint arXiv:1401.7798*, 2014.

[3] Giacomo Albi and Lorenzo Pareschi. Modeling of self-organized systems interacting with a few individuals: from microscopic to macroscopic dynamics. *Applied Mathematics Letters*, 26(4):397–401, 2013.

[4] Claudio Altafini. Dynamics of opinion forming in structurally balanced social networks. In *Decision and Control (CDC), 2012 IEEE 51st Annual Conference on*, pages 5876–5881. IEEE, 2012.

[5] Tibor Antal, Paul L Krapivsky, and Sidney Redner. Dynamics of social balance on networks. *Physical Review E*, 72(3):036121, 2005.

[6] Tibor Antal, Paul L Krapivsky, and Sidney Redner. Social balance on networks: The dynamics of friendship and enmity. *Physica D: Nonlinear Phenomena*, 224(1):130–136, 2006.

[7] Matteo Aureli and Maurizio Porfiri. Coordination of self-propelled particles through external leadership. *EPL (Europhysics Letters)*, 92(4):40004, 2010.

[8] Michele Ballerini, Nicola Cabibbo, Raphael Candelier, Andrea Cavagna, Evaristo Cisbani, Irene Giardina, Vivien Lecomte, Alberto Orlandi, Giorgio Parisi, Andrea Procaccini, et al. Interaction ruling animal collective behavior depends on topological rather than metric distance: Evidence from a field study. *Proceedings of the national academy of sciences*, 105(4):1232–1237, 2008.

[9] Alethea BT Barbaro, Kirk Taylor, Peterson F Trethewey, Lamia Youseff, and Björn Birnir. Discrete and continuous models of the dynamics of pelagic fish: application to the capelin. *Mathematics and Computers in Simulation*, 79(12):3397–3414, 2009.

[10] Nicola Bellomo and Christian Dogbe. On the modeling of traffic and crowds: A survey of models, speculations, and perspectives. *SIAM review*, 53(3):409–463, 2011.

[11] Nicola Bellomo, Miguel A Herrero, and Andrea Tosin. On the dynamics of social conflicts: looking for the black swan. *Kinetic & Related Models*, 6(3), 2013.

[12] Nicola Bellomo, Giulia Ajmone Marsan, and Andrea Tosin. *Complex Systems and Society: Modeling and Simulation*. Springer, 2013.

[13] Nicola Bellomo and J Soler. On the mathematical theory of the dynamics of swarms viewed as complex systems. *Mathematical Models and Methods in Applied Sciences*, 22(supp01):1140006, 2012.

[14] Eric Bonabeau, Marco Dorigo, and Guy Theraulaz. *Swarm intelligence: from natural to artificial systems*. Number 1. Oxford university press, 1999.

[15] Alfio Borzì and Volker Schulz. *Computational optimization of systems governed by partial differential equations*, volume 8. SIAM, 2011.

[16] Alfio Borzì and Suttida Wongkaew. Modeling and control through leadership of a refined flocking system. *Mathematical Models and Methods in Applied Sciences*, 25(02):255–282, 2015.

[17] John Charles Butcher. *The numerical analysis of ordinary differential equations: Runge-Kutta and general linear methods*. Wiley-Interscience, 1987.

[18] Scott Camazine. *Self-organization in biological systems*. Princeton University Press, 2003.

[19] José A Canizo, José A Carrillo, and Jesús Rosado. A well-posedness theory in measures for some kinetic models of collective motion. *Mathematical Models and Methods in Applied Sciences*, 21(03):515–539, 2011.

[20] Marco Caponigro, Massimo Fornasier, Benedetto Piccoli, and Emmanuel Trélat. Sparse stabilization and control of the cucker-smale model. 2013.

[21] Marco Caponigro, Massimo Fornasier, Benedetto Piccoli, and Emmanuel Trélat. Sparse stabilization and control of alignment models. *Mathematical Models and Methods in Applied Sciences*, 25(03):521–564, 2015.

[22] José A Carrillo, Massimo Fornasier, Jesús Rosado, and Giuseppe Toscani. Asymptotic flocking dynamics for the kinetic cucker-smale model. *SIAM Journal on Mathematical Analysis*, 42(1):218–236, 2010.

[23] José A Carrillo, Massimo Fornasier, Giuseppe Toscani, and Francesco Vecil. Particle, kinetic, and hydrodynamic models of swarming. In *Mathematical modeling of collective behavior in socio-economic and life sciences*, pages 297–336. Springer, 2010.

[24] José A Carrillo, Axel Klar, Stephan Martin, and Sudarshan Tiwari. Self-propelled interacting particle systems with roosting force. *Mathematical Models and Methods in Applied Sciences*, 20(supp01):1533–1552, 2010.

[25] José A Carrillo, Stephan Martin, and Vladislav Panferov. A new interaction potential for swarming models. *Physica D: Nonlinear Phenomena*, 260:112–126, 2013.

[26] Lamberto Cesari. *Optimization-theory and applications: problems with ordinary differential equations*, volume 17. Springer Science & Business Media, 2012.

[27] Yao-Li Chuang, Yuan R Huang, Maria R D'Orsogna, and Andrea L Bertozzi. Multi-vehicle flocking: scalability of cooperative control algorithms using pairwise potentials. In *Robotics and Automation, 2007 IEEE International Conference on*, pages 2292–2299. IEEE, 2007.

[28] Gabriele Ciaramella, Alfio Borzì, Gunther Dirr, and Daniel Wachsmuth. Newton methods for the optimal control of closed quantum spin systems. *SIAM Journal on Scientific Computing*, 37(1):A319–A346, 2015.

[29] Gabriele Ciaramella, Julien Salomon, and Alfio Borzì. A method for solving exact-controllability problems governed by closed quantum spin systems. *International Journal of Control*, 88(4), 2015.

[30] Philippe G Ciarlet. *Linear and nonlinear functional analysis with applications*, volume 130. SIAM, 2013.

[31] Rinaldo M Colombo and Magali Lécureux-Mercier. An analytical framework to describe the interactions between individuals and a continuum. *Journal of nonlinear science*, 22(1):39–61, 2012.

[32] Jean-Michel Coron. *Control and nonlinearity*. Number 136. American Mathematical Soc., 2009.

[33] Iain D Couzin, Jens Krause, Nigel R Franks, and Simon A Levin. Effective leadership and decision-making in animal groups on the move. *Nature*, 433(7025):513–516, 2005.

[34] Emiliano Cristiani, Benedetto Piccoli, and Andrea Tosin. Modeling self-organization in pedestrians and animal groups from macroscopic and microscopic viewpoints. In *Mathematical modeling of collective behavior in socio-economic and life sciences*, pages 337–364. Springer, 2010.

[35] Felipe Cucker and Steve Smale. Emergent behavior in flocks. *Automatic Control, IEEE Transactions on*, 52(5):852–862, 2007.

[36] Felipe Cucker and Steve Smale. On the mathematics of emergence. *Japanese Journal of Mathematics*, 2(1):197–227, 2007.

[37] Maria R D' Orsogna, Yao-Li Chuang, Andrea L Bertozzi, and Lincoln S Chayes. Self-propelled particles with soft-core interactions: patterns, stability, and collapse. *Physical review letters*, 96(10):104302, 2006.

[38] Guillaume Deffuant, David Neau, Frederic Amblard, and Gérard Weisbuch. Mixing beliefs among interacting agents. *Advances in Complex Systems*, 3(01n04):87–98, 2000.

[39] Bertram Düring, Peter Markowich, Jan-Frederik Pietschmann, and Marie-Therese Wolfram. Boltzmann and fokker–planck equations modelling opinion formation in the presence of strong leaders. In *Proceedings of the Royal Society of London A: Mathematical, Physical and Engineering Sciences*, volume 465, pages 3687–3708. The Royal Society, 2009.

[40] Werner Ebeling and Udo Erdmann. Nonequilibrium statistical mechanics of swarms of driven particles. *Complexity*, 8(4):23–30, 2003.

[41] LC Evans. Partial differential equations (graduate studies in mathematics vol 19)(providence, ri: American mathematical society), 1998.

[42] Santo Fortunato. Community detection in graphs. *Physics Reports*, 486(3):75–174, 2010.

[43] Jean Charles Gilbert and Jorge Nocedal. Global convergence properties of conjugate gradient methods for optimization. *SIAM Journal on optimization*, 2(1):21–42, 1992.

[44] Lars Grüne and Jürgen Pannek. *Nonlinear model predictive control*. Springer, 2011.

[45] Seung-Yeal Ha, Taeyoung Ha, and Jong-Ho Kim. Emergent behavior of a cucker-smale type particle model with nonlinear velocity couplings. *IEEE transactions on automatic control*, 55(7):1679–1683, 2010.

[46] Seung-Yeal Ha and Eitan Tadmor. From particle to kinetic and hydrodynamic descriptions of flocking. *arXiv preprint arXiv:0806.2182*, 2008.

[47] William W Hager. Runge-kutta methods in optimal control and the transformed adjoint system. *Numerische Mathematik*, 87(2):247–282, 2000.

[48] William W Hager and Hongchao Zhang. A new conjugate gradient method with guaranteed descent and an efficient line search. *SIAM Journal on Optimization*, 16(1):170–192, 2005.

[49] William W Hager and Hongchao Zhang. Algorithm 851: Cg_descent, a conjugate gradient method with guaranteed descent. *ACM Transactions on Mathematical Software (TOMS)*, 32(1):113–137, 2006.

[50] William W Hager and Hongchao Zhang. A survey of nonlinear conjugate gradient methods. *Pacific journal of Optimization*, 2(1):35–58, 2006.

[51] Rainer Hegselmann and Ulrich Krause. Opinion dynamics and bounded confidence models, analysis, and simulation. *Journal of Artificial Societies and Social Simulation*, 5(3), 2002.

[52] Fritz Heider. Social perception and phenomenal causality. *Psychological review*, 51(6):358, 1944.

[53] Fritz Heider. *The psychology of interpersonal relations*. Psychology Press, 2013.

[54] Hassan K Khalil and JW Grizzle. *Nonlinear systems*, volume 3. Prentice hall New Jersey, 1996.

[55] Krzysztof Kulakowski, Przemyslaw Gawronski, and Piotr Gronek. The heider balance: A continuous approach. *International Journal of Modern Physics C*, 16(05):707–716, 2005.

[56] Hanspeter Kunz and Charlotte K Hemelrijk. Artificial fish schools: collective effects of school size, body size, and body form. *Artificial life*, 9(3):237–253, 2003.

[57] Herbert Levine, Wouter-Jan Rappel, and Inon Cohen. Self-organization in systems of self-propelled particles. *Physical Review E*, 63(1):017101, 2000.

[58] Yue-Xian Li, Ryan Lukeman, and Leah Edelstein-Keshet. Minimal mechanisms for school formation in self-propelled particles. *Physica D: Nonlinear Phenomena*, 237(5):699–720, 2008.

[59] Jan Lorenz. Continuous opinion dynamics under bounded confidence: A survey. *International Journal of Modern Physics C*, 18(12):1819–1838, 2007.

[60] Jan Lorenz. *Repeated averaging and bounded confidence: Modeling, analysis and simulation of continuous opinion dynamics*. PhD thesis, 2007.

[61] Martin Macaš, Martin Saska, Lenka Lhotská, Libor Přeučil, and Klaus Schilling. Path planning for formations of mobile robots using pso technique. 2009.

[62] Lalo Magni, Davide Martino Raimondo, and Frank Allgöwer. *Nonlinear model predictive control*. Springer, 2009.

[63] Seth A Marvel, Jon Kleinberg, Robert D Kleinberg, and Steven H Strogatz. Continuous-time model of structural balance. *Proceedings of the National Academy of Sciences*, 108(5):1771–1776, 2011.

[64] Alex Mogilner, L Edelstein-Keshet, L Bent, and A Spiros. Mutual interactions, potentials, and individual distance in a social aggregation. *Journal of mathematical biology*, 47(4):353–389, 2003.

[65] Sebastien Motsch and Eitan Tadmor. Heterophilious dynamics enhances consensus. *SIAM review*, 56(4):577–621, 2014.

[66] Máté Nagy, Zsuzsa Ákos, Dora Biro, and Tamás Vicsek. Hierarchical group dynamics in pigeon flocks. *Nature*, 464(7290):890–893, 2010.

[67] Angelia Nedic and Behrouz Touri. Multi-dimensional hegselmann-krause dynamics. In *Decision and Control (CDC), 2012 IEEE 51st Annual Conference on*, pages 68–73. IEEE, 2012.

[68] Henk Nijmeijer and Arjan Van der Schaft. *Nonlinear dynamical control systems*. Springer Science & Business Media, 2013.

[69] Ryosuke Nishi and Naoki Masuda. Dynamics of social balance under temporal interaction. *EPL (Europhysics Letters)*, 107(4):48003, 2014.

[70] Yongsheng Ou and Eugenio Schuster. On the stability of receding horizon control of bilinear parabolic pde systems. In *Decision and Control (CDC), 2010 49th IEEE Conference on*, pages 851–857. IEEE, 2010.

[71] Lorenzo Pareschi and Giuseppe Toscani. *Interacting multiagent systems: kinetic equations and Monte Carlo methods*. Oxford University Press, 2013.

[72] Peter Philip. Optimal control of partial differential equations. *Lecture notes, LMU, Munich*, 2013.

[73] Luciano CA Pimenta, Nathan Michael, Renato C Mesquita, Guilherme AS Pereira, and Vijay Kumar. Control of swarms based on hydrodynamic models. In *Robotics and Automation, 2008. ICRA 2008. IEEE International Conference on*, pages 1948–1953. IEEE, 2008.

[74] David F Shanno. Conjugate gradient methods with inexact searches. *Mathematics of operations research*, 3(3):244–256, 1978.

[75] Jackie Shen. Cucker-smale flocking under hierarchical leadership. *SIAM Journal on Applied Mathematics*, 68(3):694–719, 2007.

[76] Eduardo D Sontag. *Mathematical control theory: deterministic finite dimensional systems*, volume 6. Springer Science & Business Media, 2013.

[77] Katarzyna Sznajd-Weron and Jozef Sznajd. Opinion evolution in closed community. *International Journal of Modern Physics C*, 11(06):1157–1165, 2000.

[78] John Toner and Yuhai Tu. Long-range order in a two-dimensional dynamical xy model: how birds fly together. *Physical Review Letters*, 75(23):4326, 1995.

[79] Vito Trianni and Marco Dorigo. Self-organisation and communication in groups of simulated and physical robots. *Biological cybernetics*, 95(3):213–231, 2006.

[80] Fredi Tröltzsch. Optimal control of partial differential equations. *Graduate Studies in Mathematics*, 112, 2010.

[81] Wolfgang Walter. *Ordinary Differential Equations*. Springer-Verlag New York, 1998.

[82] Suttida Wongkaew, Marco Caponigro, and Alfio Borzì. On the control through leadership of the hegselmann–krause opinion formation model. *Mathematical Models and Methods in Applied Sciences*, 25(03):565–585, 2015.

[83] Suttida Wongkaew, Marco Caponigro, Krzysztof Kulakowski, and Alfio Borzì. On the control of the heider balance model. *Preprint*, 2015.

[84] Stephen J Wright and Jorge Nocedal. *Numerical optimization*, volume 2. Springer New York, 1999.

[85] Ko Yamamoto and Masafumi Okada. Continuum model of crossing pedestrian flows and swarm control based on temporal/spatial frequency. In *Robotics and Automation (ICRA), 2011 IEEE International Conference on*, pages 3352–3357. IEEE, 2011.